

**Marta Isabel Heitor
Cerejo**

**Contribuição para a monitorização de algas tóxicas
na Ria de Aveiro – ciclo anual de sucessão
fitoplanctónica e modelização da dispersão de
microalgas**





**Marta Isabel Heitor
Cerejo**

Contribution to the assessment of toxic algae in Ria de Aveiro – phytoplankton succession annual cycle and modelling of microalgae dispersal.

Dissertação apresentada à Universidade de Aveiro para cumprimento dos requisitos necessários à obtenção do grau de Mestre em Ciências das Zonas Costeiras, realizada sob a orientação científica do Dr. António Calado, Professor Auxiliar do Departamento de Biologia da Universidade de Aveiro e Dra. Teresa Moita, Investigadora Auxiliar do Instituto Nacional de Investigação Agrária e das Pescas/ IPIMAR.

To my grandmother Queta.
When I began my path in the study of phytoplankton communities, you have asked:
"What's the purpose of your work?"
You have left this world too soon.
Here is your answer.

o júri

presidente

Doutora Cristina Maria de Almeida Bernardes
Professora Associada da Universidade de Aveiro

Doutora Ana de Jesus Branco de Melo Amorim Ferreira
Professora Auxiliar da Faculdade de Ciências da Universidade de Lisboa

Doutor António José de Brito Fonseca Mendes Calado
Professor Auxiliar da Universidade de Aveiro (Orientador)

Doutora Maria Teresa Calixto de Jesus Moita Garnel
Investigadora do Departamento do Ambiente Aquático do Instituto Nacional de Investigação Agrária e das Pescas (Co-orientadora)

Doutor João Miguel Sequeira Silva Dias
Professor Auxiliar da Universidade de Aveiro

Acknowledgements

The development of this work would have been impossible without the support and participation of several people, to which I wish to express my gratitude:

To INIAP/IPIMAR for the financial support, granted opportunities and endowment of the data used in this work.

To the director of IPIMAR/CRIPCentro, Dr. Manuel Sobral, that not only encouraged the development of this study, supplying the necessary material, but also for his friendship and sharing knowledge about Ria de Aveiro ecology.

To Prof. António Calado and Dra. Teresa Moita not only for their scientific supervision, but also for their trust in my ability for this task and their friendship.

To Prof. Dr. João Dias, co-author of Chapter V, that as initiated me in the fascinating modelling world and for all the unquestionable support and encouragement he provided me.

To Dr. Paulo Vale for his friendship and for everything he taught me about biotoxins. Thank you also for the scientific supervision of Chapter IV and by providing data.

To Prof. Dra. Marina Cunha for her precious advices and help in the data statistical analysis and interpretation.

To Eng. Carlos Vale and Enga. Paula Cabeçadas for their supervision in nutrient quantification.

To Dra. Isabel Sobral for the granted help in references search and data analysis interpretation.

To all my colleagues and friends from Departamento de Fitoplâncton do IPIMAR – Lisboa for their support, particularly to Dra. Graça Vilarinho and Armindo Morais for their supervision in the treatment of photosynthetic pigment samples and taxonomic reviews.

To all my dear colleagues of CRIPCentro, and particularly to Victor Bettencourt, Danny Bettencourt and Christian Simões that escorted me during the sampling campaign so many times.

To my dearest friend and colleague Dra. Susana Siborro for all the help she provided me, not only at a scientific level but mostly at personal level. Thanks for her smile and care, during good (and not so good) moments.

To all my friends that in some way have helped me and encouraged, particularly to Dra Ana Marta Costa and Dra Solange Burri.

To my dearest parents and sisters, for their love, constant encouragement and total support. For their comprehension for the long periods that we remained apart and for my grouchy moments.

To Pedro, for his love, care, understanding and unquestionable support and encouragement. Thank you also for the long hours dedicated to English language correction and the image of the front page.

Palavras-chave

Fitoplâncton, ciclo anual, microalgas tóxicas; biotoxinas, monitorização, modelização, Ria de Aveiro

Resumo

Este trabalho é uma contribuição para a monitorização de microalgas tóxicas na Ria de Aveiro, baseado num estudo multidisciplinar, que inclui um estudo experimental sobre a comunidade fitoplanctónica e um estudo de modelização numérica, cujo objectivo é o de avaliar a localização das estações de amostragem determinadas pelo INIAP/IPIMAR no âmbito do Plano Nacional de Salubridade de Bivalves. Durante um período de 12 meses, foi realizada uma amostragem de periodicidade semanal, uma hora antes do pico de maré-cheia, num ponto fixo localizado na entrada da Ria de Aveiro. O intuito deste trabalho foi o de fornecer maior conhecimento sobre o ciclo anual de sucessão fitoplanctónica bem como sobre os parâmetros ambientais responsáveis pelo padrão temporal observado, tanto em termos de biomassa fitoplanctónica como em termos de composição específica da comunidade. O ciclo de sucessão observado é típico de zonas temperadas onde processos de afloramento costeiro são frequentes. A sucessão sazonal do fitoplâncton foi influenciada pelo ciclo sazonal de variação da temperatura da água, pela intensidade e variabilidade dos pulsos de afloramento e pela disponibilidade em nutrientes. A persistência de eventos de afloramento costeiro contribuiu para a manutenção de elevados níveis de biomassa fitoplanctónica no Verão e também para a relativa dominância de diatomáceas durante todo o período de estudo. *Dinophysis acuminata* (incluindo morfologias presumivelmente alternantes com a morfologia típica) e *D. acuta* proliferaram em condições de relaxamento de afloramento. O primeiro foi mais abundante durante a Primavera enquanto que *D. acuta* atingiu maiores concentrações no Verão e Outono. Quando *Dinophysis acuta* estava presente na coluna de água os bivalves atingiam maiores níveis de contaminação visto que esta espécie produz tanto AO como DTX2 e PTX2. *Dinophysis acuminata* induziu contaminações exclusivamente por AO. Apesar de não ser possível inferir o nível de contaminação atingido pelos bivalves pelas concentrações de células tóxicas, particularmente devido a diferentes níveis de toxina celular, a quantificação do fitoplancton é importante na monitorização de eventos tóxicos. Os resultados obtidos sugerem maior exactidão da técnica de Utermöhl na quantificação de fitoplâncton do que o método em uso corrente no plano de monitorização de algas tóxicas do INIAP/IPIMAR – Técnica do Monitoring - sendo recomendado o uso em paralelo de ambas as técnicas. A aplicação de um modelo numérico ao estudo da dispersão de microalgas na Ria de Aveiro legitimou de um modo geral a localização das estações de amostragem de água e bivalves pré-existentes e definidas pelo INIAP/IPIMAR. No entanto, a recolha de amostras de bivalves no canal de Ílhavo foi considerada desnecessária, excepto em períodos de alerta por biotoxinas. As estações do Marégrafo e da Moacha devem ser mantidas sem qualquer alteração enquanto que o Canal de Mira deverá ser amostrado com um periodicidade bimensal; outra estação de amostragem de água na extremidade mais a montante do Canal de Espinheiro deverá ser incluída no plano de amostragem.

Keywords

Phytoplankton, annual cycle, toxic microalgae, phycotoxins, monitoring, numerical modelling, Ria de Aveiro

Abstract

This work is a contribution to the monitoring of toxic microalgae in Ria de Aveiro, based on a multidisciplinary study. It includes an experimental study on the phytoplankton community, whose aim was to provide knowledge about the annual cycle of phytoplanktonic succession and on the environmental parameters responsible for the temporal pattern observed both in terms of phytoplankton biomass and community species composition, as well as a numerical modelling study whose purpose was to evaluate the location of the water and bivalve sampling stations currently in use in the framework of 'Plano Nacional de Salubridade de Bivalves' of INIAP/IPIMAR.

Samples were collected weekly in a fixed station, located at the entrance of Ria de Aveiro, one hour before full tide, during a survey period of 12 months. The phytoplankton succession cycle observed is typical of temperate zones where coastal upwelling is a frequent event. The seasonal succession of phytoplankton biomass was determined by the seasonal cycle of surface water temperature, by the variability of the intensity of upwelling events and by the availability of dissolved nutrients. The persistency of the upwelling events contributed for the maintenance of high levels of phytoplankton biomass during summer and to the dominance of diatoms during the entire survey period. *Dinophysis acuminata* (including morphs presumably alternating with the typical form) and *D. acuta* have proliferated in conditions of upwelling relaxation. The first was more abundant in spring while *D. acuta* achieved higher concentrations in summer and autumn. When *D. acuta* was the dominant toxic species higher levels of contamination were found in shellfish, since it is a producer of OA, DTX2 and PTX2. *Dinophysis acuminata* has induced contaminations exclusively by OA. Although it is not possible to infer the level of contamination of the bivalves by the abundance of toxic cells, particularly due to different cellular toxin levels, the quantification of toxic phytoplankton is important for the monitoring of toxic events. The results suggest higher accuracy of the Uthermöhl technique for phytoplankton quantification than the method currently in use in the INIAP/IPIMAR monitoring programme of toxic microalgae – Monitoring technique - and it is recommended the use in parallel of both techniques. The application of a numerical model to the study of microalgae dispersal in Ria de Aveiro has legitimated, in a general way, the locations of the pre-existent water and bivalve sampling stations determined by INIAP/IPIMAR. However it is considered unnecessary the bivalve collection at the Ílhavo channel except in periods of occurrence of toxic microalgae. The Marégrafo and Moacha water stations should be maintained without changes while the Mira channel should be sampled bi-monthly; another station at the far end of Espinheiro channel should be included in the sampling design.

“PLANKTON”

*“We're an indolent lot...
shiftless microscopic drifters.
Here in the oceans a million trillion trillion
of us just float aimlessly and worship the sun.
We have no brains at all.
And we don't do anything except
procreate with promiscuous abandon
and generate most of the earth's oxygen.
And we have no advice at all for you diligent
bipeds who use your capacious intellects
to so industriously befoul the seas.
For about two billion years we got along
quite well without you.
And without us, you will suffocate.”*

S.E. Jørgensen

Contents

Contents	i
List of Figures	v
List of Tables	xi
List of Equations	xiii
Chapter I – Introduction	1
1. Frame, Aims and Structure	1
2. Study Area	8
2.1. Aveiro adjacent littoral coast	8
2.2. Ria de Aveiro	9
3. Sampling design	11
4. References	12
Chapter II - Comparison of different estimation methods of phytoplankton abundance	15
Abstract	15
1. Introduction	16
2. Methods	18
2.1. Toxic phytoplankton	18
2.2.1. Monitoring technique	19
2.2.2. Utermöhl technique	19
2.2. Diarrhetic toxins concentration	20
2.3. Data analysis	20
3. Results	21
4. Discussion and conclusions	28
5. References	31
Chapter III - Phytoplankton biomass and species succession during an annual cycle	35
Abstract	35
1. Introduction	36
2. Material and methods	41
2.1. Sampling procedure	41

2.2. Analytical methods	42
2.2.1. Coastal upwelling	42
2.2.2. Dissolved nutrients	42
2.2.3. Phytoplankton biomass	43
2.2.4. Phytoplankton community structure	44
2.3. Data analysis	46
2.3.1. Biological data analysis	47
2.3.1.1. Q-type analysis	48
2.3.1.2. R-type analysis	53
2.3.2. Environmental data multivariate analysis	54
2.3.3. Linking biota to environmental data	54
3. Results	55
3.1. Temporal variability of phytoplankton biomass and community structure	55
3.2. Temporal variability of environmental parameters	69
3.3. Linking biota to environmental data	75
3.4. Structure of phytoplankton communities	80
4. Discussion	84
4.1. Phytoplankton species identification	84
4.2. Temporal variability of environmental parameters	87
4.3. Annual cycle of phytoplankton biomass and species composition	92
4.4. Phytoplankton communities	102
5. Conclusions	103
6. References	106
Chapter IV - DSP toxins and pectenotoxin-2 production by <i>Dinophysis</i> cf. <i>acuminata</i> and <i>Dinophysis acuta</i>	115
Abstract	115
1. Introduction	116
1.1. Diarrhetic shellfish poisoning	117
1.2. Diarrhetic toxins	118
2. Material and methods	122
3. Results	123
4. Discussion and conclusions	128
5. References	131

Chapter V - Transport and dispersal of toxic microalgae in Ria de Aveiro	135
Abstract	135
1. Introduction	136
2. Methods	139
2.1. Numerical modelling	140
2.1.1. Hydrodynamic model	140
2.1.2. Particle-tracking model	142
3. Results and discussion	145
3.1. Preferential channel	146
3.2. Microalgae tracks characterization	146
3.2.1. Espinheiro channel	148
3.2.2. S. Jacinto channel	150
3.2.3. Mira channel	153
3.2.4. Entrance channel	154
4. Conclusions	156
5. References	158
Chapter VI – Conclusions and final considerations	163
Appendix I	i

List of Figures

Figure 1.1. Ria de Aveiro satellite image. The pink areas correspond to agglomerates of buildings (GEM, 2006).	2
Figure 1.2. Study area – Ria de Aveiro.	10
Figure 1.3. Sampling station located at the entrance of Ria de Aveiro (courtesy of Tânia Vidal).	11
Figure 2.1. Time distributions of <i>Dinophysis cf. acuminata</i> and <i>D. acuta</i> obtained by the Monitoring technique.	22
Figure 2.2. Time distributions of <i>Dinophysis cf. acuminata</i> and <i>D. acuta</i> obtained by the Utermöhl technique.	22
Figure 2.3. <i>Dinophysis cf. acuminata</i> abundance estimation with both counting techniques: Monitoring and Utermöhl.	22
Figure 2.4. <i>Dinophysis acuta</i> abundance estimation by both counting techniques: Monitoring and Utermöhl.	23
Figure 2.5. <i>Dinophysis cf. acuminata</i> abundance estimation using both counting techniques compared with OA concentration in plankton extracts.	25
Figure 2.6. <i>Dinophysis acuta</i> abundance estimation using both counting techniques compared with OA concentration in plankton extracts.	26
Figure 2.7. <i>Dinophysis acuta</i> abundance estimation using both counting techniques compared with DTX2 concentration in plankton extracts.	26
Figure 2.8. <i>Dinophysis acuta</i> abundance estimation using both counting techniques compared with PTX2 concentration in plankton extracts.	27
Figure 3.1. Main phytoplankton groups in the total phytoplankton community of Ria de Aveiro, averaged over the entire sampling period.	56

Figure 3.2. Concentration of chlorophyll <i>a</i> (a) and phytoplankton cells: b) Total phytoplankton; c) Bacillariophyceae; d) Dinophyceae; e) Prymnesiophyceae.	57
Figure 3.3. Time distribution of the abundance of small phytoflagellates at Ria de Aveiro.	59
Figure 3.4. Time distribution of Chlorophyll <i>a</i> (Chl. <i>a</i>) concentration (line) and of the percentage of chlorophyll <i>a</i> associated with the nanoplankton fraction (bars).	59
Figure 3.5. Diatom index variation during the period of study.	60
Figure 3.6. Ria de Aveiro phytoplankton community. 2D (a) and 3D (b) MDS ordination of the 52 samples performed upon the results of the ANOSIM test and based on log-transformed abundances and Bray-Curtis similarities.	63
Figure 3.7. Ria de Aveiro phytoplankton community. Proportions of different classes of phytoplankton at each season, in terms of cell numbers per litre.	64
Figure 3.8. Ria de Aveiro phytoplankton community. Species cumulative (%) abundance plotted against species rank (K-dominance curves) for each season.	65
Figure 3.9. Time distribution of frequent species of the spring phytoplankton assemblage.	66
Figure 3.10. Time distribution of frequent species of the summer phytoplankton assemblage.	67
Figure 3.11. Time distribution of frequent species of the autumn phytoplankton assemblage.	68
Figure 3.12. Time distribution of frequent species of the winter phytoplankton assemblage.	68
Figure 3.13. Upwelling index, daily and weekly average (negative values are indicators of upwelling).	70
Figure 3.14. Surface water salinity (a) and temperature (b).	70
Figure 3.15. Dissolved nutrient concentration: a) ammonium; b) nitrate and nitrite; c) silicates; d) phosphates.	71

-
- Figure 3.16.** Redfield ratio for spring, summer, autumn and winter samples. 72
- Figure 3.17.** Relation between daily upwelling index, water temperature and nitrate + nitrite concentration, during the studied period. 73
- Figure 3.18.** Ria de Aveiro phytoplankton community. 2D (a) and 3D (b) MDS ordination of the 52 samples performed upon the results of the ANOSIM test and based on normalised euclidean distances. Stress value of 0.18 for the 2D plot and of 0.13 for the 3D plot. 75
- Figure 3.19.** Ria de Aveiro environmental data. MDS of Bray-Curtis similarities from log-transformed phytoplankton abundances with superimposed circles of increasing size with increasing temperature (a); salinity (b); tidal amplitude (c); upwelling (d); nitrate + nitrite (e); ammonium (f); phosphates (g); silicates (h) (stress = 0.01). ● spring, ● summer, ● autumn, ● winter. The values presented in the legend of the circles do not correspond to real values. 76
- Figure 3.20.** Relationship between the daily upwelling index and upwelling diatoms total concentration. 79
- Figure 3.21.** Relationship between the daily upwelling index and 4 species of upwelling diatoms. 80
- Figure 3.22.** Ria de Aveiro phytoplankton assemblage. Dendrogram for hierarchical clustering of the 39 genera, using group-average linking of Bray-Curtis similarities calculated on standardized and non transformed data. 81
- Figure 3.23.** Ria de Aveiro phytoplankton assemblage. Dendrogram for hierarchical clustering of the 48 species, using group-average linking of Bray-Curtis similarities calculated on standardized and non transformed data. 82
- Figure 3.24.** Time distributions of the abundance of *Dinophysis* cf. *acuminata* and *Dinophysis acuta*. 83
- Figure 3.25.** *Druridgera compressa*, phase contrast: a-c) girdle view (200x and 400x); d) detail of the pores of the frustule; e) valvar view; f) girdle view (1000x). 85
-

Figure 3.26. Annual cycle of phytoplankton succession in Ria de Aveiro.	101
Figure 4.1. Chemical structures of okadaic acid and dinophysistoxins (adapted from FAO, 2004).	118
Figure 4.2. Chemical structure of pectenotoxins and pectenotoxin-2 seco acid (adapted from FAO, 2004).	120
Figure 4.3. Chemical structure of yessotoxins (adapted from FAO, 2004).	121
Figure 4.4. <i>Dinophysis</i> cf. <i>acuminata</i> and <i>D. acuta</i> abundance variation during the period of study.	123
Figure 4.5. Relationship between toxins concentration in plankton and <i>Dinophysis</i> spp. concentration in the water column.	124
Figure 4.6. Relationship between toxins concentration in shellfish and <i>Dinophysis</i> spp. concentration in the water column (a) and with toxin concentration in plankton (b).	125
Figure 4.7. DTX2 percentages (related do OA) in plankton, common cockle and blue mussel.	127
Figure 4.8. Relationship between toxin cellular level and <i>Dinophysis</i> spp. concentration (a) and with toxins concentration in shellfish (b).	128
Figure 5.1. Ria de Aveiro lagoon.	138
Figure 5.2. Preferential channel, in percentage to which microalgae are transported.	146
Figure 5.3. Microalgae tracks in the Espinheiro channel for minimum total exit time in spring tide (a); maximum total exit time in neap tide (b); and maximum distance attained on spring tide (c).	148
Figure 5.4. Microalgae tracks in the S. Jacinto channel for minimum (a) and maximum (b) and total exit time (c) on spring tide and minimum total exit time (d) on neap tide.	151
Figure 5.5. Microalgae tracks in the Mira channel for the minimum total exit	153

time on spring tide (a) and the maximum total exit time on neap tide (b).

Figure 5.6. Microalgae tracks in the Entrance channel for the minimum total exit time on spring tide (a) and the maximum total exit time on neap tide (b).

155

List of Tables

Table 2.1. 95% confidence limits of the counts of <i>Dinophysis acuta</i> obtained by the Utermöhl method, according to the Poisson distribution.	24
Table 3.1. Ria de Aveiro phytoplankton community. Results of the test R statistic under the H_0 of ‘no season differences’, for each biotic data matrix.	61
Table 3.2. Ria de Aveiro phytoplankton assemblages. Results of the pairwise tests, under the H_0 of ‘no season differences’, for each biotic data matrix with 999 permutations.	62
Table 3.3. Ria de Aveiro phytoplankton community. Average (\bar{x}) and standard deviation (σ) of univariate measures for each season.	69
Table 3.4. Ria de Aveiro environmental data. Results of the pairwise tests, under the H_0 of ‘no season differences’, for each data matrix with 999 permutations.	74
Table 3.5. Ria de Aveiro environmental data. Average (\bar{x}) and average deviation (σ) of the different environmental variables per season.	77
Table 3.6. Ria de Aveiro phytoplankton community. Combinations of 6 environmental variables, taken k at a time, yielding the best matches of biotic and abiotic similarity matrices for each k , as measured by Kendall rank correlation; bold type indicates overall optimum.	78
Table 3.7. Ria de Aveiro phytoplankton community. Genera groups distinguished by inverse analysis. The groups are based on the dendrogram in Figure 3.22.	81
Table 3.8. Ria de Aveiro phytoplankton community. Species groups distinguished by inverse analysis. The groups are based on the dendrogram in Figure 3.23.	82
Table 5.1. Average distance attained by microalgae at each channel, average time needed to cover that distance, average microalgae total exit time from de lagoon and average residence time for each channel.	147
Table 5.2. Average distance attained by microalgae, time needed to cover that distance and exit time, in Espinheiro channel during spring and neap tides.	149

Table 5.3. Average distance attained by microalgae, time needed to cover that distance and exit time, in S.Jacinto channel during spring and neap tides.	152
Table 5.4. Average distance attained by microalgae, time needed to cover that distance and exit time, in Mira channel during spring and neap tides.	154
Table 5.5. Average distance attained by microalgae, time needed to cover that distance and exit time, in Main channel during spring and neap tides.	155

List of Equations

Equation 1. Estimation of number of phytoplankton cells per litre by the Utermöhl technique.	19
Equation 2. 95% confidence limits of phytoplankton cells counts according to the Poisson distribution.	20
Equation 3. Absolute limit of expectation of confidence on phytoplankton cells counts.	20
Equation 4. Kendall's rank correlation	21
Equation 5. Kendall's rank correlation	21
Equation 6. Bakun index: N-S component of wind force	42
Equation 7. Bakun index: upwelling index	42
Equation 8. Chlorophyll <i>a</i> concentration	43
Equation 9. Test of the significance of Kendall's correlation	47
Equation 10. R statistic	49
Equation 11. Log-transformed data equation	49
Equation 12. Bray-Curtis coefficient	50
Equation 13. MDS stress formula	51
Equation 14. Margalef species richness index	52
Equation 15. Pielou's evenness index	52
Equation 16. Shannon-Wiener diversity index	52
Equation 17. Euclidian distance	54

Equation 18. Three-dimensional Navier Stokes equations for Ria de Aveiro hydrodynamic model	141
Equation 19. Three-dimensional Navier Stokes equations for Ria de Aveiro hydrodynamic model	141
Equation 20. Three-dimensional Navier Stokes equations for Ria de Aveiro hydrodynamic model	141
Equation 21. Lagrangean particle trajectories	143
Equation 22. Two-dimensional trajectories of the simulated particles	143
Equation 23. Fourth-order Rung-Kutta scheme	143
Equation 24. Fourth-order Rung-Kutta scheme	143
Equation 25. Fourth-order Rung-Kutta scheme	143
Equation 26. Fourth-order Rung-Kutta scheme	143
Equation 27. Fourth-order Rung-Kutta scheme	144

Chapter I

Introduction

1. Frame, Aims and Structure

Some of the most valuable and exquisite world habitats are situated within coastal zones. The richness in natural resources (aquatic and terrestrial) of these areas has induced the settlement of large human populations, either for social or economic reasons, which has exposed the already fragile equilibrium of coastal zone environments to additional pressure. Economic activities such as wild fisheries, aquaculture, nautical transports and tourism share the vital space of the coastal zone, not always in a sustainable way, leading to its progressive degradation. In an epoch where increasing effort is made to alert human populations for the non-abusive use of natural resources, it is then necessary to develop scientific studies that allow us to gain additional knowledge of coastal ecosystems functioning, in order to improve its management and assessment (Mann, 2000; CE, 2001).

Lagoons and estuaries are very productive aquatic environments frequent in coastal zones and are of high ecological importance since they constitute natural shelter environments to a wide variety of species of fish, shellfish and marine birds, which also have high economical interest (Barnes & Hughes, 1987; Mann, 2000). These systems make the transition between freshwater, marine and terrestrial environments, from which they receive large quantities of nutrients and organic matter. This contributes to their high relative productivity, the utmost among all aquatic ecosystems (Barnes & Hudes, 1987; Valiela, 1995).

In Portugal one of the most important and extensive coastal embayment occurs in the northwest Atlantic coast: Ria de Aveiro. It is a remarkable shallow coastal lagoon, very

dynamic both in physical and biophysical terms (Dias, 2001). Biologically, Ria de Aveiro is considered as a highly productive system due to its richness in nutrients and organic matter (Dias *et al.*, 2003). It guarantees natural conditions for economic activities of industry (of which fishery resources, salt and seagrasses exploitation are enhanced) navigation and recreation, supporting for that reason strong pressure caused by the abundant human population that inhabits its margins and lives upon its resources.



Figure 1.1. Ria de Aveiro satellite image. The pink areas correspond to agglomerates of buildings (GEM, 2006)

As in any marine ecosystem, very diverse communities of organisms are present in Ria de Aveiro and are interconnected originating very complex food chains. In order to know how this interconnection occurs and to understand the structure and functioning of the ecosystem is essential to know the different elements of which it is composed, i.e. the distribution of organisms in space and time (Zeitzschel, 1978; Nybakken, 1988; Valiela, 1995; Thurman, 1996).

One of the most important communities of organisms of a marine ecosystem is phytoplankton – autotrophic microscopic algae – which are the basic food for all consumers, such as zooplankton, molluscs and fish, possessing therefore great ecological significance (Zeitzschel, 1978; Gross, 1993; Summerhayes, 1996; Thurman, 1996; Hallegraeff, 2003; FAO, 2004; IOC, 2005).

Phytoplankters represent one quarter of the total planet vegetation and constitute the major portion of primary producers in the sea (Zeitzschel, 1978; Nybakken, 1988; Valiela, 1995). Consequently, phytoplankton communities study in a given area becomes crucial, because distribution and seasonal succession of the phytoplankton species present are not only of interest in themselves, but because such quantitative and qualitative differences may have effects on the higher components of the food chain and may thus also be of economic importance (Zeitzschel, 1978).

One of the most visible effects of phytoplankton distribution on the ecosystem and economy of a given area are the Harmful Algal Blooms (HABs), commonly referred as blooms, or red tides (when water coloration occurs) (Hallegraeff, 2003; Valiela, 1995; FAO, 2004). They consist in a massive proliferation of one or more phytoplankton species, usually rapid and geographically restricted (Hallegraeff, 2003; Valiela, 1995; FAO, 2004; IOC, 2005). Among the 5000 species of extant marine phytoplankton, some 300 species can at times occur in such high numbers that they obviously discolour the surface of the water (Hallegraeff, 2003).

Some species produce basically harmless water discolorations, and therefore are beneficial to wild fisheries and aquaculture activities since they provide food resources to consumers. On the other hand, some species can bloom so densely that they indiscriminately kill fish and invertebrates due to oxygen depletion. Other algal species can be harmful to fish and invertebrates by damaging or clogging their gills. Furthermore, there are microalgae (about 80 species) which have the capacity to produce potent toxins (called phycotoxins) that can find their way through levels of the food chain (e.g. molluscs, crustaceans and finfish) and are ultimately consumed by humans causing a variety of gastrointestinal and neurological illnesses (Hallegraeff, 2003; FAO, 2004; IOC, 2005).

Some algal species produce toxins at low abundances of some hundreds of cells per litre, while others must occur in some millions of cells per litre in order to cause any harm

(Hallegraeff, 2003; FAO, 2004). It is not clear why some microalgae species produce toxins; they are secondary metabolites with no explicit role in the internal economy of the organisms that produce them. Probably, they are used by their producers as a way to compete for space, fight predation or as a defence against the overgrowth of other organisms (FAO, 2004).

Until now, five groups of shellfish toxins have been distinguished, namely: (i) paralytic toxins causing paralytic shellfish poisoning (PSP); (ii) diarrhoeic toxins causing diarrhoeic shellfish poisoning (DSP); (iii) amnesic toxins causing amnesic shellfish poisoning (ASP); (iv) neurotoxic toxins causing neurotoxic shellfish poisoning (NSP); and (v) azaspiracid toxins causing azaspiracid shellfish poisoning (AZP) (Hallegraeff, 2003; FAO, 2004; IOC, 2005).

In the Portuguese coast, the most frequent toxicity events are PSP, ASP and DSP, and are caused by the ingestion of contaminated shellfish.

Symptoms of human PSP intoxication vary from a slight tingling or numbness to complete respiratory paralysis. In fatal cases, respiratory paralysis occurs within 2 to 12 hours of consumption of the PSP contaminated food. PSP toxins are a group of 21 closely related tetrahydropurines. The various PSP toxins significantly differ in toxicity with saxitoxin (STX) – the first PSP toxin chemically characterized – being the most toxic. The PSP toxins are produced mainly by dinoflagellates belonging to the genus *Alexandrium* and to *Gymnodinium catenatum* (Hallegraeff, 2003; FAO, 2004; IOC, 2005).

Amnesic shellfish poisoning (ASP), also known as domoic acid poisoning (DAP) because amnesia is not always present, was first recognised in 1987 in Prince Edward Island, Canada. At this time, ASP caused three deaths and 105 cases of acute human poisoning following the consumption of blue mussels. The symptoms included abdominal cramps, vomiting, disorientation and memory loss (amnesia). The causative toxin (the excitatory amino acid domoic acid or DA) was produced by a diatom belonging to the genus *Pseudo-nitzschia* (Hallegraeff, 2003; FAO, 2004; IOC, 2005).

Diarrhetic shellfish poisoning (DSP) in humans is due to the accumulation of fat soluble DSP toxins in the bivalve fatty tissues. DSP symptoms are diarrhoea, nausea, vomiting and abdominal pain starting 30 minutes to a few hours after ingestion and complete recovery occurs within three days. DSP toxins can be divided into different groups depending on

chemical structure. The first group, acidic toxins, includes okadaic acid (OA) and its derivatives named dynophysistoxins (DTXs). The second group, neutral toxins, consists of polyether-lactones of the pectenotoxin group (PTXs). The third group includes a sulphated polyether and its derivatives the yessotoxins (YTXs) (Hallegraeff, 2003; FAO, 2004; IOC, 2005). Diarrhetic toxins are usually produced by dinoflagellates that belong to the genus *Dinophysis*; however, the dinoflagellate genus *Prorocentrum* has also been found to be a producer of DSP toxins. The most affected areas seem to be Europe and Japan (Hallegraeff, 2003; FAO, 2004; IOC, 2005).

Despite the very different chemical nature of the phycotoxins, they do not generally change or reduce significantly in amount upon seafood products cooking neither influence the taste of the meat. The detection of contaminated seafood is not, therefore, straightforward, and neither fishermen nor consumers can determine whether seafood products are safe for consumption (IOC, 2005). Hence, to reduce the risk of serious seafood poisoning intensive monitoring of the species composition of the phytoplankton is required in the harvesting areas, in connection with bioassays and/or chemical analyses of the seafood products (IOC, 2005).

This monitoring task becomes particularly essential due to growing evidences that HABs events appear to have increased in frequency, intensity and geographical distribution, along with the number of toxic compounds found in the marine food chain (Hallegraeff, 2003). Different explanations for this trend have been given such as increased scientific awareness of toxic algal species, increased utilization of coastal waters for aquaculture, transfer of shellfish stocks from one area to another, cultural eutrophication from domestic, industrial and agricultural wastes, increased mobility of humic substances and trace metals from soil due to deforestation and/or by acid precipitation (acid rain) and unusual climatic conditions (Hallegraeff, 2003; FAO, 2004).

When toxic microalgae are registered in the water and level of toxicity found in bivalves is higher than the limit imposed by the European legislation, the competent authorities prohibit the shellfish harvest in the affected areas. This action has a strong negative impact in the economy of those areas, which main activity resides in the commercial exploitation of bivalves. This circumstance is likely to occur in Ria de Aveiro where it has been estimated (in 1996) an annual production of 5000 tons of shellfish (Sobral *et al.*, 2000).

Natural production banks of bivalve species are common in Ria de Aveiro, existing in almost every channel, but mostly in the central part of the lagoon (Sobral, pers. comm.). The most explored species are common cockle (*Cerastoderma edule*), cockle shell (*Tapes decussatus*), blue mussel (*Mytilus edulis*), carpet shell (*Venerupis pullastra*) and razor shell (*Solen marginatus*) (Sobral *et al.*, 2000).

Bivalve shellfish are an extremely successful and diversified group of aquatic organisms, from phylum Mollusca. They can occur in environments with a wide range of salinities, as sea, fresh or brackish water, and usually live at the bottom. There are some sessile species that fix themselves to solid substratum, while others live buried in bottom sediments (Storer *et al.*, 1991). Bivalve shellfish are filtering feeders that inhabit the intertidal zone and feed on phytoplankton. They pump the ambient water through filters that retain suspended matter, usually irrespective of whether this matter is of food value or not (Jørgensen, 1990). When toxic phytoplankton cells are abundant in the water column they are ingested and their toxins accumulated in the bivalve shellfish tissues (FAO, 2004; IOC, 2005).

In Portugal, the task of monitoring and control of such toxic events is performed by Instituto Nacional de Investigação Agrária e das Pescas (INIAP/IPIMAR) (Decreto-Lei n° 293/98 de 18 de Setembro). For that, water and bivalve shellfish samples are collected in different sampling stations, located along the Portuguese coast, in the frame of the project Plano Nacional de Salubridade de Bivalves.

Ria de Aveiro is one of the most affected sites by toxic events, in the Portuguese coast (Moita, 1993; Vale *et al.*, 2004; Moita *et al.*, 2005). Every year, especially in summer and autumn, toxin-producer microalgae occur in the water causing great economic losses to the bivalve shellfish harvesting activity, with the obvious consequences at the social level.

To minimize the economic and social negative impacts of the prohibition of bivalve harvesting during periods of occurrence of toxic microalgae, and also for safeguard public health, the main goal of the present dissertation is to contribute to the improvement of the toxic microalgae assessment in Ria de Aveiro. By providing additional knowledge on phytoplankton community species composition, distribution patterns of the most frequent toxic microalgae, DSP toxin production by *Dinophysis* spp. species and by testing the

applicability of different methodologies in the monitoring task, it is hoped to suggest new ideas that may improve and optimize the monitoring of toxic events in Ria de Aveiro.

Therefore this dissertation titled “*Contribution to the assessment of toxic algae in Ria de Aveiro – phytoplankton succession annual cycle and modelling of microalgae dispersal*” is divided in six chapters:

Chapter I presents the Introduction, where the frame, aims and structure of this work are described. A general description of the study area and sampling campaign is also presented.

In Chapter II, with the title “Comparison of different estimation methods of phytoplankton abundance”, a comparison between two counting techniques for estimation of toxic phytoplankton cells number per litre is made, aiming to determine the most suitable for the correct monitor of toxic microalgae in Ria de Aveiro. This comparison was accomplished by relating the toxic microalgae abundance estimated by both techniques with the toxin concentration level found in plankton extracts obtained at the same sampling station.

Chapter III, designated as “Phytoplankton biomass and species succession during an annual cycle at Ria de Aveiro” aims to describe the seasonal distribution pattern of the phytoplankton community that enters in Ria de Aveiro, during one year. The succession of phytoplankton species is also subject of study, and emphasis is given to *Dinophysis* spp. pattern of variation. Biological data results are related to several environmental parameters such as water temperature and salinity, dissolved nutrient concentration and upwelling conditions that in some way can affect the distribution and abundance of phytoplankton organisms.

In Chapter IV – “DSP toxins and pectenotoxin-2 production by *Dinophysis* cf. *acuminata* and *Dinophysis acuta*” – the relation between toxic microalgae abundance, cellular toxin concentration and bivalve shellfish toxicity is explored, in order to try to explain why at different episodes of *Dinophysis* spp. bivalve shellfish attain different levels of toxicity. Moreover, an attempt to establish a maximum limit of *Dinophysis* spp. abundance, estimated using Utermöhl technique, is performed.

In Chapter V, designated “Transport and dispersal of marine toxic plankton algae in Ria de Aveiro”, a previously developed lagrangean particle tracking model coupled to a calibrated two-dimensional hydrodynamic model of Ria de Aveiro was exploited in order to

understand how the tidal flow induces the transport and dispersal of toxic marine phytoplankton algae in this lagoon. The aim of this survey is to achieve an accurate monitoring of toxic events in Ria de Aveiro, with the obvious benefits for the local public health, by determining the optimal location of water and bivalve shellfish sampling stations and evaluating the sampling stations already existent in Ria de Aveiro, in the frame of the project Plano Nacional de Salubridade de Bivalves of INIAP/IPIMAR. This work was co-performed by Professor Doutor João Dias of Departamento de Física of the Universidade de Aveiro and has been submitted for publication in Marine Ecological Research.

Finally, Chapter VI – “Conclusions and final considerations” – synthesizes the main conclusions of this work and suggests some improvements for the monitoring of toxic microalgae in Ria de Aveiro, as well as new propositions for future work.

2. Study Area

2.1. Aveiro adjacent coast

The west Portuguese coast is located along the 9° W meridian between 37° and 42° N parallels and it is situated in the northern limit of the upwelling system associated with the Atlantic North anticyclonic gyre (Fiúza, 1983).

The predominant wind pattern of the Portuguese coast instigate two types of surface water circulation (Ekman transport¹): during periods of coastal upwelling, when northerly winds prevail, the surface waters are transported offshore and to south, existing divergence near shore. Deeper waters rise up to take the place of those divergent waters. When southerly winds prevail, Ekman transport occurs inshore and coastal convergence occurs. Events of contrary winds can exist within each period, i.e. episodes of coastal upwelling can occur during the epoch of coastal convergence and vice-versa (Fiúza, 1983; The Open University, 1989a).

Coastal convergence periods are characterized by a northerly current, of warmer and more saline waters, that flows near the coast (Fiúza, 1983). Divergence and upwelling areas are

¹ Ekman transport: The total volume of water transported at right angles to the wind direction per second (The Open University, 1989a)

characterized by colder waters than the surrounding water and contain a high concentration of inorganic dissolved nutrients which supplies the development of phytoplankton (The Open University, 1989a). In fact, it is due to this increase of primary production that coastal upwelling areas have such great ecological importance because it will condition also de productivity of higher trophic levels (The Open University, 1989a).

Coastal upwelling in the Portuguese west coast depends upon the position of the Açores anticyclone gyre, and occurs seasonally, since spring to autumn, under the forcing action of northerly winds. Patterns of coastal upwelling in Portugal are determined both by coast morphology and local wind regime and by the bathymetric characteristics of the continental shelf. North from Nazaré canyon, the coast segment where the study area is included, the coastal line is meridionally oriented and presents a wide continental shelf and a gentle slope (Fiúza, 1983).

It is in this coast segment that Ria de Aveiro, one of the most extensive Portuguese aquatic ecosystems, occurs (Barrosa, 1985; Dias, 2001).

2.2. Ria de Aveiro

Ria de Aveiro (40° 38' N, 8° 45' W) (Dias, 2001) is a shallow coastal lagoon and constitutes a highly productive environment, household of several different species of fish and invertebrates, most of them with high commercial interest. This lagoon provides natural conditions for economic activities, like industry, navigation and recreation, enduring great pressure due to the large human population that inhabits its margins and lives upon its resources (Barrosa, 1985; Dias *et al.*, 2001).

The lagoon is 45 km long and 10 km wide (Figure 1.2) and in spring tide covers an area of 83 km² at high tide, which is reduced to 66 km² at low tide (Barrosa, 1985; Dias *et al.*, 2001). It comprises a complex dendritic pattern of channels characterised by the existence of significant intertidal zones, namely mud flats and salt marshes (Dias *et al.*, 2001), where extensive natural banks of shellfish occur. It is connected to the Atlantic Ocean through an artificial channel at the west side and it exchanges most of its water with the ocean by tidal input across this narrow entrance (Vicente, 1985; Dias *et al.*, 2001).

There are numerous channels in Ria de Aveiro but in this study only the four main branches radiating from the sea entrance (Entrance channel) are considered: Mira, S. Jacinto, Ílhavo and Espinheiro channels (Figure 1.2).

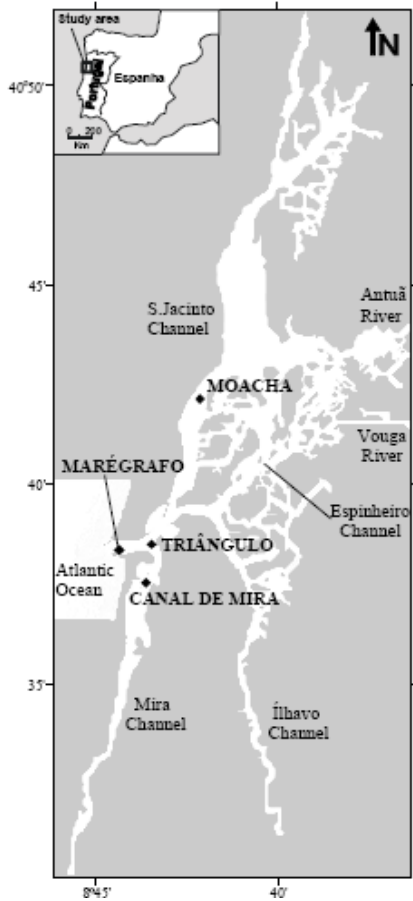


Figure 1.2. Study area – Ria de Aveiro.

(neap tide) and 3.2 m (spring tide), respectively. The tide propagates from the mouth as a mixed progressive and standing wave and it is present in the entire lagoon. It generates strong currents in deep and narrow channels, but not in the intertidal areas (Dias *et al.*, 2001). There is a small artificial headland (Triângulo Divisor das Correntes) dividing the Entrance channel in two different arms. Due to this feature the tidal prism is divided in two flows during the flood: a small one flowing into Mira channel and a second and more important one flowing to the other channels, namely S. Jacinto and Espinheiro channels, in which tidal current amplitudes may achieve values higher than $1 \text{ m}\cdot\text{s}^{-1}$ (Vicente, 1985; Dias, 2001; Dias *et al.*, 2001).

The lagoon receives freshwater mainly from two rivers, Antuã ($5 \text{ m}^3\cdot\text{s}^{-1}$ average flow) and Vouga ($50 \text{ m}^3\cdot\text{s}^{-1}$) (Vicente, 1985; Dias *et al.*, 2003; Dias & Lopes, 2006a). The Boco river,

Each of these channels has proper hydrologic characteristics, and for this reason may be considered as presenting features of individual estuaries (Dias *et al.*, 1999).

The average depth of the lagoon is about 1 m relative to the local datum, but in the inlet channel the depth is higher than 20 m. The other navigable channels, where dredging operations are frequently carried out, are about 7 m deep (Dias *et al.*, 2001).

Ria de Aveiro is a mesotidal lagoon and the tides, which are semidiurnal, are the main forcing action, with a mean tidal range of about 2 m (Vicente, 1985; Dias *et al.*, 2001; Dias & Lopes, 2006b).

Dias *et al.* (1999) referred the minimum and maximum registered tidal ranges as 0.6 m

at the southern end of Ílhavo channel, has a negligible flow, as well as the Caster and the Gonde rivers, discharging at the north end of S. Jacinto channel. There is another freshwater source at the southern end of Mira channel that consists in a small system of ponds and rivers connected with a small dam called Barrinha de Mira, and from which the flow is not well known (Dias *et al.*, 2003; Dias & Lopes, 2006a).

The estimated maximum and minimum tidal prism of the lagoon is $136.7 \times 10^6 \text{ m}^3$ and $34.9 \times 10^6 \text{ m}^3$ for the extreme spring and neap tides, respectively (Dias, 2001). The total estimated freshwater input in a spring tide is very small (about $1.8 \times 10^6 \text{ m}^3$ during a tidal cycle) when compared with the mean tidal prism at the mouth (about $70 \times 10^6 \text{ m}^3$).

A prior hydrological characterization of Ria de Aveiro lead to the conclusion that the lagoon can be considered vertically homogeneous (Dias *et al.*, 1999).

3. Sampling Design

With the purpose of monitor the phytoplankton community that enters in Ria de Aveiro preceding from the adjacent coast, sampling was performed in a fixed point located at the entrance of the lagoon (Figure 1.3). This location allowed accomplishing a systematic sampling procedure, with high frequency, and without interruptions, even when climate conditions and sea disturbance were unfavourable.

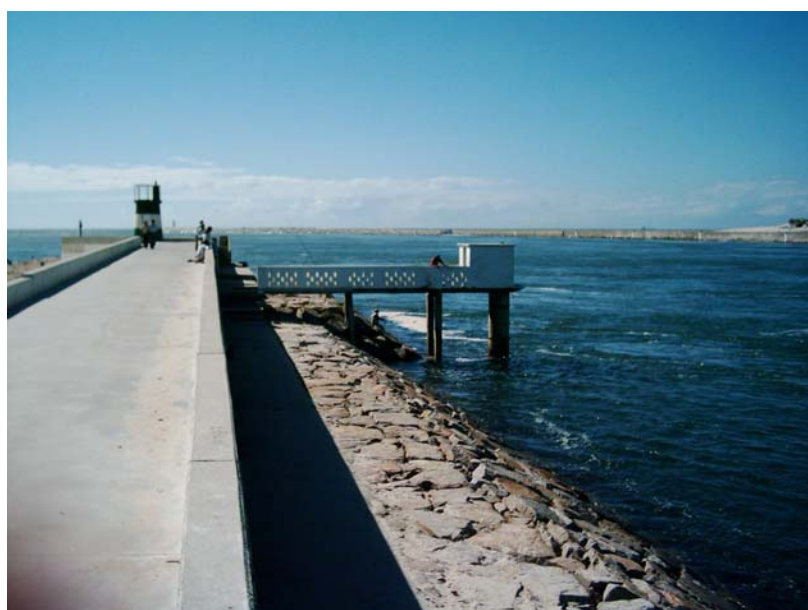


Figure 1.3. Sampling station located at the entrance of Ria de Aveiro (courtesy of Tânia Vidal).

Samples were collected weekly, since 18 May 2004 to 09 May 2005, in a total of 52 sampling campaigns. In order to minimize lagoon's water influence in the samples, sampling was performed one hour before full tide, which corresponds to a stage where flood is completely established, following the tidal prediction table, for Aveiro's seaport, of Instituto Hidrográfico of Marinha Portuguesa.

Surface water was collected to analyse the phytoplankton community, both qualitatively and quantitatively, the phytoplankton biomass, the concentration of dissolved nutrients and level of DSP toxins and pectenotoxins in plankton extracts. Measures of water temperature and salinity were also obtained. Wind direction and intensity records, provided by INMG (Instituto Nacional de Meteorologia e Geofísica), were obtained for Cabo Carvoeiro meteorological station.

4. References

- Barnes RSK & Hughes RN (1988) *An Introduction to Marine Ecology*, 2nd ed. Blackwell Science, Oxford.
- Barrosa JO (1985) Breve caracterização da Ria de Aveiro. In: *Jornadas da Ria de Aveiro*, Vol. III – Recursos da Ria de Aveiro, Câmara Municipal de Aveiro, Portugal, p 9-14.
- Comissão Europeia (CE) – Ministério do Ambiente (2001) *A União Europeia e as Zonas Costeiras* (folheto informativo). Luxemburgo, Serviço de Publicações Oficiais das Comunidades Europeias.
- Dias JM (2001) *Contribution to the study of the Ria de Aveiro hydrodynamics*. PhD dissertation, University of Aveiro, Aveiro, Portugal.
- Dias JM, Lopes JF (2006a) Calibration and validation of hydrodynamic, salt and heat transport models for Ria de Aveiro lagoon (Portugal). *Journal of Coastal Research*, SI 39 (in press).
- Dias JM & Lopes JF (2006b) Implementation and assessment of hydrodynamic, salt and heat transport models: the case of Ria de Aveiro lagoon (Portugal). *Environmental Modelling and Software* 21: 1-15.

- Dias JM, Lopes JF, Dekeyser I (1999) Hydrological characterisation of Ria de Aveiro, Portugal, in early Summer. *Oceanologica Acta* 22: 473-485
- Dias JM, Lopes JF, Dekeyser I (2001) Lagrangian transport of particles in Ria de Aveiro lagoon, Portugal. *Phys Chem Earth (B)* 26: 721-727.
- Dias JM, Lopes JF, Dekeyser I (2003) A numerical system to study the transport properties in the Ria de Aveiro lagoon. *Ocean Dynamics* 53: 220-231.
- FAO (2004) Marine Biotoxins. FAO Food and Nutrition Paper, 80. Food and Agriculture Organization of the United Nations, Rome.
- Fiúza AFG (1983) Upwelling patterns of Portugal. In: Suess E & Thiede J (eds) Coastal Upwelling. Plenum Press: New York, p 85-98.
- GEM (2001) Integrated Management of the Ria de Aveiro [on-line]. Geochemical Ecological Modelling. Faculty of Sciences and Technology, Lisbon, Portugal [consulted 25/02/2006]. Available from:
<<http://www.ecowin.org/>>
- Gross GM (1933) Principles of oceanography, 7th edn. Chesapeake Resource Consortium – University of Maryland. Prentice Hall: Englewood Cliffs, New Jersey.
- Hallegraeff GM (2003) Harmful algal blooms: a global overview. In: Hallegraeff GM, Anderson DM & Cembella AD (eds) Manual on harmful marine microalgae, 2nd edn. UNESCO Publishing, p 25-46.
- IOC (2005) The IOC harmful algal programme [on-line]. Intergovernmental Oceanographic Commission of UNESCO, Paris, France [consulted on September 2005] Available from:
<<http://ioc.unesco.org/hab/intro.htm>>
- Jørgensen CB (1990) Bivalve filter feeding: hydrodynamics, bioenergetics, physiology and ecology. Olsen & Olsen, Fredensborg, Denmark.
- Mann KH (2000) Ecology of coastal waters: with implications for management (2nd edn). Blackwell Science, Massachusetts, USA.

- Moita MT (1993) Development of toxic dinoflagellates in relation to upwelling patterns off Portugal. In: Smayda TJ & Shimizu Y (Eds.) Toxic Phytoplankton Blooms in the Sea (299-304). Elsevier, Amsterdam, The Netherlands.
- Moita MT, Palma AS, Vilarinho MG (2005) Blooms de fitoplâncton na costa Portuguesa. IPIMAR Divulgação, nº31, Lisboa, Portugal.
- Nybakken JW (1988) Marine biology: an ecological approach (2ndedn). Harper Collins Publishers, New York.
- Sobral MP, Vieira F, Sobral V (2000) Zonas de produção de moluscos bivalves da Ria de Aveiro. IPIMAR Divulgação nº 12, Lisboa, Portugal
- Storer TI, Usinger RL, Stedbins RC, Nybakken JW (1991) Zoologia geral, 6thedn. Companhia Editora Nacional, São Paulo, Brasil
- Summerhayes CP & Thorpe SA (1996) Oceanography: An illustrated guide. Southampton Oceanography Centre. Manson Publishing: London, United Kingdom.
- The Open University (1989a) Ocean circulation. Pergamon Press, Oxford, England.
- The Open University (1989b) Waves, tides and shallow-water processes. Pergamon Press, Oxford, England.
- Thurman HV (1996) Essentials of Oceanography (5thedn). Mt. San Antonio College. Prentice Hall: Upper Saddle River, New Jersey.
- Vale P, Cerejo M, Vilarinho MG (2004) Toxin production by *Dinophysis* spp. at Ria de Aveiro, Portugal. In press in: Proceedings of 5th International Conference on Molluscan Shellfish Safety, Galway, Ireland, 14-18 June 2004
- Valiela I (1995) Marine ecological processes (2ndedn). Springer-Verlag, New York.
- Vicente CM (1985) Caracterização hidráulica e aluvionar da Ria de Aveiro. Utilização de modelos hidráulicos no estudo de problemas da Ria. In: Jornadas da Ria de Aveiro, Vol III – Ordenamento da Ria de Aveiro. Câmara Municipal de Aveiro, Portugal.
- Zeitzschel B (1978) Why study phytoplankton. In: Sournia A (ed) Phytoplankton manual. UNESCO, United Kingdom, p 1-5.

Chapter II

Comparison of different estimation methods of phytoplankton abundance

Abstract

A comparative study is presented in order to evaluate the most suitable phytoplankton quantification method for the Portuguese HABs monitoring programme. At one selected station, Marégrafo, located at the entrance of Ria de Aveiro (Figure 1.2), water samples were collected for analysis and quantification of *Dinophysis* cf. *acuminata* and *D. acuta* by two microscope-based counting techniques – Utermöhl (1958) and the method currently in use in the INIAP/IPIMAR programme of toxic microalgae monitoring, here referred as Monitoring technique – and for the quantification of DSP toxins (okadaic acid – OA – and dinophysistoxin-2 – DTX2) and pectenotoxin-2 (PTX2) in plankton extracts. Both counting techniques have allowed the detection of *D. cf. acuminata* and *D. acuta* in the water when the DSP toxins were also present, and good positive correlations were obtained between the toxin profile and the estimated abundances. However, results suggest a higher accuracy of the data obtained by the Utermöhl technique than with the data obtained by the Monitoring technique, which tends to overestimate the abundance of the phytoplankton cells. The apparently lower accuracy of the data provided by the Monitoring method is thought to be a result of the method used for concentrating the sample (centrifugation), of the repeated sub-sampling involved and of the relatively small volume of the counted aliquot. For the monitoring optimization of the toxic microalgal species in Ria de Aveiro, results suggest the use of the Utermöhl method, at least for one sampling station, in parallel with the Monitoring technique that provides faster results.

1. Introduction

To reduce the risk of human intoxications caused by the ingestion of seafood products contaminated by phycotoxins, several coastal countries have developed harmful algae monitoring programmes. These programmes include, in addition to the quantification by chemical methods of the phycotoxins present in the seafood products, analyses of the specific composition of the phytoplankton community present in the water of the harvesting areas, as well as the quantification of toxic microalgae (Andersen & Thronsen, 2003; IOC, 2005).

The primary goal of sampling and analyse toxic phytoplankton is to gain some predictive ability concerning the initiation of a harmful outbreak. To acquire such an ability a good sampling programme is essential. Such a programme can be more directed to the investigation of the causes and dynamics of toxic blooms or be designed to simply assure the goals of a monitoring programme, i.e. determine the relative abundance of the toxic species present (Franks & Keafer, 2003). Thus, it is essential to define the required precision of the results in order to choose the most suitable phytoplankton quantification method. The type of method selected will determine the nature of the sample required.

There are several methods for phytoplankton quantification. Some are based in the estimation of the abundance of phytoplankton, expressed in cell numbers, and obtained by microscopic enumeration of the phytoplankton cells present in an aliquot of sample. Others involve the estimation of total phytoplankton biomass² via the quantification of chlorophyll, ATP, carbon, nitrogen, etc. These biomass measurements do not estimate phytoplankton concentration *sensu stricto*; they only provide a measurement of some constituent common to the entire population which reflects numerical abundance. For that reason, biomass measurements cannot substitute a numerical census. Other technique, although time consuming, already includes the enumeration of the phytoplankton cells and the measurement of the biomass from the cells volume characteristics (Smayda, 1978).

² Here understood as the mass of living organisms within a particular environment, measured in terms of weight per unit area or volume

The enumeration of phytoplankton presents several advantages when compared to other methods of phytoplankton concentration estimation: (a) the algae are seen, allowing the detection and evaluation of changes in appearance; (b) estimations can be made of populations whose abundance is too low for detection by proximate analyses; (c) species identification can be made and, hence, the taxonomic structure of the population can be determined (Smayda, 1978).

Microalgae quantification by microscopic counting can be accomplished by a range of different methods based on compound, inverted and epifluorescence microscopy (Andersen & Throndsen, 2003).

In Portugal, in the framework of the project 'Plano Nacional de Salubridade de Bivalves', the HABs monitoring programme includes analyses of surface water samples collected periodically in several sampling stations along the Portuguese coastal area. In Ria de Aveiro, water samples for phytoplankton analysis are collected at four locations: Marégrafo (at the mouth of the lagoon) sampled twice a week; Triângulo das Correntes (Entrance channel) and Moacha (S. Jacinto channel) sampled with a weekly periodicity; and Canal de Mira (Mira channel), sampled only when toxic microalgae are detected at the other stations.

Toxic phytoplankton quantification is made by a counting method developed by the Laboratório de Fitoplâncton of INIAP/IPIMAR, referred here as the Monitoring technique. This method is based on light microscopy and counts are performed in a Palmer & Maloney counting chamber. It is a simple method of quickly estimating the concentration of microalgae, which is a desirable characteristic to provide a rapid alert in case of occurrence of potentially toxic species. It has a preparation time of approximately 15 minutes (Andersen & Throndsen, 2003).

However, the use of inverted microscopy and sedimentation chambers, according to the Utermöhl method, is one of the most common methods of preparing phytoplankton for microscopic counting and is widely used in plankton research programmes (Paerl, 1978; Andersen & Throndsen, 2003). One of the main advantages of this method is the possibility to count with greater accuracy algae that occur at low concentrations. The preparation time ranges from 2 to 24 hours (Andersen & Throndsen, 2003) or even longer depending on the sedimentation time required for the sample volume used.

Considering that the harmful concentration of a HAB organism is species-specific and that some algae are harmful even at low concentrations (Andersen & Throndsen, 2003) it can be questioned if the sensitivity of the phytoplankton quantification method in use in the Portuguese toxic algae monitoring programme is sufficient to detect these toxic organisms at small concentrations.

It was, thus, considered pertinent to compare the accuracy of the results between the two counting techniques (Monitoring and Utermöhl) in order to determine the most suitable method of phytoplankton counting to the Portuguese HABs monitoring programme. This evaluation was achieved by comparing the results of abundance estimations of *Dinophysis* cf. *acuminata* and *D. acuta* obtained with both methods with diarrhetic toxins concentration (okadaic acid, dinophysistoxin-2) and pectenotoxin-2 measured in plankton extracts. The samples were collected at the station Marégrafo (at the mouth of Ria de Aveiro; Figure 1.2).

2. Methods

Surface water samples were collected weekly from Marégrafo from June to November 2004.

2.1. Toxic phytoplankton

From the initial field sample two sub-samples of 250 ml each were collected and immediately preserved with different fixatives, for identification and counting of phytoplankton cells. One was preserved with 10 ml of acidified formaldehyde solution (Throndsen, 1978) and employed in the estimation of phytoplankton cells abundance via the Monitoring technique, while the other was preserved with 30 ml of neutral formaldehyde solution (Throndsen, 1978) and used to estimate phytoplankton cells abundance through the Utermöhl counting technique.

Only the counts of *Dinophysis* cf. *acuminata* and *D. acuta* were used in this comparative study because of the relative high frequency of occurrence of DSP events in Ria de Aveiro lagoon, which are recurrent every year (Palma *et al.*, 1998; Moita *et al.*, 2005) and are related to the presence of the above mentioned *Dinophysis* species (Sampayo *et al.*, 1990).

2.2.1. Monitoring technique

With the Monitoring counting technique, estimation of number of phytoplankton cells per litre was made in two stages. In a first approach a 40 ml sub-sample was concentrated by a factor of 20 by centrifugation (3500 r.p.m., 20 min). The count was performed in a Palmer & Maloney counting chamber using a 0.1 ml aliquot. The conversion factor for number of cells per litre was of 500. The remaining 210 ml of the original sample was then concentrated by a factor of approximately 100 by 4 successive centrifugations (3500 r.p.m., 20 min). The count was also carried out on a 0.1 ml aliquot in a Palmer & Maloney counting chamber. The conversion factor for number of cells per litre was of 100. Counts were carried out with a 200x magnification (objective LD Plan-Neofluar 20x/0.5) in phase contrast using a Zeiss Axioskop 2 *Plus* light microscope and the final result was the arithmetic average of the two counts.

The lower estimated abundance obtainable by this method was 50 cells·L⁻¹.

2.2.2. Utermöhl technique

Phytoplankton cells counts using the Utermöhl technique were performed on a 25 ml sub-sample, which was sedimented in an Utermöhl chamber over a 1 day period (3 hours per centimetre of the liquid column) (Hasle, 1978) or longer. After sedimentation, it was considered that the entire sample volume had settled in the total chamber area, on which counts were performed with a 200x magnification (objective LD Plan-Neofluar 20x/0.5) in phase contrast with a Zeiss Axiovert 2000 inverted light microscope. Estimation of phytoplankton cells number per litre was obtained by the following equation (Equation 1):

$$Cells / L = \frac{N^{\circ} \text{ cellscounted}}{\text{vol.counted}} * 1000ml \quad (\text{Equation 1})$$

where *Cells/L* is the estimated number of cells present in one water litre; *N^o cellscounted* is the number of cells counted; *Vol.counted* is the sample volume under which counting was performed.

The lower estimated abundance obtainable by this method was 40 cells·L⁻¹.

2.2. Diarrhetic toxins concentration

From the initial field surface water sample, two-litre water samples were collected for chemical quantification of okadaic acid (OA), dinophysistoxin-2 (DTX2) and pectenotoxin-2 (PTX2) concentration.

The samples were filtered onto 10 µm nylon membranes, and frozen immediately until extraction. After thawing, toxins were extracted with aqueous 80% methanol, sonicated and left 2 hours at room temperature for spontaneous hydrolysis of esters present in the plankton. The supernatant was washed with hexane and partitioned into dichloromethane. The dichloromethane fraction was analysed on a liquid chromatograph coupled to a mass-spectrometer (LC-MS) as described in detail in Vale (2004).

2.3. Data analysis

The available data was subjected to a graphical analysis. *Dinophysis* cf. *acuminata* abundance was compared only with OA concentration because several studies have already demonstrated that this species only originates shellfish contamination with this type of DSP toxin; the periods of contamination are also of inferior toxicity (Vale & Sampayo, 2000). *Dinophysis acuta* abundance was compared with OA, DTX2 and PTX2 (Vale & Sampayo, 2000).

The 95% confidence limits of the counts of *Dinophysis acuta* obtained by the Utermöhl method were calculated according to the Poisson distribution, under the assumption that the cells are randomly distributed in the sample, by the following equation (Equation 2) (Andersen & Throndsen, 2003):

$$= \pm \frac{200\%}{\sqrt{n}} \quad \text{Equation 2}$$

where n is the number of cells actually counted (Andersen & Throndsen, 2003). This equation gives the relative limits of expectations of confidence of a given count. To obtain the absolute limit of expectation of confidence it was used Equation 3:

$$= \pm \frac{200\%}{\sqrt{n}} * \left(\frac{\text{cellconcentration}}{100\%} \right) \quad (\text{cells}\cdot\text{L}^{-1}) \quad \text{Equation 3}$$

To test for the significance of the association between the abundances of *Dinophysis* spp. estimated by both methods and the toxins concentration in plankton extracts, a rank correlation (Kendall's correlation – τ) was calculated (Equation 4). The choice of this correlation was due to the fact that it is not possible to prove that the available data follows a normal distribution and that such situation would be very improbable due to the abundance of zero values (Sokal & Rohlf, 1969; Clarke & Warwick, 1994).

$$\tau = \frac{N}{n(n-1)} \quad (\text{Equation 4})$$

where n is the conventional sample size and N is a count of ranks; it measures how well a variable corresponds to the order of the other:

$$N = 4 \sum_{i=1}^n C_i - n(n-1) \quad (\text{Equation 5})$$

To test the significance of the obtained correlations when $n \leq 40$ and under the null hypothesis of $\tau = 0$, a table with the critical values of Kendall's rank correlation coefficient should be consulted according to the number of samples (Sokal & Rohlf, 1969).

3. Results

During the study period *Dinophysis* cf. *acuminata* occurred in the water column from late spring to the beginning of summer (from June to August) whereas *D. acuta* occurred predominantly in summer and autumn (from August to November) (Figures 2.1 and 2.2).

Results obtained with the Monitoring technique (Figure 2.1) show that *Dinophysis* cf. *acuminata* attained its maximum level of abundance (1250 cells·L⁻¹) on 27 July, presenting a second abundance peak on 14 June of 1150 cells L⁻¹. *Dinophysis acuta* presented its abundance maximum on 18 October (4250 cells·L⁻¹) and on 27 July (4050 cells·L⁻¹).

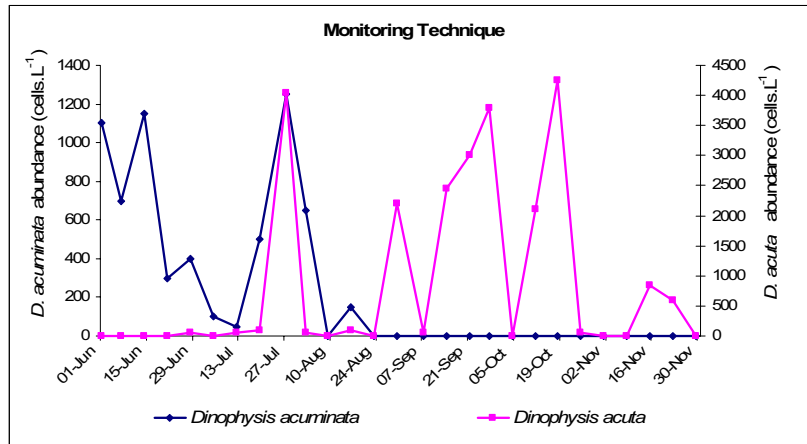


Figure 2.1. Time distributions of *Dinophysis* cf. *acuminata* and *D. acuta* obtained by the Monitoring technique.

These abundance values differ markedly from the ones obtained by the Utermöhl technique (Figure 2.2), in spite of the similarity encountered between the periods of occurrence of the toxic microalgae in question. *Dinophysis* cf. *acuminata* attained its maximum abundance on 01 June (1080 cells·L⁻¹) while *D. acuta* was present in the water column in greater numbers (2560 cells·L⁻¹) on 30 August.

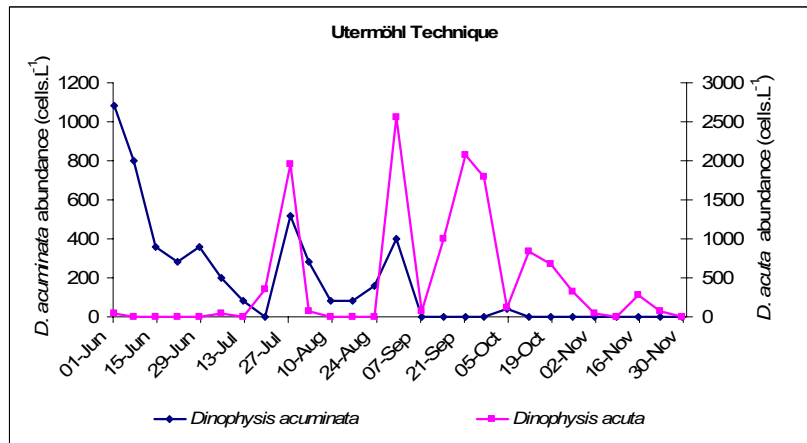


Figure 2.2. Time distributions of *Dinophysis* cf. *acuminata* and *D. acuta* obtained by the Utermöhl technique.

These results show different estimations of toxic microalgae abundance depending on the counting technique applied.

Figure 2.3 and 2.4 compare *Dinophysis* cf. *acuminata* and *D. acuta* quantifications obtained with the two microscopic counting techniques in question.

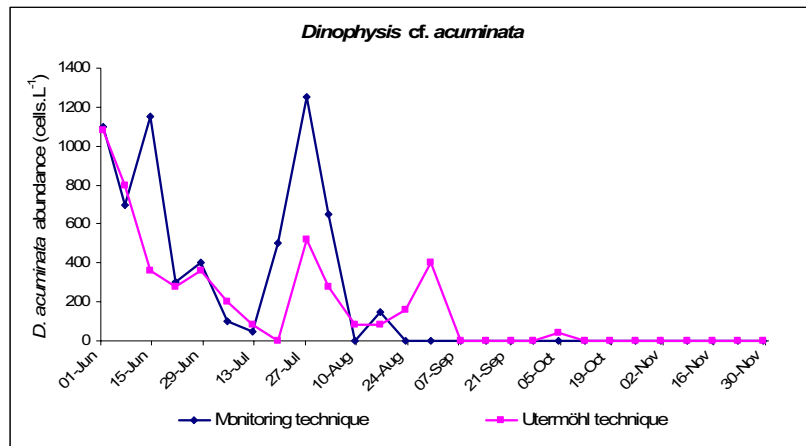


Figure 2.3. *Dinophysis cf. acuminata* abundance estimation by both counting techniques: Monitoring and Utermöhl.

Both methods registered the occurrence of the *Dinophysis* species in the same period but, generally, the abundance estimations obtained with the Monitoring technique tended to be higher than the ones estimated by the Utermöhl technique. However, exceptions occur, e.g, on 30 August (Figure 2.4) where the *Dinophysis acuta* abundance level estimated by the Utermöhl technique was higher than the estimated abundance via the Monitoring method (2560 cells.L⁻¹ and 2200 cells.L⁻¹, respectively).

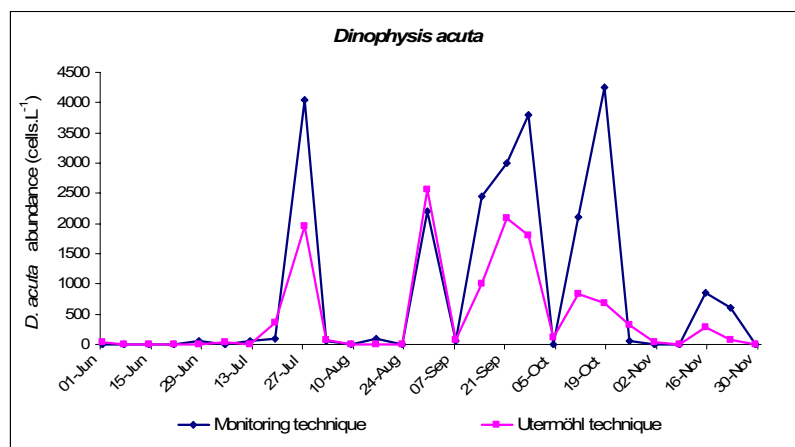


Figure 2.4. *Dinophysis acuta* abundance estimation by both counting techniques: Monitoring and Utermöhl.

Similarly in the same date (30 August) *Dinophysis cf. acuminata* was not registered by the Monitoring method while using Utermöhl method a 400 cells.L⁻¹ concentration was obtained (Figure 2.3). Identical situation occurred on 4 November, when by the Monitoring method, no *Dinophysis* species occurrence was registered, whereas by the Utermöhl

method *D. cf. acuminata* presented 40 cells·L⁻¹ abundance (Figure 2.3), and *D. acuta* occurred with 120 cells·L⁻¹ abundance (Figure 2.4).

In order to test the significance of the differences observed between the estimations of the abundance of *Dinophysis* spp. obtained with both methods, a calculation of the 95% confidence limits, accordingly to the Poisson distribution, for the results obtained by the Utermöhl technique was performed, under the assumption that the cells are randomly distributed in the sample (Andersen & Throndsen, 2003). The calculation of the same confidence limits for the counts obtained by the Monitoring method was not straightforward due to the sub-sampling procedure and phased counts that the method involves. Therefore, Table 2.1 only shows the 95% confidence limits for the counts of *Dinophysis acuta* obtained by the Utermöhl method.

Table 2.1. 95% confidence limits of the counts of *Dinophysis acuta* obtained by the Utermöhl method, according to the Poisson distribution.

Date	Monitoring (cells·L ⁻¹)	Utermöhl (cells·L ⁻¹)	95% Confidence limits (±)
31/05/04	0	40	80
07/06/04	0	0	0
14/06/04	0	0	0
21/06/04	0	0	0
28/06/04	50	0	0
05/07/04	0	40	80
12/07/04	50	0	0
19/07/04	100	360	240
27/07/04	4050	1960	561
02/08/04	50	80	113
09/08/04	0	0	0
16/08/04	100	0	0
23/08/04	0	0	0
30/08/04	2200	2560	640
07/09/04	50	80	113
14/09/04	2450	1000	400
21/09/04	3000	2080	578
27/09/04	3800	1800	537
04/10/04	0	120	141
11/10/04	2100	840	367
18/10/04	4250	680	331
25/10/04	50	320	227
01/11/04	0	40	80
08/11/04	0	0	0
15/11/04	850	280	212
22/11/04	600	80	113
29/11/04	0	0	0

The results show that for most of the sampling dates the abundance data obtained with the Monitoring method is out of the confidence interval of the results provided by the Utermöhl method; when they are included in this confidence interval usually they are higher than the result obtained by the Utermöhl technique and situated within the maximum limit. These results suggest again a trend of the Monitoring technique to overestimate the abundance of the phytoplankton cells.

Figures 2.5 and 2.6 illustrate the results obtained by the comparison between *Dinophysis cf. acuminata* and *D. acuta* abundances with okadaic acid (OA) concentration measured from plankton extracts.

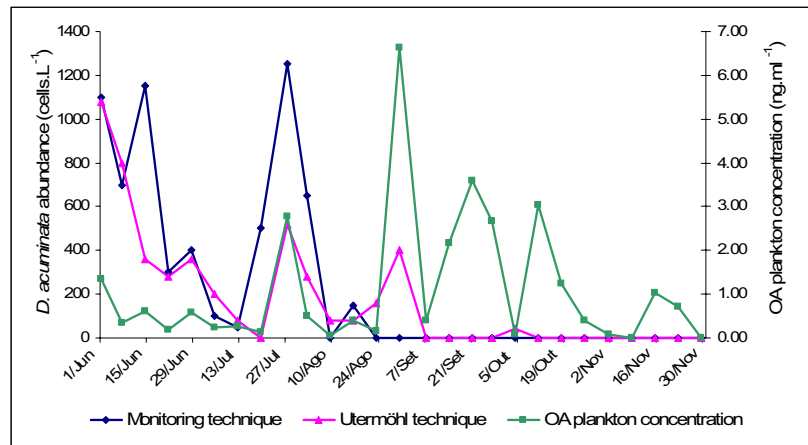


Figure 2.5. *Dinophysis cf. acuminata* abundance estimation using both counting techniques compared with OA concentration in plankton extracts.

For the period comprised between 01 June and 24 August (Figure 2.5), during which *Dinophysis cf. acuminata* occurred in the water column, the results obtained with the Utermöhl technique are more concurrent with the OA toxicity level found in plankton extracts than with the abundance results obtained by the Monitoring method.

Higher OA toxicity levels were found after this period, when *Dinophysis acuta* was the dominant toxic species present in the water column (Figure 2.6). In this case, plankton extracts presented not only OA, but also DTX2 and PTX2 (Figure 2.6, 2.7 and 2.8), which is in agreement with the observations of Vale & Sampayo (2000) and Vale (2004).

Here again, better correspondence was achieved between the Utermöhl *Dinophysis acuta* abundance estimates and OA concentration in plankton extracts than with estimates obtained by the Monitoring technique (Figure 2.6).

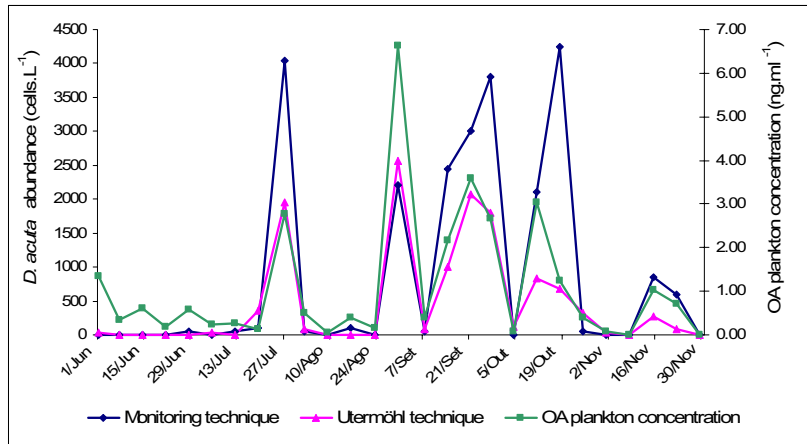


Figure 2.6. *Dinophysis acuta* abundance estimation using both counting techniques compared with OA concentration in plankton extracts.

To test the significance of the association between the variation of *Dinophysis* spp. abundances estimated by both methods and the OA concentration in plankton extracts, the Kendall's rank correlation was calculated. It was obtained a value of $\tau = 0.7$ between the sum of the abundances of *Dinophysis* cf. *acuminata* and *D. acuta* obtained with the Utermöhl method and OA concentration in plankton extracts. With the data obtained by the Monitoring technique it was obtained the same value of τ (0.7). Under the null hypothesis (H_0) of $\tau = 0$, these values of τ are different from zero and H_0 can be rejected to a level of significance >0.01 ; hence both techniques present good positive correlation with the level of toxins found in plankton extracts.

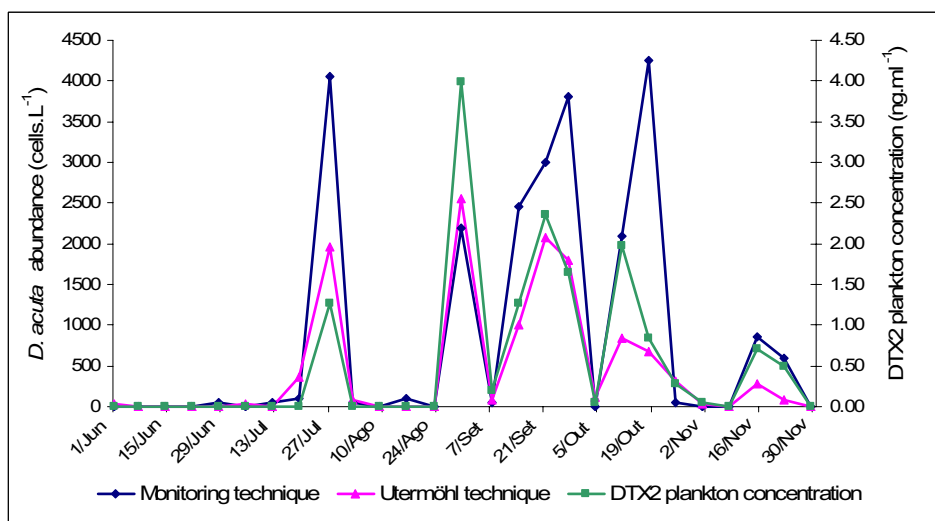


Figure 2.7. *Dinophysis acuta* abundance estimation using both counting techniques compared with DTX2 concentration in plankton extracts.

When *Dinophysis acuta* abundances are compared with DTX2 concentration (Figure 2.7) again, better correspondence is observed between the Utermöhl *Dinophysis acuta* abundance estimates and DTX2 concentration in plankton extracts. In this case, the correspondent value of τ obtained between DTX2 concentration and the Utermöhl abundance estimates is 0.4 whereas with the Monitoring technique is 0.3. Both τ values are very significant ($p > 0.01$).

Dinophysis acuta's production of pectenotoxin-2 (see FAO, 2004) was also compared with the cellular abundance (Figure 2.8).

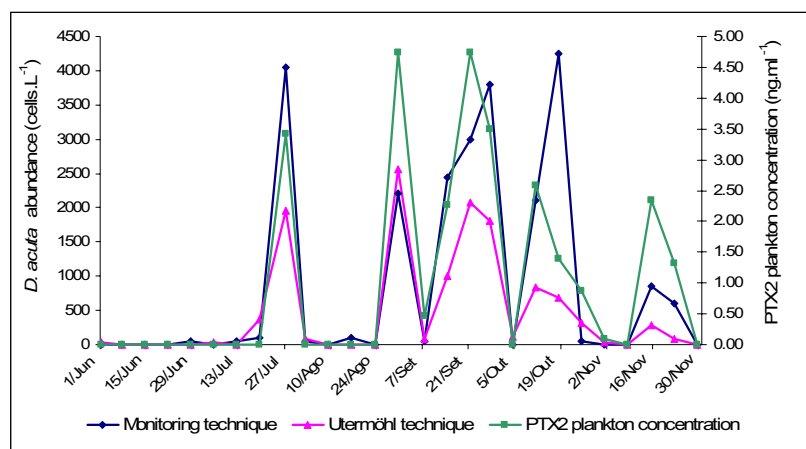


Figure 2.8. *Dinophysis acuta* abundance estimation using both counting techniques compared with PTX2 concentration in plankton extracts.

Once more, better parallelism between the abundance variation of *Dinophysis acuta* obtained with the Utermöhl technique and the concentration of PTX2 was observed. Also, the τ correlation obtained with the *Dinophysis acuta* quantification by Utermöhl method ($\tau = 0.3$) is higher than the τ correlation obtained with the data provided by the Monitoring method: 0.2. Both values are considered significant ($p > 0.1$).

Although both counting techniques revealed the occurrence of *Dinophysis cf. acuminata* and *D. acuta* in the water column whenever diarrhetic toxins were detected in plankton extracts, the graphics shown suggest better connection between *Dinophysis* spp. abundance estimation based on the Utermöhl method and diarrhetic toxin concentration in plankton extracts. However, the rank correlations calculated show that both techniques provide results significantly positively correlated with the toxins concentration in plankton extracts.

Better positive correlation between the data provided by the Utermöhl method and toxin level was found for the concentrations of DTX2 and PTX2.

4. Discussion and Conclusions

It is important to emphasize that any method of phytoplankton microscopic quantification involves a great deal of errors with respect to specimens identification. These errors will, consequently, influence the accuracy of the final abundance values obtained. Many phytoplankton organisms cannot be determined to species level (or even to genus) due to the position that they acquire in the slide during preparation of the sample. Frequently they settle in a position that prevents their correct identification or in confuse aggregates that render impossible the task of distinguishing one species from another (Hasle, 1978; Estrada, 1982). Moreover, the type of fixative used in the preservation of the sample also influences the quality of the organism's identification, due to the qualitative selectivity of such solutions, which normally better preserve certain group of organisms in detriment of others (Thronsen, 1978).

Bearing in mind these kinds of imprecision, which are common to both phytoplankton quantification methods in discussion, the differences observed in the graphical analysis of the accuracy of the results obtained by both techniques have to be explained by other reasons.

Both counting methods succeed in detecting the presence of toxic microalgae in the water column and their periods of occurrence were coherent with the presence of diarrhetic toxins found in plankton extracts. When *Dinophysis* cf. *acuminata* was the dominant toxic algae present in the water, the diarrhetic toxin found in the plankton extracts was okadaic acid, whereas when *D. acuta* was the dominant species other diarrhetic toxins were present, such as DTX2 and PTX2. These results are concomitant with studies performed by Vale & Sampayo (2000). However, the results suggest better concomitance between the level of DSP toxins and *Dinophysis* spp. abundance peaks estimated with the Utermöhl technique, in spite of the positive and significative correlations obtained between the toxin levels and toxic microalgae concentration estimated by both methods. The correlations obtained between DTX2 and PTX2 concentration and *Dinophysis acuta* concentration were higher for the data estimated by the Uthermöhl method than by the Monitoring

technique. These results suggest a higher accuracy of the Utermöhl method in estimating *Dinophysis* spp. concentrations.

From a general point a view, the Monitoring method tends to overestimate phytoplankton cell abundances when the microalgae are present in the water column above a certain threshold concentration, and underestimates it when microalgae occur at lower concentrations. This statement is supported by the results shown in Figures 2.3 and 2.4 where, at least for two occasions, Utermöhl technique detected *Dinophysis* cf. *acuminata* and *D. acuta* at low concentrations, but the Monitoring technique failed to register these species when they were rare. These results agree with the known fact that the sensitivity of the Utermöhl method is higher than the sensitivity of any method that uses counting chambers such as Palmer & Maloney chambers, as is the case of the Monitoring method (Andersen & Thronsen, 2003). Regarding species which are harmful even at low concentrations, this technique may not succeed in providing a reliable prediction of the toxicity events initiation. Moreover, if research programmes are in course, the overestimation of phytoplankton cells that are present in the water at considerable concentrations, can introduce errors when, for example, the study aims are to compare the toxic microalgae concentration with the toxin level found in bivalve shellfish. On the other hand, in three occasions, namely 28 June, 12 July and 16 August, *Dinophysis acuta* was registered in the water column by the Monitoring technique and not by the Utermöhl method. Due to the small abundances recorded, these situations are probably the result of the count of one or two cells in the second count of the Monitoring method, number that is not very significantive (Anderson & Thronsen, 2003). The same statement is true for the Utermöhl method; estimations of $40 \text{ cells} \cdot \text{L}^{-1}$ are a result of the counting of a single cell.

There are several possible explanations for the differences observed between toxic microalgae abundance estimated by both counting methods, connected with the sub-sampling design applied in each method.

Between the collection of the initial field sample and the calculation of the final data there are several steps (preservation, sub-sampling, counting, etc) each of which is a potential source of variability. Many of these sources of variability can be avoided with proper care when dealing with the sample. However, the variability introduced by removing a sub-

sample from a larger sample can never be eliminated since there is no way of assuring that a sub-sample is a perfect representation of the sample (Venrick, 1978b).

In routine plankton work, usually the initial field sample is successively sub-sampled two or more times so that the final count is based on a fraction of the initial sample. At each sub-sampling stage a component of variability is introduced into the data (Venrick, 1978b). In the Monitoring technique the number of sub-samples made was higher than in the Utermöhl method. In fact, in the Monitoring technique the sub-sampling procedure had at least 3 levels, since the initial field sample: initial field sample, 250 ml sample, 40 ml/50 ml sample and 0.1 ml aliquot. In the Utermöhl technique sub-sampling occurs only two times: from the initial field sampling, a 250 ml sub-sample is preserved and from this, a 25 ml sub-sample is made and counted.

Another fact that can explain the apparently smaller accuracy of the Monitoring technique is the sub-sample volume subject of microscopic count and the number of organisms counted. This volume is also of considerable importance regarding the significance of the results (Hasle, 1978). A sample is always an estimate of a larger body of information, in this case, the phytoplankton community (Venrick, 1978a). So, the higher the sample volume used the higher will be the significance of the results when extrapolated to the population (Hasle, 1978). In the Monitoring technique, only an aliquot of 0.1 ml of the sub-sample is subject of microscopic counting, while in Utermöhl technique a sub-sample of 25 ml is used. But more important than the sample volume counted is the number of organisms counted; the more cells counted, the more precision gained (Anderson & Throndsen, 2003). The reduced size of the sample volume counted may influence the number of organisms within the counting chamber and hence available for counting.

Besides the ones mentioned above, the Monitoring technique may also be affected by errors connected with the sample concentration technique used: centrifugation. Although the centrifugation procedure allows us to observe a large variety of sub-sample volumes and it is an easy and rapid process, some phytoplankton species may be destroyed or deformed by the centrifugal force applied, resulting in a modest quantitative precision and reproducibility (Hasle, 1978; Jacques, 1979). Moreover, in a procedure involving successive centrifugations with supernatant rejection between them, partial loss of phytoplankton cells cannot always be avoided. The Utermöhl technique has a greater

limitation in the sub-sample volumes that can be sedimented and requires the use of an inverted light microscope; however loss of cells is less likely to occur, because the sample recipient is always the same and the method supernatant rejection is “safer” (Hasle, 1978). Due to the sedimentation time the preparation of samples for microscopic counting by the Utermöhl method can be more time consuming. However it is a standard method with a very good reproducibility (Jacques, 1979).

Concluding, even though the higher preparation time for microscopic counting by Utermöhl technique is a disadvantage, it may be advisable to use this method for toxic microalgae abundance estimations whenever accuracy is of primary importance. Experience with the parallel use of both methods suggests that the application of the Utermöhl method should be maintained at least once a week for the Marégrafo sampling station, which during flood tide is a useful representation of the water entering Ria de Aveiro. The Monitoring technique should probably remain the routine method, since it detects toxic microalgae occurrence in the water column and provides quick results, which are essential to provide rapid alerts of toxicity events that can be harmful to human health.

5. References

- Andersen P, Throndsen J (2003) Estimating cell numbers. In: Hallegraeff GM, Anderson DM & Cembella AD (eds) Manual on harmful marine microalgae (2nd ed). UNESCO Publishing, p 99-128.
- Estrada M (1982) Ciclo anual del fitoplancton en la zona costera frente a Punta Endata (Golfo de Vizcaya). *Inv. Pesq.* 46(3): 469-491.
- FAO (2004) Marine Biotoxins. FAO Food and Nutrition Paper, 80. Food and Agriculture Organization of the United Nations, Rome.
- Franks PJS, Keafer, BA (2003) Sampling techniques and strategies for coastal phytoplankton blooms. In: Hallegraeff GM, Anderson DM & Cembella AD (eds) Manual on harmful marine microalgae (2nd ed). UNESCO Publishing, p 51-75.

- Hasle GR (1978) The inverted-microscope method. In: Sournia A (ed) Phytoplankton manual. UNESCO Publishing, United Kingdom, p 88-96.
- IOC (2005) The IOC harmful algal programme [on-line]. Intergovernmental Oceanographic Commission of UNESCO, Paris, France.[consulted in September 2005] Available from:
<<http://ioc.unesco.org/hab/intro.htm>>
- Jacques G (1979) Méthodes de mesure. In: Jacques G (ed) Phytoplankton – biomasse, production, numération et culture. Université Pierre et Marie Curie, Banyuls-sur-Mer, France.
- Moita MT, Palma AS, Vilarinho MG (2005) Blooms de fitoplâncton na costa Portuguesa. IPIMAR Divulgação, nº31, Lisboa, Portugal.
- Paerl HW (1978) Effectiveness of various counting methods in detecting viable phytoplankton. NZ Journal of Marine and Freshwater Research 12 (1): 67-72.
- Palma AS, Vilarinho, MG, Moita MT (1998) Interannual trends in the longshore variation of *Dinophysis* off The Portuguese coast. In: Harmful Algae Reguera B, Blanco J, Fernández ML, Wyatt T (eds) Xunta de Galicia and Intergovernmental Oceanographic Commission of UNESCO, Paris, p. 124-127.
- Sampayo MA de M, Alvito P, Franca S, Sousa I (1990) *Dinophysis* spp. toxicity and relation to accompanying species. In: Graneli E, Sundstrom B, Edler L, Anderson DM (eds) Toxic Marine Phytoplankton. Elsevier, New York, p. 215-220.
- Smayda TJ (1978) Estimating cell numbers: What to count? In: Sournia A (ed) Phytoplankton manual. UNESCO Publishing, United Kingdom, p 165-166.
- Sokal RR & Rohlf FJ (1969) Introduction to Biostatistics (2ndedn). WH Freeman and Company. New York. p 363.
- Thronsen J (1978) Preservation and storage. In: Sournia A (ed) Phytoplankton manual. UNESCO Publishing, United Kingdom, p 69-74.

Vale P (2004) Differential dynamics of dinophysistoxins and pectenotoxins between blue mussel and common cockle: a phenomenon originating from the complex toxin profile of *Dinophysis acuta*. *Toxicon* 44:123-134. Elsevier.

Vale P, Sampayo, MA (2000) Dinophysistoxin-2: a rare diarrhoeic toxic associated with *Dinophysis acuta*. *Toxicon* 38: 1599-1606.

Venrick EL (1978a) Sampling strategies. In: Sournia A (ed) *Phytoplankton manual*. UNESCO Publishing, United Kingdom, p 8-16.

Venrick EL (1978b) The implications of subsampling. In: Sournia A (ed) *Phytoplankton manual*. UNESCO Publishing, United Kingdom, p 75-87.

Chapter III

Phytoplankton biomass and species succession during an annual cycle at Ria de Aveiro

Abstract

A study of the seasonal annual cycle of phytoplankton biomass and assemblages succession in the coastal area of Aveiro is presented. Using a high frequency sampling strategy, performed at the entrance of Ria de Aveiro, it was possible to characterize the pattern of succession of phytoplankton species and correlate it with the environmental conditions. Four distinct periods were identified and in each a different phytoplankton assemblage was recognized (spring, summer, autumn and winter). A seasonal phytoplankton succession cycle typical of temperate zones was observed, despite some differences found with respect to the theoretical model of succession. The typical decrease of phytoplanktonic biomass during summer did not occur and the dinoflagellates did not become dominant in the summer community, probably as a result of the persistency of upwelling events. The phytoplankton development was limited by the concentration of nutrients during the warmer seasons (mainly by phosphorus) and by irradiance during winter. The high frequency sampling allowed the identification of phytoplankton succession cycles associated with processes of upwelling and upwelling relaxation. Small phytoflagellates were registered in high abundances as well as the dinoflagellate *Prorocentrum* cf. *minimum*, a producer of phycotoxins. The characteristic communities of upwelled waters and higher water mixture, and of water column stratification were identified as well as the accompanying communities of *Dinophysis* cf. *acuminata* and *Dinophysis acuta*.

1. Introduction

In the basis of the extremely complex food chains present in marine coastal ecosystems (Barnes & Hedges, 1986) there is a group of organisms, called primary producers, which are able to fix inorganic carbon into organic compounds using external sources of energy, such as light or inorganic compounds. Examples are pelagic phytoplankton, benthic micro- and macroalgae, higher plants, like seagrasses and mangroves, and bacteria (Nybakken, 1988; Valiela, 1995). Despite the variety of primary producers, pelagic phytoplankton constitutes the most important group, contributing about 95% to total marine primary production³ (Zeitzschel, 1978; Nybakken, 1988; Valiela, 1995).

The term phytoplankton refers to the large group of planktonic plants that live in surface waters, passively drifting along with water movements due to their reduced mobility capacity (Zeitzschel, 1978; Nybakken, 1988; Harris, 1986; Valiela, 1995). Phytoplankton organisms are unicellular (exceptionally multicellular) microscopic algae, which can either be solitary or colonial (Zeitzschel, 1978; Harris, 1986). Phytoplankton organisms are photosynthetic, i.e. they use the energy of sunlight (captured by photosynthetic pigments such as chlorophylls and carotenoids) to synthesize the energy-rich organic molecules (Zeitzschel, 1978; Nybakken, 1988; Valiela, 1995). Because they are able to produce their own food they are also called autotrophs and constitute the basic food for all consumers (zooplankton, molluscs and fish) (Zeitzschel, 1978; Nybakken, 1988; Valiela, 1995; Hallegraeff, 2003; FAO, 2004). However, other phytoplankton organisms can be mixotrophic or heterotrophic, i.e. they build up organic particulate matter from dissolved organic substances (osmotrophy) or even particulate organic matter (phagotrophy) (Zeitzschel, 1978).

The main taxa of microscopically visible planktonic producers that are found over most of the world's oceans are diatoms (Bacillariophyceae), dinoflagellates (Dinophyceae), coccolithophorids (Prymnesiophyceae), silicoflagellates and other flagellates (Dictyochophyceae, Euglenophyceae, Prasinophyceae), and blue-green algae (Cyanophyceae) (Zeitzschel, 1978; Nybakken, 1988; Valiela, 1995).

³ Primary production is the rate of formation of energy-rich organic compounds from inorganic materials. (Nybakken, 1988).

Phytoplankton organisms can also be classified by size in nanoplankton, cells $<20\ \mu\text{m}$, such as many diatoms, coccolithophorids and silicoflagellates, and microplankton, cells ranging from 20 to $200\ \mu\text{m}$ in size, with diatoms and dinoflagellates being the most common organisms in this size class (Zeitzschel, 1978; Nybakken, 1988; Valiela, 1995).

The phytoplankton groups and the different species that compose them present diverse morpho- and physiological features which allow them to adapt to different environmental conditions. The composition of phytoplankton community in a given area is, therefore, extremely variable, due to a great number of environmental parameters whose possible combinations are almost infinite (Margalef, 1978a). The rate of primary production of a parcel of a marine environment depends thus on the chemical and physical conditions of that parcel, such as light intensity, temperature, nutrient supply and physics of water masses (Margalef, 1978b; Harris, 1986; Nybakken, 1988; Valiela, 1995).

All these major factors affecting primary production change in large spatial and temporal scales (Margalef, 1978a). In temperate seas they change seasonally and thus phytoplankton total biomass also varies over the year (Nybakken, 1988; Valiela, 1995). In these areas the production pattern presents a major peak in spring, a smaller peak in autumn and low productivity in winter and summer (Nybakken, 1988). This pattern is mainly due to changes in the stratification of water column surface layers and nutrient supply (Harris, 1986) that occurs in temperate latitudes.

During winter the nutrients regenerated by mineralization are resuspended from the bottom and accumulate at the water surface. They will not be depleted by algal uptake because the light intensity (necessary for photosynthesis) is low and the depth at which water is mixed by wind action exceeds the critical depth⁴, so algae are often too deep for photosynthesis to be very active (Nybakken, 1988; Valiela, 1995).

In early spring, the increasing light intensity decreases the depth of the critical depth. The depth of mixing decreases as wind strength decreases and there is warming of near-surface water that increases thermal stratification. A seasonal thermocline⁵ establishes between the warmer, less dense, surface water and the deeper, colder, and hence denser, water. High

⁴ Critical depth is the depth at which photosynthesis for the water column equals respiration for the water column. If critical depth is less than the depth to which surface waters are mixed, no net production in the water column takes place. If it is greater than the depth of mixing, net production takes place in the water column and phytoplankton growth occurs (Valiela, 1995).

availability of light and nutrients allows high phytoplankton growth and the spring bloom develops. At some point, nutrients of the surface layer will become depleted by algal uptake, and phytoplankton growth will diminish. This depletion of nutrients in surface waters may persist through summer if the thermally stratified water column, that prevents the vertical mixing of deeper and nutrient-rich water with surface nutrient-poor water, persists. There may be intermittent periods of mixing that give rise to short bursts of algal production during summer, but generally primary production is low in this season (Nybakken, 1988; Valiela, 1995).

In the autumn, with cooling temperatures and increased meteorological disturbances, mixing occurs and nutrient concentration in surface water increases. Even though light intensity is reduced, there may still be enough for phytoplankton growth. The second annual peak of primary production then occurs. Soon, however, light levels become low and the mixed layer deepens due to breakdown of stratification of the water, and the seasonal cycle of production ends, with nutrients accumulating once again in the surface layers (Nybakken, 1988; Valiela, 1995).

In addition to the marked changes in abundance observed in the phytoplankton over the course of a year, there is also a marked change in species composition of the phytoplankton community. This change in the dominant species from season to season is called seasonal succession. Under seasonal succession, one or more species of diatoms, dinoflagellates or coccolithophorids dominate the plankton for a shorter or longer period and then are replaced by another set of species (Nybakken, 1988; Valiela, 1995).

In general, the succession progresses in several steps. From initial phases where strong vertical mixing favours the dominance of chain-forming diatoms, to mature phases where water column stratification favours the strategy of dinoflagellates and other flagellates that can swim to zones rich in light and nutrients (Margalef, 1978b; Nybakken, 1988; Valiela, 1995).

However, in areas where oceanographic processes, such as coastal upwelling, are frequent, as it is the case of the Iberian Peninsula Atlantic coast, the upwelling of cold and nutrient-rich waters to surface layers of the water column (in response to northerly winds) radically

⁵ Thermocline: area with high gradient of temperature (Valiela, 1995).

changes the seasonal pattern of stratification, keeping the phytoplankton community of these areas in the initial stages of succession (Margalef, 1978a).

In the western Portuguese coast Moita (2001) has described a phytoplankton community associated with upwelling events mainly composed by diatoms, many of them chain-forming, like *Chaetoceros* spp., *Guinardia striata*, *Pseudo-nitzschia* spp., *Leptocylindrus danicus*, *Eucampia zodiacus*, *Hemiaulus sinensis*, *Thalassiosira* spp., *Lauderia annulata*, *Detonula pumila* and *Thalassionema nitzschioides*. Also the benthic species *Cylindrotheca closterium* is registered in this community, probably due to the higher sediment movement, which brings these organisms to surface waters (Calado, pers. com.).

Moita (2001) also describes for the coastal Portuguese waters, in periods of greater vertical mixing of the water column (winter), a phytoplankton community characterized by the presence of *Paralia sulcata*, *Thalassiothrix* spp., *Thalassiosira eccentrica*, *Navicula* spp., *Odontella mobiliensis*, *Pleurosigma* spp., *Diploneis* spp., and *Thalassionema nitzschioides*. To this group coccolithophorid species are associated, such as *Emiliana huxleyii* and *Gephyrocapsa oceanica*, especially during periods of less turbulence.

The dinoflagellate group is most abundant under water column stratification conditions. The community composed by the genera *Ceratium*, *Dinophysis*, *Protoperidinium*, *Prorocentrum*, *Gymnodinium*, *Gyrodinium* and by the diatom *Proboscia alata*, is therefore most abundant in summer (Moita, 2001).

Using a high frequency sampling strategy, in Cascais Bay, Palma (2003) has identified short-term succession cycles, related with the process of upwelling and upwelling relaxation events. During these episodes the succession diatom-dinoflagellates is maintained, but a different phytoplankton community which overlays the species of the several stages of seasonal succession, can be registered, during relatively rapid successions of short upwelling pulses.

Regarding the known toxic microalgae species that occur in the Portuguese coast, blooms of *Gymnodinium catenatum* have been associated, since 1985, with PSP events (Hallegraeff, 2003; FAO, 2004; IOC, 2005), especially during summer and autumn seasons (Moita & Silva, 2001). These events are usually connected with episodes of upwelling relaxation and with water column stratification (Moita & Silva, 2001). This chain-forming

dinoflagellate and saxitoxin producer, does not occur every year in the Portuguese coast (Moita & Silva, 2001; Vale, 2004).

Toxic events related to species of *Pseudo-nitzschia* spp. (ASP), producer of the toxin domoic acid (Hallegraeff, 2003; FAO, 2004; IOC, 2005), occur in Portugal generally between spring and autumn (Vale, 2004). Conditions of strong vertical mixture of the water column favour the dominance of diatoms in the phytoplankton community (Margalef, 1978a) also including *Pseudo-nitzschia* species. In the Portuguese coast, this genus belongs to the phytoplankton community characteristic of upwelled waters (Moita, 2001; Moita *et al.*, 2005a).

Diarrhetic shellfish poisoning toxins are usually produced by dinoflagellates that belong to the genus *Dinophysis*; however, the dinoflagellate genus *Prorocentrum* has also been found to be a producer of DSP toxins (Hallegraeff, 2003; FAO, 2004; IOC, 2005). In Portugal, the first confirmed occurrence of diarrhetic toxins associated with *Dinophysis acuminata*, *D. acuta* and *D. fortii* was registered in 1987 (Sampayo *et al.*, 1990). With exception of the year 1993, DSP events were signed every year, especially from late spring to mid autumn (Palma *et al.*, 1998), with Ria de Aveiro being the most affected site (Moita, 1993; Vale *et al.*, 2004; Moita *et al.*, 2005). Most of the *Dinophysis* species are associated with upwelling relaxation events and the highest numbers of cells per litre are found under water column stratification conditions (Palma *et al.*, 1998; Moita *et al.*, 2005). *Dinophysis acuminata* is adapted to minor temperatures and salinities, occurring preferably in spring and summer. *Dinophysis acuta* proliferations present their epicentre between Figueira da Foz and Aveiro coast, being most abundant during hot and dry summers and can be northward transported by currents that establish in the end of the summer (Moita *et al.*, 2005).

The scope of the present work is therefore to study the seasonal annual cycle of phytoplankton biomass and assemblages succession in the coastal area of Aveiro, by means of a high frequency (weekly) sampling strategy, performed at the entrance of Ria de Aveiro, during the tidal flood period. This sampling will also permit to identify and characterize short-term succession cycles associated with upwelling events. Additionally, the temporal pattern of the biomass and species composition of the phytoplankton community will be linked with environmental factors, such as seawater temperature and

salinity, dissolved nutrients and tidal amplitude. Finally, toxic microalgae occurrence will be placed in the annual succession cycle obtained, given particular emphasis to the distribution of *Dinophysis acuminata* and *D. acuta*.

2. Material and Methods

2.1. Sampling procedure

Measures of water temperature (°C) and salinity (Practical Salinity Units - PSU) were obtained using a portable sounding lead WTW-LF 197.

For quantification of dissolved nutrients concentration, 15 ml water samples were collected with a syringe and filtered with Seitz-Filter-Werke membrane filters with 25 mm diameter and 0.45 µm size pore. Samples were stored in plastic bottles previously decontaminated with HCl 10% (0.1 M), involved in aluminium paper and frozen at -18°C.

For estimation of total phytoplankton photosynthetic biomass, 3 surface water replicates of 250 ml each were collected and stored in opaque plastic bottles, kept in the dark. Other 3 replicates of the same volume were also collected in order to estimate photosynthetic biomass in the nanoplankton sample fraction (organisms of size inferior to 20 µm).

The qualitative and quantitative study of phytoplankton community composition was performed via two sampling strategies:

- (1) collection of water samples of living material with a Hydro-Bios plankton net with a 20 µm size pore, destined to a initial and rapid qualitative analysis of phytoplankton community structure, and
- (2) collection of one 250 ml water sample immediately preserved with 30 ml of neutral formaldehyde solution (final concentration of 2.4%), stored in opaque plastic bottles, and used for the quantitative analysis of phytoplankton community species composition.

2.2. Analytical methods

2.2.1. Coastal upwelling

The records of wind direction and intensity were used to calculate an index representative of coastal upwelling conditions, due to the wind forcing action in the seawater surface, of the northwest Portuguese coast. It was used Bakun index (1973), where the N-S component of wind force is calculated accordingly to the drag quadratic law:

$$\tau^{(x,y)} = C_D \rho_A \left| \vec{V} \right| (u, v) \quad (\text{Equation 6})$$

where C_D is the drag coefficient (1.2×10^{-3}); ρ_A is the air density ($1.22 \text{ kg}\cdot\text{m}^{-3}$); $\left| \vec{V} \right|$ is the wind velocity vector ($\text{m}\cdot\text{s}^{-1}$) and (u, v) is the north wind component.

The upwelling index V_E ($\text{m}^3\cdot\text{s}^{-1}\cdot\text{km}^{-1}$), which quantifies the surface current due to Ekman's transport, was calculated from the N-S wind stress component by the following equation:

$$V_E = \tau^{(y)} / \rho_w f \quad (\text{Equation 7})$$

where ρ_w represents the seawater density ($1025 \text{ kg}\cdot\text{m}^{-3}$) and f is the Coriolis parameter ($2\Omega \sin\phi$, where $\Omega = 7.29 \times 10^5 \text{ s}^{-1}$ and $\phi = \text{latitude}$ ($37\ 45'$ N)).

Negative values of this index will correspond to coastal upwelling events.

2.2.2. Dissolved nutrients

Quantification of nitrate plus nitrite ($\text{NO}_3^- + \text{NO}_3^{2-}$), ammonium (NH_4^+), phosphate (PO_4^{3-}) and silicate (SiO_4^{4-}) concentration was made by means of a auto-analyser TRAACS 2000, Analytical Console, BRAN+LUEBBE.

2.2.3. Phytoplankton biomass

Total phytoplankton biomass and nanoplankton biomass was estimated through the quantification of chlorophyll *a* (Chl.*a*) and pheopigments, since these photosynthetic pigments are considered good indicators of such parameter (Zeitzschel, 1978; Moita, 2001).

After the collection, the samples were immediately filtered onto Whatman 0.45 µm cellulose nitrate membrane filters. Three of the 250 ml water samples were additionally filtered previously with a 20 µm pore size net for quantification of chlorophyll *a* and pheopigments associated with the nanoplankton. The resulting membrane filters were stored in centrifuge plastic tubes involved in aluminium paper (in order to avoid pigment photodegradation), frozen and kept at -18°C.

The pigments quantification was carried out by fluorometric analysis, in agreement with the Holm-Hansen *et al.* (1965) method, after pigment extraction with 8 ml of 90% acetone aqueous solution. Fluorescence emission readings were performed in a spectrofluorometer Perkin-Elmer Mod. 204-A, before and after sample acidification with 5% HCl. Chlorophyll *a* concentration was calculated by the equation:

$$Chla = F_d^a \frac{\tau}{\tau - 1} (R_b - R_a) \frac{V}{V} \quad (\text{Equation 8})$$

where *Chla* is chlorophyll *a* concentration (mg·m⁻³); *F_d^a* corrected port factor (mg·m⁻³); *R_b* and *R_a* are the sample fluorescence values before and after acidification, respectively; *τ* is the maximum acidification ratio (*R_b/R_a*) of calibration; *v* acetone solution volume used in the extraction (ml) and *V* filtered sample volume (ml).

The spectrofluorometer was previously calibrated with Sigma chlorophyll *a* pure solutions. A pheophytin *a* solution was also used as a secondary calibration pattern, which allowed the computation of a corrected door factor before any reading was performed (Pissarra & Cavaco, 1984).

2.2.4. Phytoplankton community structure

Samples of living material were immediately observed in an Zeiss Axioskop 2 *plus* light microscope, in order to qualitatively examine the sample, this way establishing which species could be misinterpreted during the quantification, as recommended by Hasle (1978a) and Andersen & Thronsen (2003). For each sample a list of the occurring phytoplankton species was made before the counting procedure.

Total phytoplankton community counts were performed through the Utermöhl technique (Utermöhl, 1958) using a Zeiss Axiovert 135 inverted light microscope, with phase contrast and, in the case of cocolithophorids, bright field microscopy. A 25 ml sample was sedimented and the counting procedure was made as follows:

- (1) greater organisms were counted with a 200x magnification (Zeiss objective Plan-Neofluar 20x/0.5 Ph2) in the entire chamber area;
- (2) smaller organisms were counted with a 400x magnification (Zeiss objective LD A-Plan 40X/0.50 Ph2 infinit/1.0) in selected random optic fields, distributed in the entire chamber area and corresponding to 1 ml of sample;
- (3) species of high abundance were counted with a 200x magnification (Zeiss objective Plan-Neofluar 20x/0.5 Ph2), in one or more chamber transects, until a number equal or superior to 200 organisms was obtained.

The identification of phytoplankton organisms was made, whenever possible, to species level. When this was not possible, organisms were classified in their respective genus or in higher taxonomic groups or even in artificial categories such as phytoflagellates, armoured and unarmoured dinoflagellates and pennate and centric diatoms. As it has been previously referred in Chapter II, it should be regarded that the phytoplankton estimations obtained by any microscope-based method for microalgae quantification may be inaccurate due to the several errors that can be made during the specimens identification. These errors are particularly determined by the position that the organisms acquire after their settlement in the slide and by the qualitative selectivity of the fixative (Hasle, 1978).

The total phytoplankton was considered as the sum of organisms belonging to Bacillariophyceae, Dinophyceae, Prymnesiophyceae, Euglenophyceae, Dictyochophyceae, Prasinophyceae, Chlorophyceae, Chrysophyceae, and Cyanophyceae.

Results obtained from Prymnesiophyceae counts should be regarded with caution, since the methodology applied is not the most suitable for this kind of organisms, underestimating their real abundance. This is partially due to the low magnification used in the counting procedure and to problems of sample preservation with the neutral formaldehyde solution that tends to acidify with time, causing coccolithophorid destruction (Thronsen, 1978; Bollmann *et al.*, 2002)

Identification of unarmoured dinoflagellates and phytoflagellates was difficult since most species tend to be partially destroyed by formaldehyde fixation solutions (Thronsen, 1978).

Each cell of colonial phytoplankton organisms was counted, as in *Leptocylindrus danicus* and *Pseudo-nitzschia* spp.. Exception was made to *Leptocylindrus mediterraneus* that usually lives in symbiosis with *Solenicola* spp., which lives attached to the frustule, hiding the number of cells in the colony. Counts of diatoms with large frustules like *Proboscia alata* and *Rhizosolenia* spp., that sometimes can occupy more than one observation field, were performed by counting the frustule ends, and then dividing the resulting number by two. Dead phytoplankton cells and empty thecae or frustules were not counted.

Counts of *Dinophysis acuta* took into account the existence of several intermediate forms between the vegetative cell (*D. acuta*) and the gamete represented by *Dinophysis dens* morphology (Moita & Sampayo, 1993; Reguera, 2003). Those intermediate forms were designated as *Dinophysis* morpho *acuta* and the gamete as *D. acuta* morpho *D. dens*. However, since these intermediate forms have appeared in small concentrations, their abundance was added to *Dinophysis acuta* abundances, for data analysis purposes.

The several different morphologies that have been connected with the life cycle of *Dinophysis acuminata* (Reguera, 2003) were placed in the same category and designated as *Dinophysis* cf. *acuminata*.

Due to the considerable confusion that exists with regard to the identification of *Prorocentrum minimum* (Heil *et al.* 2005) as a result of its extremely variable cell shape and the presence of a small anterior spine, which is not always recognizable under light microscopy, in the present work a category named *Prorocentrum* cf. *minimum* was used to designate all of the different life forms that have been usually identified as *Prorocentrum minimum*.

In addition, heterotrophic and phagotrophic forms such as *Erythrospidinium* spp., *Gyrodinium spirale*, many *Protooperidinium* and *Noctiluca scintillans* were also included in the counting procedure. Some zooplankton organisms were also enumerated and placed in large categories. The blooming ciliate *Mesodinium rubrum* was also counted.

Estimation of number of phytoplankton cells per litre was obtained with Equation 2 (see Chapter II). The volume of sample subject of counts varied accordingly to the counting procedure and thus the multiplication factor to estimate the number of cells per litre as also varied: for organisms counted in 25 ml the multiplication factor was 40; for organisms counted in 1 ml, the multiplication factor was 1000 and counts performed in one transect were multiplied by 37.42 to obtain the estimation of number of cells per litre.

The lower estimated abundance obtainable by this method for organisms counted with a 200x magnification was 40 cells·L⁻¹ and for organisms counted with a 400x magnification was 1000 cells·L⁻¹.

Phytoplankton species identification and classification was carried out taking into consideration the checklist of phytoplankton species previously described for the coastal Portuguese waters (Moita & Vilarinho, 1999).

The principal monographs used for species identification were: Peragallo & Peragallo (1908) and Hasle & Syvertsen (1996) for diatoms, Heimdal (1996) for coccolithophorids, Throndsen (1996) for phytoflagellates, Steidinger & Tangen (1996), Shiller (1937) and Dodge (1982) for dinoflagellates.

2.3. Data analysis

Biological and environmental data were subjected to a graphical analysis and to a multivariate analysis.

Multispecies distribution patterns and associated environmental variables were analysed following the strategy suggested by Field *et al.* (1982) and Clarke & Warwick (1994), which keeps the analysis of biotic and environmental data completely separate. This strategy avoided the influence of any previous assumptions about relationships between the biota and environment, minimizing the danger of circular argument in seeking to deduce relationships.

The statistical analysis was performed with the computer software package PRIMER (Plymouth Routines in Multivariate Ecological Research) developed at the Plymouth Marine Laboratory, United Kingdom (Clarke & Warwick, 1994). Graphical presentation was made by the use of Golden Software Grapher 3 and Microsoft Office Excel 2003.

2.3.1. Biological data analysis

The abundance values of each phytoplankton category at each sample were organized in an array of p rows (phytoplankton species or other taxa and artificial categories) and n columns (samples).

Total phytoplankton number of cells per litre was obtained by the addition of the abundances of Bacillariophyceae, Dinophyceae, Prymnesiophyceae and Other Classes (Euglenophyceae, Prasinophyceae, Chlorophyceae, Chrysophyceae, Dictyochophyceae and Cyanophyceae). Correlations between the concentration of chlorophyll a and the abundance of total phytoplankton cells was established using the Kendall's rank correlation (Sokal & Rohlf, 1969) previously described in Chapter II (Equations 4-5). Since the number of samples is superior to 40, the test for the significance of the obtained correlation was calculated by using the normal approximation to test the null hypothesis that the true value of $\tau = 0$ (Equation 9):

$$t_s = \frac{\tau}{\sqrt{2(2n+5)/9n(n-1)}} \quad \text{Equation 9}$$

compared with $t_{\alpha}[\infty]$ (Sokal & Rohlf, 1969).

Kendall's correlations were also calculated between the concentration of total phytoplankton and the concentration of Bacillariophyceae, Dinophyceae, Prymnesiophyceae and Other Classes. This nonparametric method was used due to the high improbability of the available data to follow a normal distribution (Sokal & Rohlf, 1969).

From the original data set, three matrices were constructed differing in the taxonomic level of the phytoplankton categories: class, genus and species. This aggregation of the original set of biological descriptors counted was necessary due to the different variability levels

involved in the different categories of phytoplankton. Each data matrix was subjected to the same statistical multivariate analyses procedure.

The class matrix was used to determine the proportions of the most important phytoplankton classes, namely Bacillariophyceae, Dinophyceae and Prymnesiophyceae, on the total phytoplankton community.

Concerning the multivariate study, the original data was first analysed in order to measure the similarity between samples (*q*-type analysis), aiming to describe patterns occurring over time, and then between variables (*r*-type analysis or inverse analysis) with the purpose of determine the most probable assemblages of different phytoplankton species, giving particular emphasis to the toxic species *Dinophysis* cf. *acuminata* and *D. acuta* (Field *et al.*, 1982; Legendre & Legendre, 1984a).

2.3.1.1. Q-type analysis

Testing differences between groups of samples

Groups of samples collected in the same season were considered as replicates of four periods: Spring, Summer, Autumn and Winter (ex.: samples collected in the 12 weeks of the spring season were considered replicates of one sample representative of spring).

Having defined this structure within the set of samples a test for statistically significant differences between groups was performed. Due to the fact that the data array had a higher number of variables than of samples and to the improbability of the distribution of counts be reduced to approximate (multivariate) normality, by any transformation, because of the dominance of zero values, the test of differences between seasons was performed by an analysis of similarities (ANOSIM) rather than by an analysis of variance (ANOVA) (Field *et al.*, 1982; Clarke & Warwick, 1994).

The ANOSIM test is based on a simple non-parametric permutation procedure and it is applied to the data similarity matrix underlying the ordination of samples. It has this designation in analogy with the acronym ANOVA. It has the advantage of making few assumptions about the data and there is also no restriction in the use of a different number of replicates between groups (Clarke & Warwick, 1994).

The similarity analysis is based on a statistic test named R Statistic (Equation 10) (Clarke & Warwick, 1994). The null hypothesis (H_0) taken into consideration in this study was that there are no differences in phytoplankton assemblages composition between seasons.

$$R = \frac{(\bar{r}_b - \bar{r}_w)}{\left(\frac{M}{2}\right)} \quad (\text{Equation 10})$$

where \bar{r}_w is defined as the average of all rank similarities among replicates within seasons; \bar{r}_b is the average of rank similarities arising from all pairs of replicates between different seasons; $M = n(n-1)/2$ and n is the total number of samples under consideration (Clarke & Warwick, 1994).

The R statistic usually falls between 0 and 1, indicating some degree of discrimination between conditions, in this case, seasons. If the R value is approximately zero, H_0 is true, so that similarities between and within seasons will be the same on average; if R is 1 all replicates within seasons are more similar to each other than any replicates from different seasons, and H_0 is rejected (Clarke & Warwick, 1994).

The above is a global test, indicating if there are differences between seasons somewhere that could be worth examining further. This additional exam is made by comparison of specific pairs of seasons (*pairwise tests*). The obtained R value allows the rejection (or not) of H_0 at a certain level of significance (Clarke & Warwick, 1994). In this study, the rejection of H_0 was made when the significance value of differences between seasons was inferior to 5%.

This analysis of similarities (ANOSIM) was performed upon a Bray-Curtis similarity matrix with log-transformed data (Equation 11):

$$Y_{ij} = \log(X_{ij} + 1) \quad (\text{Equation 11})$$

where X_{ij} is the raw data score of the i th species in the j th sample; Y_{ij} is the corresponding transformed score (Clarke & Warwick, 1994). The logarithmic transformation has the

effect of scaling down the scores of abundant species so that they do not swamp the other data (Field *et al.*, 1982; Clarke & Warwick, 1994).

The Bray-Curtis coefficient (Equation 12) was the similarity measure adopted due to the fact that it is not affected by scale changes in the measurements and joint absences, i.e. similarity depends on species which are present in one or other (or both) samples, and not on species which are absent from both. However, it gives more weight to abundant species than to rare ones, which is what most ecologists do intuitively (Field *et al.*, 1982; Clarke & Warwick, 1994).

$$S_{jk} = 100 \left(1 - \frac{\sum_{i=1}^p |Y_{ij} - Y_{ik}|}{\sum_{i=1}^s (Y_{ij} + Y_{ik})} \right) \quad (\text{Equation 12})$$

where Y_{ij} represents the entry in the i th species in the j th sample; Y_{ik} is the entry for i th species in the k th sample; S_{jk} is the similarity between the j th and k th samples summed over all p species (Clarke & Warwick, 1994).

S_{jk} ranges from 0 (no species in common) to 100 (identical species between the samples).

Ordination analysis – non-metric multidimensional scaling (MDS)

An ordination analysis was performed upon the results of the ANOSIM test, by the method of non-metric multidimensional scaling (MDS).

Like other methods of ordination, the MDS produces a map of the samples, usually in two or three dimensions, in which the placement of samples, rather than representing their geographical location, reflects the similarity of their biological communities (Field *et al.*, 1982; Legendre & Legendre, 1984b; Clarke & Warwick, 1994).

Firstly, MDS interprets some function of the similarity measure between each pair of samples as a distance in ordinary Euclidean space. It then seeks the best possible reconciliation (according to some optimality criterion) of these $n(n-1)/2$ inter-station ‘distances’ with the physical distances between n points on a 2 (or higher) dimensional map (Field *et al.*, 1982; Clarke & Warwick, 1994).

The ‘goodness-of-fit’ of this ordination is measured by the stress formula (Equation 13):

$$Stress1 = \frac{\sum_j^n \sum_{k>j}^n (d_{jk} - \hat{d}_{jk})^2}{\sum_j^n \sum_{j>k}^n d_{jk}^2} \quad (\text{Equation 13})$$

where \hat{d}_{jk} is the distance estimated from the regression, corresponding to similarity S_{jk} .

Stress may be thought of as the distortion involved in ‘compressing’ the data to a small number of dimensions. It increases with reducing dimensionality and quantity of data. If stress <0.1 the ordination obtained gives a good representation of the similarities between samples, with no prospect of misinterpretation; if stress <0.2, it still gives a potentially useful 2-dimensional picture. Values superior to 0.2 should be treated with great deal of scepticism (Clarke & Warwick, 1994).

Multi dimensional scaling presents several advantages over other ordination techniques such as principal co-ordinates analysis, reciprocal averaging and correspondence analysis (Field *et al.*, 1982; Clarke & Warwick, 1994). The latter are essentially based on the method of principal components and are relatively inflexible, particularly with regard to the large number of zero counts generally present in a species-samples matrix. By contrast, great flexibility is bestowed on MDS by its less direct approach (Field *et al.*, 1982). Multi dimensional scaling is very simple in concept in spite of the complexity of the numerical algorithm. It is based on the relevant sample information, working on the sample similarity matrix and not on the original data array. Species deletions are unnecessary, since the number of species on which it was based is largely irrelevant to the amount of calculation required. Multi dimensional scaling is generally applicable, i.e. fewer assumptions are made about the nature and quality of the data. Nevertheless, MDS is computationally demanding, convergence to the global minimum of stress is not guaranteed and the algorithm places most weight on the large distances (Field *et al.*, 1982; Clarke & Warwick, 1994).

Indicator species

After the analysis of distribution patterns by ordination, an analysis of the raw data was made in order to extract information about the phytoplankton organisms or categories that caused the pattern. For that the average abundance of each phytoplankton class was

calculated and the relative importance of each class determined in percentage for each season.

Several univariate measures were also applied. This type of community measures collapses the full set of descriptors counts for a sample into a single coefficient (Clarke & Warwick, 1994). The calculated measures were: total number of species (S), total number of individuals (N), species richness (Margalef's index – d – Equation 14), species diversity (Shannon's index – H' – Equation 15) and species evenness (Pielou index – J' – Equation 16). Species richness is usually given by S , which is very dependent on sample size; the Margalef index also incorporates the total number of individuals (N) and it is a measure of the number of species present for a given number of individuals. The J' index expresses how evenly the individuals are distributed among the different species in the samples (Pielou, 1977; Clarke & Warwick, 1994). This concept is the reverse of dominance that occurs when one sample is highly dominated by one species (Clarke & Warwick, 1994). The Shannon species diversity index incorporates both the species richness and evenness components (Clarke & Warwick, 1994). These univariate measures were calculated regarding the following equations, accordingly with Clarke & Warwick (1994):

Margalef species richness index:

$$d = (S - 1) / \log(N) \quad (\text{Equation 14})$$

where S is the total number of species and N is the total number of individuals .

Pielou's evenness index:

$$J' = H' / \log_2 S \quad (\text{Equation 15})$$

where H' is the species diversity index and $\log_2 S$ is the maximum possible diversity which would be achieved if all species were equally abundant.

Shannon-Wiener diversity index:

$$H' = -\sum_i p_i (\log p_i) \quad (\text{Equation 16})$$

where p_i is the proportion of the total count arising from the i th species.

To determine the most abundant species within each season phytoplankton assemblage, cumulative ranked abundances were plotted against species rank in order of decreasing abundance. This approach has been promoted as K-dominance plots. The most elevated curve indicates the most dominated assemblage (Clarke & Warwick, 1994).

2.3.1.2. R-type analysis

The inverse or r -type analysis is an appropriate complement of the sample analysis, since it allows determining different groups of species which are more likely to occur together than separate (Field *et al.* 1982).

A classification analysis was applied upon a Bray-Curtis similarity matrix over standardized data. In this case, two species will be thought of as “similar” if their numbers tend to fluctuate in parallel across samples (Field *et al.*, 1982).

Data standardization was necessary prior to inverse comparison because when quantitative data is used, perfectly correlated species, which always occur together but in different abundances, might be separated from one another by their different scores (Clarke & Warwick, 1994).

Due to the fact that some species occur too seldom to form an analysable pattern (Clarke & Warwick, 1994), those rare species were eliminated prior to classification and ordination analysis. Species selection was made based on the dominance of the species, at any one station, above an arbitrary percentage. In other words, species accounting for $>p\%$ of the total abundance in any one sample were retained (p is chosen to reduce species to the required number). The percentage used in this work was of 2%, resulting in a 48 species and 39 genera array, according to the suggestions of Field *et al.*, (1982).

Classification

A classification analysis was performed upon the species and genera matrixes by the method of hierarchical clustering by group average sorting. This method joins two groups of species together at the average level of similarity between all members of one group and all members of the other (Clarke & Warwick, 1994).

2.3.2. Environmental data multivariate analysis

Having determined statistical differences between phytoplankton assemblages of the different seasons, environmental variables were also explored in order to examine the temporal variability of each variable, possible connection between the variables and potential relationships between the abiotic and biotic data. The probable limiting nutrient for phytoplankton growth for each season was also estimated using the Redfield ratio.

As done in the biota data analysis groups of samples were considered as replicates of the four seasons and a similarity analysis using a 1-way layout ANOSIM test was performed in order to determine if there were significant interpretable differences between the physical/chemical parameters of each season. This analysis of similarities was performed upon a Normalised Euclidian Distance matrix with non-transformed data.

The Euclidian distance is defined as the natural distance between any two points in space. It is defined algebraically as (Clarke & Warwick, 1994):

$$d_{jk} = \sqrt{\sum_{i=1}^p (y_{ij} - y_{ik})^2} \quad \text{Equation 17}$$

Normalised Euclidian distance was used because the variables presented different measurement units (Clarke & Warwick, 1994).

An ordination analysis was performed upon the results of the ANOSIM test, by the method of non-metric multidimensional scaling (MDS), previously described (see pages 47 and 48).

A calculation of the average and standard deviation of each variable for each season was performed.

2.3.3. Linking biota to environmental data

A graphical analysis was used to investigate possible relationships between the biotic and abiotic data, particularly concerning upwelling and its influence over species composition of the phytoplankton community. For that, the temporal variability of the abundances of a set of diatom species known to respond to upwelling events was plotted against the daily

upwelling index: *Chaetoceros* spp., *Pseudo-nitzschia* spp., *Thalassiosira* spp., *Thalassionema nitzschioides* and *Leptocylindrus danicus*.

Each environmental variable was represented by symbols of differing size and these symbols were superimposed on the biotic ordination of the corresponding samples. In this way it was possible to examine the variation of the different environmental variables along with the pattern observed with the biotic ordination.

The match between the biotic (species matrix) and environmental data was made through the Primer sub-routine BIOENV, upon the similarity matrices underlying both biotic and abiotic ordinations. These were chosen differently to match the respective form of the data (Bray-Curtis upon log-transformed data for biotic data and normalised euclidean distance for environmental data). Their ranks were compared through a rank correlation coefficient based on similarity ranks designated as Kendall's rank coefficient (τ) (Sokal & Rohlf, 1969). The arithmetic expression of this coefficient is shown in Chapter II, Equations 4-5.

Combinations of environmental variables were considered at steadily increasing levels of complexity, i.e. k variables at a time ($k = 1, 2, 3, \dots, v$) each one with the corresponding τ value.

The test for the significance of the associations found between the biotic and abiotic data was performed by means of the RELATE sub-routine of the PRIMER software and, again, the Kendall's rank coefficient was used.

3. Results

3.1. Temporal variability of phytoplankton biomass and community structure

A list of the phytoplankton species and other taxa or artificial categories identified and subject to count, in a total of 52 samples collected from 18 May 2004 to 17 May 2005, is presented in attachment (Appendix 1, Table 1).

The percentage of occurrence of the main phytoplankton groups, during the study period, is presented in Figure 3.1.

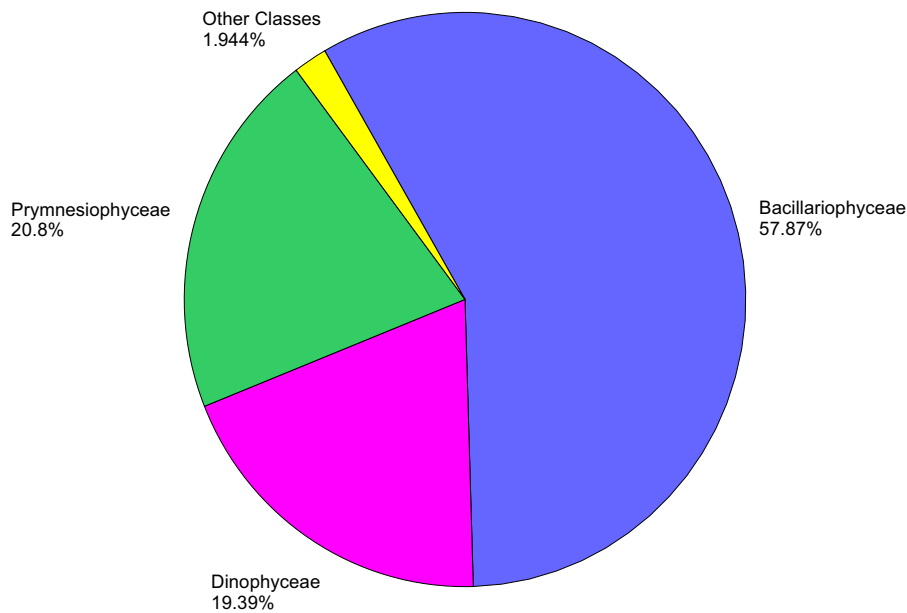


Figure 3.1. Main phytoplankton groups in the total phytoplankton community of Ria de Aveiro, averaged over the entire sampling period.

The most significant group was Bacillariophyceae, contributing with 58% of cell numbers to total phytoplankton community, followed by Pymnesiophyceae (21%) and Dinophyceae (19%). Other classes, including the groups Euglenophyceae, Dictyochophyceae, Chlorophyceae, Chrysophyceae, contributed with 1.9% to total phytoplankton community.

Phytoplankton concentration showed a seasonal variation, both in terms of chlorophyll *a* and number of cells (Figure 3.2). The highest values were observed during spring and summer.

Concentration of total phytoplankton was obtained by the addition of Bacillariophyceae, Dinophyceae, Pymnesiophyceae, Euglenophyceae, Prasinophyceae, Chlorophyceae, Chrysophyceae, Dictyochophyceae and Cyanophyceae abundances.

Chlorophyll *a* (Chl.*a*) concentration varied between $4.72 \mu\text{g}\cdot\text{L}^{-1}$, on 30 August 2004, and $0.22 \mu\text{g}\cdot\text{L}^{-1}$, attained on 17 and 24 January 2005. The highest values of Chl.*a* were observed during the spring and summer. During the autumn, Chl.*a* values decreased to a minimum in winter and increased again during the spring.

The highest chlorophyll *a* values (Figure 3.2a) were observed on 5 July and 30 August and were mainly due to high concentrations of diatoms ($8.6 \times 10^5 \text{ cells}\cdot\text{L}^{-1}$) and $1.6 \times 10^6 \text{ cells}\cdot\text{L}^{-1}$, respectively).

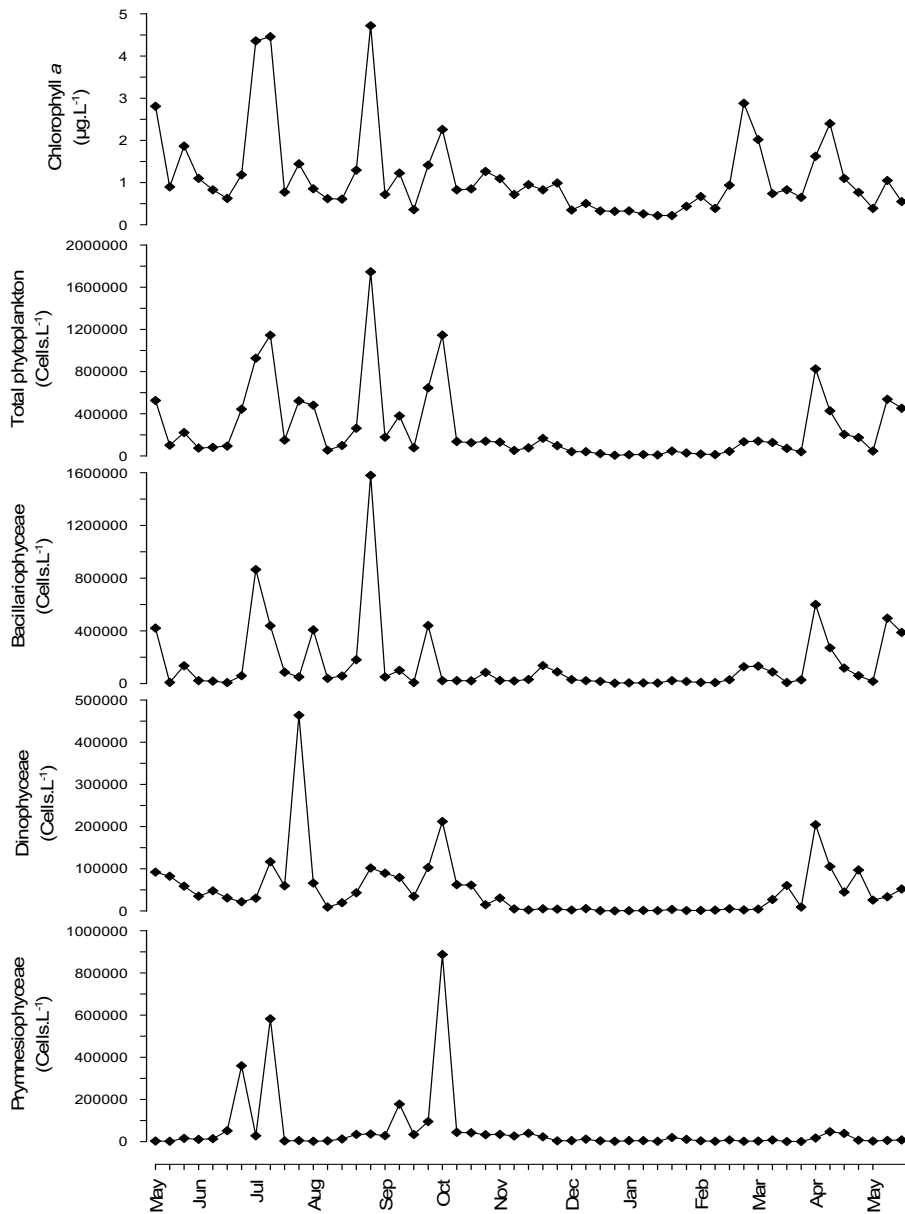


Figure 3.2. Concentration of chlorophyll *a* (a) and phytoplankton cells: b) Total phytoplankton; c) Bacillariophyceae; d) Dinophyceae; e) Prymnesiophyceae.

Total phytoplankton concentrations varied in the range of 1.7×10^5 cells·L⁻¹ (30 August) and 6.8×10^3 cells·L⁻¹ (27 December) (Figure 3.2b). Generally there was a good correspondence between Chl.*a* concentration and total phytoplankton number of cells per litre, except for the period of February 2005, when an elevated biomass concentration was not matched by a high cellular concentration (Figure 3.2a, b). A good correlation was calculated between Chl.*a* concentration and total number of phytoplankton cells by the Kendall's rank coefficient, with $\tau=0.68$. Under the null hypothesis of 'no association

between the two sets of variables', i.e. $\tau=0$, the test for the significance of this correlation was made by using Equation 9 (page 47) and comparing the resulting value with the Student's t distribution ($t_{\alpha}[\infty]$). The obtained t_s value was 7.21, and the minimal significant value of the coefficient at a probability of 0.001 is 3.29, thus the obtained value of τ is very significantly different from zero and there is a strong correlation between the concentration of Chl.*a* and total phytoplankton number of cells per litre.

The distribution pattern of Bacillariophyceae over the study period (Figure 3.2c) was similar to the variation pattern of the total phytoplankton concentration (Figure 3.2b). This was probably due to the higher significance in the phytoplankton community of the diatom group (Figure 3.1 and 3.2b, c). A higher value of Kendall's correlation was obtained between total phytoplankton abundance and total diatom abundance ($\tau=0.68$) than with total abundances of the other groups: dinoflagellates ($\tau=0.61$), other classes ($\tau=0.45$) and coccolithophorids ($\tau=0.35$). All these values of τ are very significantly different from zero and hence H_0 (no association between the two variables) can be rejected at a probability level of 0.001%. Maximum number of diatom cells per litre occurred on 30 August (1.6×10^6 cells·L⁻¹) and the minimum on 27 December, corresponding to 4.4×10^3 cells·L⁻¹. High concentrations of diatoms were observed in July and August.

High concentrations of dinoflagellates (Figure 3.2d) occurred in July, particularly on 27 July when a concentration of 4.6×10^5 cells·L⁻¹ was found. Smaller peaks of abundance occurred on 4 October and 8 April with corresponding values of 2.1×10^5 and 2.0×10^5 cells·L⁻¹. The lowest concentration occurred on 27 December (2.4×10^2 cells·L⁻¹)

Regarding coccolithophorids (Figure 3.2e), their concentration over the year was overall stable, except on three occasions: 28 June 2004, with 3.6×10^5 cells·L⁻¹, 12 July 2004 (5.8×10^5 cells·L⁻¹) and 04 October 2004, when the maximum concentration of coccolithophorids was reached at 8.9×10^5 cells·L⁻¹. The lowest concentration – 1.0×10^3 cells·L⁻¹ – occurred at March 28 2004.

Small phytoflagellates, category that contains species from various taxa, were abundant throughout the study period (Figure 3.3).

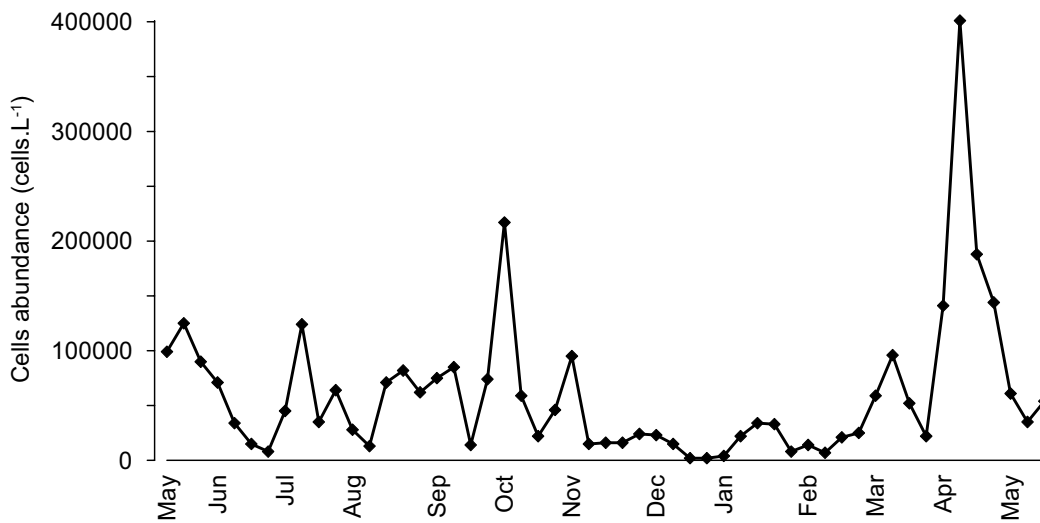


Figure 3.3. Time distribution of the abundance of small phytoplagellates at Ria de Aveiro.

As for the other groups of organisms (Figure 3.2) small phytoplagellates occurred in the water column in smaller concentrations from the end of autumn to winter (from November 2004 to February 2005) (Figure 3.3). The highest concentration (4.0×10^5 cells·L⁻¹) was found on 11 April 2005. In spring, summer and beginning of autumn small phytoplagellates concentration was, most part of the times, higher than 5.0×10^4 cells·L⁻¹.

Figure 3.4 presents the variation of total Chl.*a* concentration and the percentage of Chl.*a* associated with the nanoplankton fraction of the phytoplankton community.

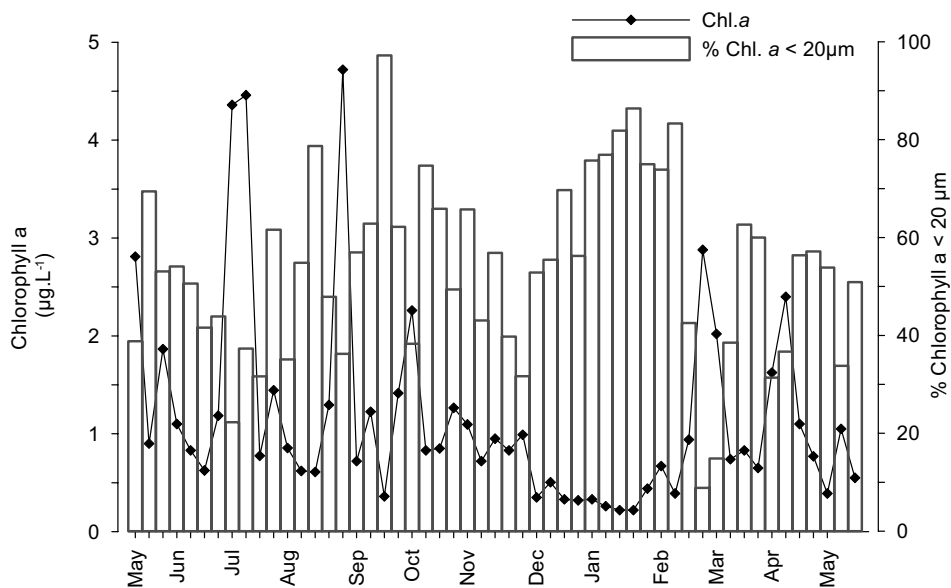


Figure 3.4. Time distribution of Chlorophyll *a* (Chl.*a*) concentration (line) and of the percentage of chlorophyll *a* associated with the nanoplankton fraction (bars).

For the majority of samples, Chl.*a* percentage associated with the nanoplankton was above 40%. The lowest percentage was encountered on 28 February 2005 (8.8%). Despite the fact that maximum percentage of Chl.*a* (97.2%) was observed on 21 September 2004, nanoplankton contributed most to total photosynthetic biomass during winter (December, January and February), with an average percentage of 60%.

The abundance of diatoms was usually high throughout the period of study. An index calculated by dividing the total number of diatoms by the total number of diatoms plus dinoflagellates shows values higher than 0.5 on most occasions. Sporadic periods of dinoflagellate relative dominance occurred more often between May and June 2004 and between September and November of the same year.

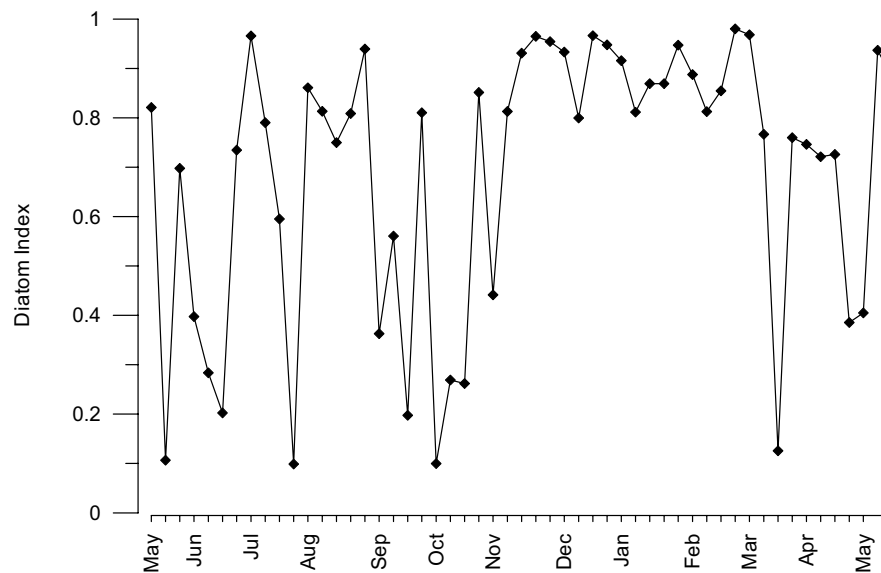


Figure 3.5. Diatom index variation during the period of study.

The graphical analysis (Figure 3.2-3.5) suggests that seasonality is an important source of variation and supports grouping of samples according to season.

To test the statistical significance of the observed seasonal differences it was performed a 1-way layout ANOSIM test, with 999 permutations, upon a Bray-Curtis similarity matrix with log-transformed data, considering that the samples collected were replicates of the four seasons typical of temperate zones: spring, summer, autumn and winter. Thus, samples collected from 18 May 2004 to 14 June 2004 and from 21 March 2005 and 09 May 2005 were assembled in the Spring group; from 21 June 2004 to 14 September 2004,

samples characterized the Summer season; Autumn group included samples collected from 21 September 2004 to 20 December 2004, and Winter group was composed by samples collected from 27 December 2004 to 14 March 2005.

The phytoplankton categories were aggregated in three different ways depending on their taxonomic level: class, genera and species. For simplicity, these matrixes are below designated as class, genera and species matrix.

Results of the Global R statistic, for each biotic data matrixes, are shown in Table 3.1, under the null hypothesis (H_0) of ‘no difference between seasons’:

Table 3.1. Ria de Aveiro phytoplankton community. Results of the test R statistic under the H_0 of ‘no season differences’, for each biotic data matrix.

Matrix	Class	Genera	Species
Global R	0.223	0.424	0.513
Significance level	0.1%	0.1%	0.1%
Number of permuted statistics \geq Global R	0	0	0

The obtained R values fall between 0 and 1, indicating that there are significant differences between seasons. Values of R equal to or higher than 0.223 for the class matrix, 0.424 for the genera matrix and 0.513 for the species matrix do not occur since, in 999 permutations, zero of the permuted statistics was equal or superior to the observed global R. Therefore, H_0 is rejected at a significance level of 0.1%. The results obtained with each data matrix are coherent, demonstrating that there are differences between the phytoplankton assemblages of each season which are worth exploring further.

R statistic tests were performed between pairs of seasons in order to determine where the differences demonstrated by the global R are visible (Table 3.2).

Regarding the results of the pairwise tests for the class matrix, the significance level of the R statistic for the pair Spring/Summer is largely superior to the significance level used in this study to allow H_0 rejection: 5%. Therefore, H_0 is, in a first instance, accepted, and there are no significant differences between phytoplankton assemblages of these two seasons. However, when the pairwise tests were performed upon the genera and species matrixes, the R statistic obtained in the test of spring vs. summer falls in the range 0 to 1, and H_0 can be rejected at a significance level of 0.1%. Concerning the R statistic of the

other pairs of seasons, for each data matrix, H_0 is always rejected and, therefore, all seasons possess significantly different phytoplankton assemblages.

Table 3.2. Ria de Aveiro phytoplankton assemblages. Results of the pairwise tests, under the H_0 of ‘no season differences’, for each biotic data matrix with 999 permutations.

Class Matrix			
Groups	R Statistic	Significance level (%)	Number \geq observed
Spring, Summer	-0.006	50.5	504
Spring, Autumn	0.172	1.4	13
Spring, Winter	0.4	0.1	0
Summer, Autumn	0.184	0.7	6
Summer, Winter	0.508	0.1	0
Autumn, Winter	0.17	1.4	13
Genera Matrix			
Groups	R Statistic	Significance level %	Number \geq observed
Spring, Summer	0.238	0.1	0
Spring, Autumn	0.41	0.1	0
Spring, Winter	0.636	0.1	0
Summer, Autumn	0.299	0.1	0
Summer, Winter	0.687	0.1	0
Autumn, Winter	0.438	0.1	0
Species Matrix			
Groups	R Statistic	Significance level %	Number \geq observed
Spring, Summer	0.348	0.1	0
Spring, Autumn	0.452	0.1	0
Spring, Winter	0.695	0.1	0
Summer, Autumn	0.373	0.1	0
Summer, Winter	0.787	0.1	0
Autumn, Winter	0.475	0.1	0

An ordination analysis by the non-metric multidimensional scaling (MDS) method was performed upon the results of the ANOSIM test and is presented in Figure 3.6. Regarding the 2D ordination (Figure 3.6a) a clear pattern between the groups of samples was not observed, mostly due to the fact that changes in the phytoplankton community are gradual.

The stress value of this ordination (0.17) is superior to 0.1 and hence the representation should be regarded with some caution. However, bearing in mind the results of the ANOSIM test, which have confirmed the existence of differences between season phytoplankton assemblages, this stress value is probably due to the high quantity of data (Clarke & Warwick, 1994) and it still provides a useful 2-D representation of the biological data (Clarke & Warwick, 1994). Moreover, whenever in presence of temporal

data or gradient it can be considered normal a high stress value since the dissimilarities between the groups of samples will be less marked or, in other words, smaller (M. Cunha, pers. comm.). A gradient between the different seasons seems, therefore, to exist: winter appears distinguished from the other groups of samples. The distance between spring and summer samples is smaller when compared with the other groups of samples, which means that the phytoplankton assemblages of these two seasons, even though different, are more closely related. Autumn samples appear to make the transition between the warmer seasons and winter.

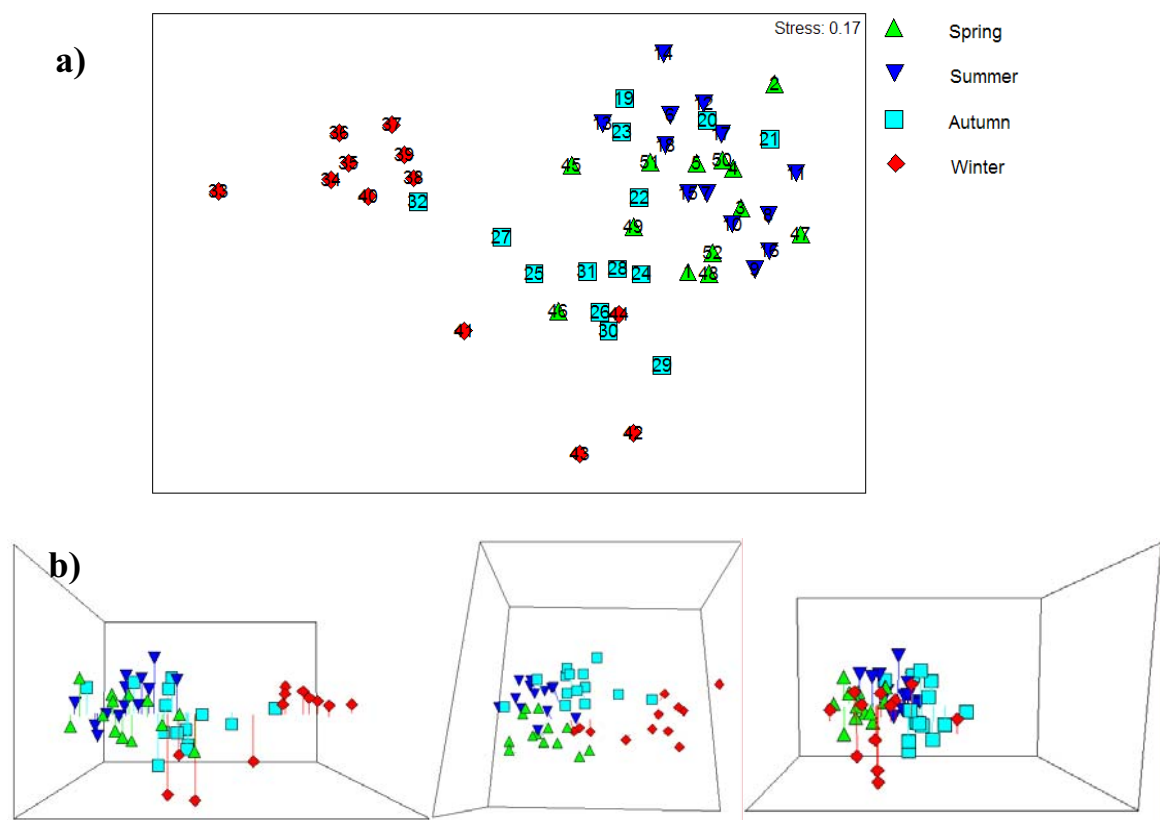


Figure 3.6. Ria de Aveiro phytoplankton community. 2D (a) and 3D (b) MDS ordination of the 52 samples performed upon the results of the ANOSIM test and based on log-transformed abundances and Bray-Curtis similarities.

The 3D MDS has a smaller stress value, 0.12, which indicates a better ordination of samples; as it is shown in Figure 3.6b, groups of samples appear more separated from one another than in the 2D plot. A temporal gradient, from spring to winter samples is visible.

Having summarized the pattern of distribution of the biological data over the study period with the ordination plot, it was performed a search for the phytoplankton organisms which

are responsible for that pattern, i.e. which are responsible for the existing differences of phytoplankton assemblages between seasons, by returning to the raw data.

Figure 3.7 shows the proportions of the different phytoplankton classes between seasons, in terms of cell numbers per litre.

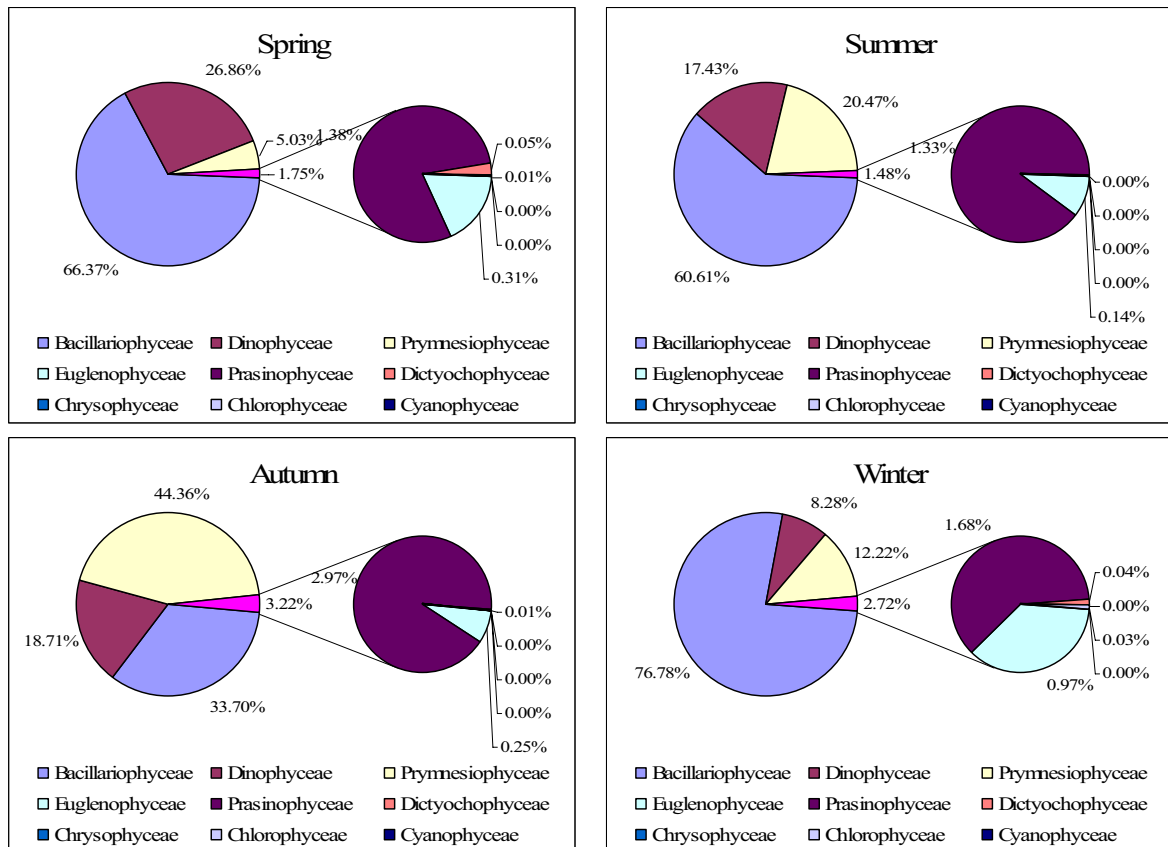


Figure 3.7. Ria de Aveiro phytoplankton community. Proportions of different classes of phytoplankton at each season, in terms of cell numbers per litre.

During all seasons except autumn, diatoms were the dominant group of the phytoplankton community. During autumn, cocolithophorids were dominant (number of cells per litre). Regarding spring and summer phytoplankton communities, diatoms continue to be the dominant group, but the cocolithophorids increased in relative importance while the dinoflagellates decreased. The percentage of abundance of the Prasinophyceae remained approximately the same while there was a decrease of importance of the Dictyochophyceae from spring to summer. From summer to autumn the differences in community were again due mostly to an increase in the abundance of cocolithophorids, which substituted the diatom group in the dominance of the community. During this period the relative

abundance of the Dinophyceae remained almost unchanged and the porportion of the Prasinophyceae increased slightly. From autumn to winter, diatoms became again the dominant phytoplankton group and a marked decrease of the other main groups was observed. The Prasinophyceae somewhat decreased in relative importance while Euglenophyceae reached, in this season, its higher significance. Closing the cycle, from winter to spring, dinoflagellates increased in numbers as well as the Dictyochophyceae. Euglenophyceae decreased in relative abundance from winter to spring.

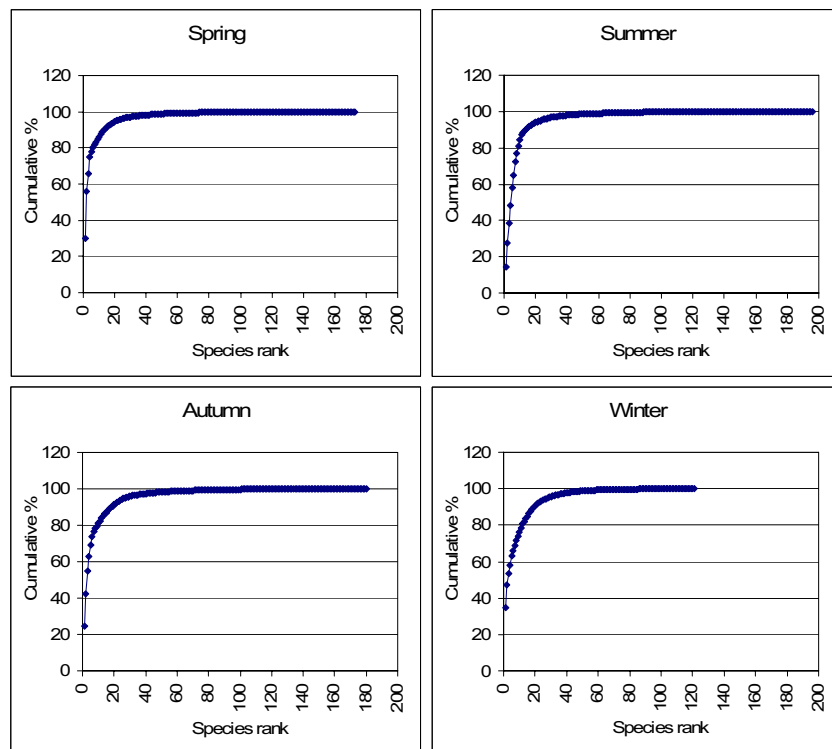


Figure 3.8. Ria de Aveiro phytoplankton community. Species cumulative (%) abundance plotted against species rank (K-dominance curves) for each season.

In order to extract information on patterns of relative species abundances without reducing that information to a single statistic summary, k-dominance curves were constructed based on the cumulative frequencies of the abundances of each phytoplankton category present in the phytoplankton assemblage of each season (Appendix I - Tables 2, 3, 4 and 5). The curves presented in Figure 3.8 show that the winter phytoplankton community has the lowest species diversity and the dominance of the phytoplankton assemblage is shared by a higher number of species. The summer phytoplankton assemblage presents higher species diversity but it is strongly dominated by a smaller number of species.

The species with cumulative frequencies inferior to roughly 70% were considered the most abundant and thus the dominant of the phytoplankton assemblage of each season (see Appendix 1). There are no “perfect indicators”, i.e. species which occur in all samples of one season and in none of the compared seasons.

The spring phytoplankton assemblage was essentially dominated by small phytoflagellates (phytoplankton category which contains organisms of various classes), diatoms like *Leptocylindrus danicus* and *Pseudo-nitzschia* spp., *Prorocentrum* cf. *minimum* and other small armoured dinoflagellates (Figure 3.9).

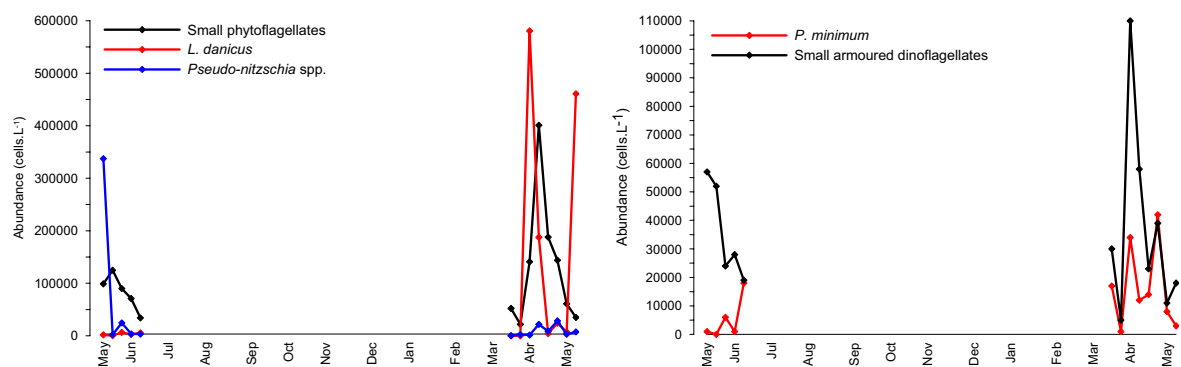


Figure 3.9. Time distribution of frequent species of the spring phytoplankton assemblage

Small phytoflagellates were the most abundant in the spring of 2005 reaching a maximum of abundance of 4.0×10^5 cells·L⁻¹ on 11 April 2005. *Leptocylindrus danicus* was also most abundant in the spring of 2005, attaining a maximum of abundance of 5.8×10^5 cells·L⁻¹ on 08 April 2005. A second and minor peak of abundance occurred on 09 May 2005 (4.6×10^5 cells·L⁻¹). *Pseudo-nitzschia* spp. occurred in higher numbers in the spring of 2004, at the first sampling data (18 May 2004). It has reached a concentration of 3.4×10^5 cells·L⁻¹. Small armoured dinoflagellates were very abundant in the spring phytoplankton assemblage and reached its higher abundance of 1.1×10^5 cells·L⁻¹ on 08 April 2005. *Prorocentrum* cf. *minimum* attained its maximum concentration of 4.2×10^4 cells·L⁻¹ on 27 April 2005, but its proliferation had started in March 2005.

During summer, *Leptocylindrus danicus* continued to dominate the phytoplankton assemblage accompanied by *Syracosphaera pulchra*, *Chaetoceros* spp., small forms of *Thalassiosira* spp., small phytoflagellates, *Pseudo-nitzschia* spp. and small armoured dinoflagellates (Figure 3.10).

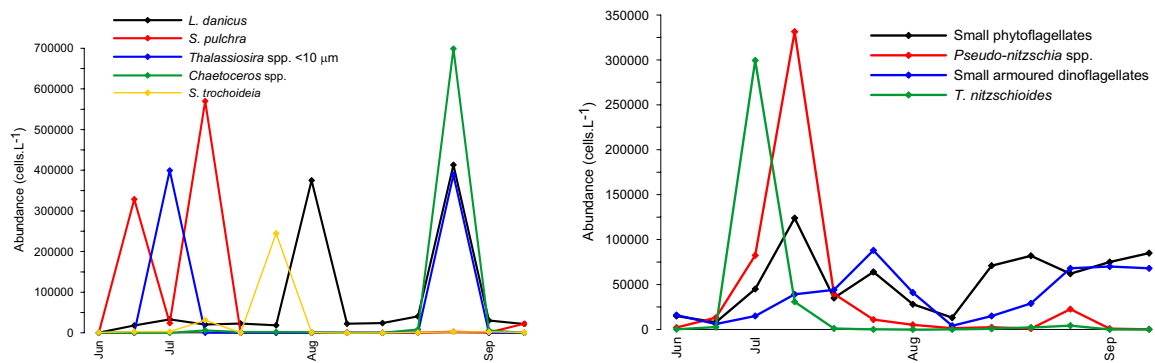


Figure 3.10. Time distribution of frequent species of the summer phytoplankton assemblage

Large proliferations of *Syracosphaera pulchra* occurred on 28 June (3.3×10^5 cells·L⁻¹) and July 12 2004 (5.7×10^5 cells·L⁻¹). *Leptocylindrus danicus* also occurred in higher numbers for two times, on 02 and 30 August 2004, with corresponding abundances of 3.7×10^5 cells·L⁻¹ and 4.1×10^5 cells·L⁻¹. Small forms of the genera *Chaetoceros* spp. and *Thalassiosira* spp. occurred mostly on 30 August 2004 (7.0×10^5 cells·L⁻¹) and 3.9×10^5 cells·L⁻¹). The latest had occurred previously on 05 July 2004 with a concentration of 4.0×10^5 cells·L⁻¹. *Pseudo-nitzschia* spp. was most abundant on 12 July 2004 (3.3×10^5 cells·L⁻¹). Small forms of phytoflagellates and armoured dinoflagellates occurred generally at the same concentration during this period. The highest concentration of the small armoured dinoflagellates (8.8×10^4 cells·L⁻¹) and *Scrippsiella* cf. *trochoidea* (2.4×10^5 cells·L⁻¹) took place on 27 July 2004. These proliferations of different phytoplankton organisms follow one another over time.

Syracosphaera pulchra was again dominant in the autumn phytoplankton assemblage (Figure 3.11), as a result of a large proliferation, with a concentration of 8.7×10^5 cells·L⁻¹ that occurred on 04 October 2004. Other coccolithophorids were also abundant, such as *Emiliania huxleyii*, which reached a maximum concentration of 6.5×10^4 cells·L⁻¹ on 27 September 2004, and *Gephyrocapsa* spp., whose concentrations ranged from 2.0×10^3 to 3.0×10^4 cells·L⁻¹. Small phytoflagellates, some of the Prasinophyceae class, were again abundant in this phytoplankton assemblage, occurring in concentrations ranging from 2.0×10^4 to 2.1×10^5 cells·L⁻¹. *Leptocylindrus danicus* bloomed in this season on 27 September 2004 with a concentration of 4.0×10^5 cells·L⁻¹ but in the rest of the season its numbers remained low. Small armoured dinoflagellates were more abundant at the beginning of the season reaching concentrations of 8.7×10^4 cells·L⁻¹.

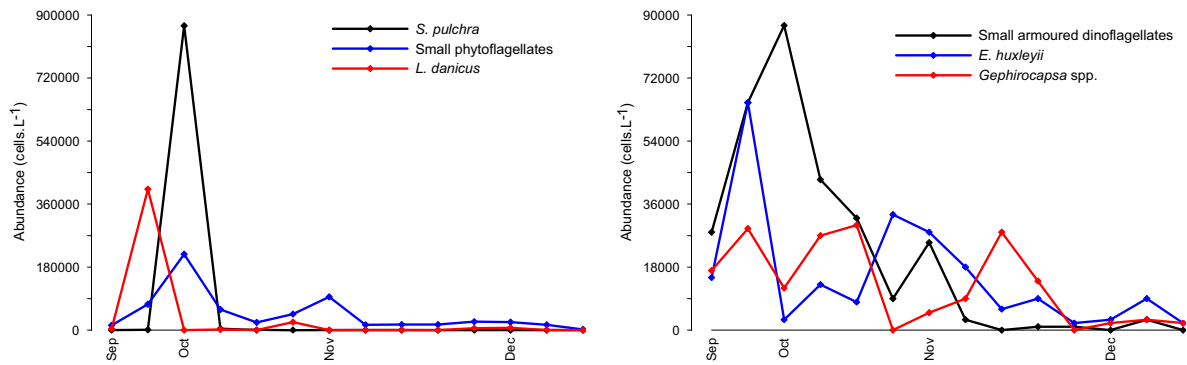


Figure 3.11. Time distribution of frequent species of the autumn phytoplankton assemblage

During winter (Figure 3.12), small phytoflagellates were, once more, dominant, as well as *Chaetoceros* spp., *Guinardia delicatula*, *Lauderia annulata*, *Pseudo-nitzschia* spp., *Cylindrotheca closterium* and *Thalassiosira* spp.. The cocolithophorids *Emiliana huxleyii* and *Gephyrocapsa* spp. also occurred with significant abundances.

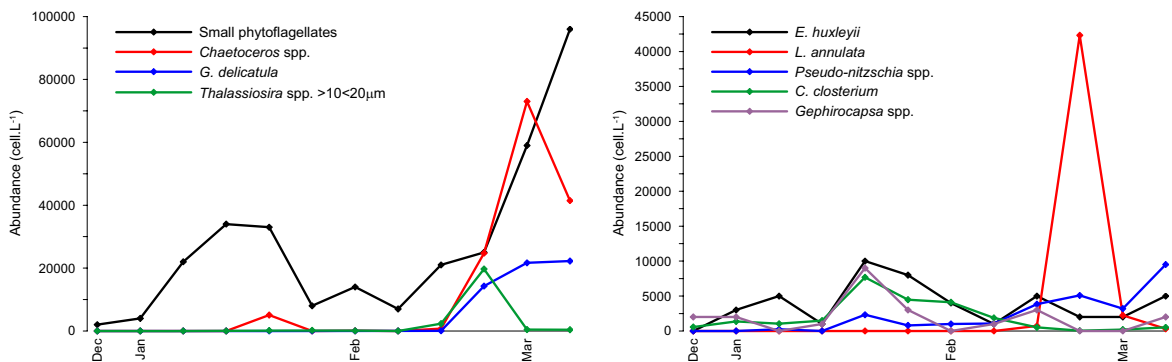


Figure 3.12. Time distribution of frequent species of the winter phytoplankton assemblage

Exception made to the small phytoflagellates, which were present in the water column throughout this season in relative high concentrations, the concentration of the other phytoplankton groups was more expressive from the middle of February. On 28 February 2005 *Chaetoceros* spp., *Lauderia annulata*, *Thalassiosira* spp. experienced an increase in concentration reaching the values of, respectively, 2.5×10^4 , 4.2×10^4 , 1.9×10^4 cells L⁻¹. *Guinardia delicatula* also increased in numbers from 28 February 2005, but in March reached higher concentrations. *Emiliana huxleyii* occurred in smaller concentrations than in the other seasons but it was present in all the samples, with concentrations ranging from 1.0×10^3 to 1.0×10^4 cells L⁻¹. *Cylindrotheca closterium* and *Pseudo-nitzschia* spp. never reached high concentrations but they were present in all the samples.

Table 3.3 summarizes the average of the univariate measures calculated for each season. The standard deviation of each measure is also presented.

Table 3.3. Ria de Aveiro phytoplankton community. Average (\bar{x}) and standard deviation (σ) of univariate measures for each season.

Season	Total Species (S)		Total individuals (N)		Species Richness (d)		Species Evenness (J')		Species Diversity (H')	
	\bar{x}	σ	\bar{x}	σ	\bar{x}	σ	\bar{x}	σ	\bar{x}	σ
Spring	68	11.56	37647	29418.63	6.50	0.74	0.48	0.12	2.00	0.46
Summer	75	19.84	55798	51400.23	6.99	1.36	0.48	0.10	2.06	0.39
Autumn	64	12.64	25559	36490.78	6.54	1.10	0.58	0.11	2.40	0.42
Winter	39	15.06	7824	7566.81	4.39	1.29	0.60	0.11	2.16	0.41

The summer phytoplankton assemblage was characterized by the highest number of species (S) and individuals (N) while the winter phytoplankton assemblage showed the smallest values for the same parameters. The number of phytoplankton species present during spring and autumn was rather similar. The highest species richness (d) was calculated for the summer phytoplankton assemblage even though the difference between this value and the species richness for spring is not very high. As for species evenness (J'), which is a measure of how species are distributed among the samples, winter presents the highest value in opposition to spring and summer. This means that in the winter phytoplankton assemblage a larger number of species divides the highest proportion of the community than in other seasons, which are clearly dominated by a small number of species (Figure 3.8). The phytoplankton assemblage with highest species diversity (H') was autumn.

3.2. Temporal variability of environmental parameters

Figure 3.13 presents the daily upwelling index calculated from the records of wind direction and strength for Cabo Carvoeiro meteorological station. A weekly index is also accessible, obtained from the average of the daily upwelling values recorded in the week preceding the sampling date.

Negative values of this index are indicators of upwelling events.

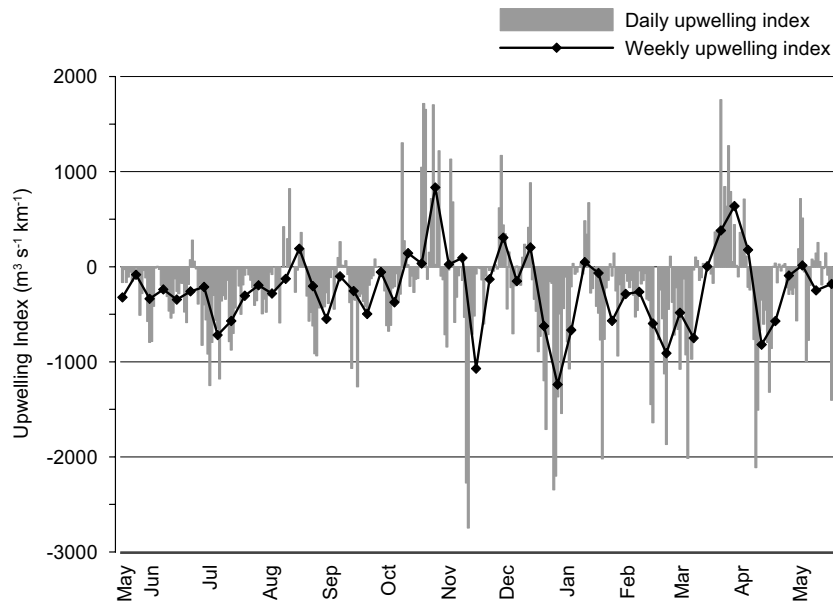


Figure 3.13. Upwelling index daily and weekly average (negative values are indicators of upwelling).

Coastal upwelling events were persistent throughout the year and stronger during winter and beginning of spring. However, it was not a continuous process being interrupted by periods of upwelling unfavourable winds, for example between October 2004 and March 2005. The most intense upwelling event occurred on 11 November 2004. Another strong upwelling event occurred on 02 May 2004.

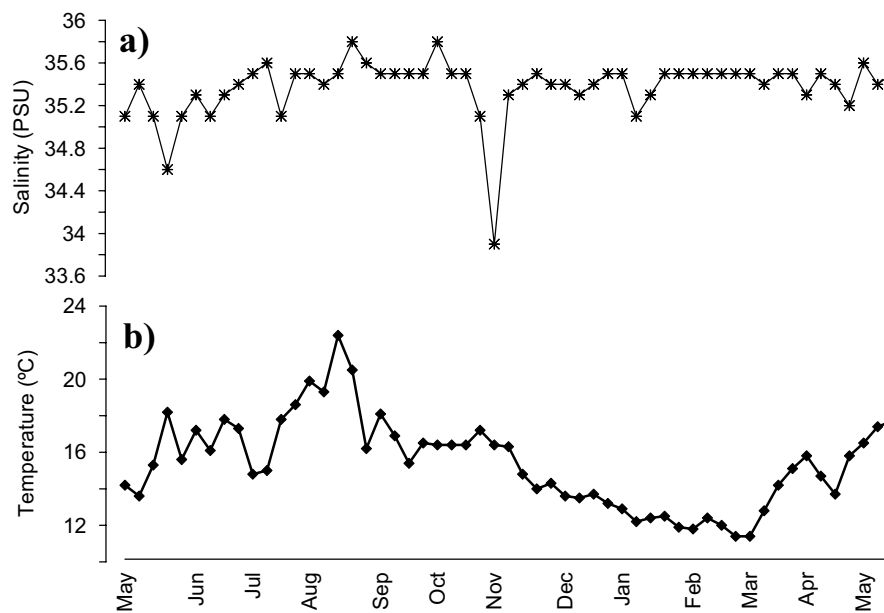


Figure 3.14. Surface water salinity (a) and temperature (b).

Salinity values (Figure 3.14a) varied between 33.9 PSU and 35.8 PSU remaining, however, more or less stable around 35.37 PSU. The smallest value was observed on 01 November 2004 and was probably due to the higher precipitation that occurred in the days preceding the collection of samples.

Higher values of surface water temperature (Figure 3.14b) were registered during spring and summer, decreasing progressively from autumn to winter. Temperature varied between a minimum of 11.4°C recorded on 28 February 2005 and a maximum of 22.4°C on 16 August 2004. The average surface water temperature during the study period was of 15.4°C.

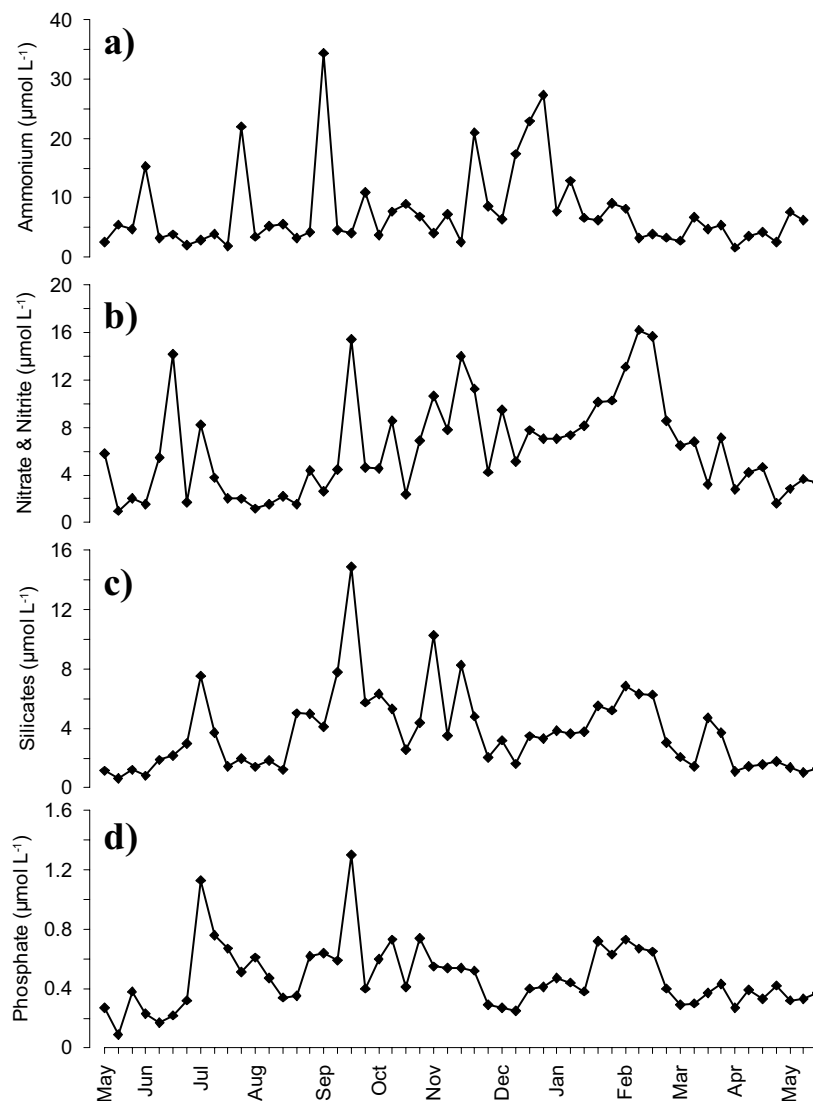


Figure 3.15. Dissolved nutrient concentration: a) ammonium; b) nitrate and nitrite; c) silicates; d) phosphates.

Dissolved nutrient concentration variation over the survey period is presented in Figure 3.15. The most abundant nutrient over the year was ammonium (Figure 3.15a), whose concentration varied between a maximum of $34.4 \mu\text{mol}\cdot\text{L}^{-1}$ attained on 07 September 2004 and a minimum of $1.6 \mu\text{mol}\cdot\text{L}^{-1}$, reached on 08 April 2005. Although the 3 major peaks of ammonium concentration were detected in spring 2004 and summer 2005, this nutrient occurred in high average concentrations during autumn and winter.

Nitrate and nitrite concentrations (Figure 3.15b) somewhat followed the same tendency of ammonium, reaching higher average concentrations during autumn and winter. The highest concentration in the water surface of these nutrients was achieved on 14 February 2005 with the value $16.2 \mu\text{mol}\cdot\text{L}^{-1}$. The lowest concentration was $1.0 \mu\text{mol}\cdot\text{L}^{-1}$ and occurred on 24 May 2004.

Silicates (Figure 3.15c) occurred at smaller concentrations during spring and higher values took place during summer and autumn. The smaller concentration of silicates, $0.6 \mu\text{mol}\cdot\text{L}^{-1}$, was reached on 24 May 2004 and the maximum value of $14.9 \mu\text{mol}\cdot\text{L}^{-1}$ occurred on 21 September 2004.

Phosphates (Figure 3.15d) were the less abundant nutrients in the water surface during the study period, with values ranging $0.1 \mu\text{mol}\cdot\text{L}^{-1}$ and $1.3 \mu\text{mol}\cdot\text{L}^{-1}$ attained on 24 May 2004 and on 21 September 2004, respectively.

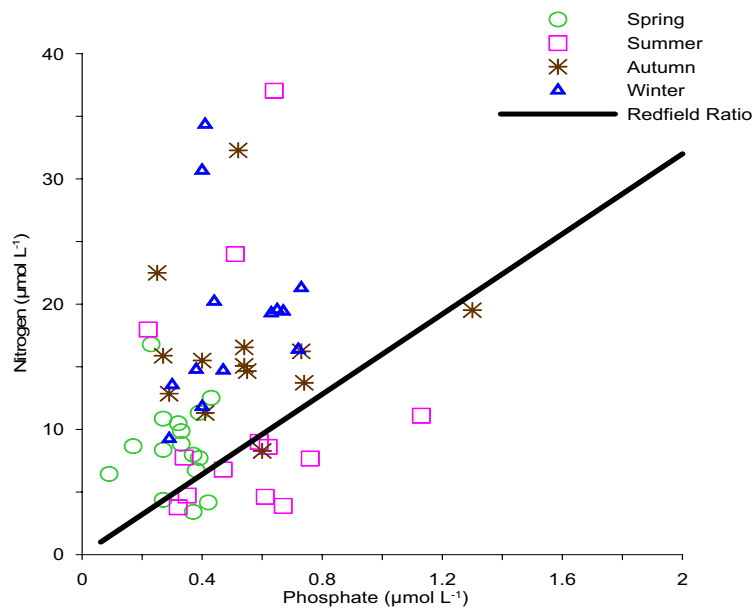


Figure 3.16. Redfield ratio for spring, summer, autumn and winter samples.

With the purpose of determining the limiting nutrient for phytoplankton development, Figure 3.16 shows a graphic where total dissolved nitrogen (nitrate + nitrite + ammonium) is plotted against phosphate concentration.

Regarding the theoretical Redfield ratio values of 16:1 for N:P ratio (Harris, 1986), generally, nitrogen was always in excess during the study period, phosphate being the limiting nutrient for the phytoplankton nutrient. Exception is made for the majority of the summer samples, two samples in autumn and 2 stations in spring.

Figure 3.17 shows the relationship between three environmental variables known to be interconnected.

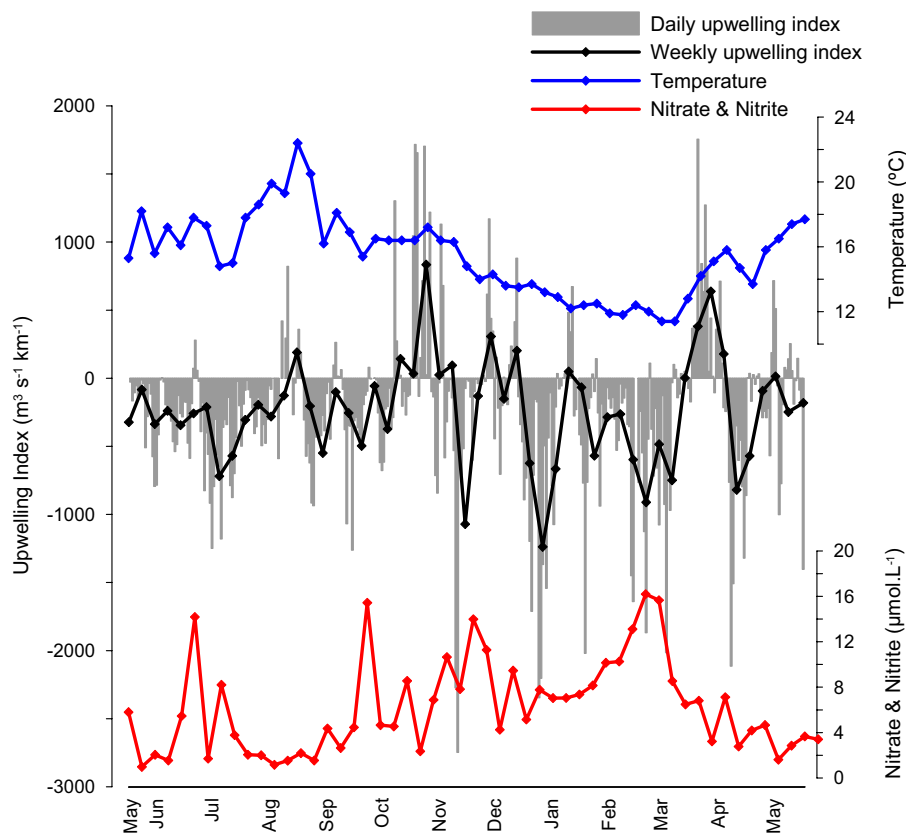


Figure 3.17. Relation between daily upwelling index, water temperature and nitrate + nitrite concentration, during the studied period.

Upwelling events correspond to a decrease in water surface temperature and an increase of the concentration of nitrates + nitrites.

The multivariate analysis of the environmental data followed a strategy similar to that applied to the biotic data.

The set of variables measured at each date of sampling were assembled in different groups corresponding to the four seasons, and a one-way layout ANOSIM test was performed in order to determine if the temporal pattern of variation verified for the biological data was also true for the environmental data. The analysis of similarities was done upon the normalised euclidean distance triangular matrix of the environmental data. The global R value obtained was 0.244 and, since in 999 permutations none of the permuted statistic originated values was equal or greater than this value, H_0 was rejected at a significance level of 0.1%.

Table 3.4 presents the results of the test of differences between pairs of seasons (pairwise tests).

Table 3.4. Ria de Aveiro environmental data. Results of the pairwise tests, under the H_0 of ‘no season differences’, for each data matrix with 999 permutations.

Groups	R Statistic	Significance level (%)	Number \geq observed
Spring, Summer	0.189	0.1	0
Spring, Autumn	0.161	0.3	2
Spring, Winter	0.493	0.1	0
Summer, Autumn	0.11	0.9	8
Summer, Winter	0.468	0.1	0
Autumn, Winter	0.14	1.1	10

Bearing in mind, once again, the level of significance used in this study that allows the rejection of H_0 – 5% – the results of the pairwise tests between seasons using the environmental data consent the rejection of H_0 and, thus, the different seasons possess significant differences in respect to physical and chemical parameters.

The ordination analysis of the 52 samples based on the ANOSIM test results of the environmental data of Ria de Aveiro is presented in Figure 3.18.

As for the biological data, sample 2D ordination using the environmental data did not show a clear pattern of temporal variation, as suggested by the stress value of 0.18. However, the 3D ordination of samples, which has a much better stress value, 0.13, shows the same seasonal variability of environmental data, as was demonstrated with the biotic data.

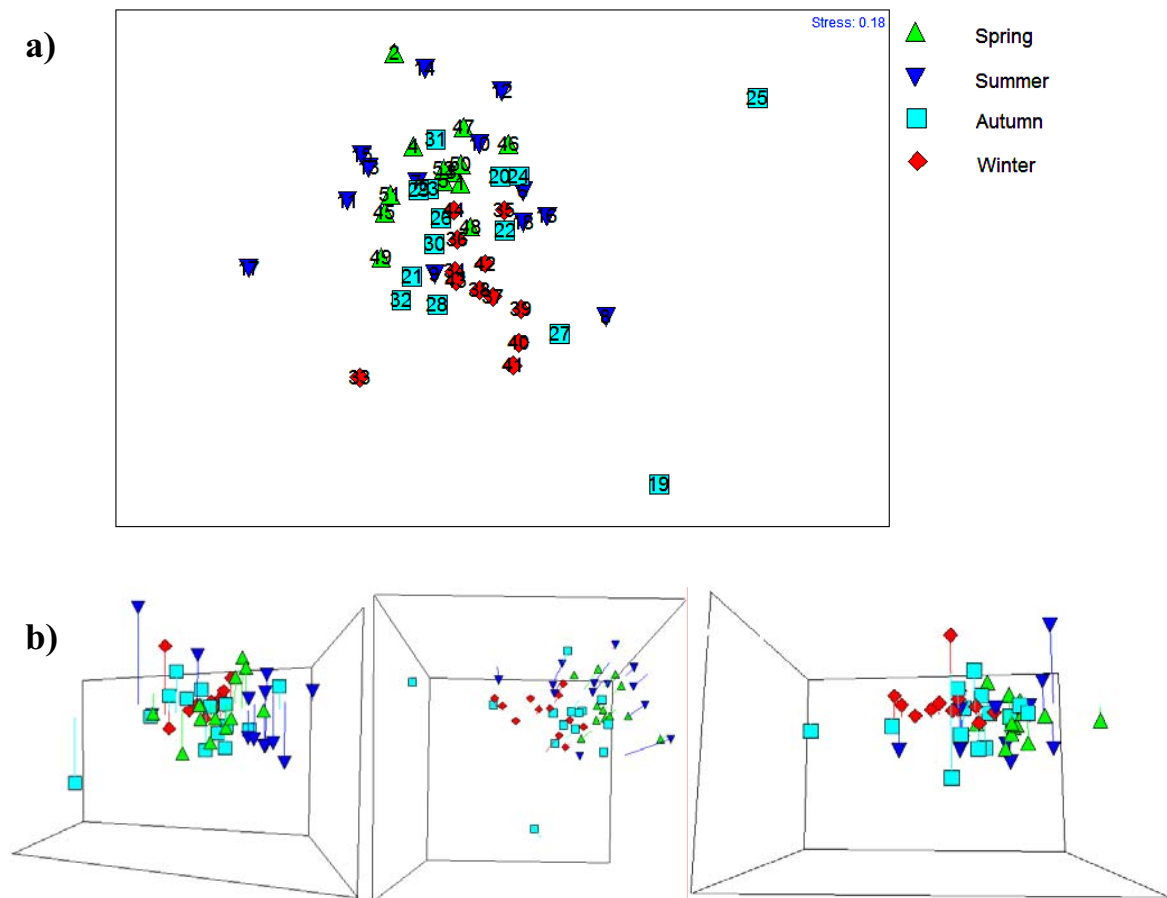


Figure 3.18. Ria de Aveiro phytoplankton community. 2D (a) and 3D (b) MDS ordination of the 52 samples performed upon the results of the ANOSIM test and based on normalised euclidean distances. Stress value of 0.18 for the 2D plot and of 0.13 for the 3D plot.

3.3. Linking biota to environmental data

The relation of the biological data ordination and the different environmental variables taken in consideration in this study was visualized by representing the values of each variable as symbols (circles) of differing size and superimposing these symbols on the biotic ordination (Figure 3.6a) of the corresponding samples using the species matrix (Figure 3.21).

While salinity values were more or less stable throughout the period of study (Figure 3.19b), water surface temperature was higher during spring and summer (Figure 3.19a), as expected.

Tidal high values ranged from 2.4 to 3.6 m and the higher values took place in spring and summer, especially in August (Figure 3.19c).

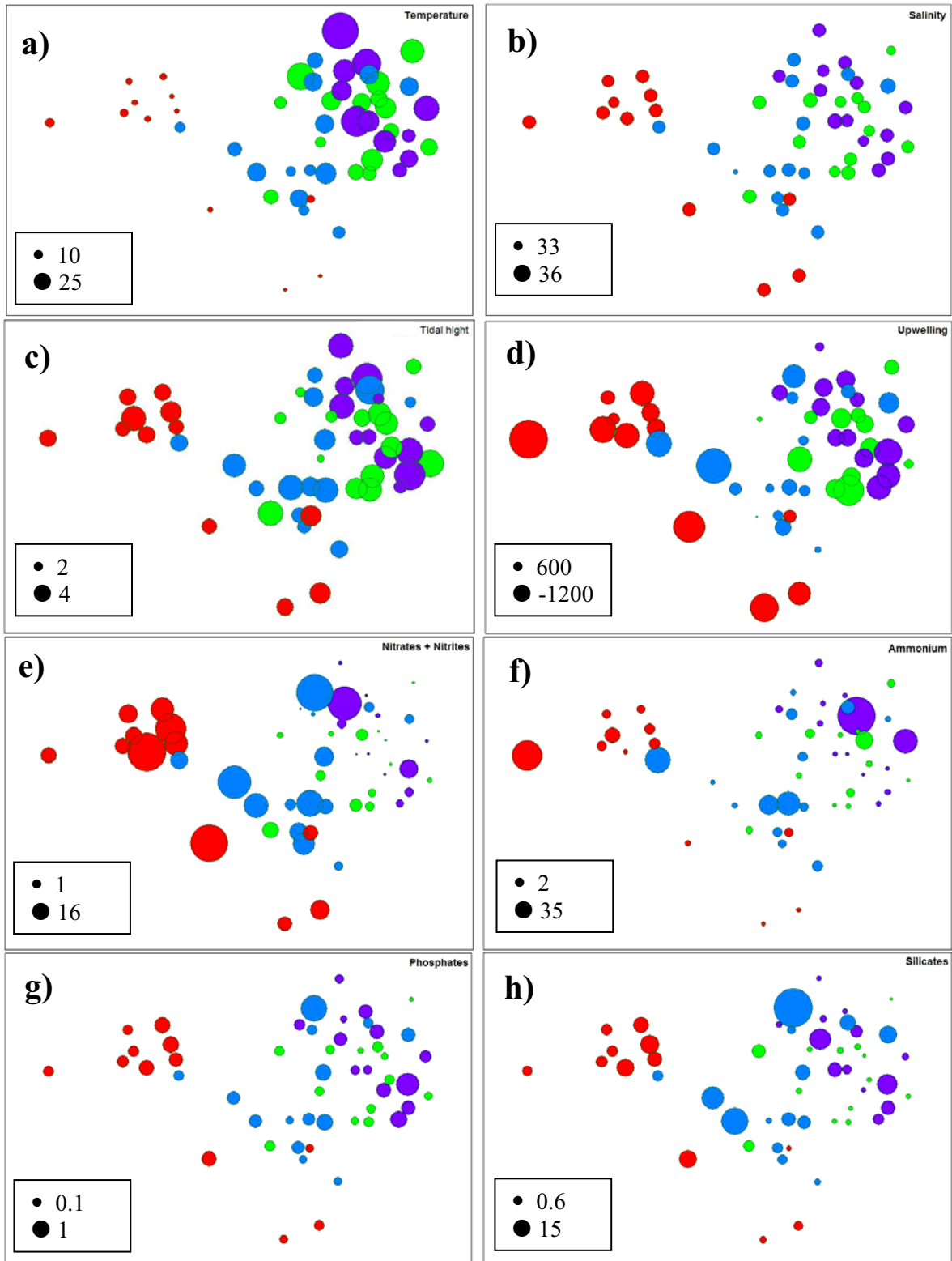


Figure 3.19. Ria de Aveiro environmental data. MDS of Bray-Curtis similarities from log-transformed phytoplankton abundances with superimposed circles of increasing size with increasing temperature (a); salinity (b); tidal amplitude (c); upwelling (d); nitrate + nitrite (e); ammonium (f); phosphates (g); silicates (h) (stress = 0.01). ● spring, ● summer, ● autumn, ● winter. The values presented in the legend of the circles do not correspond to real values.

Northerly winds were frequent during the studied period and, consequently, so were the daily values of the upwelling index (Figure 3.19d). The upwelling was stronger during winter, but since no significant phytoplankton development occurs in this season, due mostly to low light intensity necessary for photosynthesis, the upwelling occurring during spring and summer has a higher importance.

The nutrients that occurred in smaller concentrations at the water surface were phosphates (Figure 3.19g). It was in the summer season that, on average, higher concentrations of this element was measured; the smallest concentrations occurred during spring. Nitrate + nitrite concentration (Figure 3.19e) in the water surface was higher during autumn and winter, and the smallest values occurred mostly during summer. The highest ammonium concentrations (Figure 3.19f) were found during summer and winter. Silicates occurred in higher concentrations during autumn and winter (Figure 3.19h).

For each season the averages of the different environmental variables measured at each sampling campaign were calculated and follow the same pattern as described above (summarized in Table 3.5.).

Table 3.5. Ria de Aveiro environmental data. Average (\bar{x}) and average deviation (σ) of the different environmental variables per season.

		Spring	Summer	Autumn	Winter
Temperature (°C)	\bar{x}	15.70	18.07	15.35	12.24
	σ	1.44	2.25	1.32	0.57
Salinity (PSU)	\bar{x}	35.28	35.49	35.32	35.44
	σ	0.24	0.16	0.44	0.12
Tidal hight (m)	\bar{x}	2.99	3.05	2.99	2.96
	σ	0.32	0.39	0.26	0.16
Upwelling ($m^3s^{-1}km^{-1}$)	\bar{x}	-250.98	-277.46	-143.11	-481.69
	σ	455.93	241.97	379.28	388.17
Nitrates + Nitrites ($\mu mol \cdot L^{-1}$)	\bar{x}	4.75	2.97	8.06	9.73
	σ	3.37	1.99	3.82	3.46
Ammonium ($\mu mol \cdot L^{-1}$)	\bar{x}	4.82	7.78	9.44	8.14
	σ	3.18	9.96	6.46	6.70
Silicates ($\mu mol \cdot L^{-1}$)	\bar{x}	1.95	3.67	5.45	4.27
	σ	1.20	2.31	3.62	1.75
Phosphates ($\mu mol \cdot L^{-1}$)	\bar{x}	0.31	0.58	0.54	0.51
	σ	0.10	0.22	0.27	0.16

A correspondence between the biological data (species matrix) and environmental patterns, was performed by using a rank correlation coefficient (τ -Kendal coefficient), a non-parametric test which measures the strength of the association between two or more variables. Combinations of environmental variables were considered at steadily increasing levels of complexity (k). Table 3.6 displays the outcome for the Ria de Aveiro phytoplankton community.

Table 3.6. Ria de Aveiro phytoplankton community. Combinations of 6 environmental variables, taken k at a time, yielding the best matches of biotic and abiotic similarity matrices for each k , as measured by Kendall rank correlation; bold type indicates overall optimum.

k	Best variable combinations			
1	Temp (0.285)			
2	Temp, Upw (0.301)	Temp, Nit (0.295)		
3	Temp, Upw, Nit (0.315)	Temp, Upw, Amo (0.273)	Temp, Nit, Sil (0.27)	
4	Temp, Upw, Nit, Sil (0.284)	Temp, Upw, Nit, Pho (0.28)	Temp, Sal, Upw, Nit (0.276)	Temp, Upw, Nit, Amo (0.268)

The single environmental variable which best distinguished seasons, in a manner consistent with the biological patterns is the temperature ($\tau=0.285$). Of course, since the biotic ordination is not one-dimensional, it could not be expected a single environmental variable to provide a very successful match, though knowledge of the temperature variable alone does distinguish the winter season (Figure 3.21a). The best two-variable combination also involves temperature but adds the weekly upwelling index. The correlation (0.301) is approximately similar to the other two-variable subset (temperature and nitrates + nitrites). The best three-variable combination retains temperature and weekly upwelling index and adds the concentration of dissolved nitrates (nitrates + nitrites). It gives the overall optimum value for τ of 0.315. The correlation values decrease for the four-way combinations and it is observed that the adding of the others classes of nutrients originates approximately similar correlations.

To test the significance of these correspondence between the biotic and abiotic data a test with the Kendall's rank correlation, upon the similarity matrix of both types of data, was

performed under the null hypothesis of ‘no relationship between the biotic information and a specific abiotic pattern’, i.e. $\tau=0$. The obtained τ value was 0.182, and since in 999 permutations none was greater than or equal to 0.182, H_0 can be rejected at a significance level of 0.1%. Therefore there is significant correspondence between the biotic and abiotic data and it is the interconnection between water surface temperature, upwelling events and concentration of dissolved nitrites and nitrates that has largely influenced the temporal distribution of the phytoplankton assemblages.

Variations in physical and chemical characteristics of water masses are reflected in the phytoplankton community. Using the abundance distribution of 5 chain forming diatoms known to respond to upwelling events (*Chaetoceros* spp., *Pseudo-nitzschia* spp., *Thalassiosira* spp., *Thalassionema nitzschioides* and *Leptocylindrus danicus*), it was observed, during the spring and summer months, that there was an increase in the abundance of these diatoms whenever deep cold rich-nutrient water upwelled (Figure 3.20). However, at different upwelling events phytoplankton cells achieved different concentrations and the proliferations were dominated by different species (Figure 3.21).

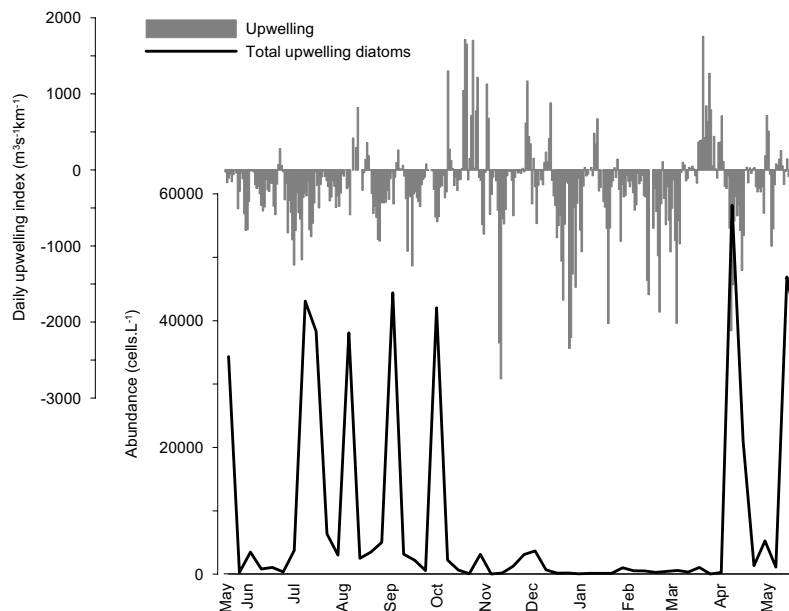


Figure 3.20. Relationship between the daily upwelling index and upwelling diatoms total concentration.

Pseudo-nitzschia spp. was more abundant in May and July 2004. *Thalassionema nitzschioides* and *Thalassiosira* spp. were also present in the proliferation of July 2004.

The abundance peaks that took place in August and October 2004 and in April and May 2005 were mostly due to proliferations of *Leptocylindrus danicus*. The latter species was also abundant in September 2004 accompanied by *Thalassiosira* spp. and *Chaetoceros* spp. (Figure 3.21).

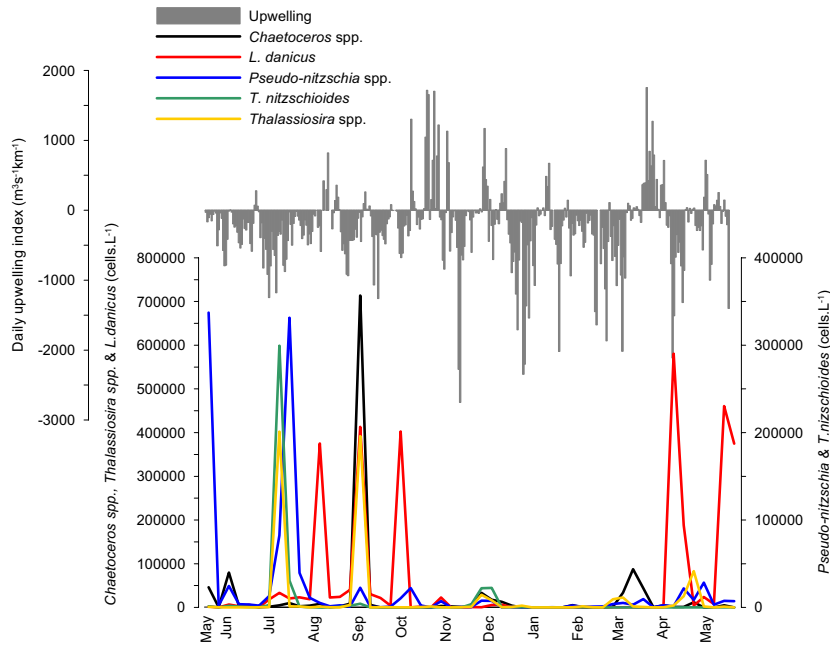


Figure 3.21. Relationship between the daily upwelling index and 4 species of upwelling diatoms.

No proliferations of these diatoms occurred from the end of autumn until the end of winter, in spite of the strong upwelling events recorded, probably as a result of the small irradiance and water column mixing conditions characteristic of this period.

3.4. Structure of phytoplankton communities

For the inverse or *r*-type analysis, both the genera and species matrix were used. Phytoplankton categories accounting for >2% of the total abundance in any one sample were chosen, resulting in a data array of 39 genera from the initial 113, and 48 species from the initial 139. The similarity analysis between variables was performed with a Bray-Curtis coefficient upon standardized and non transformed data. The dendrograms of the classification analysis of the species and genera matrixes are presented in Figures 3.22 and 3.23, respectively.

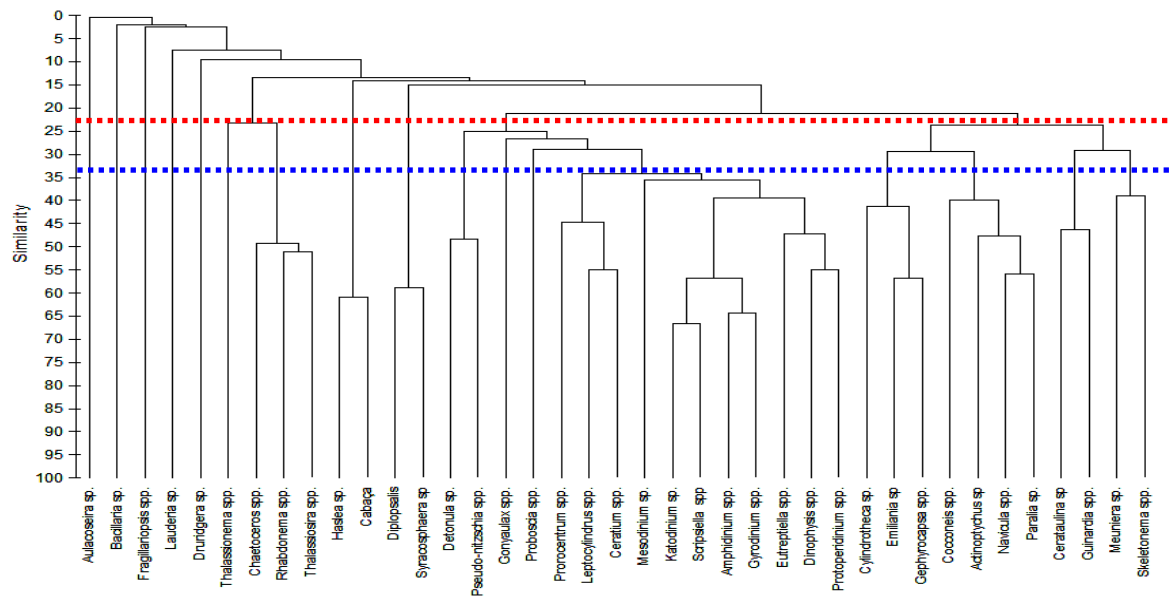


Figure 3.22. Ria de Aveiro phytoplankton assemblage. Dendrogram for hierarchical clustering of the 39 genera, using group-average linking of Bray-Curtis similarities calculated on standardized and non transformed data.

A list of the genera in each cluster, at a similarity level of 23% (red hatched line) is given in Table 3.7.

Table 3.7. Ria de Aveiro phytoplankton community. Genera groups distinguished by inverse analysis. The groups are based on the dendrogram in Figure 3.22.

Group A <i>Aulacoseira</i> sp.	Group H <i>Dipllopsalis</i> ; <i>Syracosphaera</i> sp.
Group B <i>Bacillaria</i> sp.	Group I <i>Amphidinium</i> spp.; <i>Ceratium</i> spp.; <i>Detonula</i> sp.; <i>Dinophysis</i> spp.; <i>Eutreptiella</i> spp.; <i>Gonyaulax</i> spp.; <i>Gyrodinium</i> spp.; <i>Katodinium</i> sp.; <i>Leptocylindrus</i> spp.; <i>Mesodinium</i> sp.; <i>Proboscia</i> spp.; <i>Prorocentrum</i> spp.; <i>Protoperidinium</i> spp.; <i>Pseudo-nitzschia</i> spp.; <i>Scripsiella</i> spp.
Group C <i>Fragillariopsis</i> sp.	Group J <i>Actinoptychus</i> spp.; <i>Cerataulina</i> sp.; <i>Cocconeis</i> spp.; <i>Cylindrotheca</i> sp.; <i>Emiliana</i> sp.; <i>Gephyrocapsa</i> spp.; <i>Guinardia</i> spp.; <i>Meuniera</i> sp.; <i>Navicula</i> spp.; <i>Paralia</i> sp.; <i>Skeletonema</i> spp.
Group D <i>Lauderia</i> sp.	
Group E <i>Druridgia</i> sp.	
Group F <i>Chaetoceros</i> spp.; <i>Rhabdonema</i> spp.; <i>Thalassionema</i> spp.; <i>Thalassiosira</i> spp.	

At a similarity level of approximately 36% (blue hatched line), *Pseudo-nitzschia* spp. appears associated with *Detonula* sp.. Both genera have already been considered as diatoms that respond to upwelling events (Moita, 2001). At the same similarity level, *Dinophysis* spp. appears associated with the armoured dinoflagellates *Scripsiella* spp., *Prorocentrum* spp., *Ceratium* spp. and *Protoperidinium* spp. Also the unarmoured dinoflagellate genera *Katodinium*, *Gyrodinium* and *Amphidinium* varie together with

Dinophysis spp., as well as the euglenophyta *Eutreptiella* spp. and the ciliate *Mesodinium* sp..

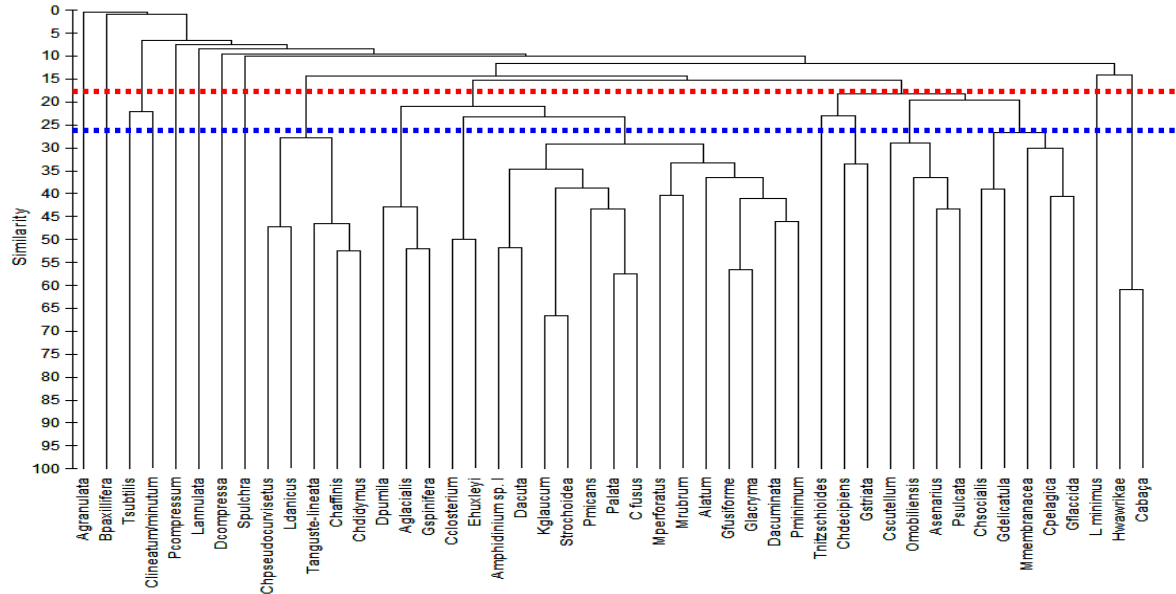


Figure 3.23. Ria de Aveiro phytoplankton assemblage. Dendrogram for hierarchical clustering of the 48 species, using group-average linking of Bray-Curtis similarities calculated on standardized and non transformed data.

A list of the species in each cluster, at a similarity level of 18% (red hatched line) is given in Table 3.8.

Table 3.8. Ria de Aveiro phytoplankton community. Species groups distinguished by inverse analysis. The groups are based on the dendrogram in Figure 3.23.

Group A <i>Aulacoseira granulata</i>	Group I <i>Asterionellopsis glacialis</i> ; <i>Amphidinium</i> sp.; <i>A. latum</i> ;
Group B <i>Bacillaria paxillifera</i>	<i>Ceratium fusus</i> ; <i>Cylindrotheca closterium</i> ; <i>Detonula pumila</i> ;
Group C <i>Thalassiosira subtilis</i> ; <i>Ceratium lineatum/minutum</i>	<i>Dinophysis acuta</i> ; <i>D. acuminata</i> ; <i>Emiliana huxleyii</i> ;
Group D <i>Prorocentrum compressum</i>	<i>Gonyaulax spinifera</i> ; <i>Gyrodinium fusiforme</i> ; <i>G. lacryma</i> ;
Group E <i>Lauderia annulata</i>	<i>Katodinium glaucum</i> ; <i>Mesoporus perforatus</i> ;
Group F <i>Druridgia compressa</i>	<i>Proboscia alata</i> ; <i>Prorocentrum micans</i> ; <i>P. minimum</i> ;
Group H <i>Chaetoceros pseudocurisetus</i> ; <i>Ch. affinis</i> ; <i>Ch. didymus</i> ;	<i>Scrippsiella</i> cf. <i>trochoidea</i>
<i>Leptocylindrus danicus</i> ; <i>Thalassiosira anguste-linneata</i>	Group J <i>Actinoptychus senarius</i> ; <i>Cerataulina pelagica</i> ;
	<i>Chaetoceros decipiens</i> ; <i>Ch. socialis</i> ; <i>Cocconeis</i> cf. <i>scutellum</i> ;
	<i>Guinardia delicatula</i> ; <i>G. flaccida</i> ; <i>G. striata</i> ;
	<i>Mesocera membranacea</i> ; <i>Odontella mobiliensis</i> ; <i>Paralia sulcata</i> ;
	<i>Thalassionema nitzschioides</i>
	Group K <i>Leptocylindrus minimus</i> ; <i>Haslea wawriake</i> ; Unidentified dinoflagellate I

Grouping of species was considered particularly important since it was desired to describe the species whose abundance tends to fluctuate in parallel with the abundances of *Dinophysis acuta* and *Dinophysis acuminata*, responsible for the most frequent events of shellfish contamination in Ria de Aveiro – DSP.

At a similarity level of 26% (Figure 3.23, blue hatched line) the species that tend to co-occur with *Dinophysis acuta* and *D. acuminata* appear dissociated. The species whose abundance tends to vary in parallel with *Dinophysis acuta* abundance are the unarmoured dinoflagellates *Amphidinium* sp. and *Katodinium glaucum*, the armoured dinoflagellates *Ceratium fusus*, *Scrippsiella* cf. *trochoidea* and *Prorocentrum micans* and the centric diatom *Proboscia alata*. *Dinophysis acuminata* appears associated with *Amphidinium latum*, *Gyrodinium fusiforme*, *G.lacryma* (unarmoured dinoflagellates), *Mesoporus perforatus* and *Prorocentrum* cf. *minimum* (armoured dinoflagellates of the order Prorocentrales) and, additionally, with the ciliate *Mesodinium rubrum*.

Dinophysis acuminata was most abundant during spring and at the beginning of summer it co-existed with *D. acuta* (Figure 3.24). The latter was most abundant from summer to the beginning of autumn. The maximum abundance peak of *Dinophysis acuta* was reached on 30 August 2004 corresponding to a concentration of 2560 cells·L⁻¹. *Dinophysis acuminata* highest value of abundance was 1080 cells·L⁻¹ and occurred on 31 May 2004.

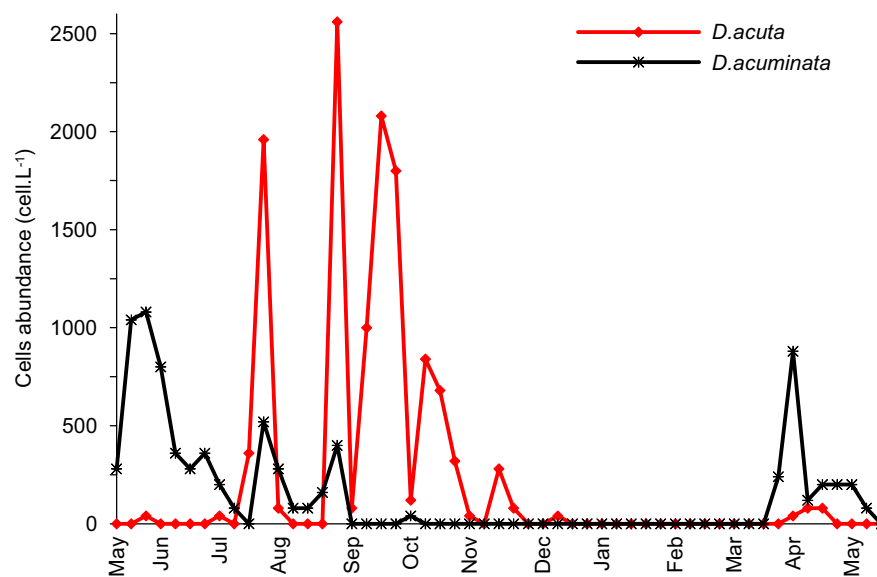


Figure 3.24. Time distributions of the abundance of *Dinophysis* cf. *acuminata* and *Dinophysis acuta*.

In the majority of times that both *D. cf. acuminata* and *D. acuta* occurred in the water column, the system was apparently limited by the concentration of phosphorus, occurring an excess of nitrogen nutrients. Their distributions were also restricted by the physical conditions of the water column, being more abundant during episodes of weak upwelling and upwelling relaxation (Figure 3.13). *Dinophysis cf. acuminata* proliferations occurred in the range of water surface temperatures of 12.8 and 22.4°C and *D. acuta* of 14.8 to 22.4°C (Figure 3.14).

4. Discussion

4.1. Phytoplankton species identification

Most phytoplankton species enumerated in this study have already been reported for Portuguese coastal waters (Moita & Vilarinho, 1999). Exceptions have occurred such as *Asterolampra* spp., *Asteromphalus sarcophagus*, *Odontella longicuris*, *Amphidinium latum* and *Gonyaulax birostris*. Particular emphasis is given to the centric diatom *Druridgia compressa* (West) Donkin 1861 (Figure 3.25), a relatively rarely cited species (Round *et al.*, 1990). It was first placed in the *Podosira* genus by T. West in 1860 (Guiry *et al.*, 2006). In this study it was identified by means of bright field and phase contrast microscopy using water samples fixed with neutral formalin. Cells usually appeared in pairs and in girdle view; in this view each cell had a square form and possessed four well distinguished chloroplasts, each one placed at one corner of the cell. In valve view, cells were ellipsoidal. Due to its resemblance with species of *Podosira* and *Melosira* in girdle view it is possible that this was not, truly, a first occurrence in the Portuguese waters and that it may have been confused previously with these other genera.

The difficulties and inaccuracies associated with the identification and enumeration of phytoplankton organisms have already been stressed in the Methods section and in Chapter II. Although the total number of identified species exceeds 200, the largest percentage of cells present in each sample could have never been identified under the light microscope. Being obtained by the same person, however, the numbers may retain some comparative value (Margalef, 1978b).

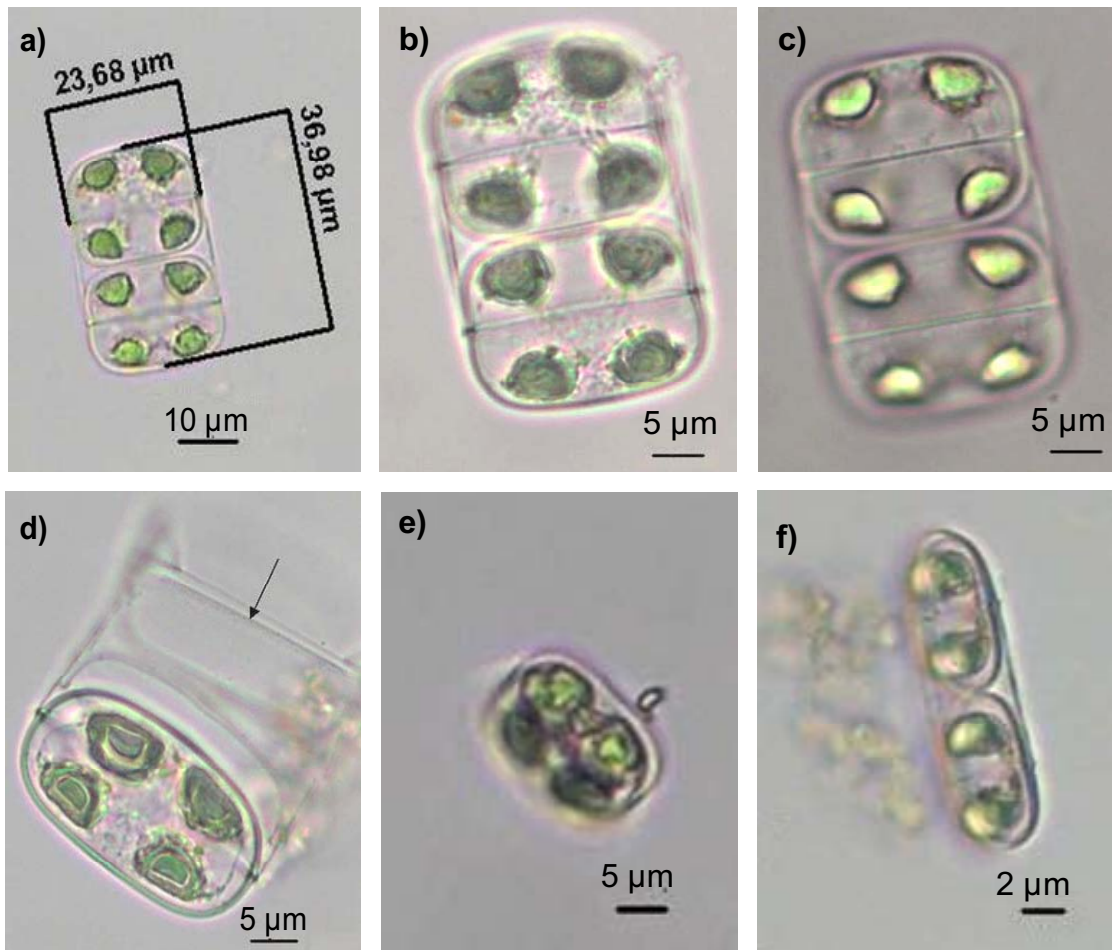


Figure 3.25. *Druridgera compressa*, Phase contrast. a-c) girdle view; d) detail of the pores of the frustule; e) valvar view; f) girdle view.

Some of the most common and largest diatom genera were identified to species level without too many problems during the routine counting. This was usually true for centric diatoms, which are large and possess unique features that ease their identification. However, due to the large storage time in neutral formaldehyde solution, that tends to acidify with time (Thronsen, 1978), it was found that the silica of the frustules of many species of centric diatoms, like *Leptocylindrus danicus* and *Dactyliosolen fragilissimus* became damaged. When compared to samples preserved with Lugol's solution, the storage time of samples preserved using formalin is higher and it is not necessary to periodically verify the condition of the samples (Thronsen, 1978), although the preservation of organisms is better with Lugol's solution. To avoid this kind of damages in some phytoplankton organisms, an effort should be made to decrease, as much as possible, the time between collection of samples and its observation, and consider the use of neutral Lugol's solution to preserve the samples.

Other genera, such as *Thalassiosira*, *Coscinodiscus* and *Melosira* were found to be indistinguishable with certainty from one another in valve view. For this reason many of the centric diatoms that appeared solitary and in valve view were included in artificial categories depending on cell diameter. Particularly for *Thalassiosira* and *Chaetoceros*, confusion also arose when specimens were in girdle view and almost no species names have been used. Nevertheless it should be remembered that unidentified species belong to the same life-forms as identified species in the same genera and may show similar ecological behaviour (Margalef, 1978b)

Pennate diatoms species identification was found to be more difficult not only because the usual small size of the specimens (the smallest ones could be less than 5 μm) but also due to the cells organic content that masked frustule ornamentation, which provides most species-specific characteristics used in diatom identification (Van Den Hoek *et al.*, 1995). This limitation in identifying pennate diatoms was especially felt with *Pseudo-nitzschia* species, considered important due to the capacity that some species have of producing domoic acid (Skov *et al.* 1999; FAO, 2004; IOC, 2005). *Pseudo-nitzschia* species in light microscopy form easily identifiable colonies characterized by overlapping cells. Each cell contains two chloroplasts, one at each end, and a central nuclear area. However, the species distinctive characteristics, like the number of interstriae, fibulae and poroids are only well distinguished in SEM, and for that reason the use of electron microscopy is of critical importance in the identification of these group of organisms (Skov *et al.*, 1999).

In respect to dinoflagellates some identification problems were experienced as well. Specimens with very thin plates, or no wall at all, were only poorly fixed by this method, many disintegrating rapidly or deforming unrecognizably on contact with the fixative (Hasle, 1978a). Thus, many of the unarmoured dinoflagellates were placed in an artificial category. Unfortunately it seemed to be a very abundant group and further investigation on the species composition of this group should be made in future work, probably appealing to the use of other fixatives like Lugol's solution, osmium tetroxide or glutaraldehyde (Hasle, 1978a). The fixation and preservation of the species with cell walls (armoured species) consisting of heavily developed cellulose plates was readily accomplished with the neutral formalin added to samples. However, their identification was sometimes difficult due to the position that the specimens acquire during the settlement in the slide, hiding the plate boundaries necessary for correct identification.

Ideally, identification of dinoflagellates with thecae should involve thecal dissociation in a controlled manner, with sodium hypochlorite (bleach), and records should be made of the form and relative position of the different plates (Taylor, 1978).

As already mentioned in the Methods section, the technique used for enumeration of the phytoplankton species in this work is not the most appropriate for coccolithophorid identification (Bollmann *et al.*, 2002). The classification of coccolithophorids is based almost entirely upon the structure and arrangement of the coccoliths, with only minor emphasis to other features such as cell shape. Identification to genus and species levels is hampered in most cases by the small size of the cells and their individual coccoliths (Heimdal, 1978). Coccolithophorids can only be satisfactorily described through the combined use of light microscopy, scanning electron microscopy and transmission electron microscopy (Heimdal, 1978). In this study a large part of the coccolithophorids present in the samples were identified only to genus level, and counts of each genus should be regarded with caution. Nevertheless they provide a useful idea of the probable relative importance of this group of organisms on the littoral coast of Aveiro.

The most common flagellates in marine phytoplankton, excluding dinoflagellates and coccolithophorids, are those that are part of the nanoplankton (cells < 20 µm) (Harris, 1986; Leadbeater, 1978). In this category, pigmented flagellates belonging to the algal classes Haptophyceae, Chrysophyceae and Prasinophyceae are the most common. In the present work, small phytoflagellates were particularly difficult to identify by means of light microscopy due to their small size and lack of flagella as a result of the action of the fixative agent. In fact, the satisfactory description of nanoplankton flagellates requires correlated light and electron microscopical observations (Leadbeater, 1978). In this study nanoplankton microflagellates were usually very abundant and thus, even knowing that their counts would have a great amount of errors it was decided to include them in this work.

Summarizing, other techniques of identification could have been used in order to accurately identify many organisms. Nevertheless, the technique of phytoplankton quantification and identification used in this study (Utermöhl method) was considered suitable for the achievement of the main objectives of this work, which were focused mostly in seasonal ecological variations of the phytoplankton community in general and of

the most important constituents of that community (diatoms, dinoflagellates and coccolithophorids). The use of additional techniques of phytoplankton identification, for example scanning electron microscopy, would have greatly increased the necessary time for the achievement of results. Nevertheless, studies with finer taxonomic discrimination should be performed in near future and ought to include specific microscopic techniques for each phytoplankton group. Moreover, in further work it could be considered the use of larger volumes of samples (ex.: 1 L) preserved with neutral Lugol's solution and counts performed upon a larger sample volume to increase the precision of the counts.

4.2. Temporal variability of environmental parameters

Upwelling

Upwelling events were frequent in Aveiro littoral region during the study period and the stronger events occurred during spring and winter (Figure 3.13). Although frequent, upwelling was not a continuous process occurring as pulses of maximum intensity separated by intermediate periods of upwelling-unfavourable winds.

The occurrence of upwelling in this region has already been reported by other authors such as Fiúza *et al.* (1982) and Moita (2001), which described an upwelling season with higher intensities in the summer months (July, August and September). In another area of the west Portuguese coast (Cascais Bay) the upwelling season also occurred during spring and summer (Palma, 2003). The reported upwelling season on the NW coast of Spain occurs between March and October (Bode & Varela, 1994).

In spite of the large season of upwelling observed, the upwelling that has occurred during spring and summer was more relevant for phytoplankton growth than the upwelling that took place during winter, since in this season, the phytoplankton growth appears to be limited by light intensity (Figure 3.2 and 3.20) and not by the lower availability of nutrients (Figure 3.15, Table 3.6). The upwelling events which have occurred during spring and summer have transported to the surface waters new stocks of dissolved inorganic nutrients (Figure 3.17) which have contributed to the development of phytoplankton cells (Figure 3.20 and 3.21).

Temperature

Water surface temperature varied seasonally as is typical of temperate zones (Harris, 1986; Nybakken, 1988; Valiela, 1995) with increasing temperatures from spring to summer and progressive decrease to autumn and winter. The measured temperatures fall within the range of others previously reported by Moita (2001) and Ambar *et al.* (2002) for the Portuguese coast. The average temperature was 15.4°C and the maximum of 22.4°C, attained in August, can be correlated with a period of prevailing southerly winds. The conjunction between the warm waters that these winds have probably transported to near-shore and the high light intensities usual in August, may have contributed to this temperature maximum.

Short-term variations of water surface temperature were related to upwelling pulses (Figure 3.17). The introduction of deep colder water to the surface layers induced a decrease of the water temperature (Harris, 1986; Nybakken, 1988; Valiela, 1995; Mann, 2000).

Salinity

The average salinity value measured in this study was 35.4 PSU. The results obtained are consistent with the ones acquired by Moita (2001) for the Portuguese coast and by Casas *et al.* (1997) for the northwest Spanish coast. Dias (2001) has also reported similar values for Ria de Aveiro entrance channel in his studies of Ria de Aveiro hydrodynamics.

Salinity values remained stable most part of the period of study. Variations in salinity in semi-enclosed coastal waters are a result of evaporation, precipitation, oceanic water inflow and river discharge (Denes & Caffrey, 1988). The most important factors causing salinity changes in Ria de Aveiro are freshwater inflow along with the oceanic water inflow (Dias, 2001). Both flows become mixed at each tidal cycle and in periods when the freshwater inflow becomes negligible as a result of low precipitation (as it has occurred in Portugal during the period of study (IM, 2005) complete mixing of these water masses occurs (Dias, 2001). In this case salinity in the lagoon is close to the salinity of the oceanic water (Dias, 2001). Moreover, the timing of sampling, always in high tide, has assured that the water samples collected would be of marine source.

Nutrients

The nutrients measured in this study are usually considered essential and potentially limiting for phytoplankton growth. These include nitrogen (N) in different chemical forms (nitrates + nitrites, ammonium), phosphorus (P) in one chemical form (phosphate) and silicon (Si), an essential element for diatom development (Harris, 1986; The Open University, 1989; Valiela, 1995; Mann, 2000).

A limiting nutrient is an element that is essential for the development of phytoplankton but that is available in smaller quantities than are required by the algae to increase in abundance (Harris, 1986; Valiela, 1995). In non-limiting conditions the molar ratio of carbon (C), nitrogen and phosphorus in phytoplankton (Redfield Ratio) is C:N:P=106:16:1 (Harris, 1986; Valiela, 1995). When one of these nutrients is below this molar ratio it is considered to be limiting. However, the definition of limiting nutrient is not always that straightforward. Precisely which element is limiting will depend on the relative turnover times of the pool of the different dissolved nutrients and not on their concentrations (Harris, 1986).

The vertical and horizontal distribution of a given nutrient in surface waters is dependent of geochemical, biological and physical processes (Harris, 1986). After the nutrient uptake by the living organisms and the decay and sink of those organisms, the nutrient regeneration occurs in deep water and at the sediment interface (Harris, 1986; Valiela, 1995). The transport of these regenerated nutrients to the surface is made possible through physical processes, such as wind mixing, river runoff, tidal mixing and upwelling events (Harris, 1986; Valiela, 1995; Mann, 2000).

The measured values of nitrogen nutrients were substantially higher than previously obtained by Moita (2001) for the same region of the Portuguese coast. On the contrary, the concentration of phosphates and silicates measured was smaller. Moreover, Moita (2001) has identified higher nutrient concentrations during winter and spring whereas in this study autumn and winter were the seasons with higher average concentration of all the classes of nutrients in question. In the present work, maximum nutrient concentrations have occurred in spring and summer associated with upwelling events.

Phosphorus was the nutrient found in smaller concentrations and exerted a limiting action on the phytoplankton growth in the majority of the samples. This was not the expected result since the conventional wisdom is that nitrogen is limiting in the oceans and coastal areas and phosphorus is limiting in freshwater (Harris, 1986; Nybakken, 1988; Valiela, 1995).

The limiting role of nitrogen on phytoplankton development in coastal areas is justified by the complex cycling of this element. Nitrogen must be released from macromolecules by digestion or decomposition before it can be made available for further algal growth, and it must undergo changes in oxidation state before metabolism. Thus, it may be expected a smaller velocity of nitrogen recycling when compared to that of phosphorus (Harris, 1986). Moreover, the dynamics of nitrogen recycling is further intricate as a result of the various inorganic forms in which this element can occur in the water column: N_2 , NH_4^+ , NO_2^- , NO_3^- . These compounds can only be interconverted by bacterial action in the environment or within living cells. In surface waters the pools of dissolved inorganic nitrogen are therefore very much dependent on biological uptake and regeneration (Harris, 1986).

Phosphorus is to some extent a simpler element than nitrogen as the single ionic form PO_4^{3-} is the ubiquitous form of the element found in both the organisms and in the environment (Harris, 1986; Valiela, 1995). It seldom achieves concentrations comparable to those of nitrate because it is strongly adsorbed by particles and forms insoluble salts, while nitrates are highly soluble (Valiela, 1995). No oxidation and reduction steps are required for environmental cycling, metabolism and macromolecular synthesis (Harris, 1986).

However, the limiting nutrient for phytoplankton growth in coastal areas is not nitrogen in many occasions (Harris, 1986). The coastal systems may be phosphorus limited when nitrogen concentrations are high and $N:P > 16:1$ (Harris, 1986) as it seems to be the case in the present study. Many factors could have contributed to this observation. One of them refers to the strategy and location of sampling that was carried out under completely established conditions of high tide, in an attempt to assure that the water collected was almost exclusively of marine source; however, the samples collection was performed close to one of the walls that limit the artificial entrance of Ria de Aveiro. The existing water flow near that wall could be somewhat different from the flow of the entrance channel

central area, particularly regarding to the direction and intensity of the flow and it can exist some susceptibility of nutrient entrapment during successive stages of the tidal cycle. Nevertheless, the hypothesis that these observations are real and are not only a sampling artefact has to be taken into consideration, because the high amounts of nitrogen may be indicative of the eutrophication of Aveiro coastal area, a situation that would require careful monitoring. There are several studies which point to the eutrophication of coastal areas, situation that is characterized by the increase in frequency and abundance of phytoplankton blooms as a result of higher nutrient availability (GEOHAB, 2005). This eutrophication is mainly due to a high input of nitrogen nutrients (organic and inorganic) proceeding from a number of sources. In the present case the relative abundance of nitrogen can be due to (1) inputs from domestic and industrial sewage effluents (Mann, 2000); (2) increase of the deposition of atmospheric nitrogen (Harris, 1986; Mann, 2000; Whitall & Paerl, 2001) whose concentrations have been increasing due to the pollution, particularly in very industrialized areas (Whitall & Paerl, 2001), which is the case of Aveiro region; and (3) higher regeneration rates of this class of nutrients through the microbial loop, as a result of the activity of the very abundant group of small phytoflagellates (Nielsen & Richardson; 1989; Bode & Varela, 1994).

4.3. Annual cycle of phytoplankton biomass and community structure

The values of phytoplankton abundance and biomass observed in the present study fall within the range of those previously described by other authors for Iberian waters: Margalef (1978b), Estrada (1984), Casas *et al.* (1997), Casas *et al.* (1999), Moita (2001) and Palma (2003).

The succession model observed is similar to that expected for this area of the northwest Atlantic, corresponding to a temperate zone (Margalef, 1978b; Harris, 1986; Nybakken, 1988; Valiela, 1995), with significant differences between phytoplankton assemblages of different seasons (Table 3.1 and 3.2).

Chlorophyll *a* and total number of phytoplankton cells maximums were observed in the warmer months while minimum values were observed during winter (Figure 3.2a,b). The good and highly significant Kendall's correlation obtained between the phytoplankton

cells counts and the measured levels of chlorophyll *a* indicates a reasonable accuracy in the quantification procedure.

This seasonal variation of phytoplankton in the littoral of Aveiro can be linked with the occurrence of upwelling, with the seasonal cycle of water surface temperature, which was considered as an indicator of the conditions of stratification of the water column in this study, and the availability of dissolved nutrients, namely nitrates and nitrites (Table 3.6). All these environmental variables are interconnected (Figure 3.17), since events of upwelling are one of the mechanisms that introduce nutrients to the surface water layer, enhancing phytoplankton growth (Harris, 1986; Valiela, 1995; Mann, 2000). The input of deeper and, thus, colder waters to the surface is reflected in the temperature of the surface waters which, most of the times and even during periods of high irradiance, decrease. The variability of intensity and direction of the winds responsible for upwelling originate different hydrographic regimes which, ultimately, will condition the species composition of the phytoplankton assemblages (Margalef, 1978b; Harris, 1986; Nybakken, 1988; Valiela, 1995). In this way, the high photosynthetic biomass values observed in spring, summer and autumn were a result of the combination of upwelling events with introduction of nutrients and sufficient light intensities for the completion of photosynthesis. In winter, the higher mixture of the water column and hence higher turbulence were not translated in high phytoplankton abundances due to low light intensities characteristic of this season (Harris, 1986; Valiela, 1995; Fernández & Bode, 1994; Casas *et al.*, 1999).

Differences were found with respect to the theoretical model of phytoplankton biomass variation over the year. As expected, the spring bloom was not a continuous phenomenon with maximum abundances appearing in various pulses with the entire process taking several weeks (Figure 3.2) (Casas *et al.*, 1999). After the spring bloom a decrease in phytoplankton biomass during the summer months was expected, due to the stratification of the water column caused, in part, by the increase of the water surface temperature (evidence in Figure 3.14 – increase of surface water temperature in July, August and September). The stratification would not allow the transport of nutrients to the surface, which at this time would have been depleted by algal uptake during the spring bloom, and phytoplankton number of cells would decrease. On the contrary, probably as a result of the persistency of upwelling events during summer (Figure 3.13) there was transport of cold,

deeper and nutrient-rich waters to the photic zone (Figure 3.15), which may have allowed relative high concentrations of phytoplankton cells (Figure 3.2). In fact, the two major peaks of chlorophyll *a* concentration, which occurred in summer, were superior to those found in spring and autumn (Figure 3.2a) in such a way that the expected second annual peak of primary production in autumn was not evident. In winter, the decrease in light intensity and surface water temperature (Figure 3.14) and the increase of the water mixture due to wind action that in turn increased the turbulence of the water instigated the expected decay of the phytoplankton community, in spite of the high availability of nutrients (Figure 3.15).

Other main difference found relatively to the classical model of phytoplankton species succession was the high abundance of unidentified small phytoflagellates throughout the period of study (Figure 3.3). These organisms had a higher proportion on the total phytoplankton community than that of coccolithophorids and dinoflagellates (results not shown) (Figure 3.1). This relative high abundance is evident in Figure 3.4 where the concentration of chlorophyll *a* associated with the nanoplankton fraction (constituted mostly by small phytoflagellates) was above 40% during all the studied period. Small phytoflagellates have been previously reported as the most abundant group of phytoplanktonic organisms by Fernández & Bode (1994) and Casas *et al.* (1999). Their abundance distribution followed the pattern of the other groups of organisms with higher concentrations during spring and summer and a continuous decrease in abundance from autumn to winter. However while the other groups of organisms (namely diatoms, dinoflagellates and coccolithophorids) experienced a drastic decrease in cell numbers during winter (Figure 3.2), small phytoflagellates seemed to be able to maintain a considerable abundance during the same period (Figure 3.3). The nanoplankton biomass contributed, during this season, 60% to the total photosynthetic biomass (Figure 3.4). Small phytoflagellates seem to have, thus, a great importance in primary production. Also, their important role in nutrient recycling has been stated previously (Harris, 1986; Fernández & Bode, 1994; Casas *et al.*, 1999). Generally, these organisms predominate in waters with low nutrient concentrations, because their high surface/volume ratio enables them to advantageously utilise light and nutrients during summer stratification and downwelling periods (Margalef, 1978a). In the present study, however, when the small phytoflagellates were more abundant than the other main groups of the phytoplankton

community (particularly in winter) there was no shortage of any essential nutrient (Figure 3.11) mainly due to winter convection, which leads to a higher mixture of the water column that resuspended the nutrients from the bottom to the surface waters (Harris, 1986; Nybakken, 1988; Valiela, 1995). Relatively higher numbers of small phytoflagellates were, most probably, a result of their capacity of taking advantage of the higher turbulence of the water column to be transported to areas where the light intensity was sufficient for photosynthesis. Their small size and high division rate would enable them to compensate the cell losses due to that turbulence maintaining their abundance (Margalef, 1978a) and to take advantage of temporally more favourable conditions to increase in numbers. Many of these small flagellates are auxotrophs, heterotrophs or mixotrophs and thus play an important role in the alternative pathway of nutrient recycling called microbial loop (Harris, 1986; Fernández & Bode, 1994; Casas *et al.*, 1999). It has been estimated that at the end of an upwelling event the microbial system could generate more than 50% of the nitrogen consumed by the phytoplankton (Bode & Varela, 1994). This component makes the identification of small phytoflagellates group of Ria de Aveiro a priority matter in the near future.

Small phytoflagellates aside, diatoms formed the bulk of phytoplankton in the area studied, the results being consistent with the ones previously described for other regions of the Portuguese coast by Moita (2001) and Palma (2003) and for the northwest Spanish coast (Casas *et al.*, 1997; Casas *et al.*, 1999; Estrada, 1982) (Figure 3.2c). However, an exception occurred in autumn, when the proportion of coccolithophorids in the phytoplankton assemblage was superior to that of diatoms, most probably due to a very large bloom of *Syracosphaera pulchra* that began during the end of summer but whose abundance maximum ($8.7 \times 10^5 \text{ cells} \cdot \text{L}^{-1}$) was achieved on 04 October 2004.

Another marked difference found in respect to other coastal zones was the non dominance of dinoflagellates during the summer (Margalef, 1978a; Estrada, 1982; Harris, 1986; Nybakken, 1988; Valiela, 1995). In fact, their relative dominance has decreased from spring to summer (Figure 3.7). The succession did not progress up to the establishment of well defined associations of dinoflagellates, possibly because of the persistency of upwelling events that may have prevented the formation of a permanent stratified surface layer and destabilized the water column (Figure 3.13), allowing the enhanced phytoplankton growth and keeping the succession at its initial stages (Margalef, 1978a).

However, samples were collected in a coastal sampling station which is subjected to higher water turbulence. It is possible that dinoflagellates could be dominant of assemblages of phytoplankton occurring offshore (Moita & Silva, 2001). Diatoms were almost always present and were dominant most of the times (Figure 3.5), which may also be a consequence of the frequency of upwelling and mixing events (Margalef, 1978b; Casas *et al.*, 1997). The periods when dinoflagellates were dominant were related to upwelling relaxation events (Figure 3.5 and 3.13) that temporarily decreased the instability of the water column allowing the proliferation of dinoflagellates (k-strategists), which are slow growers but have the capability of moving to areas with higher nutrient availability. This mobility capacity represents an advantage when in conditions of stratification and consequent nutrient depletion (Margalef, 1978a; Harris, 1986). During periods of higher water mixture, like upwelling events or storm seasons, like winter, diatoms (r-strategists) possess greater competitive advantage (Margalef, 1978a; Harris, 1986). Many species are colony-forming and lack mobility and have a tendency to sink due to their heavy silicified cell wall. In this way the water mixture allows them to be transported to areas of the water column where light intensity is sufficient for photosynthesis and nutrients storage (Harris, 1986; Mann, 2000). Moreover, their fast reproduction rates enable them to multiply rapidly maintaining or increasing the numbers of the initial population and thus assuring their survival in unpredictable climate conditions (Margalef, 1987a; Harris, 1986). The high availability in nutrients usually correlated with the periods of higher turbulence sustains these high division rates (Margalef, 1978a).

The ANOSIM tests performed upon the biological and environmental data allowed the establishment of four main epochs both in terms of species composition of phytoplankton assemblages (Table 3.2) and of environmental parameters (Table 3.4): spring, summer, autumn and winter. The results obtained with the biological data class matrix did not dissociate spring and summer phytoplankton assemblages (Table 3.2) but the following analysis with the genera and species matrix have demonstrated significant differences between these epochs concerning lower phytoplankton taxa ranks. These results indicate a similarity between the relative abundance of large groups, namely diatoms and dinoflagellates that have more or less maintained the same proportions, between spring and summer, in the phytoplankton community (Figure 3.7). The more significant difference was due to an increase of coccolithophorid proportion in the summer phytoplankton

assemblage. The similarities between these assemblages are probably a result of the influence of upwelling and upwelling relaxation events that were abundant in both seasons.

The change in the specific composition of the phytoplankton community between these four periods was gradual as shown in the MDS plot presented in Figure 3.6. A certain temporal gradient occurs that initiates with spring and summer phytoplankton assemblages, which are more similar, and an autumn community that appears to make the transition between this community and the winter phytoplankton assemblage. These gradual changes are also visible by the joint observation of the pie charts presented in Figure 3.7. Moreover, the non-existence of perfect indicators, i.e. phytoplankton species that were present in one group and absent from the others, also reflects the gradual variations of the species composition of the phytoplankton community.

The results obtained suggest that, in a general way, the annual cycle of phytoplankton succession in Ria de Aveiro progressed as follows:

Spring phytoplankton assemblage

In spring, with the increase of light intensity and high availability of nutrients, due to their transport to the surface waters during winter and to the persistence of upwelling events, the phytoplankton biomass increased. The growth of phytoplankton was apparently nutrient limited, particularly by phosphorus, except on two occasions (27 April 2005 and 17 May 2005), when the Redfield ratio was N:P < 16:1 and thus phytoplankton growth was limited by nitrogen.

The phytoplankton community was dominated by small phytoflagellates, diatoms like *Leptocylindrus danicus* and *Pseudo-nitzschia* spp., small unidentified armoured dinoflagellates and *Prorocentrum* cf. *minimum*. Both proliferations of *Leptocylindrus danicus* (08 April and 09 May 2005) occurred in response to upwelling events (Figure 3.13), the first one of $-2114 \text{ m}^3\text{s}^{-1}\text{km}^{-1}$ and the second of $-1002 \text{ m}^3\text{s}^{-1}\text{km}^{-1}$. In both cases the concentration of all nutrients analysed was brought to very low levels except in the case of nitrate + nitrite concentration on 09 May 2005, when an increase was observed. The high abundance of phytoplankton in conditions of nutrient depletion is probably due to the necessary time of adaptation of the phytoplankton cells to the conditions of high availability of nutrients after the upwelling pulses (Dugdale *et al.*, 1990; Bode & Varela,

1994). This nutrient depletion may also be due to consumption by the phytoplankton cells. Maximum abundances of phytoplankton cells are usual when the nutrients concentrations of the surrounding waters are low and the upward flow of water diminished (Dugdale *et al.*, 1990; Bode & Varela, 1994).

Prorocentrum cf. minimum, a common, neritic, bloom-forming dinoflagellate widely distributed in the northern hemisphere waters, especially in estuarine areas (Denardou-Queneherve, 1999; Witek, 2000; Heil *et al.*, 2005) occurred with relative expression during spring. Its occurrence in Ria de Aveiro waters raises another area of importance in the assessment of toxic microalgae, since this species has been related to shellfish and human poisonings in Japan, Portugal (Lagoa de Óbidos) and Norway (Silva, 1985; Silva & Peixoto, 1987; Denardou-Queneherve, 1999; Sierra-Beltrán, 2004; Heil *et al.*, 2005). There is still no consensus on whether *P. minimum* is toxic (Wikfors, 2005) despite different studies on toxicity have reported it as a producer of a PSP-like toxin, a toxin that causes liver damage and is designated as venerrupin (Denardou-Queneherve, 1999; Witek, 2000; Sierra-Beltrán, 2005) and a diarrhetic shellfish toxin (Witek, 2000). There is also evidence that it produces neurotoxins (Grzebyk *et al.*, 1997). These different toxins are related to different strains of *Prorocentrum minimum* (Denardou-Queneherve, 1999; Witek, 2000). In the Mexican coast there is indication that the geographical spread of *P. minimum* is associated with climate changes and that bloom formation is related to anthropogenic activities and, in this sense, *P. minimum* blooms are a signal of changing water quality (Sierra-Beltrán, 2005) and a response to increasing coastal eutrophication (Heil *et al.*, 2005). At the moment, this species is not included in the set of marine toxic phytoplankton species that are monitored in Ria de Aveiro. It is then recommended to include this species in the monitoring program both in terms of phytoplankton quantification and toxin identification and quantification.

Summer phytoplankton assemblage

The summer season was characterized by the progressive increase in temperature of the surface waters, most probably as a result of the increase in the light intensity characteristic of this season. The phytoplankton growth limiting factor was again the availability of nutrients, in this case nitrogen.

Phytoplankton biomass values remained high due to the input of new supplies of dissolved nutrients to the surface waters by upwelling pulses. In opposition to what was expected, there was not a change in the dominance of the phytoplankton community from diatoms to dinoflagellates. The persistency of the upwelling events and thus the higher turbulence of the water column continued to favour the diatom strategy. Nevertheless, during periods of upwelling relaxation and more stable conditions of the water column dinoflagellates assemblages have dominated the phytoplankton community.

The most frequent species in the summer assemblage continued to be *Leptocylindrus danicus* accompanied by other diatoms like *Chaetoceros* spp., *Thalassiosira* spp., *Pseudonitzschia* spp. and *Thalassionema nitzschioides*. These are diatoms typical of upwelled waters (Moita, 2001) and their high abundance in this season is a result of the strong upwelling events that have occurred. Small phytoflagellates were also abundant as well as the coccolithophorid *Syracosphaera pulchra*, and other armoured dinoflagellates, especially *Scrippsiella* cf. *trochoidea*. Although not dominant, the dinoflagellates genera *Dinophysis*, *Ceratium*, *Protoperidinium* and *Prorocentrum* increased in numbers.

The highest number of species and individuals, and the higher species richness (d) was encountered in this season but it was also this phytoplankton assemblage who was strongly dominated, namely by *Leptocylindrus danicus* and *Syracosphaera pulchra* (Appendix I, Table 3).

Autumn phytoplankton assemblage

The phytoplankton assemblage of the autumn season was dominated by organisms of the Prymnesiophyceae class (coccolithophorids), namely *Syracosphaera pulchra*, *Emiliania huxleyi* and *Gephyrocapsa* spp.. Small phytoflagellates and small armoured dinoflagellates were also abundant. The diatom group has lost much of its expression in the community while the dinoflagellates kept, more or less, the same expression inside the phytoplankton community from summer to autumn. This was probably due to a decrease in the upwelling intensity that has allowed more stable conditions in the water column which favoured the dinoflagellates strategy (Margalef, 1978a) and coccolithophorids development.

Once more, the phytoplankton development was, in general, apparently limited by the availability of nutrients in the surface waters, namely phosphorus.

Winter phytoplankton assemblage

In winter, the decrease in the water surface temperature corresponded to the decrease in irradiance. The increase in wind strength, usual in this time of year, intensified the water column mixture and the regenerated nutrients in the deeper layers were transported to the surface. Moreover, the upwelling pulses attained their higher significance at this season. However, the phytoplankton biomass and cell numbers have significantly decreased during this period. Phytoplankton growth was probably limited by the availability of light intensity, necessary for photosynthesis, being unable to take full advantage of the higher dissolved nutrients concentration.

Diatoms continued to dominate the phytoplankton assemblage, and the dominance of the assemblage was shared by a variety of species: *Chaetoceros* spp., *Guinardia delicatula*, *Lauderia annulata*, *Pseudo-nitzschia* spp., *Thalassiosira* spp. and *Cylindrotheca closterium*. Many of these species are described by Moita (2001) as typical of periods of stronger water mixing or of upwelling waters. Dinoflagellates and coccolithophorids have decreased largely in abundance, but *Emiliania huxleyii* and *Gephyrocapsa* spp., in spite of their smaller abundance, were always present in the water column. Phytoflagellates, such as Euglenophyceae, increased in relative importance. Small phytoflagellates were really the most abundant group in terms of cells numbers being able to maintain their abundance even when the conditions of the water column were not the most favourable.

This period is characterized by a smaller number of species present and also by a decrease on total phytoplankton number of cells. It has the smallest richness index but higher evenness i.e. the organisms are more equitably distributed among the different species and thus the dominance of some species in the assemblage is less marked.

This annual cycle of succession can be summarized by the following figure (Figure 3.26):

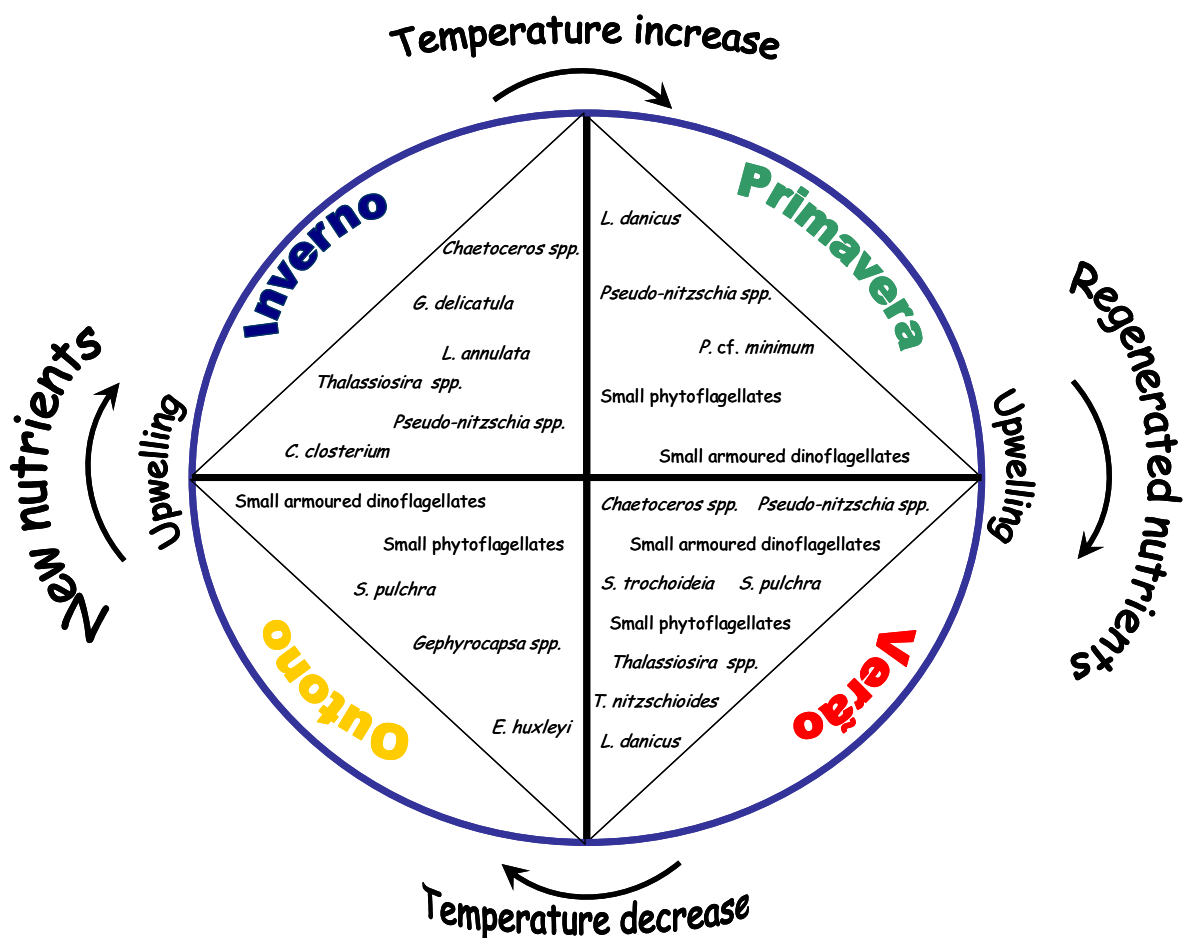


Figure 3.26. Annual cycle of phytoplankton succession in Ria de Aveiro

Phytoplankton succession cycles associated with upwelling events

As previously referred, one of the main contributors for the observed seasonal variation of phytoplankton was the frequency and intensity of the upwelling events in parallel with the seasonal cycle of stratification of the water column, here inferred by the changes of the temperature of the surface waters. This influence of the upwelling in the abundance of phytoplankton species can be observed in Figure 3.20. Although the response of the microalgae to the upwelling events by increasing in abundance is clear the peaks are not exactly correlated with the stronger upwelling pulses, probably due to the necessary time of adaptation of the phytoplankton cells to the new conditions of the water column (Dugdale *et al.*, 1990).

Margalef (1978a) has stated that a phytoplankton succession cycle associated with upwelling events can be divided in three stages: (1) when small diatoms like *Skeletonema* spp., *Chaetoceros* spp., and *Thalassiosira* spp. proliferate due to quicker rates of division;

(2) when larger diatoms begin to dominate the phytoplankton assemblage, such as *Thalassiosira rotula*, *Lauderia* spp., *Eucampia* spp., *Chaetoceros* spp., *Rhizosolenia* spp., *Thalassionema* spp. and *Nitzschia* spp.; (3) and dominance of *Dinophysis* spp., *Peridinium* spp., *Ceratium* spp. and other dinoflagellates that increase in abundance when the turbulence of the water column decreases after an upwelling pulse.

In the present study area each phytoplankton proliferation episode associated with upwelling pulses is dominated by a different diatom species or set of species characteristic of upwelled waters (Moita, 2001). This difference observed in the species composition and abundance of the blooming diatoms may reflect the period between the beginning of the upwelling event and the date of sampling (Palma, 2003). For example the upwelling pulse that gave rise to the proliferation of small forms of *Thalassionema nitzschioides* and *Thalassiosira* spp. on 05 July 2004 had occurred 4 days before the date of sampling, thus the sample corresponded to the final phase of the first stage of the phytoplankton succession (Margalef, 1978a; Moita, 2001; Palma, 2003). The proliferation of *Pseudo-nitzschia* spp. that took place on 12 July 2005 happened in response to an upwelling pulse that had occurred 6 days before the date of sampling (Figure 3.21). This corresponds to the second stage of phytoplankton succession when larger diatom species proliferate. In spite of these examples it was often very difficult to identify the pattern of variation in the specific composition of the diatom community perhaps because this variation is a very rapid progress; the dominance of dinoflagellates in conditions of upwelling relaxation or convergence is not evident also. In order to observe with detail the evolution of the diatom community through time it would be necessary to increase the frequency of sampling from weekly to daily when upwelling favourable winds establish. This increase in the sampling frequency could also allow the analysis of the diatom-dinoflagellate succession associated with episodes of upwelling and upwelling relaxation.

4.4. Phytoplankton communities

The classification analysis of the genera matrix revealed a community similar to the previously described by Moita (2001), common in conditions of water column stratification. It was composed by the genera *Dinophysis*, *Scrippsiella*, *Prorocentrum*, *Ceratium*, *Protoperidinium*, *Katodinium*, *Gyrodinium* and *Amphidinium*. At a lower

similarity level, this community emerged together with *Pseudo-nitzschia* and *Detonula*. For this reason it is thought that this assemblage is more abundant during periods of alternation between upwelling conditions, when diatoms will prevail, and upwelling relaxation conditions, where dinoflagellates will be more frequent.

The community comprising *Actinopterychus* spp., *Cerataulina* sp., *Emiliana* sp., *Gephyrocapsa* sp., *Guinardia* spp., *Meuniera* sp., *Navicula* spp., *Paralia* sp. and *Skeletonema* spp. appears to be more frequent under conditions of higher vertical mixture of the water column, mainly in winter, although the species occur during the entire study period. The assemblage that includes *Chaetoceros* spp., *Thalassiosira* spp., *Thalassionema* spp. and *Rhabdonema* spp. also occurs in higher abundances in periods of water mixture.

The phytoplankton species whose abundance fluctuation was similar to that of *Dinophysis* cf. *acuminata* were *Amphidinium latum*, *Gyrodinium fusiforme*, *G. lacryma*, *Mesoporus perforatus* and *Prorocentrum* cf. *minimum*. The species that tended to co-occur with *Dinophysis acuta* were the dinoflagellates *Amphidinium* sp. (unidentified species), *Katodinium glaucum*, *Ceratium fusus*, *Scrippsiella* cf. *trochoidea*, *Prorocentrum micans* and the centric diatom *Proboscia alata* (Table 3.8). These genera have been referred by Moita (2001) as members of the summer community of Portuguese coastal waters.

In the present study, harmful algal blooms of *Dinophysis* cf. *acuminata* occurred in spring (2004 and 2005) and of *D. acuta* in summer and autumn. Both species proliferated during conditions of upwelling relaxation as it has been reported previously (Palma *et al.*, 1998; Moita *et al.*, 2005a). *Dinophysis* cf. *acuminata* occurred in colder surface waters than *Dinophysis acuta*. The abundances of these species recorded during the studied period are relatively small when compared to other years: in 2003 *Dinophysis acuta* achieved a concentration of 50×10^3 cells·L⁻¹ (Moita *et al.* 2004) and in the autumn of 2005 this maximum was overcome by a bloom of 203×10^3 cells·L⁻¹ (Moita *et al.*, 2005b). These values were obtained with the Monitoring method of phytoplankton quantification, that tends to overestimate the abundance of the cells (see Chapter II), and must be compared with caution with the data of the present study, which were obtained by the Uthermöhl method. However, the corresponding values of *Dinophysis* spp. abundance obtained with the Monitoring technique for the same period (Figure 2.1) continue to be significantly smaller than the ones recorded by Moita *et al.* (2004, 2005b).

Despite these relative small abundances, bivalve shellfish were heavily contaminated with DSP toxins during the studied period, considering the maximum limit of DSP toxins established by the European Commission Decision 2002/225/CE: 16 µg of DSP toxins per 100 g of bivalve meat. In fact, during the period of proliferation of *Dinophysis* cf. *acuminata* a maximum contamination by OA in *Mytilus edulis* close to 100µg.100g⁻¹ was measured and when *Dinophysis acuta* was the dominant toxic species, OA reached the level of 156 µg·100 g⁻¹ and DTX2 of 85 µg·100 g⁻¹ (unpublished data from Plano Nacional de Salubridade de Bivalves supplied by Laboratório de Biotoxinas do INIAP/IPIMAR).

Both *Dinophysis* species have occurred in conditions of rich supply of nitrogen. Episodes of proliferation of harmful algae have already been related to increasing eutrophication of the coastal areas (Mann, 2000; GEOHAB, 2005; Heil *et al.* 2005).

5. Conclusions

The adopted sampling strategy was considered adequate for the study of the temporal patterns of phytoplankton distribution as well as for the identification of the phytoplankton species succession during one annual cycle. However, for the study of the short-term succession cycles associated with upwelling events a daily frequency of sampling, during the appropriate periods, may be recommended.

The technique of phytoplankton quantification and identification used in this study (Utermöhl method) was also considered suitable for the achievement of the main objectives of this work, which were focused mostly in seasonal ecological variations of the phytoplankton community in general and of the most important constituents of that community (diatoms, dinoflagellates and coccolithophorids). However, in future work specific techniques of identification should be applied to each phytoplankton group in order to identify the organisms that make part of the marine phytoplankton community that enters in Ria de Aveiro in a more accurate way. These additional techniques of identification should include both the use of other fixatives, like for example Lugol's solution, and of other types of microscopy, such as electron microscopy.

The approach used for the multivariate analysis of the biotic and environmental data – the use of MDS upon an ANOSIM test - has proven to be efficient in separating the different

assemblages of phytoplankton species that occur in different seasons, correlating them with different hydrographic regimes. The followed strategy revealed the patterns of the temporal distribution of the data without making previous assumptions. However further work should be done in order to associate the phytoplankton communities, found during the r-analysis, to the physical and chemical conditions of the water column.

The variation in the specific composition of the four phytoplankton assemblages identified was correlated with the seasonal cycle of water surface temperature, which was considered an indicator of the conditions of stratification or mixture of the water column in this study, the occurrence and intensity of upwelling, and the availability of dissolved nutrients, namely nitrates and nitrites.

A typical seasonal phytoplankton succession cycle of upwelling temperate zones was observed in Aveiro. The period from May 2004 to May 2005 was characterized by high values of photosynthetic biomass and microalgae abundance during the warmer months and accentuated decrease of these values during winter. Differences, however, were found with respect to the theoretical model of phytoplankton biomass variation and species succession over the year. It was not observed the typical decrease of phytoplanktonic biomass during summer neither the increase in the relative dominance of dinoflagellates during the same season. These differences were correlated with the persistency and variability of intensity of the upwelling pulses, recorded during the period of study, which prevented the formation of a permanent stratified surface layer and destabilized the water column, allowing the enhanced phytoplankton growth and keeping the succession at its initial stages.

Other main difference found relatively to the classical model of phytoplankton species succession was the high abundance of unidentified small phytoflagellates. This group of organisms not only includes photosynthetic organisms, and thus has great importance in primary production, but also comprises auxotrophic organisms which have been recently involved by several authors in the recycling of nutrients through the microbial loop. This statement is particularly important because the recycling of nutrients through the microbial loop may be one of the sources of the high concentrations of nitrogen nutrients found in the coastal waters of Aveiro, in parallel with other causes such as: inputs from domestic and industrial sewage effluents and increased deposition of atmospheric nitrogen. All these

factors may have a role in the high concentrations of several chemical forms of nitrogen which may be indicative of the eutrophication of the coastal waters of Aveiro, situation that should deserve future and careful monitoring. These relative high nitrogen concentrations were revealed by the results which indicated phosphorus as the limiting factor for phytoplankton growth, in the majority of samples, instead of nitrogen, the nutrient which is usually pointed out as limiting for the phytoplankton development in coastal areas. This probable limitation of phytoplankton development by the availability of dissolved nutrients took place in spring, summer and beginning of autumn. At the end of autumn and winter the limitation of phytoplankton growth was probably exerted by the decrease in solar irradiance.

The high frequency sampling strategy adopted revealed the existence of phytoplankton succession cycles associated with processes of upwelling and upwelling relaxation; however it was not sufficiently frequent to allow the clear identification of the phytoplankton species involved in those succession cycles. Often, during the summer, it was verified a succession diatoms-dinoflagellates, with the diatoms of rapid growth and deprived of mobility prevailing in periods of upwelling, with higher water mixture and availability of nutrients. The dinoflagellates of slow growth but that are capable of moving to areas of higher light intensity and nutrient availability, dominated in conditions of upwelling relaxation or water column stratification.

Proliferations of *Prorocentrum cf. minimum*, a dinoflagellate indicated by several authors as a potential producer of several types of phycotoxins and harmful to humans via shellfish poisoning, were recorded during the entire studied period particularly during spring. At the moment, this species is not included in the set of marine toxic phytoplankton species that are monitored in Ria de Aveiro. It is then advised to include this species in the monitoring program both in terms of phytoplankton quantification and toxin identification and quantification.

The multivariate statistical method applied in the present work also allowed determining different communities of phytoplankton species whose abundance tends to fluctuate in parallel through time. The characteristic communities of upwelled waters and higher water mixture and of water column stratification previously described by Moita (2001) were identified, although the fact that they were not correlated with the physical state of the

water column. Moreover, the accompanying communities of *Dinophysis* cf. *acuminata* and *D. acuta* were identified and were associated with upwelling relaxation events. *Dinophysis* cf. *acuminata* proliferated during spring and beginning of summer while *D. acuta* was most abundant during summer and beginning of autumn. Most part of the times both *Dinophysis* species occurred during conditions of high levels of nitrogen.

6. References

- Ambar I, Serra N, Brogueira MJ, Cabecadas G, Abrantes F, Freitas P, Goncalves C & Gonzalez N (2002) Physical, chemical and sedimentological aspects of the Mediterranean outflow off Iberia. *Deep-Sea Research II* 49: 4163-4177.
- Bakun A (1973) Coastal upwelling indices, west coast of North America. NOAA Tech. Report NMFS SSRF-671: 1946-71.
- Barnes RSK & Hughes RN (1988) *An Introduction to Marine Ecology* (2nd edn). Blackwell Science, Oxford.
- Bode A & Varela M (1994) Planktonic carbon and nitrogen budgets for the N-NW Spanish shelf: the role of pelagic nutrient regeneration during upwelling events. *Scientia Marina* 58 (3):221-231.
- Bollmann J, Cortés MY, Haidar AT, Brabec B, Close A, Hofmann R, Palma S, Tupas L & Thierstein HR (2002) Techniques for quantitative analyses of calcareous marine phytoplankton. *Marine Micropaleontology* 44: 163-185.
- Casas B, Varela M & Bode A (1999) Seasonal succession of phytoplankton species on the coast of A Coruña (Galicia, northwest Spain). *Boletín del Instituto Español de Oceanografía* 15 (1-4): 413-429.
- Casas B, Varela M, Canle M, González N & Bode A (1997) Seasonal variations of nutrients, seston and phytoplankton, and upwelling intensity off La Coruña (NW Spain). *Estuarine, Coastal and Shelf Science* 44: 797-778.
- Clarke KR & Warwick RM (1994) *Change in marine communities: an approach to statistical analysis and interpretation*. Plymouth Marine Laboratory, UK, 141 p.

- Daget J (1976) Les modèles mathématiques en écologie (2^{ème} ed). In: Collection d'Écologie 8. Masson, Paris, France.
- Denardou-Queneherve A, Grzebyk D, Pouchus YF, Sauviat MP, Alliot E, Biard JF, Berland B & Verbist JF (1999) Toxicity of French strains of the dinoflagellate *Prorocentrum minimum* experimental and natural contaminations of mussels. *Toxicon* 37:1711-1719.
- Dias JM (2001) Contribution to the study of the Ria de Aveiro hydrodynamics. PhD dissertation, University of Aveiro, Aveiro, Portugal, 288 p.
- Dodge JD (1982) Marine dinoflagellates of the British Isles. HM Stationery Office, London, 303 p.
- FAO (2004) Marine Biotoxins. FAO Food and Nutrition Paper, 80. Food and Agriculture Organization of the United Nations, Rome, 278 p.
- Field JG, Clarke KR & Warwick RM (1982) A practical strategy for analysing multispecies distribution patterns. *Marine Ecology Progress Series* 8:37-52.
- Fiúza A, Macedo ME & Guerreiro MR (1982) Climatological space and time variation of the Portuguese coastal upwelling. *Oceanologica Acta* 5:31-40.
- GEOHAB (2005) Global Ecology and Oceanography of Harmful Algal Blooms, GEOHAB Core Research Project: HABs in Upwelling Systems. G. Pitcher, T. Moita, V. Trainer, R. Kudela, P. Figueiras, T. Probyn (Eds.) IOC and SCOR, Paris and Baltimore. 82 p.
- Gross GM (1933) Principles of oceanography (7th edn). Chesapeake Resource Consortium – University of Maryland. Prentice Hall, Englewood Cliffs, New Jersey.
- Guiry MD, Rindi F & Guiry GM (2006). AlgaeBase version 4.0. World-wide electronic publication, National University of Ireland, Galway [consulted on February 2006]. Available from:
<<http://www.algaebase.org>>

- Hallegraeff GM (2003) Harmful algal blooms: a global overview. In: Hallegraeff GM, Anderson DM & Cembella AD (eds) Manual on harmful marine microalgae (2nd edn). UNESCO Publishing, p 25-46.
- Harris GP (1986) Phytoplankton ecology: structure, function and fluctuation. Chapman and Hall, London, 384 p.
- Hasle GR (1978) Identification problems: Some specific preparations - Diatoms. In: Sournia A (ed) Phytoplankton manual. UNESCO, United Kingdom, p 136-142.
- Hasle GR & Syvertsen EE (1996) Marine Diatoms. In: Tomas CR (ed) Identifying marine diatoms and dinoflagellates. Academic Press, Inc., New York, p 5-385.
- Heil CA, Glibert PM & Chunlei F (2005) *Prorocentrum minimum* (Pavillard) Schiller: A review on a harmful algal bloom species of growing worldwide importance. In: Gilbert PM & Sellner KG (eds) Harmful algae 4(3): 447-650
- Heimdal BR (1978) Identification problems: Some specific preparations - Coccolithophorids. In: Sournia A (ed) Phytoplankton manual. UNESCO, United Kingdom, p 148-150.
- Heimdal BR (1996) Modern Coccolithophorids. In: Tomas CR (ed) Marine phytoplankton: a guide to naked flagellates and coccolithophorids. Academic Press, Inc., New York, p 147-247.
- Holm-Hansen O, Lorenze CJ, Wolmes W & Strickland JD (1965) Fluorometric determination of chlorophyll. CIEM 30:3-15.
- Instituto de Meteorologia [IM] (2005) Acompanhamento da situação de seca meteorológica [on-line]. Ministério da Ciência, Inovação e Ensino Superior, Portugal [consulted in February 2006]. Available from:
<<http://www.inag.pt/inag2004/port/divulga/actualidades/seca>>
- IOC (2005) The IOC harmful algal programme [on-line]. Intergovernmental Oceanographic Commission of UNESCO, Paris, France. [consulted in September 2005] Available from:
<<http://ioc.unesco.org/hab/intro.htm>>

- Leadbeater BSC (1978) Identification problems – Some specific preparations: other flagellates. In: Sournia A (ed) *Phytoplankton manual*. UNESCO, United Kingdom, p 151-153.
- Legendre L & Legendre P (1984a) *Écologie numérique: Le traitement multiple des données écologiques* (2 ed). Presses de L'Université du Québec, Québec, Canada, 260 p.
- Legendre L & Legendre P (1984b) *Écologie numérique: La structure des données écologiques* (2 ed). Presses de L'Université du Québec, Québec, Canada, 335 p.
- Mann KH (2000) *Ecology of coastal waters: with implications for management* (2nd edn). Blackwell Science, Massachusetts, USA, 406 p.
- Margalef R (1978a) Life-forms of phytoplankton as survival alternatives in an unstable environment. *Oceanologica acta* Vol I (4): 493-508.
- Margalef R (1978b) Phytoplankton communities in upwelling areas: the example of NW Africa. *Oecologia aquatica* 3:97-132.
- Moita MT (1993) Development of toxic dinoflagellates in relation to upwelling patterns off Portugal. In: Smayda TJ & Shimizu Y (Eds.) *Toxic Phytoplankton Blooms in the Sea*. Elsevier, Amsterdam, The Netherlands, p 299-304.
- Moita MT (2001) Estrutura, variabilidade e dinâmica do fitoplâncton na costa de Portugal continental. PhD dissertation. Faculdade de Ciências da Universidade de Lisboa. Lisboa, Portugal. 272 p.
- Moita MT & Sampayo MA de M (1993) Are there cysts in the genus *Dinophysis*? In: Smayda TJ & Shimizu Y (Eds.) *Toxic Phytoplankton Blooms in the Sea*. Elsevier, Amsterdam, The Netherlands, p 153-154.
- Moita MT & Vilarinho MG (1999) Checklist of phytoplankton species off Portugal: 70 years of studies. *Portugaliae Acta Biol., Sér.B, Sist.* 18:5-50.
- Moita MT, Silva AJ (2001) Dynamic of *Dinophysis acuta*, *D. acuminata*, *D. tripos* and *Gymnodinium catenatum* during an upwelling event of the Northwest coast of Portugal. In: Hallegraeff GM, Blackburn SI, Bolch CJ & Lewis RJ (Eds.) *Harmful Algal Blooms 2000*, IOC of UNESCO.

- Moita MT, Palma AS, Vilarinho MG (2005a) Blooms de fitoplâncton na costa Portuguesa. IPIMAR Divulgação, nº31, Lisboa, Portugal.
- Moita MT, Palma S, Gonçalves L, Vilarinho G, Cerejo M, Silva A & Oliveira PB (2004) The highest blooms of *Dinophysis acuminata* and *Dinophysis acuta* on the NW coast of Portugal (2002 and 2003). In: XI International Conference on Harmful Algal Blooms, Cape Town, South Africa.
- Moita MT, Silva A, Gonçalves AS, Vilarinho G, Cerejo M, Palma S, Vidal T & Quental T (2005b) Relatório INAG/IPIMAR 2005, Lisboa, Portugal.
- Nielsen TG & Richardson K (1989) Food chain structure of the North Sea plankton communities: seasonal variations of the role of the microbial loop. Marine Ecology Progress Series 56:75-87.
- Nybakken JW (1988) Marine biology: an ecological approach (2nd edn). Harper Collins Publishers, New York 513 p.
- Palma AS (2003) Estudo de um ciclo anual de sucessão fitoplanctónica na Baía de Cascais. Master dissertation. Faculdade de Ciências da Universidade do Porto, Porto, Portugal, 64p.
- Palma AS, Vilarinho, MG, Moita MT (1998) Interannual trends in the longshore variation of *Dinophysis* off the Portuguese coast. In: Reguera B, Blanco J, Fernández ML, Wyatt T (eds) Harmful Algae. Xunta de Galicia and Intergovernmental Oceanographic Commission of UNESCO, Paris, p 124-127.
- Peragallo H & Peragallo M (1908) Diatomées marines de France. Tempere HJ (ed). Grez-sur-Loing, 491 p.
- Pielou EC (1977) Mathematical ecology. John Wiley & Sons, Inc., USA.
- Pissarra JL & Cavaco MH (1984) Análise fluorimétrica de pigmentos fotossintéticos: calibração e controlo das medições. Relatório INIP nº 23, p 5-12.

- Reguera B (2003) Biología, autoecología y toxicología de las principales especies del género *Dinophysis* asociadas a episodios de intoxicación diarreogénica por bivalvos (DSP) [on-line]. Tesis Doctoral, Universidad de Barcelona, Barcelona, España. 298p. [consulted on January 2006]. Available from:
<http://www.tdx.cesca.es/TESIS_UB/AVAILABLE/TDX-0628104-12836//TESISREGUERA.pdf>
- Round FE, Crawford RM & Mann DG (1990) The diatoms: Biology and morphology of the genera. Cambridge University Press, Cambridge, 747 p.
- Sampayo MA de M, Alvito P, Franca S, Sousa I (1990) *Dinophysis* spp. toxicity and relation to accompanying species. In: Graneli E, Sundstrom B, Edler L, Anderson DM (eds) *Toxic Marine Phytoplankton*. Elsevier, New York, p 215-220.
- Schiller J (1937) Dinoflagellatae. Akad. Verlagsgesellschaft MBH, Leipzig, Vol. I 617 p; Vol.II, 589 p.
- Sierra-Beltrán AP, Cortés-Altamirano R & Cortés-Lara MC (2005) Occurrences of *Prorocentrum minimum* (Pavillard) in México. In: Gilbert PM & Sellner KG (eds) *Harmful algae* 4(3): 507-517.
- Silva ES & Peixoto ME (1987) Factores ecológicos relacionados com duas “Marés Vermelhas” na Lagoa de Óbidos. *Arquivos do Instituto Nacional de Saúde* 12: 129-168.
- Silva ES (1985) Ecological factors related to *Prorocentrum minimum* blooms in Óbidos lagoon (Portugal). In: Anderson, White & Baden (eds) *Toxic Dinoflagellates*. Elsevier Science Publishing Co., Inc., p 251-256.
- Sokal RR & Rohlf FJ (1969) *Introduction to Biostatistics* (2nd edn). WH Freeman and Company. New York. p 363.
- Steidinger KA, Tangen K (1996) Dinoflagellates. In: Tomas CR (ed) *Identifying marine diatoms and dinoflagellates*. Academic Press, Inc., New York, p 387-598.
- Summerhayes CP & Thorpe SA (1996) *Oceanography: An illustrated guide*. Southampton Oceanography Centre, Manson Publishing, London, United Kingdom.

- Taylor FJR (1978) Identification problems – Some specific preparations: Dinoflagellates. In: Sournia A (ed) *Phytoplankton manual*. UNESCO, United Kingdom, p 143-147.
- The Open University (1989) *Seawater: its composition, properties and behaviour*. Pergamon Press, Oxford, England, 164p.
- Thronksen J (1978) Preservation and storage. In: Sournia A (ed) *Phytoplankton manual*. UNESCO Publishing, United Kingdom, p 69-74.
- Thronksen J (1996) The planktonic marine flagellates. In: Tomas CR (ed) *Identifying marine phytoplankton*. Academic Press, Inc., New York, p 7-145.
- Thurman HV (1996) *Essentials of Oceanography* (5th edn). Mt. San Antonio College. Prentice Hall: Upper Saddle River, New Jersey.
- Utermöhl H (1958) Zur vervollkommnung der quantitativen phytoplankton-methodik. *Mitt. Int. Ver. Theor. Angew. Limnol* 9: 1-38.
- Vale P (2004) Differential dynamics of dinophysistoxins and pectenotoxins between blue mussel and common cockle: a phenomenon originating from the complex toxin profile of *Dinophysis acuta*. *Toxicon* 44:123-134.
- Vale P, Cerejo M & Vilarinho MG (2004). Toxin production by *Dinophysis* spp. at Ria de Aveiro, Portugal. In press in: *Proceedings of 5th International Conference on Molluscan Shellfish Safety*, Galway, Ireland, 14-18 June 2004.
- Valiela I (1995) *Marine ecological processes* (2nd ed). Springer-Verlag, New York, 686 p.
- Van Den Hoek C, Mann DG & Jahns HM (1995). *Algae: an introduction to phycology*. Cambridge University Press, Cambridge, U.K, 623p.
- Whitall DR & Paerl HW (2001) Atmospheric pollutants and trace gases: spatiotemporal variability of wet atmospheric nitrogen deposition to the Neuse River Estuary, North Carolina. *Journal of Environmental Quality* 30: 1508-1515.
- Wikfors GH (2005) A review and new analysis of trophic interactions between *Prorocentrum minimum* and clams, scallops, and oysters. In: Gilbert PM & Sellner KG (eds) *Harmful algae* 4(3): 585-592.

Witek B & Plinski M (2000) The first recorded bloom of *Prorocentrum minimum* (Pavillard) Schiller in the coastal zone of the Gulf of Gdansk. *Oceanologia* 42(1): 29-36.

Zeitzschel B (1978) Why study phytoplankton. In: Sournia A (ed) *Phytoplankton manual*. UNESCO, United Kingdom, p 1-5.

Chapter IV

DSP toxins and pectenotoxin-2 production by *Dinophysis cf. acuminata* and *Dinophysis acuta*

Abstract

Water samples were collected weekly in order to estimate *Dinophysis cf. acuminata* and *D. acuta* abundances over a 6 month period and to determine the concentration of dinophysistoxins and pectenotoxin-2 in plankton extracts. The relation between *Dinophysis cf. acuminata* and *D. acuta* abundances, DSP toxins and pectenotoxin-2 concentration in plankton extracts, cellular toxin concentration and bivalve shellfish toxicity was exploited. Okadaic acid data was correlated with the sum of *Dinophysis cf. acuminata* plus *D. acuta* concentration; dinophysistoxin-2 (DTX2) and pectenotoxin-2 (PTX2) with *D. acuta* concentration only. Whenever *Dinophysis* spp. species were registered in the water column, bivalve shellfish were contaminated with DSP toxins. These results evidence the value of toxic microalgae quantification in HABs monitoring programs. *Dinophysis cf. acuminata* caused bivalve contamination exclusively with OA. *Dinophysis acuta* induced shellfish contamination by OA, DTX2 and PTX2 and, thus, more toxins were available for shellfish contamination. Blue mussel attained higher concentrations of DTX2 partially due to its higher filtrating capacity but mostly by slowest elimination of this toxin. Common cockle attained higher concentrations of PTX2sa also as a result of higher elimination times. Cellular toxin levels increased during the decay of *Dinophysis* spp. proliferation partially due to lowest rates of cellular division. A first attempt to establish a maximum limit of *Dinophysis* abundance estimated by means of the Utermöhl method was performed.

1. Introduction

Bivalve shellfish are filter-feeding animals, i.e. they obtain their food resources by pumping large quantities of the ambient water through filters that retain suspended matter, usually irrespective of whether this matter is of food value or not (Jørgensen, 1990). The particles removed from the environment are concentrated to levels many times those found in the water, a phenomenon called bioaccumulation⁶; the concentration factor may be in the range of 10 to 1000 or more. Some of these captured particles are destined to be partially or completely degraded, thus making their components available to the nutritional pool of the bivalve (Sampayo *et al.*, 1990).

Bivalve shellfish are known as important vectors of food intoxications in humans. The ingestion of toxic microalgae, which produce toxic compounds called phycotoxins, induces the accumulation of those chemicals in the bivalve tissues. These organisms are not visibly affected by the accumulation of phycotoxins but when later consumed by humans they will cause a variety of gastrointestinal illnesses (Valiela, 1995; Hallegraeff, 2003; FAO, 2004; IOC, 2005). The increase of phycotoxins concentration throughout different levels of the food chain is referred by the term biomagnification.

Previous depuration and/or cooking of shellfish before ingestion does not reduce the toxin concentration neither contamination influence the taste of the meat (IOC, 2005). Detection of contaminated shellfish is not, thus, straightforward, and the determination of whether bivalves are safe for consumption or not can not be made visually. Therefore, in order to reduce the risk of serious food intoxications in humans, intensive monitoring of the species composition of the phytoplankton is required in the shellfish harvesting areas in connection with bioassays and/or chemical analyses of the bivalve species (IOC, 2005). When toxic microalgae are detected in the harvesting areas, the competent authorities involved in the monitoring of the toxic events ban the harvest of shellfish (Sobral *et al.*, 2000; IOC, 2005).

⁶ Bioaccumulation: accumulation of substances, such as phycotoxins or other organic chemicals in an organism or part of an organism. The accumulation process involves the biological sequestering of substances that enter the organism through respiration, food intake, epidermal contact with the substance, and/or other means. The sequestering results in the organism having a higher concentration of the substance than the concentration in the organism surrounding environment. The level at which a given substance is bioaccumulated depends on the rate of uptake, the mode of uptake, how quickly the substance is eliminated from the organism, transformation of the substance by metabolic processes, the lipid (fat) content of the organism, the hydrophobicity of the substance, environmental factors, and other biological and physical factors (URL: <http://toxics.usgs.gov/definitions/bioaccumulation.html>).

Several illnesses related to the occurrence of toxic microalgae have been registered in Europe. The most relevant are Paralytic Shellfish Poisoning (PSP), Diarrhetic Shellfish Poisoning (DSP) and Azaspiracid Poisoning (AZP). Amnesic Shellfish Poisoning (ASP), although detected in Europe, has never caused any reported incidents (Hallegraeff, 2003; FAO, 2004; IOC, 2005).

1.1. Diarrhetic Shellfish Poisoning

The most frequent toxic event in Portugal, representing for that reason the main risk for human health, is DSP (Vale & Sampayo, 2000; Vale, 2004). The main symptoms are gastrointestinal disorders such as diarrhoea, nausea, vomiting and abdominal pain starting 30 minutes to a few hours after ingestion of contaminated shellfish and complete recovery occurs within three days (Hallegraeff, 2003; FAO, 2004; IOC, 2005).

Diarrhetic shellfish poisoning events are particularly recurrent in the northwest coast, and Ria de Aveiro is one of the most affected sites (Palma *et al.*, 1998; Vale *et al.*, 2003; Moita *et al.*, 2005). Almost every year, especially since late spring till mid-autumn (Palma *et al.*, 1998), bivalve harvesting and related business (such as depuration plants), the most important economic activities related with the exploitation of natural resources in Ria de Aveiro, suffer great financial losses due to the occurrence of toxic microalgae in the water (Sobral *et al.*, 2000).

The microalgae responsible for the production of phycotoxins of the DSP group belong to the dinoflagellate genera *Dinophysis* and *Prorocentrum* (Hallegraeff, 2003; FAO, 2004; IOC, 2005). In Portugal, DSP events are usually correlated with *Dinophysis acuminata* Claparède & Lachmann and *Dinophysis acuta* Ehrenberg occurrence in the water column (Sampayo *et al.*, 1990; Palma *et al.*, 1998).

Most of the *Dinophysis* species are associated with upwelling relaxation events and the largest numbers of cells per litre are encountered in conditions of stratification (Palma *et al.*, 1998; Moita *et al.*, 2005). *Dinophysis acuta* and *D. acuminata* distributions are restrained by water salinity, temperature and stratification. Although these two species often coexist, blooms are not coincident in space or in time. When there are widespread blooms of *Dinophysis* cf. *acuminata*, *D. acuta* is nearly absent along the coast and vice versa (Palma *et al.*, 1998).

Dinophysis cf. acuminata blooms, adapted to minor temperatures and salinity, occur preferably in spring and summer and are normally preceded by upwelling relaxation conditions. *Dinophysis acuta* blooms present their epicentre in Figueira da Foz – Aveiro region, during hot and dry summers and can be northward transported by currents that establish in the end of summer (Moita *et al.*, 2005).

1.2. Diarrhetic toxins

Diarrhoeic toxins can be divided into different groups depending on chemical structure. The first group, acidic toxins, includes okadaic acid (OA) and its derivatives named dinophysistoxins (DTXs) (Figure 4.1). The second group, neutral toxins, consists of polyether-lactones of the pectenotoxin group (PTXs). The third group includes a sulphated polyether and its derivatives the yessotoxins (YTXs) (FAO, 2004). Only the first ones are unequivocally diarrhetic in test animals, while the other two groups become very controversial regarding their possible effects on humans and therefore their inclusion under the ‘DSP’ denomination (Vale & Sampayo, 2002b).

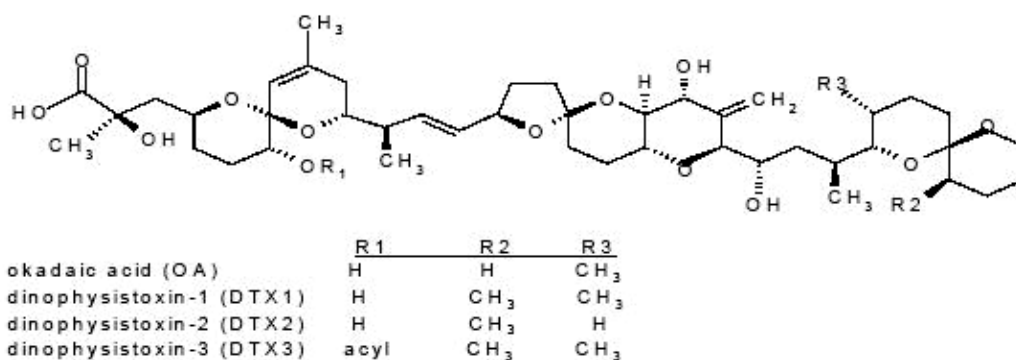


Figure 4.1. Chemical structures of okadaic acid and dinophysistoxins (adapted from FAO, 2004)

Okadaic acid and its derivatives (DTX1 and DTX2) are lipophilic and accumulate in the fatty tissue of shellfish (FAO, 2004). These compounds are potent phosphatase inhibitors and this property is linked to inflammation of the intestinal tract and diarrhoea in humans (Hallegraef, 2003; FAO, 2004).

Dinophysistoxin-3 originally described a group of DSP toxin derivatives in which saturated or unsaturated fatty acyl groups were attached to the 7-OH group of DTX1. More recently it has been shown that any of the parent toxins, OA, DTX1 and DTX2, can be

acylated with a range of saturated and unsaturated fatty acids from C14 to C18 (Hallegraeff, 2003; FAO, 2004). These acylated compounds also possess toxic activity and due to the fact that they have only been detected in contaminated shellfish, and not in algae, it has been suggested that they are probably metabolic products originated in the bivalve (Lee *et al.*, 1989; FAO, 2004).

Okadaic acid has a global distribution having been detected in bivalve shellfish throughout Japan, Europe and North America (Kumagai *et al.* 1986; Cembella, 1989). Dinophysistoxin-1 has been detected in bivalve shellfish proceeding from Japan and Norway (Lee *et al.* 1988, FAO, 2004) while DTX2 occurs in Irish and Galician bivalve shellfish as well as in Portuguese shellfish (Vale & Sampayo, 1999, 2002a).

The diarrhetic parent toxins found in Portuguese shellfish are only OA and DTX2, and not DTX1 (Vale & Sampayo, 1999). When *Dinophysis acuta* is the dominant toxic species present in the water column, shellfish contamination is due to the presence of both OA and DTX2 in a proportion of 3:2 (Vale, 2004). *Dinophysis cf. acuminata* originates exclusively contamination of shellfish with OA (Vale & Sampayo 1999, 2000).

Relative levels of free and acylated diarrhetic toxins forms can differ extremely, depending on the bivalve shellfish species in question. Thus, in blue mussel (*Mytilus edulis*) and in the clam *Donax trunculus* it is common to detect the free toxin forms (OA and DTX2) in variable percentages but never at trace levels. In other bivalve shellfish species, namely common cockle (*Cerastoderma edule*), carpet shell (*Venerupis pullastra*), razor clam (*Solen marginatus*) and oysters (*Crassostrea angulata*), percentages of free toxin forms are usually undetectable or found at trace levels, and only in situations of high contamination it is possible to detect free toxin forms, being contamination dominated only by acylated forms (Vale & Sampayo, 2002a).

The second group, neutral toxins (Figure 4.2), consists of polyether-lactones of the pectenotoxin group (PTXs). Ten PTXs have been isolated until now and six out of these have been chemically identified (FAO, 2004).

Studies performed by Vale & Sampayo (2002b) demonstrated that in plankton extracts the major pectenotoxin found is PTX2, followed by trace levels of PTX2 seco acid (PTX2sa) (Figure 4.2). Nevertheless, the screening for pectenotoxins in Portuguese bivalve shellfish has shown a contamination mainly with PTX2sa, followed by its epimer 7-epi-PTX2sa.

These last structures differ from the other known pectenotoxins in having an open ring structure (Vale & Sampayo, 2002b). Traces of PTX2 have been detectable only in shellfish very contaminated with pectenotoxins. These findings strongly suggest that shellfish are responsible for the conversion of PTX2 in PTX2sa by oxidation, has was demonstrated in New Zealand shellfish (Suzuki *et al.*, 2001; FAO, 2004).

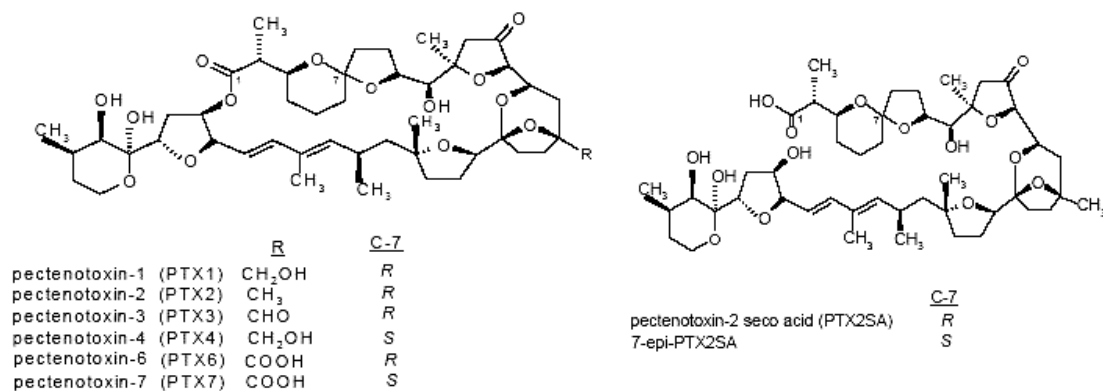


Figure 4.2. Chemical structure of pectenotoxins and pectenotoxin-2 seco acid (adapted from FAO, 2004).

Pectenotoxins in Portuguese shellfish have a strong association with the occurrence of *Dinophysis acuta* but not with *D. cf. acuminata*. *Dinophysis fortii* is implicated also (Vale & Sampayo, 2002b; Vale, 2004).

The third group of DSP toxins (Figure 4.3) includes a sulphated compound called yessotoxin (YTX), a brevetoxin-type polyether, and its derivative 45-hydroxyessotoxin (45-OH-YTX). The yessotoxins do not cause diarrhoea; yessotoxin attacks the cardiac muscle in mice after intraperitoneal injection, while desulphated yessotoxin damages the liver. The algae from the *Dinophysis* genera do not produce YTXs. Microalgae such as *Gonyaulax polyedra* and *Lingulodinium* spp. have been implicated in its production (FAO, 2004).

Vale & Sampayo (2000) have demonstrated, for Ria de Aveiro lagoon, with a four year time series, that at different episodes of *Dinophysis* spp. occurrence in the water, bivalves reach different toxicity levels. These toxicity levels are difficult to predict with precision from phytoplankton cell quantification alone and one of the causes may reside in the proportion of toxic phytoplankton in relation to non-toxic accompanying species (Sampayo *et al.*, 1990).

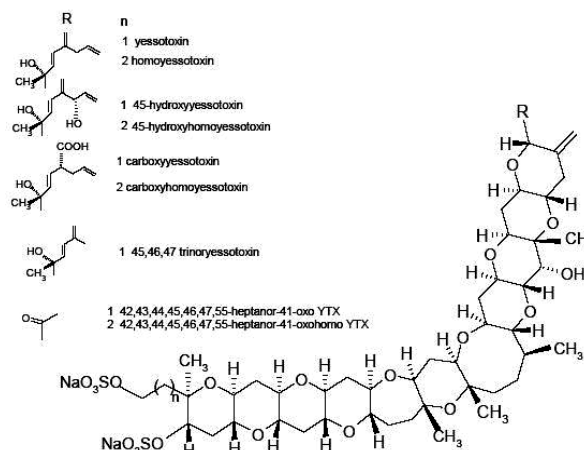


Figure 4.3. Chemical structure of yessotoxins (adapted from FAO, 2004).

Another fact to take into account is the different toxin profiles, as well as different cellular concentrations of toxins confirmed in several *Dinophysis* species, obtained by liquid chromatography after microscopic isolation of *Dinophysis* spp. specimens (Lee *et al.*, 1989; Cembella, 1989; James *et al.*, 1998). Still, scarce data on toxin production by this genus is available, due to the fact that *Dinophysis* spp. has not been cultured with success (Sampayo, 1993).

The aim of this work is therefore to provide additional data in order to explain why different *Dinophysis* spp. proliferations originate different toxicity levels in bivalve shellfish. For that, the relation between toxin-producer microalgae abundance, DSP toxins and pectenotoxin-2 concentration in plankton extracts, cellular toxin concentration and bivalve shellfish toxicity will be exploited. Moreover, an attempt to establish a maximum limit of *Dinophysis* spp. abundance, estimated using Utermöhl technique is performed. The existent limits, expressed in number of cells per liter of water, are for application with the Monitoring phytoplankton quantification technique (described in Chapter II). Considering the conclusions of Chapter II, that Utermöhl technique, due to higher results accuracy, should be included in the Portuguese HABs monitoring programme, at least for one sampling station, it is considered important to establish such a limit for use with Utermöhl technique, above which alert of DSP toxicity should be given.

At one sampling station located at Ria de Aveiro lagoon entrance – Marégrafo – periodic water samples were collected weekly in order to estimate *Dinophysis* cf. *acuminata* and *D. acuta* abundance, over a 6 month period. Plankton extracts proceeding from the same sampling station were analyzed weekly for DSP toxins and pectenotoxin-2 concentration.

Levels of DSP toxins and pectenotoxins found in two bivalve shellfish species, namely common mussel (*Mytilus edulis*) and common cockle (*Cerastoderma edule*), were provided by Laboratório de Biotoxinas from INIAP/IPIMAR.

2. Material and Methods

At one selected station, Marégrafo, located at the entrance of Ria de Aveir, 250 ml water samples were collected weekly for phytoplankton identification and counting, during a 6 month period, ranging from June to November 2004.

The water samples were immediately preserved with 30 ml of neutral Formalin, and used to estimate cellular abundance of *Dinophysis* cf. *acuminata* and *D. acuta* by the Utermöhl counting technique, as described earlier in Chapter II.

For quantification of toxin level in plankton extracts, two-litre water samples were filtered onto 10 µm nylon membranes, and frozen immediately until extraction. After thawing, toxins were extracted with aqueous 80% methanol, sonicated and left 2 hours at room temperature for spontaneous hydrolysis of esters present in the plankton. The supernatant was washed with hexane and partitioned into dichloromethane. The dichloromethane fraction was analyzed on a liquid chromatograph coupled to a mass-spectrometer (LC-MS) as described in detail in Vale (2004).

Okadaic acid cellular level was calculated by dividing OA concentration in plankton extracts by the sum of the *Dinophysis* species abundances. Dinophysistoxin-2 and PTX2 cellular level was calculated in the same way, but only the abundance of *Dinophysis acuta* was taken into consideration.

Correlations were established between *Dinophysis* spp. quantification and level of diarrhoeic toxins present in plankton extracts by means of the Kendall's rank coefficient (see Chapter II).

A first attempt to establish the maximum limit of *Dinophysis* spp. concentration at which bivalves may be contaminated with DSP toxins above the European Commission maximum limit (European Commission Decision 2002/225/CE) was performed by means of a Type II Regression Model. Simple linear regression could not be applied since this methodology presumes that one variable is fixed, i.e. controlled by laboratory conditions and measured

without error, and the other is random, and measured with error. In the present case, both variables are measured with error since they correspond to samples collected in the field and thus a Model II of Regression must be applied in order to determine the functional relationship between the two variables (Sokal & Rohlf, 1969). This regression was performed upon the *Dinophysis* spp. (*D. acuminata* + *D. acuta*) abundances and OA toxicity in common cockle, but not with OA toxicity in common mussel, due to the constant toxicity of this bivalve species, almost always with a toxicity value above the maximum limit.

3. Results

During the study period, *Dinophysis* cf. *acuminata* occurred in the water column from late spring to beginning of summer (from June to August) whereas *D. acuta* occurred predominantly during summer and autumn (from August to November) (Figure 4.4).

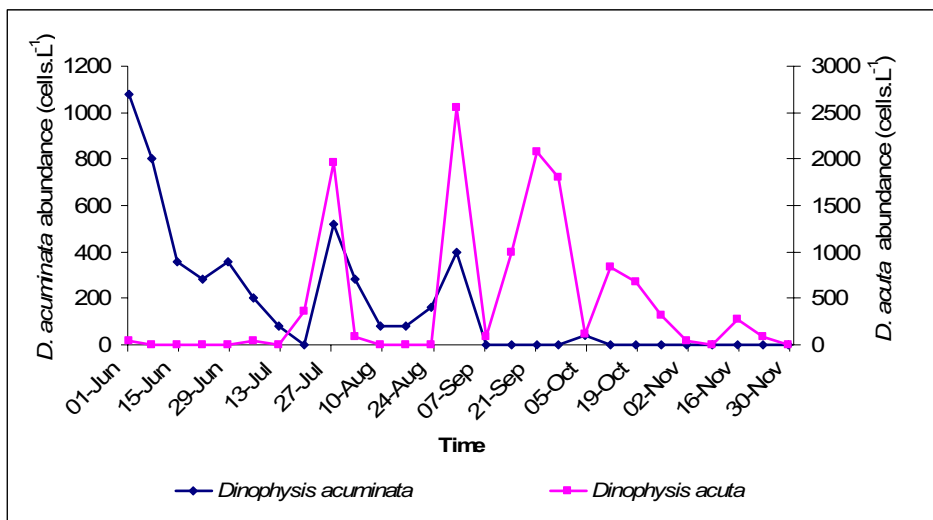


Figure 4.4. *Dinophysis* cf. *acuminata* and *D. acuta* abundance variation during the period of study.

Dinophysis cf. *acuminata* reached a maximum abundance on 01 June (1080 cells·L⁻¹) while *D. acuta* was present in the water in higher numbers on 30 August (2560 cells·L⁻¹). In July and in the end of August both species co-occurred with *Dinophysis* cf. *acuminata* occurring in smaller abundances than that of *D. acuta*.

The maximum DSP toxins concentration found in the plankton occurred on 30 August, when a concentration of 2560 cells·L⁻¹ of *Dinophysis acuta* originated toxin concentrations of 6.63 ng·L⁻¹ of OA, 3.99 ng·L⁻¹ of DTX2 and 4.75 ng·L⁻¹ of PTX2 (Figure 4.5).

When *Dinophysis cf. acuminata* occurred in highest abundances (01 June) OA was found in the plankton extracts with a concentration of 1.34 ng·L⁻¹; DTX2 and PTX2 were not observed.

Good parallelism was obtained between *Dinophysis* spp. quantification and level of diarrhoeic toxins present in plankton extracts (Figure 4.5); the presence of DSP toxins in plankton extracts is positively correlated with the abundances of *Dinophysis* : $\tau_{(OA)} = 0.71$; $\tau_{(DTX2)} = 0.39$; and $\tau_{(PTX2)} = 0.31$, at a probability level of 0.01. However, in different bloom episodes, concentration of toxins in the water was not always tightly related to *Dinophysis* spp. abundance (Figure 4.5).

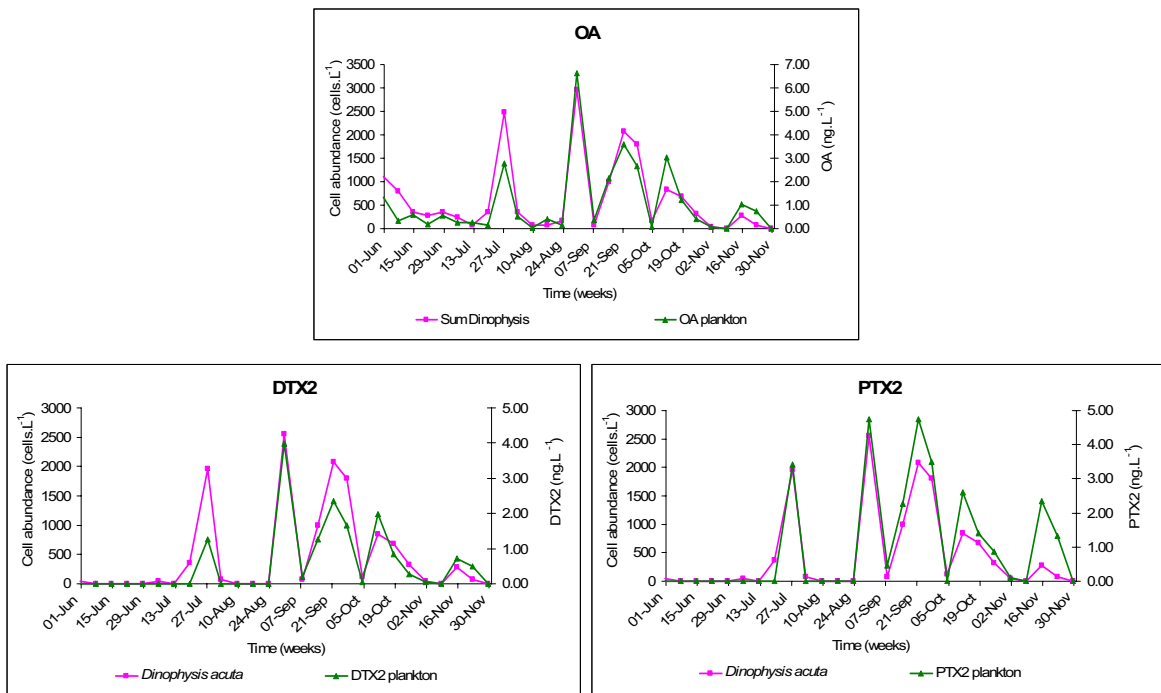


Figure 4.5. Relationship between toxins concentration in plankton and *Dinophysis* spp. concentration in the water column.

Figure 4.6 presents the relationship between *Dinophysis* spp. concentration and shellfish level of DSP toxicity.

Unquestionable correspondence was not obtained, but toxicity in shellfish was registered whenever *Dinophysis* spp. were present in the water column. When *Dinophysis acuminata* was the dominant toxic species, shellfish contamination was due to OA while when *Dinophysis acuta* was present, DTX2 and PTX2sa were also present (Figure 4.6a). Figure 4.6b reveals the same results: when DSP toxins are found in plankton, bivalve shellfish are contaminated.

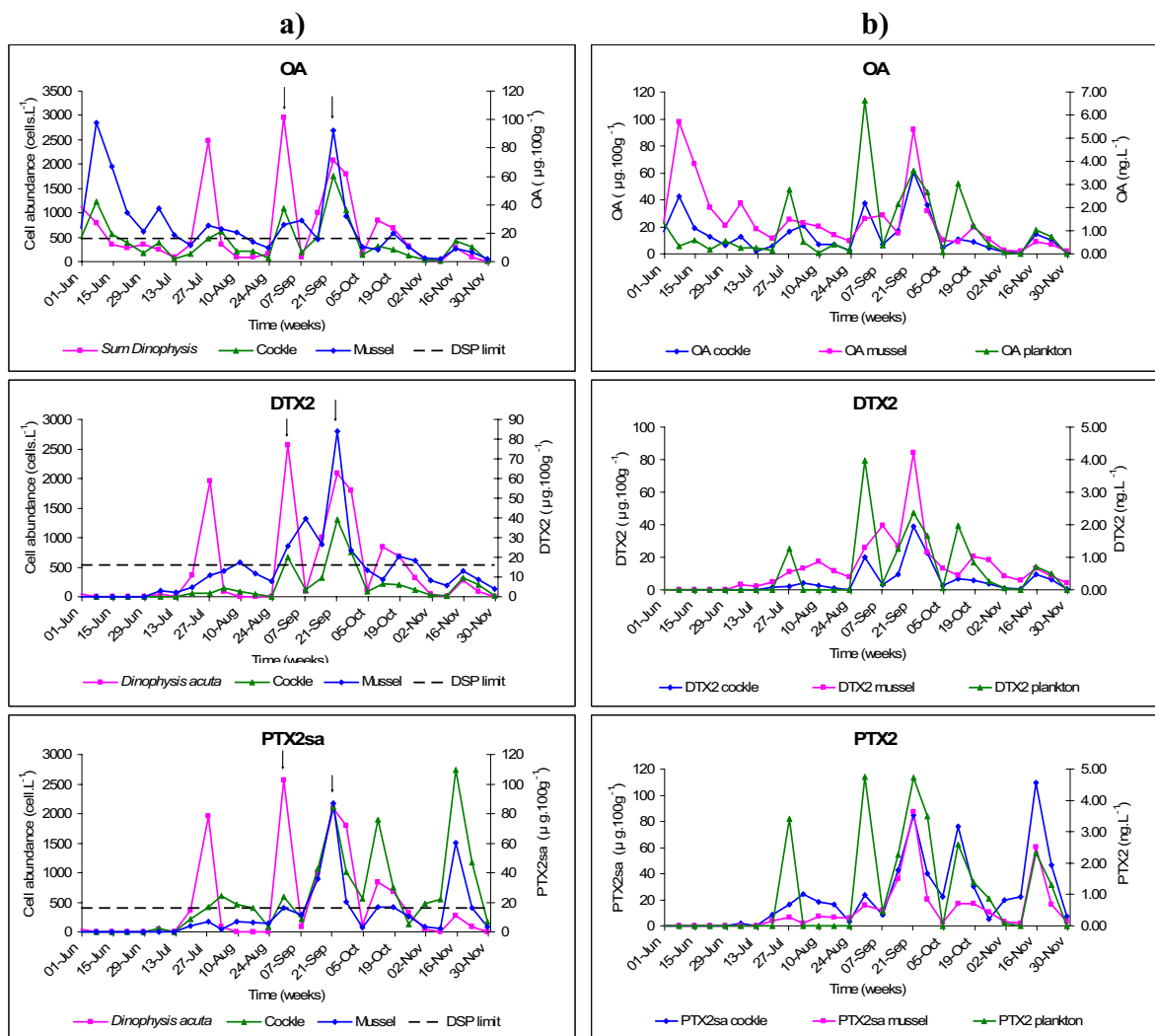


Figure 4.6. Relationship between toxins concentration in shellfish and *Dinophysis* spp. concentration in the water column (a) and with toxin concentration in plankton (b).

Regarding the European Commission Decision 2002/225/CE, which postulates the maximum level of okadaic acid, dinophysistoxins and pectenotoxins in conjunction, in 16 µg of okadaic acid equivalents per 100 g of bivalve meat, toxicity above this limit in common cockle was observed from 01 to 14 June and from 27 July to 22 November

(exception is made for the common cockle samples collected at 23 August, 25 October and 29 November, whose toxicity level was below of the $16 \mu\text{g}\cdot 100\text{g}^{-1}$). Considering blue mussel, toxicity levels registered in the study period were always superior to the maximum limit, except for the analysis performed at November 01, 08 and 21.

To describe the dependence of OA toxicity in common cockle upon the abundances of *Dinophysis* spp. (*D. acuminata* + *D. acuta*) obtained by the Utermöhl technique and to predict the concentration of *Dinophysis* spp. at which bivalves may be contaminated, considering the maximum level of DSP toxins in $16 \mu\text{g}\cdot 100\text{g}^{-1}$, a Model II Regression was applied. The choice of this type of regression was due to the fact that both variables taken into consideration are measured with error, none controlled by laboratory conditions (Sokal & Rohlf, 1969). No attempt of relating blue mussel OA toxicity and *Dinophysis* spp. abundances was made due to the constant toxicity of this bivalve species, almost always with a toxicity value above the maximum limit.

Therefore, OA toxicity in common cockle (Y) is related with the abundance of *Dinophysis* spp. (X) accordingly to the following equation:

$$Y = 0.017X + 2.9$$

To a value of $Y = 16 \mu\text{g}\cdot 100\text{g}^{-1}$ corresponds, therefore a value of $729 \text{ cells}\cdot\text{L}^{-1}$ of *Dinophysis* spp. This value can be approximated to $700 \text{ cells}\cdot\text{L}^{-1}$ for monitoring purposes. This value has to be considered only as a first approach; further studies should be endeavoured, perhaps following the same methodology, but appealing to replicate water and bivalve samples, collected at the same time and location in several sampling stations.

Regarding Figure 4.6a it is possible to see that, mainly for OA and DTX2, blue mussel achieved higher levels of contamination than common cockle.

Dinophysistoxin-2 percentages, related to the OA level, in plankton, common cockle and blue mussel are presented in Figure 4.7. As shown, DTX2 percentage in blue mussel is higher than the DTX2 percentage in common cockle and increases over time. The DTX2 percentage in common cockle presents a better correspondence with the DTX2 percentage in plankton.

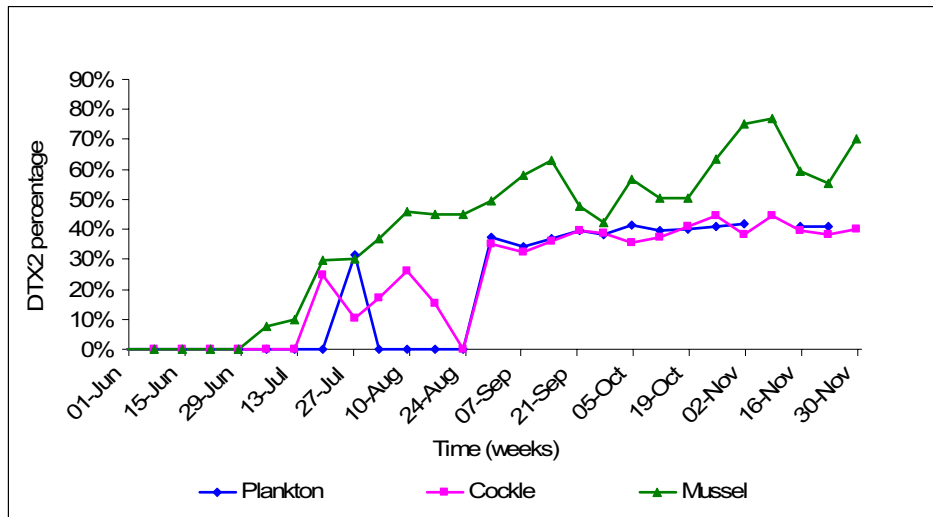


Figure 4.7. DTX2 percentages (related do OA) in plankton, common cockle and blue mussel.

In respect to pectenotoxins, PTX2sa concentrations are higher in common cockle than in blue mussel (Figure 4.6b).

Figure 4.6a also reveals that at different episodes of *Dinophysis* spp. proliferation, bivalve shellfish attain different levels of toxicity. For example, considering *Dinophysis acuta* abundance peaks of 2560 and 2080 cells·L⁻¹ attained at, respectively, 30 August and 21 September, the DSP toxins levels recorded, both in common cockle and blue mussel, were substantially higher in the 21 September sample, despite the resemblance between the values of abundance of *Dinophysis acuta*.

It was hypothesized, in agreement with Vale *et al* (2004) work, that different cellular toxin levels could play some role in the observed differences in bivalve shellfish toxicities (Figure 4.6) and toxin level in plankton (Figure 4.5) at different *Dinophysis* spp. episodes. Figure 4.8 shows different cellular toxin concentrations found at maximum cell numbers during *Dinophysis* spp. proliferation. However, no pattern was observed in relating cellular toxin levels and *Dinophysis* spp. abundances. In the situations signed, cellular toxin levels increased when *Dinophysis* spp proliferation entered in a decay period.

This increase in cellular toxin levels did not contribute for further bivalve shellfish contamination (Figure 4.8b).

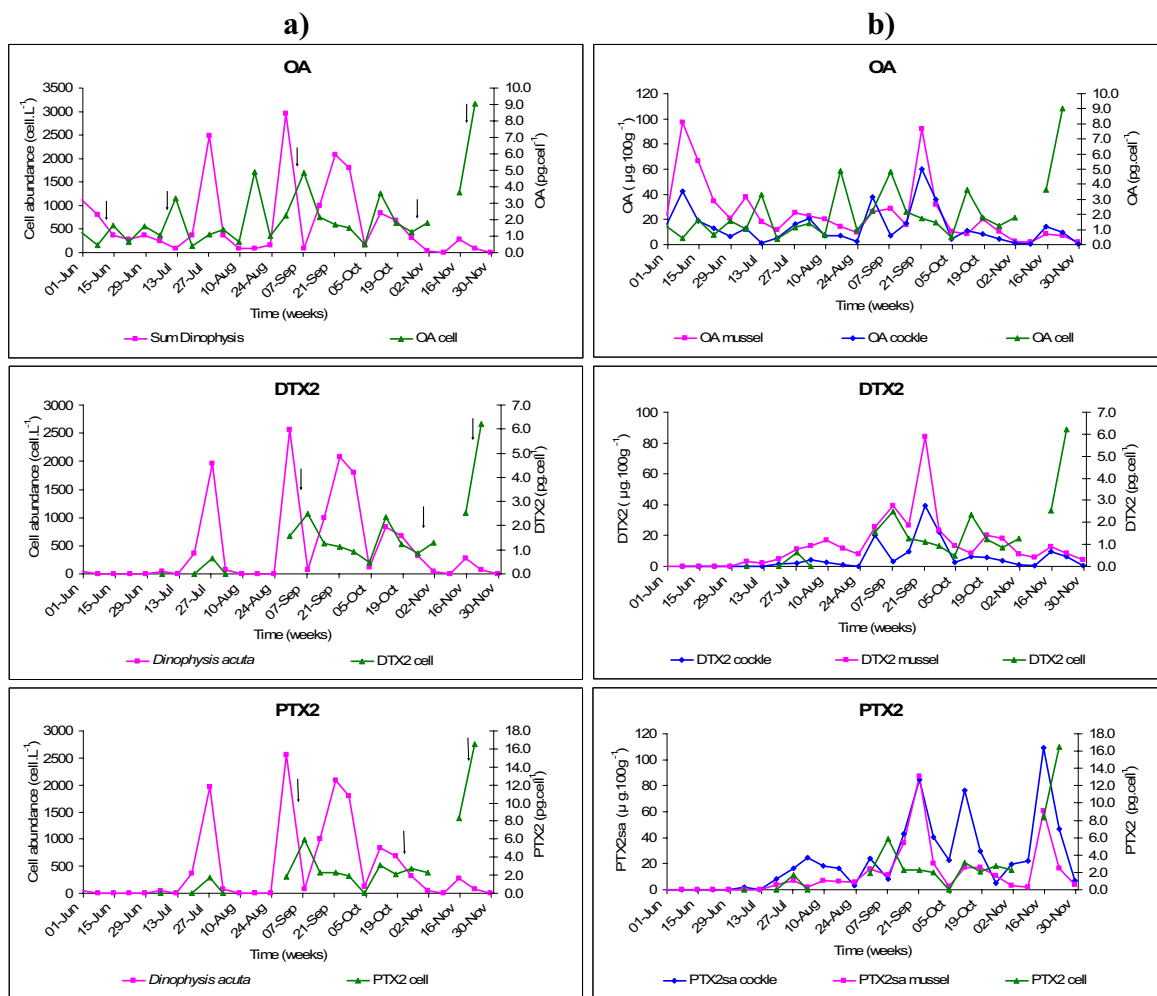


Figure 4.8. Relationship between toxin cellular level and *Dinophysis* spp. concentration (a) and with toxins concentration in shellfish (b).

4. Discussion and conclusions

During the study period, *Dinophysis* cf. *acuminata* and *D. acuta* coexisted, but their maximum abundances did not coincide in time as observed previously by Palma *et al.* (1998), Moita *et al.* (2005) and Vale *et al.* (2004). *Dinophysis* cf. *acuminata* was more abundant from late spring to beginning of summer, while *D. acuta* occurred during summer and autumn (Palma *et al.*, 1998; Moita *et al.* 2005; Vale *et al.*, 2004).

Quantification of DSP toxins (OA and DTX2) and pectenotoxins (PTX2) in plankton extracts related to *Dinophysis* spp. counts obtained with Utermöhl technique permitted, again, to demonstrate the production of those toxic compounds by *Dinophysis* spp.. Perfect correspondence between *Dinophysis* spp. number of cells per litre and bivalve shellfish

contamination was not obtained, probably due to the fact that shellfish and water samples were collected at different locations in Ria de Aveiro; however, whenever *Dinophysis* spp species were registered in the water column, bivalve shellfish chemical analysis demonstrated the presence of diarrhetic toxins. These results evidence the value of toxic microalgae quantification in HABs monitoring programs.

The data reinforce previous results obtained by Vale & Sampayo (2000, 2002) and Vale *et al.* (2004), which attributed to *Dinophysis* cf. *acuminata* bivalve contamination exclusively with OA. *Dinophysis acuta* induces shellfish contamination by OA, DTX2 and PTX2 and hence more diarrhetic toxins were available for shellfish contamination.

Blue mussel attained higher contamination levels than common cockle, mainly in respect to OA and DTX2, probably due to the larger volumes of water filtrated by blue mussels, when compared with common cockles. Larger volumes of water implicate larger quantity of toxic cells retained and consequently higher toxicity. Moreover, it is also possible that the higher DSP contamination levels attained by blue mussel are due to higher abundances of *Dinophysis* spp. at the surface of the water column than at the bottom (Moita & Silva, 2001); blue mussels are organisms found attached to rock surfaces, close to the surface of the water column (Tyler-Walters, 2002) whereas common cockles usually live at the surface of the sediments bottom (Tyler-Walters, 2005), and hence less exposed to this type of toxic microalgae proliferation.

Another fact that may contribute to the higher levels of DSP contamination in blue mussels is the differential times of toxin elimination, depending on the type of toxin. For example, DTX-2 percentage in blue mussel was found to be higher than the DTX2 percentage found in common cockle, and increased over time in blue mussel. A detoxification experiment performed by Vale (2004) demonstrated that this higher concentration of DTX2 in blue mussels is due to slowest elimination times of this toxin, when compared with the necessary time to eliminate OA. This higher elimination time induces higher contamination of blue mussels due to accumulation of the toxin for longer periods.

In respect to pectenotoxins, PTX2 was found in plankton extracts only when *Dinophysis acuta* was the toxic species present, and it was not registered in the bivalves. In these organisms, PTX2sa was the pectenotoxin present, observation that is in agreement with the hypothesis launched by several authors, which claims that PTX2sa is a result of PTX2

transformation by metabolic processes in shellfish (Suzuki *et al.*, 2001; Vale & Sampayo, 2002b; FAO, 2004).

Pectenotoxin-2-seco-acid concentrations were higher in common cockle profiles than in blue mussel. Vale (2004) has also provided a possible explanation for this fact, demonstrating that the lower levels of PTX2sa in blue mussel are due to quicker elimination of this toxin by mussels than by cockles.

Relationships established between *Dinophysis* spp number of cells per litre and DSP toxins and pectenotoxin-2 concentration in plankton extracts and with bivalve shellfish toxicity levels, showed that at different proliferations of *Dinophysis* spp. different levels of toxicity in the water and in bivalves are attained. This observation has been made previously by other authors, namely, Sampayo *et al.* (1990), Vale & Sampayo (2000) and Vale *et al.* (2004). In these studies, several aspects were pointed as causes for the impossibility to predict the bivalve shellfish toxicity from the toxic microalgae concentration: (i) bivalve shellfish species physiology – depending of bivalve shellfish species ecology and physiology, some species will accumulate toxins at a higher rate than others. As well, the depuration process can develop at different species-specific velocities, depending also of the DSP toxin in question (Vale, 2004); (ii) relative abundance of accompanying non toxic microalgae species (Sampayo *et al.*, 1990) and (iii) cellular toxin concentration (Vale & Sampayo, 2000; Vale *et al.*, 2004).

The increase of cellular toxin levels during the decay of *Dinophysis* spp. proliferation has been observed previously by Vale *et al.* (2004) and the probable explanation may be lower rates of cellular division (Vale *et al.*, 2004). This situation was observed in some occasions in the presented data, but no clear pattern was visible. One of the explanations that could account for these results resides in the probable existence of inaccuracies during the analytical processing of the samples. Nevertheless, the higher cellular toxin levels did not contribute for further shellfish contamination, maybe because the rapid decrease of *Dinophysis* spp. abundances (Vale *et al.*, 2004).

A first attempt of providing a maximum limit of *Dinophysis* spp. concentration, estimated by the Utermöhl method, and under which contamination of shellfish does not endanger public health was performed. The resulting value was 700 cells·L⁻¹ and should merely be considered as indicative, since it is very difficult to predict the concentration of toxins in

bivalve shellfish by the abundance of toxic microalgae, for the reasons described above. However, this limit is necessary for monitoring purposes and the methodology used in this work may be applied in future and more accurate attempts of achieving such a limit. These attempts may also include the use of replicate water and bivalve samples, collected at the same time, in the same location, and at several sampling stations.

5. References

- Cembella AD (1989) Occurrence of okadaic acid, a major diarrhetic shellfish toxin, in natural populations of *Dinophysis* spp. from the eastern coast of North America. *J. Appl. Phycol.* 1: 307-310.
- Decisão da Comissão 2002/225/CE de 15 de Março de 2002. JO N° 75, 15.03.2002 , p.62.
- FAO (2004) Marine Biotoxins. FAO Food and Nutrition Paper, 80. Food and Agriculture Organization of the United Nations, Rome. 278 p.
- Hallegraeff GM (2003) Harmful algal blooms: a global overview. In: Hallegraeff GM, Anderson DM & Cembella AD (eds) Manual on harmful marine microalgae (2nd edn). UNESCO Publishing, p 25-46.
- IOC (2005) The IOC harmful algal programme [on-line]. Intergovernmental Oceanographic Commission of UNESCO, Paris, France.[consulted on September 2005] Available from:
<<http://ioc.unesco.org/hab/intro.htm>>
- James KJ, Bishop AG, Gillman M, Kelly SS, Roden C, Draisci R, Lucentini L & Giannetti L (1998) The diarrhoeic shellfish poisoning toxins of *Dinophysis acuta*: identification and isolation of dinophysistoxin-2. In: Reguera B, Blanco J, Fernández ML & Wyatt T (eds.), Harmful Algae. Xunta de Galicia and IOC of UNESCO, Spain, pp. 489-492.
- Jørgensen CB (1990) Bivalve filter feeding: hydrodynamics, bioenergetics, physiology and ecology. Olsen & Olsen, Fredensborg, Denmark.

- Kumagai M, Yanagi T, Murata M, Yasumoto T, Kat M, Lassus P, Rodríguez-Vázquez A (1986) Identification of okadaic acid as the causative toxin of diarrhetic shellfish poisoning in Europe. *Agricultural and Biological Chemistry* 50: 2853-2857
- Lee JS, Igarashi T, Fraga S, Dahl E, Hovgaard P and Yasumoto T (1989) Determination of diarrhetic shellfish toxins in various dinoflagellate species. *Journal of Applied Phycology* 1: 147-152
- Lee JS, Tangen K, Dahl E, Hovgaard P, Yasumoto T (1988) Diarrhetic shellfish toxins in Norwegian mussels. *Nippon Suisan Gakkaishi* 54 (11): 1953-1957
- Moita MT, Palma AS, Vilarinho MG (2005) Blooms de fitoplâncton na costa Portuguesa. IPIMAR Divulgação, nº31, Lisboa, Portugal.
- Nybakken JW (1988) *Marine Biology: an ecological approach* (2nd ed). Harper Collins Publishers, New York.
- Palma AS, Vilarinho, MG, Moita MT (1998) Interannual trends in the longshore variation of *Dinophysis* off The Portuguese coast. In: Harmful Algae Reguera B, Blanco J, Fernández ML, Wyatt T (eds) Xunta de Galicia and Intergovernmental Oceanographic Commission of UNESCO, Paris, p. 124-127.
- Sampayo MA de M, Alvito P, Franca S, Sousa I (1990) *Dinophysis* spp. toxicity and relation to accompanying species. In: Graneli E, Sundstrom B, Edler L, Anderson DM (eds) *Toxic Marine Phytoplankton*. Elsevier, New York, p. 215-220.
- Sobral MP, Vieira F, Sobral V (2000) Zonas de produção de moluscos bivalves da Ria de Aveiro. IPIMAR Divulgação nº 12, Lisboa, Portugal.
- Suzuki T, Mackenzie L, Stirling D & Adamson J (2001) Pectenotoxin-2 seco acid: a toxin converted from pectenotoxin-2 by the New Zealand Greenshell mussel, *Perna canaliculus*. *Toxicon* 39: 507-514.
- Toxic Substances Hydrology Program [online]. US Department of the Interior, US Geological Survey [cited 17/11/2005] Available from:
<<http://toxics.usgs.gov/definitions/bioaccumulation.html>>

- Tyler-Walters, H. (2002). *Mytilus edulis*. Common mussel. Marine Life Information Network: Biology and Sensitivity Key Information Sub-programme [on-line]. Plymouth: Marine Biological Association of the United Kingdom. [consulted in August 2005]. Available from:
<<http://www.marlin.ac.uk/species/Mytilusedulis.htm>>
- Tyler-Walters, H. (2005). *Cerastoderma edule*. Common cockle. Marine Life Information Network: Biology and Sensitivity Key Information Sub-programme [on-line]. Plymouth: Marine Biological Association of the United Kingdom. [consulted in 2005]. Available from:
<<http://www.marlin.ac.uk/species/Cerastodermaedule.htm>>
- Vale P, Sampayo MA de M (1999) Esters of okadaic acid and dinophysistoxin-2 in Portuguese bivalves related to human poisonings. *Toxicon* 37:1109-1121
- Vale P, Sampayo MA de M (2000) Dinophysistoxin-2: a rare diarrhoeic toxin associated with *Dinophysis acuta*. *Toxicon* 38: 1599-1606. Elsevier Science Publishing.
- Vale P, Sampayo MA de M (2002a) Esterification of DSP toxins by Portuguese bivalves from the Northwest coast determined by LC-MS – a widespread phenomenon. *Toxicon* 40: 33-42
- Vale P, Sampayo MA de M (2002b) Pectenotoxin-2 seco acid, 7-epi-pectenotoxin-2 seco acid and pectenotoxin-2 in shellfish and plankton from Portugal. *Toxicon* 40: 979-987.
- Vale P, Botelho MJ, Rodrigues S (2003) Reflexão sobre os episódios de DSP de 2002: nova legislação comunitária e métodos alternativos. In: *Actas 6º Encontro de Química dos Alimentos*, p. 896-903.
- Vale P (2004) Differential dynamics of dinophysistoxins and pectenotoxins between blue mussel and common cockle: a phenomenon originating from the complex toxin profile of *Dinophysis acuta*. *Toxicon* 44:123-134. Elsevier.
- Vale P, Cerejo M & Vilarinho MG (2004). Toxin production by *Dinophysis* spp. at Ria de Aveiro, Portugal. In press in: *Proceedings of 5th International Conference on Molluscan Shellfish Safety*, Galway, Ireland, 14-18 June 2004.

Valiela I (1995) Marine ecological processes. Springer-Verlag, New York.

Chapter V

Transport and dispersal of toxic microalgae in Ria de Aveiro*

Abstract

A numerical model was used to predict toxic microalgal transport and dispersion in Ria de Aveiro. A previously developed Lagrangean particle tracking model coupled to a calibrated two-dimensional hydrodynamic model of Ria de Aveiro was used. Microalgae were regarded as passive particles and the methodology used allowed the determination of their trajectories, as induced by the tidal currents predicted by the hydrodynamic model. The model assumes Ria de Aveiro as vertically homogeneous and does not take into account the vertical distribution patterns of microalgae. Simulations were carried out during extreme spring and neap tides, with microalgae release at the mouth of the lagoon at the local flood. The maximum and minimum areas affected during the occurrence of toxic microalgae blooming were estimated, in order to evaluate the suitability of the distribution of the sampling stations included in the toxic events local monitoring program. It was found that tidal currents greatly determine the microalgal horizontal distribution and dispersal in the lagoon. The results identify possible refinements to the locations of water and bivalve sampling stations postulated by INIAP/IPIMAR, in the frame of the local HAB's program: bivalve sampling station at the Ílhavo channel was considered unnecessary since no microalgal transport for this channel was registered. Marégrafo, Moacha and Triângulo das Correntes water sampling stations and sample collection periodicity should be preserved. The definition of a water sampling station at the far end of Espinheiro channel is also advised.

1. Introduction

Ria de Aveiro is the most affected area in the Portuguese coast, and in a more recurrent way, by harmful algae blooms (HABs) and resulting contamination of bivalve shellfish, especially of the DSP type (Vale, 2004; Moita & Silva, 2001; Palma *et al.*, 1998). This situation does not only constitute a threat to public health but also has strong negative impacts in the economy of the area. In fact, bivalve shellfish exploitation and related business (such as depuration plants) constitute the most important economic activity, related to the exploration of fishing resources, of Ria de Aveiro. The bivalve harvest takes place most of the year, except in periods of phycotoxin occurrence. In these periods the competent authorities forbid the capture and commercialization of shellfish, safeguarding public health but harming, in a certain way, the economy of the area (Sobral *et al.*, 2000).

The HABs impacts in public health and economy appear to have increased in frequency, intensity and geographical distribution in the past two decades (Hallegraeff, 2003). These toxic events are predominantly coastal phenomena and their effects are most often manifested upon coastal biota. Much of the global production of seafood and exploitation of fish and shellfish resources is situated within the coastal zone. The monitor and control of HABs is, therefore, of critical importance to coastal-zone management of marine resources and protection of public health (Cembella *et al.*, 2005).

In Portugal, the task of monitoring and controlling harmful algal blooms is performed by Instituto Nacional de Investigação Agrária e das Pescas (INIAP/IPIMAR). To accomplish this task water and bivalve shellfish samples are collected in various sampling stations, located along the Portuguese coast, in the frame of the project Plano Nacional de Salubridade de Bivalves.

As it has been defined in chapter III, phytoplankton refers to a large group of planktonic plants that live in surface waters, passively drifting along with water movements due to their reduced mobility capacity (Zeitzschel, 1978; Nybakken, 1988; Harris, 1986; Valiela, 1995). Phytoplankters represent one quarter of the total planet vegetation and constitute the major portion of primary producers in the sea (Zeitzschel, 1978; Nybakken, 1988; Valiela,

1995). They are critical food for several aquatic organisms such as molluscs, crustaceans and finfish (Hallegraeff, 2003; FAO, 2004; IOC, 2005).

Phytoplankton distribution in the water column is influenced by many physical/chemical parameters, such as light intensity, temperature and availability of nutrients (Valiela, 1995). Moreover their distribution is also influenced by external inputs of energy like currents (Margalef, 1978b). Due to their microscopic size and short live-time they can also easily be deposited at the bottom or increase and decrease their concentration relatively fast (Margalef, 1978b). However, in such a dynamic environment like Ria de Aveiro, where the tidal currents are the main forcing action (Dias, 2001), and because this lagoon is considered as vertically homogeneous (Dias, 2001), in this study it is assumed that microalgae distribution in this coastal environment is mainly due to tidal forcing.

High concentrations of phytoplankton cells, usually referred to as blooms, are generally favourable to aquaculture and fishing activities. However, the proliferation of some species can, at times, be responsible for the occurrence of harmful effects in the trophic relationships, public health, and economic activities (Hallegraeff, 2003; FAO, 2004; IOC, 2005). Among the 5000 species of extant marine phytoplankton, some 300 species can at times occur in such high numbers that they obviously discolour the surface of the sea (so-called 'red tides'), while only about 80 species have the capacity to produce potent toxins (phycotoxins) that can find their way through fish and shellfish to humans causing a variety of gastrointestinal illnesses (Sournia *et al.*, 1991; Hallegraeff, 2003).

Essentially there are 3 kinds of illnesses caused by the ingestion of bivalve shellfish contaminated by phycotoxins: paralytic shellfish poisoning (PSP); amnesic shellfish poisoning (ASP); and diarrhetic shellfish poisoning (DSP).

Diarrhetic shellfish poisoning is the most frequent toxic event in Ria de Aveiro, and it is caused by microalgae proliferations of the dinoflagellate genera *Dinophysis* spp. (*Dinophysis acuminata* and *D. acuta*) (Moita, 1993; Vale *et al.*, 2004; Moita *et al.*, 2005). The first confirmed occurrence of diarrhetic toxins (okadaic acid, dinophysistoxins and pectenotoxins) in Portugal associated with *Dinophysis* species was registered in 1987 (Sampayo *et al.*, 1990). Exception made to the year 1993, DSP events are registered every year, especially since late spring till mid-autumn (Palma *et al.* 1998). Most of the *Dinophysis* species are associated with upwelling relaxation events in the Portuguese

northwest coast, and the largest numbers of cells per litre are encountered in conditions of stratification (Palma *et al.*, 1998; Moita *et al.*, 2005). These marine toxic phytoplankton cells are transported to the interior of Ria de Aveiro by the action of tidal flood and contaminate the existing bivalve shellfish banks.

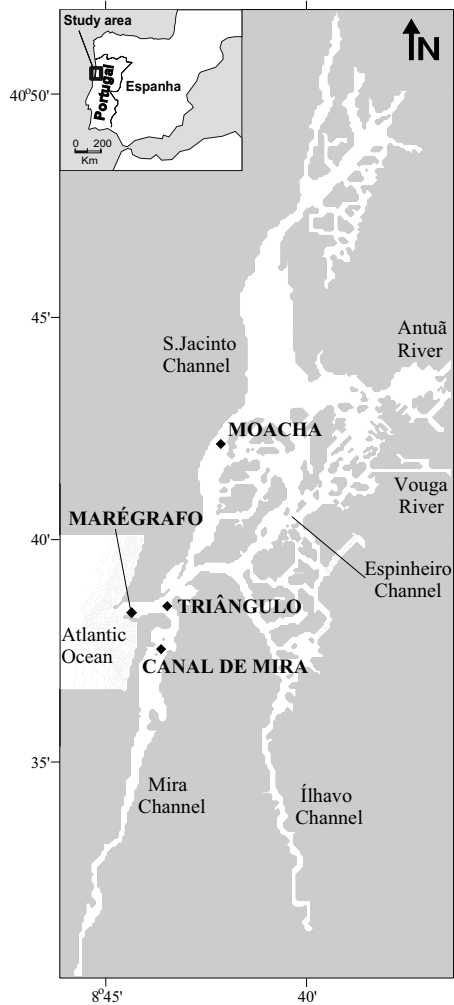


Figure 5.1. Ria de Aveiro lagoon sediments (Storer *et al.*, 1991).

In the frame of the monitoring program of toxic events defined for Ria de Aveiro, periodic collection of water samples is made at four sampling stations (Figure 5.1), namely, Marégrafo (at the mouth of the lagoon) sampled twice a week, Triângulo das Correntes (Entrance channel) and Moacha (S. Jacinto channel) sampled once a week, and Canal de Mira (Mira channel), sampled only in case of occurrence of toxic microalgae at the other stations. These samples are used for the identification and quantification of phytoplankton species known to be toxic.

Bivalve shellfish are an extremely successful and diversified group of animals, from phylum Mollusca. They are exclusively aquatic organisms, but they can occur in environments with a wide range of salinities, as sea, fresh or brackish water. The majority of species lives at the bottom. There are some sessile species that fix themselves to solid substratum, while others live buried in bottom

sediments. Bivalve shellfish are filter feeders that inhabit the intertidal zone. They filter large quantities of water from which they withdraw microscopic food particles, such as phytoplankton cells. Filter feeders pump the ambient water through filters that retain suspended matter, usually irrespective of whether this matter is of food value or not (Jørgensen, 1990). When toxic phytoplankton cells are abundant in the water column they will be ingested and their toxins accumulated in the bivalve shellfish tissues.

Natural production banks of bivalve shellfish are common in Ria de Aveiro lagoon, existing in almost every channel, but mostly in the central part of the lagoon, and particularly in areas close to the entrance (Sobral, personal communication).

In the frame of the national program of assessment of HABs in the Portuguese coast, Ria de Aveiro is one of the locations more frequently subject to sampling. A variety of bivalve shellfish sampling stations exist along the lagoon: blue mussel is collected every week at the Entrance channel, twice a month in S. Jacinto channel and once a month in Espinheiro channel; common cockle is sampled every week at S. Jacinto channel, and once a month in Espinheiro and Ílhavo channel; carpet shell is collected twice a month in Mira channel and once a month in Espinheiro channel; and razor shell is sampled twice a month in Mira channel. Due to the decrease of natural productions banks of cockle shell in Ria de Aveiro lagoon, this species, as well as oysters, is sampled from the existing molluscan shellfish farming of Costa Nova, with a monthly periodicity.

The location of the shellfish sampling stations was determined by INIAP/IPIMAR considering the largest production banks existent, their relative commercial exploitation and also considering the existing points for microbiological assessment of water quality.

For the purpose of contributing to the optimization of the monitoring program of HABs developed in Ria de Aveiro, it is considered important to study and understand how the tidal flow induces the horizontal transport and dispersal of toxic microalgae in this lagoon. The methodology adopted in this work comprises the application of a previously developed Lagrangean particle tracking model (Dias et al., 2001; 2003) coupled to a calibrated two-dimensional hydrodynamic model of Ria de Aveiro (Dias & Lopes, 2006a,b). This study provides an example of the applicability of the numerical modelling in the management of coastal areas and shows ways of improving the sampling design of a monitoring program.

2. Methods

In this study microalgae are considered as passive particles, assuming the absence of effective means of locomotion. Their movement is assumed to be entirely induced by the tidal currents and the modelling system allows following their tracks. Simulations are carried out during the extreme spring and neap tides, with release of particles at the mouth

of the lagoon at the local flood, in order to estimate the maximum and minimum areas affected during the occurrence of HABs, and therefore evaluate the adequate distribution of the sampling stations included in the monitoring program. The maximum and minimum residence time of microalgae for the lagoon, as well as for each channel were estimated. This work was carried out under no wind and in the absence of river discharges, therefore maximizing the residence time.

2.1. Numerical modelling

One of the most common tools in the study of coastal zones, lagoons and estuaries are numerical models which are increasingly applied in the planning and management of hydrologic basins (Santos & Costa, 1985).

A numerical model is, by definition, an approximate reconstruction of a real phenomenon (Dias & Lopes, 2005b). In shallow coastal water systems, the mathematical modelling of physical processes has undergone a large development. However, due to the complexity of the processes involved, its development will surely pursue for a long time in order to reproduce more accurately the processes that actually occur in these systems (Dias & Lopes, 2005b). Some models are already considered in a mature stage as it is the case for the two-dimensional vertically integrated (2HD) hydrodynamic models. 2HD models can be used as reliable and useful tools to study shallow coastal waters (Dias *et al.*, 2003; Dias & Lopes, 2005b).

2.1.1. Hydrodynamic model

Attending to the hydrodynamic characteristics of the study domain, Ria de Aveiro, a two-dimensional vertically integrated hydrodynamic model based on finite differences techniques was considered suitable for the simulation of the lagoon hydrodynamic by Dias (2001). This model was developed from the SIMSYS2D model (Leendertse & Gritton, 1971; Leendertse, 1987) and solves the second order partial differential equations for the depth average fluid flow derived from the full three-dimensional Navier-Stokes equations. This result in a system consisting of an equation for the mass continuity and two horizontal momentum equations that are vertically averaged by integrating from the bottom to the surface (Dias & Lopes, 2005b):

$$\frac{\partial \zeta}{\partial t} + \frac{\partial(HU)}{\partial x_1} + \frac{\partial(HV)}{\partial x_2} = 0 \quad (\text{Equation 18})$$

$$\frac{\partial U}{\partial t} + U \frac{\partial U}{\partial x_1} + V \frac{\partial U}{\partial x_2} = fV - g \frac{\partial \zeta}{\partial x_1} - \frac{\tau_{x_1}^b}{H\rho_0} + A_h \nabla^2 U \quad (\text{Equation 19})$$

$$\frac{\partial V}{\partial t} + U \frac{\partial V}{\partial x_1} + V \frac{\partial V}{\partial x_2} = -fU - g \frac{\partial \zeta}{\partial x_2} - \frac{\tau_{x_2}^b}{H\rho_0} + A_h \nabla^2 V \quad (\text{Equation 20})$$

where U is the depth integrated velocity component in the x_1 direction (eastward); V is the depth integrated velocity component in the x_2 direction (northward); ζ is the surface water elevation; H is the water height; t is the time; f is the Coriolis parameter; g is the acceleration of gravity; ρ is the water density; A_h is the kinematics constant turbulent horizontal viscosity; and τ^b is the magnitude of the shear stress on the bottom caused by the flow of water over the bed.

The last parameter, τ^b , is related to the frictional dissipation of momentum at the water-sediment interface and it is approximated by a quadratic drag law using the Manning-Chezy formulation (Dronkers, 1964; Dias *et al.*, 2003).

The system of equations (18)-(20) was discretized using a finite difference method and the difference equations solved by the ADI method (alternating direction implicit), using a space-staggered grid (Leendertse & Gritton, 1971; Dias *et al.*, 2003).

With appropriate boundary and initial conditions, this system of equations constitutes a well-posed initial boundary value problem whose solution describes the depth-averaged circulation in a tidal basin (Dias *et al.*, 2003).

At the ocean open boundary the water elevation over the reference level was imposed by using tidal predictions determined in the web page *Tidal Prediction for the Western Iberian Peninsula* (URL: <http://neptuno.fis.ua.pt/tidal>). The initial conditions were horizontal level and null velocity in all the grid points. Along the solid boundaries a null normal velocity was imposed and a free slip condition was assumed (Dias *et al.*, 2003).

The simulation of flow in this complex domain requires the use of the finest possible grid. The model grid must be sufficiently fine to resolve the essential features of depth and geometry variations, but as grid resolution is refined, the total number of grid points and the computational time increase geometrically. For this domain the ideal cell's dimension would be around 50 m, but the compromise solution was to develop a grid with dimensions $\Delta x = \Delta y = 100$ m, resulting in 160 cells in the x_1 direction (eastward) and 393 cells in the x_2 direction (northward). In this case, the narrower channels had their width exaggerated, but it was guaranteed that they conserve their water volume (Dias *et al.*, 2003).

A computational time step of 40 s was considered, with a 3 day spin up period. A typical value of $20 \text{ m}^2 \text{ s}^{-1}$ was adopted for A_b , in order to increase the stability of the numerical solution.

The hydrodynamic model was calibrated and validated for Ria de Aveiro by Dias & Lopes (2006a; 2006b). The calibration procedure consisted in adjusting the bottom friction comparing the harmonic constants of the main tidal constituents determined from simulated time series of water level with those determined from observed data for 21 stations distributed throughout the main channels of the lagoon. The validation process of the model was achieved by comparing simulated water level and currents with independent observed data concerning 11 stations (Dias *et al.*, 2003; Dias & Lopes, 2006a,b).

Results from the calibration and validation processes indicated that the hydrodynamic model accurately predicts the water level and the currents in the lagoon.

2.1.2. Particle-tracking model

Lagrangian modelling constitutes a powerful tool for studying the processes of dispersion in coastal waters, estuaries and lagoons (Gomez-Gesteira *et al.*, 1999; Inoue & Wiseman, 2000; Dias, 2001). It allows analysis of dispersion of water masses, represented as passive particles, as well as estimation of residence times, at a low computational cost compared to Eulerian models. For this reason, Lagrangian models are now widely applied in the study of transport of passive particles in coastal areas (Hofmann *et al.*, 1991; Gomez-Gesteira *et al.*, 1999; Dias, 2001).

In recovering Lagrangean information from a Eulerian currents data set, the purpose is to obtain Lagrangean particles trajectories, X_i^n , given an Eulerian velocity field, $U_i(X_i^n, t)$, by integrating the following equation:

$$\frac{dX_i^n}{dt} = U_i(X_i^n, t) \quad (\text{Equation 21})$$

where particles are identified as $i= 1,2,\dots$, and the vectors X_i^n and U_i give the 2-D particle positions and velocities (Dias, 2001; Dias *et al.*, 2003).

Therefore, the two-dimensional trajectories of the simulated particles are computed using a Lagrangean approach, solving the equation:

$$X_i(x_0, y_0)^{n+1} = X_i(x_0, y_0)^n + \int_{t_0+n\Delta t}^{t_0+(n+1)\Delta t} U_i(x_0, y_0, t) dt \quad (\text{Equation 22})$$

at each time step. $X_i(x_0, y_0)^{n+1}$ is the position at the instant $n+1$ of the particle released at the point $X_i(x_0, y_0)^0$ (Dias, 2001; Dias *et al.*, 2003).

In this study the time integral was computed using a fourth-order Rung-Kutta scheme (Hofmann *et al.*, 1991; Dias, 2001; Dias *et al.*, 2003):

$$K_{1i} = \Delta t \times U_i \left[X_i(x_0, y_0)^n, t \right] \quad (\text{Equation 23})$$

$$K_{2i} = \Delta t \times U_i \left[X_i(x_0, y_0)^n + \frac{K_{1i}}{2}, t + \frac{\Delta t}{2} \right] \quad (\text{Equation 24})$$

$$K_{3i} = \Delta t \times U_i \left[X_i(x_0, y_0)^n + \frac{K_{2i}}{2}, t + \frac{\Delta t}{2} \right] \quad (\text{Equation 25})$$

$$K_{4i} = \Delta t \times U_i \left[X_i(x_0, y_0)^n + K_{3i}, t + \Delta t \right] \quad (\text{Equation 26})$$

$$X_i(x_0, y_0)^{n+1} = X_i(x_0, y_0)^n + \frac{K_{1i}}{6} + \frac{K_{2i}}{3} + \frac{K_{3i}}{3} + \frac{K_{4i}}{6} \quad (\text{Equation 27})$$

where $X_i(x_0, y_0)^{n+1}$ represents the new location of a particle that was advected from its previous position $X_i(x_0, y_0)^n$ by the velocity $U_i = (U_i, V_i)$ in a time interval Δt , and K_{ji} represents the Runge-Kutta coefficients.

The implementation of the model described above is straightforward, provided that a velocity field such as the one simulated by the two-dimensional hydrodynamic model is available. In reality, particles may move in response to additional processes such as diffusion, dissolution or aggregation and deposition, which are important in some areas of the lagoon. The implicit assumption made in this work was that the particle distribution was dictated primarily by passive advection within the 2-D flow field (Dias, 2001; Dias *et al.*, 2003).

In this study, particle tracks will be used to simulate the paths of microalgae in Ria de Aveiro. In the model used, microalgae are regarded as passive particles, i.e. the model assumes that they do not possess effective means of locomotion, being their distribution mainly due to the transport induced by tidal currents.

Once the two velocity components of the tidal currents at the particle location are known (interpolated for the current particle position from the discrete velocities computed by the hydrodynamic model), the particle location is advanced forward in time by the fourth-order Runge-Kutta scheme (Eqs. 23 to 27) (Dias, 2001; Dias *et al.*, 2003).

The time step and the grid used for the lagrangean simulations were the same considered for the hydrodynamic model.

The accuracy of the particle-tracking model was tested by advecting a particle in a well-known velocity field. The particles were advected by a two-dimensional periodic velocity field, with a strong semidiurnal constituent and a weak diurnal one. The relations and values adopted are typical of Ria de Aveiro (Dias *et al.*, 2001). The computed particle trajectory was compared with the trajectory determined by solving the analytical equations, and the results showed a good accuracy (Dias 2001; Dias *et al.*, 2001).

3. Results and Discussion

The model was used to simulate two different tidal cases in September 2004. This period was chosen considering that, during this month, toxic microalgae were sure to be observed in Ria de Aveiro, namely *Dinophysis acuta*. Simulations were performed emitting particles at 3 cells located in the lagoon mouth, during one tidal cycle, in extreme spring and neap tides (tidal ranges of 3.1 and 0.7 m, respectively). The highest and the lowest tidal prism in Ria de Aveiro (and therefore the maximum and minimum tidal currents) occur in the extreme spring and neap tides, respectively. A tide prediction for the periods referred was imposed at the ocean open boundary. Through this methodology was determined the maximum and minimum trajectories performed by the microalgae in the lagoon. The simultaneous tracks obtained for all particles emitted were represented using animations (not shown). Assuming that microalgae behave in the same manner as the particles, these animations revealed that their distribution in Ria de Aveiro lagoon is unquestionably determined by tidal currents. In the extreme spring tide case microalgae reach further into the lagoon than in neap tide, affecting also a larger distribution area. This behaviour is due to the stronger tidal currents induced by the higher tidal wave amplitude, characteristic of spring tides (The Open University, 1989), and transport microalgae further into the lagoon. Additionally, at the end of the spring tide ebb stage, some particles still remain inside the lagoon, near Triângulo das Correntes sampling station. This may occur as a consequence of the higher distances that particles achieve in this type of tide. This result has considerable importance because it shows that a certain level of microalgae retention may exist in Ria de Aveiro lagoon. In both cases, microalgae transport occurs mainly into Espinheiro channel, induced by the stronger currents expected in this channel (Dias, 2001).

Other simulations were carried out for the same period, again during one tidal cycle in the extreme spring and neap tides, with 15 emission points located along the lagoon mouth (particles released at the beginning of the local flood). It was observed that the majority of the emitted particles did not return to the ocean after one tidal cycle, which did not allow the calculation of all the desired results. For that reason, further simulations, again with 15 emission points, were performed over a 4 day period starting at the same instants.

3.1. Preferential channel

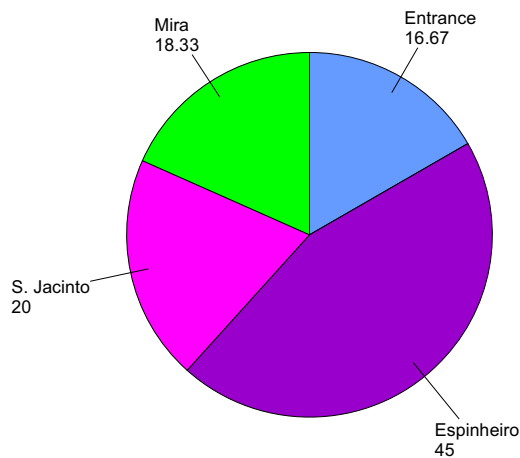


Figure 5.2. Preferential channel, in percentage, to which microalgae are transported.

Using the microalgae tracks obtained for both simulations (tidal cycle period - 12.25 h and 4 day period – 96 h), the channels into which microalgae were preferentially transported were determined (Figure 5.2).

The results reveal that microalgae transport occurred mainly into Espinheiro channel (45% of the cases) followed by S. Jacinto channel (20%), Mira channel (18.33%) and finally to the Entrance channel (16.67%). No

microalgae transport to Ílhavo channel was recorded. These results were similar for neap and spring tides. The hydrodynamic characterization of Ria de Aveiro lagoon performed by Dias (2001), gives an explanation of these results in terms of the highest current flux observed in these channels.

Since no microalgae transport was recorded to Ílhavo channel, it is considered that it is not necessary to continue with the monthly common cockle sampling programme in this channel. The occurrence of significantly higher tidal currents that could induce microalgae transport to this channel is unlikely. In situations of flooding and increased river flow, besides the consequent decrease of the tidal currents in Ílhavo Channel, the resulting higher influence of freshwater would be a strong restrictive condition for marine toxic microalgae and shellfish survival in this area. Even so, in periods of toxic microalgae occurrence it is considered wise to perform samplings at Ílhavo channel, both of water and bivalve shellfish, in order to confirm this hypothesis.

3.2. Microalgae tracks characterization

Using the tracks obtained for the 4 day period simulations in neap and spring tides, the far distance attained by microalgae at each channel before returning back to the ocean and the time needed to cover that distance, as well as the total time taken by the microalgae to exit

from Ria de Aveiro lagoon were calculated. The residence time for each channel was determined by subtracting the time microalgae needed to reach the far distance in that channel to the total exit time of microalgae from the lagoon. In this case the residence time should be interpreted as the time that particles emitted at the far distance in each channel take to leave the lagoon. The average results are summarized in Table 5.1.

Table 5.1. Average distance attained by microalgae at each channel, average time needed to cover that distance, average microalgae total exit time from de lagoon and average residence time for each channel.

Channel	Distance (km)	Time(h)	Exit time (h)	Resid. Time (h)
Espinheiro	6.18	9.11	20.09	10.97
S. Jacinto	5.21	14.82	54.09	39.26
Mira	1.70	6.72	18.97	12.25
Entrance	1.52	7.13	8.66	1.53

Microalgae achieve greater distances within the lagoon in Espinheiro and S. Jacinto channels, 6.18 km and 5.21 km, respectively, probably due to the higher strength of the tidal currents that occur in these channels (Dias, 2001). In S.Jacinto channel, microalgae needed more time to travel a shorter distance and also to exit the lagoon. Once more, the tidal currents pattern may explain this behaviour, since in S.Jacinto channel the tidal current intensity strongly reduces landward.

Microalgae in Mira channel achieved an average maximum distance of 1.70 km in a 6.72 h period. Even though the shorter distance, they have a total exit time very similar to that of Espinheiro channel, due to the lower current intensities in this channel (Dias, 2001).

On average the maximum distance travelled by particles before turning back to the ocean is shorter in the Entrance channel than in all others. In this case they always exit the lagoon in a time less than one complete tidal cycle (8.66 h).

S.Jacinto channel presents the highest average residence time (39.26 h), corresponding to about 1 day 15 h 15 min. The second highest average residence time occurs in Mira channel (12 h 15 min), followed by Espinheiro channel (10 h 58 min) and Entrance channel (1 h 31 min). S.Jacinto channel possesses higher residence times due to the greater distances achieved by the microalgae. When microalgae start their path to exit the lagoon, carried by the ebb currents, they are caught by the next flood currents and consequently dispersed again into the channels. The residence time in Mira channel is not related to the

distances that microalgae achieve, but with a certain level of retention that apparently occurs in the area of Triângulo das Correntes.

To better understand how microalgae dispersal and distribution occurs in the different channels and the possible consequence in toxicity level presented by bivalve shellfish, a more detailed characterization for each channel follows.

3.2.1. Espinheiro channel

The microalgae trajectory maps obtained for this channel over a 4 day period simulation (Figure 5.3) show that for both spring and neap tides, microalgae always reach the shellfish sampling stations in this channel. Some times microalgae can reach even more remote areas, being transported into both branches that arise from Espinheiro channel.

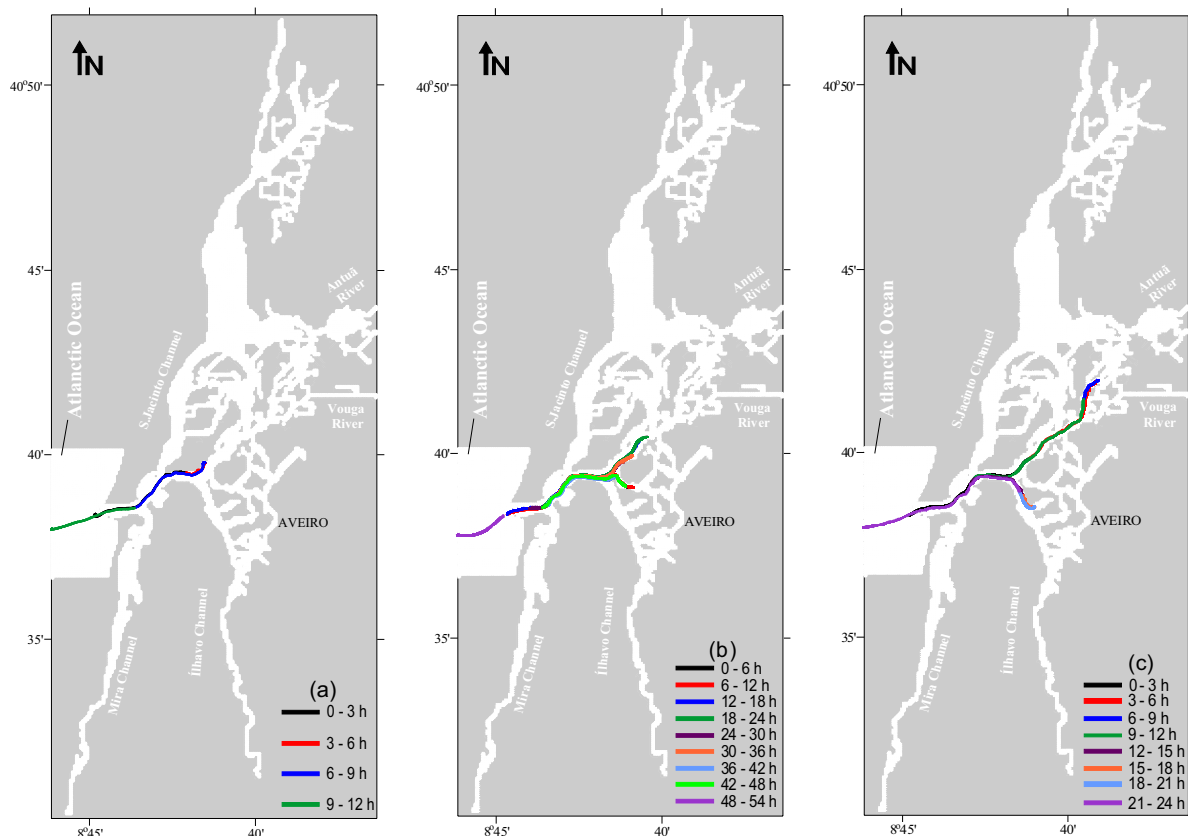


Figure 5.3. Microalgae tracks in the Espinheiro channel for minimum total exit time in spring tide (a); maximum total exit time in neap tide (b); and maximum distance attained on spring tide (c).

The results show that 60% of microalgae leave the lagoon during the first tidal cycle. Results (not shown) also indicate that, however, on spring tides, microalgae can remain in

the lagoon for a period of 22.74 h to 36.28 h. On neap tide, this retention time can reach 49.62 h (1 d 22 h 37 min).

Analysis of Figures 5.3a-b reveals that on spring tides microalgae remain in the lagoon less time than on the neap tides but achieve higher distances (Figure 5.3c).

Average values of the calculated parameters are presented in Table 5.2. In Espinheiro channel microalgae reach major distances in spring tide (track of maximum distance attained shown in Figure 5.3c) than in neap tide, but the necessary time to cover that distance is largest in neap tide.

Table 5.2. Average distance attained by microalgae, time needed to cover that distance and exit time, in Espinheiro channel during spring and neap tides.

Espinheiro channel	Distance (km)	Time (h)	Exit time (h)	Residence time (h)
Spring tide	6.686	8.121	15.535	7.410
Neap tide	5.599	10.267	25.397	15.130

This pattern is probably due to the stronger currents on spring tides, which transport microalgae to more remote areas of the channel more rapidly. On neap tides, lower current velocities reduce the microalgae transport into the channel and increase the time needed for that transport.

The same tendency is reproduced in the microalgae total exit time parameter which is also higher during neap tide. It is believed that the stronger currents of the ebb in spring tide are responsible for a faster exit of microalgae from the lagoon in comparison with neap tides. In the last situation, particles that enter Espinheiro channel do not exit the lagoon after one tidal cycle; they are transported back and forward inside the channel due to the influence of successive ebb and flood currents.

The average total exit time of microalgae after their dispersal into this channel is of 20.09 h (Table 5.1). This time for microalgae maintenance in Espinheiro channel is considered enough for growth of the phytoplankton cells concentration (Margalef, 1978b), leading to high food availability to filter-feeding bivalve shellfish. If potential toxin producer microalgae are present in the set of phytoplankton species, time exposure of filter-feeding bivalve shellfish to those organisms will be high and the level of toxicity found in their tissues will also be higher.

The residence time of this channel is shorter on spring tides (7 h 25 min) than on neap tides (15 h 8 min) (Table 5.2). Although higher distances are achieved in spring tide, current velocities are also significantly higher in this situation (Dias *et al.*, 2000), which may explain that fact.

These results show that the existing bivalve shellfish sampling stations located in Espinheiro channel postulated by INIAP/IPIMAR may be considered adequate for monitoring purposes. Nevertheless, there are no records of microalgae concentrations that actually occur in this channel (such records would be interesting to obtain correlations between toxicity level in bivalve shellfish and toxic microalgae abundance). Water samples are only collected at Marégrafo and Triângulo das Correntes sampling stations; this analysis reveals the phytoplankton species composition that effectively enter in Ria de Aveiro. The phytoplankton community composition observed in samples collected at these locations may be the same that would be found in samples from monitoring stations located at Espinheiro channel (if they exist), because the main component of the tidal flow is directed to this channel. Besides, considering the time that microalgae can be retained in Espinheiro channel, it is possible that concentrations can increase due to cellular multiplication; this possibility may be important in the toxicity level in bivalve shellfish if microalgae toxin-producers are present. The collection of water samples during an experimental period, at the same points and with the same periodicity of bivalve shellfish sampling is, therefore, recommended. This procedure will show if there are significant differences between the phytoplankton species abundance in each location, and whether the water sampling stations of Marégrafo and Triângulo das Correntes are enough to perform the HABs monitoring in Espinheiro channel.

3.2.2. S. Jacinto channel

Microalgae trajectory maps obtained from the simulations over one single tidal cycle period showed that microalgae cannot exit the lagoon in a period less than 12.25 h, after their entrance in S. Jacinto channel.

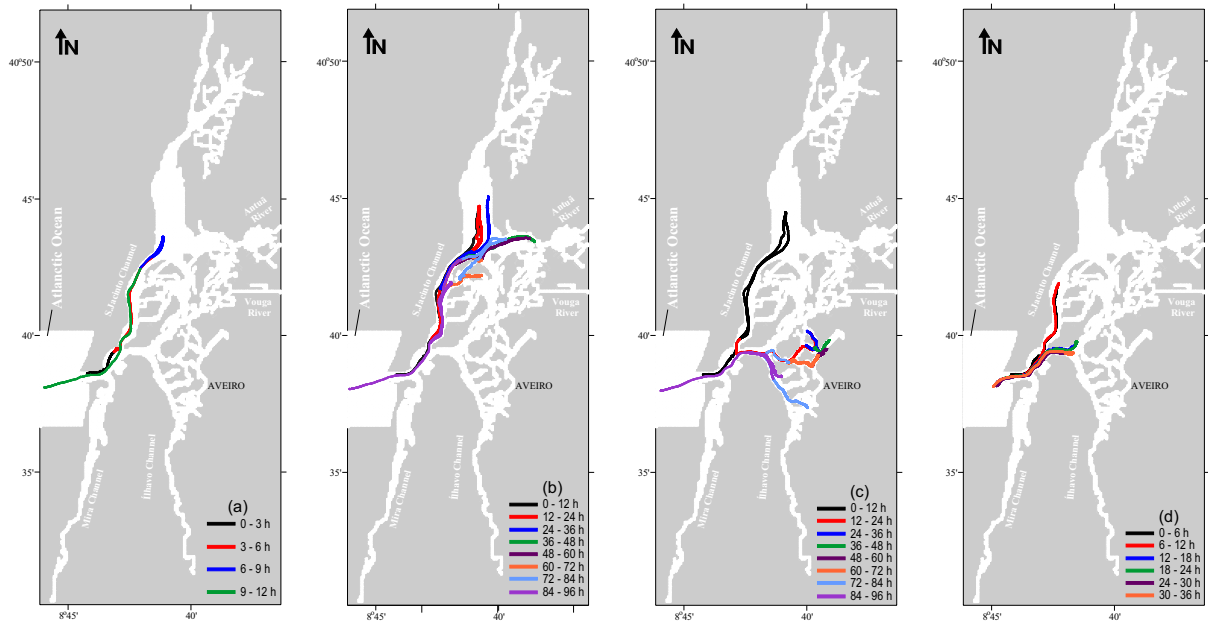


Figure 5.4. Microalgae tracks in the S. Jacinto channel for minimum (a) and maximum (b) and total exit time (c) on spring tide and minimum total exit time (d) on neap tide.

The results obtained from a 4 day period simulation, on spring and neap tides (Figure 5.4), demonstrated that, most of the times, ebb currents were not strong enough to carry microalgae out of Ria de Aveiro during one tidal cycle so they were, caught in the next flood current. In this case they were transported back to S. Jacinto channel (Figure 5.4b), where they reached areas far from the mouth, or were transported to the Espinheiro channel (Figure 5.4c). In both cases the total time that microalgae take to exit from the lagoon is increased. An exception was found in one situation during spring tide where microalgae left Ria de Aveiro lagoon in a period of less than one tidal cycle (Figure 5.4a). It is believed that this different microalgae path was essentially determined by the northward location of the particle emission point in Ria de Aveiro mouth and its proximity with the land boundary. Microalgae proceeding from this point were subjected to a flood flux different from the one in the middle of the channel, which transports the microalgae to a small bay (S.Jacinto bay) near the entrance of S.Jacinto channel. This could have delayed the microalgae course and reduced the distance attained in the channel. This shorter distance (4.9 km) could be enough to lead the microalgae to exit from the lagoon in a period of 11.18 h, under the influence of the ebb current.

Through the analysis of the other trajectories, it was observed that the total exit time reached maximums of 96.39 h (Figure 5.4b) and of 49.04 h (Figure 5.4d), during spring and neap tides, respectively. The maximum distance attained within the S. Jacinto channel was

of 9.097 km (Figure 5.4b) in spring tide and minimum distance was of 3.121 km during neap tide.

The analysis of Table 5.3 confirms the results discussed above. In addition the total exit time, average maximum distances attained by microalgae and time needed to cover those distances, were also higher during spring tide.

Table 5.3. Average far distance attained by microalgae, time needed to cover that distance and exit time, in S.Jacinto channel, in spring and neap tides.

S. Jacinto channel	Distance (km)	Time (h)	Exit time (h)	Residence time (h)
Spring tide	6.566	18.747	67.973	49.227
Neap tide	3.853	10.897	40.197	29.300

The stronger currents characteristic of spring tides are believed to be the cause for the greater microalgae transport into S.Jacinto channel. Due to the greater distances achieved, ebb currents were not strong enough to transport microalgae out of the lagoon. Instead, they were caught by the next flood current which carried microalgae to other areas of the lagoon, consequently increasing the period of retention. Considering the weaker tidal currents of neap tides it would be expected that microalgae total exit time would be enhanced, as happened in Espinheiro channel. However, it was found that this period was shorter than during spring tide. A probable explanation is that the microalgae travel shorter distances on neap tide. In fact, if microalgae are transported far from the mouth in S.Jacinto channel (as in spring tide), the local current intensity is strongly reduced (Dias *et al.*, 2000) and they are trapped in the central area of the channel. In the Espinheiro channel the current intensity remains high even for large distances to the mouth, and therefore the microalgae are able to be transported back to the lagoon's mouth during the ebb.

The bivalve shellfish sampling stations are located in the central area of the channel, as well as in S.Jacinto bay and in Moacha. Therefore it is not considered relevant to add other sampling locations. Concerning water sampling, one monitoring station exists in Moacha, which is located close to the greatest distances attained by microalgae. The impact of the implementation of another water sampling point at the beginning of the channel could be evaluated; however, it is thought that no additional knowledge would be obtained, considering the good information on phytoplankton species composition and concentrations already obtained at Marégrafo and Triângulo das Correntes sampling stations. In conclusion, implementation of new sampling stations at S.Jacinto channel is

not recommended. A weekly periodicity at Moacha water sampling station is considered necessary, since phytoplankton community composition can change in a week, due to the period that algae remain in this constrain (see Table 5.1 - average of 54.09 h and maximum of 96.39 h).

3.2.3. Mira channel

In Mira channel the dispersal of microalgae presents a different pattern depending on the type of tide (spring or neap) that induces their transport. From the trajectories obtained with the 4 day simulations, it was found that during spring tide microalgae entry and departure from the lagoon occurs on one tidal cycle (Figure 5.5a). The time that microalgae remain in the lagoon on neap tides is, to some extent, enhanced due to the fact that they are caught by the next flood current before they can exit the lagoon. Some are retained in the area of Triângulo das Correntes and then re-transported back into Ria de Aveiro, this time in the direction of Espinheiro channel (Figure 5.5b).

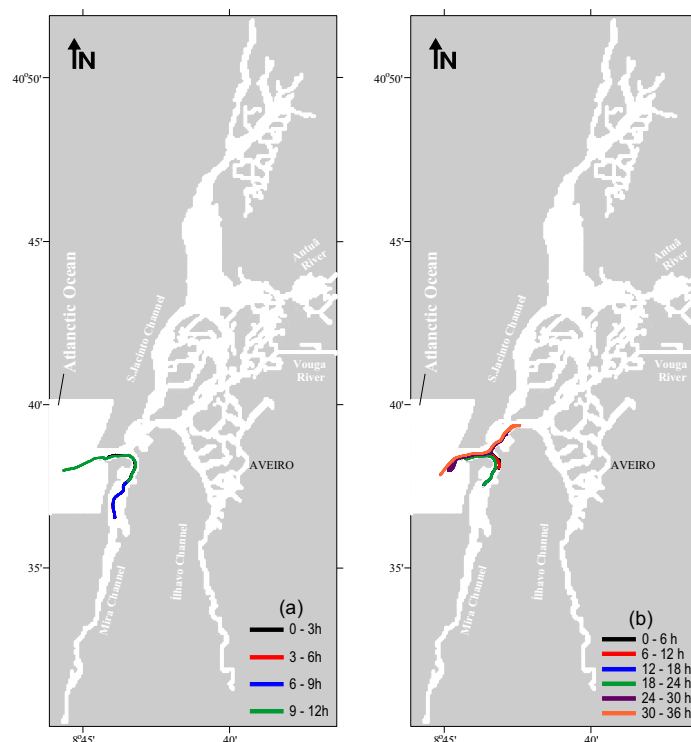


Figure 5.5. Microalgae tracks in the Mira channel for the minimum total exit time on spring tide (a) and the maximum total exit time on neap tide (b).

In Mira channel (Table 5.4) microalgae achieve approximately the same maximum distance in spring and neap tides (1.716 km and 1.693 km, respectively), and the time

needed for that transport is also closely the same. However, numerical results for microalgae total exit time and residence time, confirms the assumptions made exclusively from the analysis of the trajectory maps.

Table 5.4. Average far distance attained by microalgae, time needed to cover that distance and exit time, in Mira channel in spring and neap tides.

Mira channel	Distance (km)	Time (h)	Exit time (h)	Residence time (h)
Spring tide	1.716	7.000	11.127	4.127
Neap tide	1.693	6.440	26.807	20.367

The time that microalgae remain in the lagoon is higher in neap tide (average of 26.807 h) mainly due to greater residence time (20.367 h).

Bivalve sampling stations in this channel (natural productions banks and molluscan shellfish farming areas) are located close to the areas attained by microalgae in the simulations. As a result the location of these sampling sites is considered appropriate. The periodicity of sampling already existent is also considered sufficient for this channel, because microalgae are not preferentially transported for this branch. The water sampling is made at the same area of bivalve shellfish collection, and for that reason it is also considered appropriated. Nevertheless, water samples are only collected in periods of strong occurrence of marine toxic microalgae. The collection of water samples more frequently, maybe twice a month, is recommended.

3.2.4. Entrance channel

In this channel, average maximum distance attained by microalgae is similar in spring and neap tides, as well as the time needed to cover that distance (Table 5.5). Nevertheless, in neap tide larger periods for complete microalgae exit from the lagoon were found, due to the shorter residence time in spring tide. This channel presents an average residence time of 1.53 h (Table 5.1).

Figure 5.6 shows microalgae retention close to the northern jetty of the inlet channel. This retention occurs due to the location of the microalgae emission point.

Table 5.5. Average far distance attained by microalgae, time needed to cover that distance and exit time, in Main channel in spring and neap tides.

Main channel	Distance (km)	Time (h)	Exit time (h)	Residence time (h)
Spring tide	1.554	7.090	7.825	0.730
Neap tide	1.500	7.160	9.220	2.060

Such emission was performed northward of the lagoon mouth. Therefore particles were possibly transported by a flux different from the one that occurs in the central area of the inlet channel, displaying weaker current velocity and different direction due to the proximity of the land boundary. Nevertheless, this case is considered relevant in this study, because a dense mass of common mussel exists at this jetty, which constitutes a suitable substratum for the fixation of these organisms (Tyler-Walters, 2002). If microalgae are retained at this location, the time exposure of bivalve shellfish to toxic microalgae is higher; which also increases the level of toxicity that could be found in bivalve shellfish samples collected at this spot (Triângulo das Correntes common mussel sampling station).

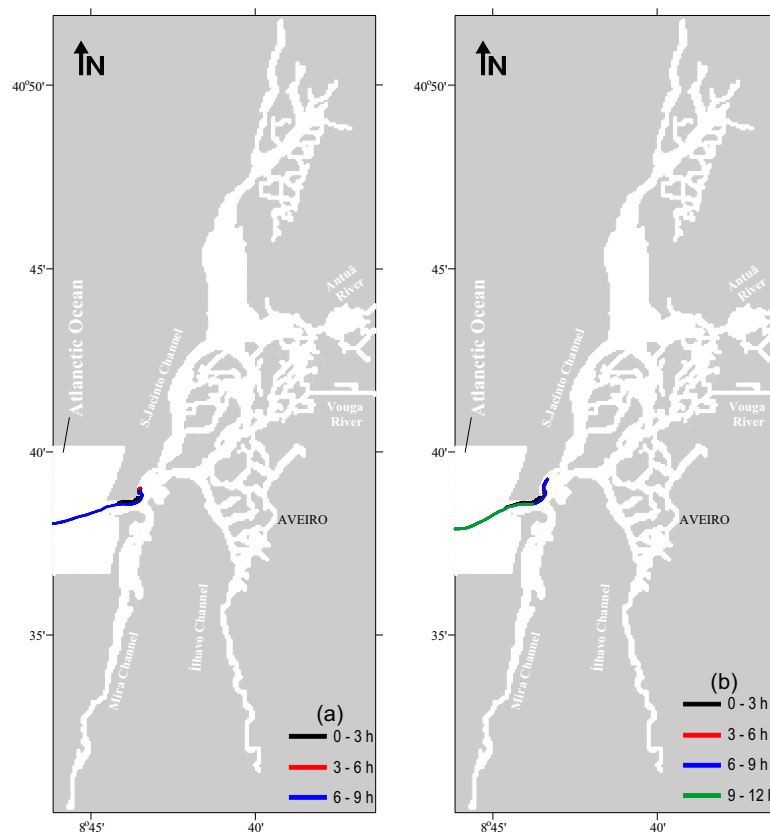


Figure 5.6. Microalgae tracks in the Entrance channel for the minimum total exit time on spring tide (a) and the maximum total exit time on neap tide (b).

4. Conclusions

Numerical modelling proved to be a very useful tool in the management and assessment of this coastal area, namely in the monitoring of toxic events related to the presence of marine toxic microalgae that enter in Ria de Aveiro lagoon proceeding from the littoral waters. It has legitimated the location of water and bivalve shellfish sampling stations postulated by INIAP/IPIMAR, in the frame of Plano Nacional de Salubridade de Bivalves for Ria de Aveiro. It also provides additional knowledge about the horizontal distribution and dispersal of microalgae in this lagoon. The reduced time and financial resources required to apply this methodology, comparatively to the ones usually implicated in conventional monitoring programmes should be emphasized.

Nevertheless, one should bear in mind that the model used in this study does not take in account the possible, and most probable, microalgae vertical distribution patterns determined by light intensity, nutrients availability, water temperature and salinity (Valiela, 1995). Although Ria de Aveiro is shallow and considered vertically homogeneous, it is considered advisable, and in agreement with Cembella *et al.* (2005), a model enhancement. This improvement would have the purpose of evaluate the importance of microalgae vertical distribution patterns in the level of toxicity found in the tissues of bivalve shellfish and of obtain accurate correlations between cellular abundance and level of toxicity.

The results obtained show that microalgae horizontal distribution and dispersal in Ria de Aveiro lagoon are mainly due to tidal currents. According to the hydrological characterization provided by Dias (2001), the preferential channels to which microalgae are transported to (Espinheiro and S. Jacinto channels) are the ones to which the main component of the tidal flux is directed.

Pre-existent bivalve shellfish sampling stations cover reasonably well the area of Ria de Aveiro most influenced by tidal currents and, consequently, the maximum area that microalgae can achieve in each channel in a few days. The selection of the sampling stations made by INIAP/IPIMAR was based on the high commercial interest of natural production banks and their location is precisely in the maximum area under the direct

marine influence of Ria de Aveiro. The location of the sampling stations and periodicity is considered adequate, except in Ílhavo channel, where microalgae transport was never found in this study. Therefore, it is considered that the bivalve sampling station existent in this channel is not necessary. Nevertheless, it is advisable the collection of bivalve shellfish in Ílhavo channel in periods of toxic microalgae occurrence.

Considering the water sampling stations, which have the purpose of identify and count the phytoplankton cells, Marégrafo should be maintained due to its ideal location at the entrance of the lagoon, which gives the general idea of phytoplankton community species composition. The sampling periodicity at this site is also considered optimal (two times a week) bearing in mind the different times that microalgae remains in each channel.

Triângulo das Correntes sampling station existence can generate some controversy. On one hand, analysis of the water samples collected at this site permit to determine the toxic microalgae abundance that affects the common mussel dense mass existent at the northern jetty of the inlet channel, where a certain level of retention was found (see Entrance channel results); it also allows to monitor the microalgae that enter in S.Jacinto and Espinheiro channels. On the other hand, results obtained for Mira channel reveal that Triângulo das Correntes, that divide the tidal prism, can be a retention area due to the convergence of water flows coming from different channels in ebb stages. Therefore, phytoplankton cells concentrations found in the analysis of water samples collected at this location can overestimate the real cell concentrations that enter in the different channels. Moreover, it is considered probable (confirmed by the experience of observation of phytoplankton samples) that the species composition found in Triângulo das Correntes is the same found in Marégrafo. It is then recommended a comparative study between the level of toxicity found in common mussel and toxic microalgae abundance encountered in water samples proceeding from Marégrafo and Triângulo das Correntes in order to verify where the best correlation is established.

The water sampling station in Moacha (S. Jacinto channel) and the weekly periodicity of collection is considered enough, since it is in this area that the largest and with highest commercial interest, natural production banks of bivalve shellfish are encountered. Taking into account the time that microalgae remain in this channel and its residence time (the most elevated), studies based on a higher frequency of water collection in Moacha (one for

day, for example) could be interesting to evaluate if toxic microalgae abundance really increases over time, after their entrance in this channel.

Water sample collection in Mira channel should be increased to, at least, two times a month and not only in periods of toxic microalgae occurrence.

Considering Espinheiro channel, it is advised the definition of a water sampling station at the far end of this channel, close to the areas where collection of bivalve shellfish is made.

5. References

- Barrosa JO (1985) Breve caracterização da Ria de Aveiro. In: Jornadas da Ria de Aveiro, Vol. III – Recursos da Ria de Aveiro, Câmara Municipal de Aveiro, Portugal, p 9-14
- Cembella AD, Ibarra IA, Diogene J, Dahl E (2005) Harmful Algal Blooms and their assessment in fjords and coastal embayments. *Oceanography* 18: 158-171
- Dias JM (2001) Contribution to the study of the Ria de Aveiro hydrodynamics. PhD dissertation, University of Aveiro, Aveiro, Portugal
- Dias JM, Lopes JF (2006a) Calibration and validation of hydrodynamic, salt and heat transport models for Ria de Aveiro lagoon (Portugal). *Journal of Coastal Research*, SI 39 (in press)
- Dias JM, Lopes JF (2006b) Implementation and assessment of hydrodynamic, salt and heat transport models: the case of Ria de Aveiro lagoon (Portugal). *Environmental Modelling and Software* 21: 1-15
- Dias JM, Lopes JF, Dekeyser I (1999) Hydrological characterisation of Ria de Aveiro, Portugal, in early Summer. *Oceanologica Acta* 22: 473-485
- Dias JM, Lopes JF, Dekeyser I (2000) Tidal Propagation in Ria de Aveiro Lagoon, Portugal. *Phys Chem Earth (B)* 25: 369-374
- Dias JM, Lopes JF, Dekeyser I (2001) Lagrangian transport of particles in Ria de Aveiro lagoon, Portugal. *Phys Chem Earth (B)* 26: 721-727

- Dias JM, Lopes JF, Dekeyser I (2003) A numerical system to study the transport properties in the Ria de Aveiro lagoon. *Ocean Dynamics* 53: 220-231
- Dronkers JJ (1964) Tidal Computations in Rivers and Coastal Waters. North-Holland Publishing Company, Amsterdam, The Netherlands
- FAO (2004) Marine Biotoxins, FAO Food and Nutrition Paper, 80. Food and Agriculture Organization of the United Nations, Rome. 278 pp.
- Gesteira-Gomez M, Montero P, Prego R, Taboada JJ, Leitão P, Ruiz-Villarreal M, Neves R, Perez-Villar V (1999) A two-dimensional particle tracking model for pollution dispersion in A Coruña and Vigo Rias (NW Spain). *Oceanologica acta* 22: 167-177
- Hallegraeff GM (1995) Harmful algal blooms: a global overview. In: Hallegraeff GM, Anderson DM & Cembella AD (eds) *Manual on Harmful Marine Microalgae* (pp. 25-50). UNESCO Publishing.
- Hofmann EE, Hedström KS, Moisan JR, Haidvogel DB, Mackas DL (1991) Use of simulated drifter tracks to investigate general transport patterns and residence times in the coastal transition zone. *Journal of Geophysical Research* 96 C8: 15041-15052
- Inoue M, Wiseman Jr. WJ (2000) Transport, mixing and stirring processes in a Louisiana estuary: a model study. *Estuarine, Coastal and Shelf Science* 50: 449-466
- IOC (2005) The IOC harmful algal programme [on-line]. Intergovernmental Oceanographic Commission of UNESCO, Paris, France.[cited 26/09/2005]
Available from:
<<http://ioc.unesco.org/hab/intro.htm>>
- Jørgensen CB (1981) Feeding and cleaning mechanisms in the suspension feeding bivalve *Mytilus edulis*. *Marine Biol* 65: 159-163
- Jørgensen CB (1990) Bivalve filter feeding: hydrodynamics, bioenergetics, physiology and ecology. Olsen & Olsen, Fredensborg, Denmark

- Leendertse JJ (1987) Aspects of SIMSYS2D, a system for two-dimensional flow computation. Report R-3572-USGS. The Rand Corporation, New York, USA
- Leendertse JJ, Gritton EC (1971) A water-quality simulation model for well-mixed estuaries and coastal seas: volume II, Computation Procedures. Memorandum R-708-NYC. The Rand Corporation, New York, USA
- Margalef R (1978a) Phytoplankton communities in upwelling areas - the example of NW Africa. *Oecologia Acta* 3: 97-132
- Margalef R (1978b) Life-forms of phytoplankton as survival alternatives in an unstable environment. *Oceanologica Acta* 4: 493-508
- Moita MT (1993) Development of toxic dinoflagellates in relation to upwelling patterns off Portugal. In: Smayda TJ & Shimizu Y (Eds.) *Toxic Phytoplankton Blooms in the Sea* (299-304). Elsevier, Amsterdam, The Netherlands.
- Moita MT (2001) Estrutura, variabilidade e dinâmica do fitoplâncton na costa de Portugal Continental. PhD dissertation, Faculdade de Ciências da Universidade de Lisboa, Lisboa, Portugal
- Moita MT, Palma AS, Vilarinho MG (2005) Blooms de fitoplâncton na costa Portuguesa. IPIMAR Divulgação nº 31, Lisboa, Portugal
- Moita MT, Silva AJ (2001) Dynamic of *Dinophysis acuta*, *D. acuminata*, *D. tripos* and *Gymnodinium catenatum* during an upwelling event of the Northwest coast of Portugal. In: Hallegraeff GM, Blackburn SI, Bolch CJ & Lewis RJ (Eds.) *Harmful Algal Blooms 2000*, IOC of UNESCO
- Palma AS, Vilarinho MG, Moita MT (1998) Interannual trends in the longshore variation of *Dinophysis* off Portuguese coast. In: Reguera B, Blanco J, Fernández ML & Wyatt T (Eds.) *Harmful Algae*: 124-127
- Saldanha L (1995) Fauna submarina atlântica. Publicações Europa América, Mem Martins, Portugal
- Sampayo MAM, Alvito P, Franca S and Sousa I (1990) *Dinophysis* spp. toxicity and relation to accompanying species. In: Graneli E, Sundstrom B, Edler L & Anderson DM (eds.) *Toxic Marine Phytoplankton* (215-220). Elsevier, New York

- Santos MA, Costa JR (1985) Modelação matemática e gestão da qualidade da água em rios. Laboratório Nacional de Engenharia Civil, Lisboa, Portugal
- Sobral MP, Vieira F, Sobral V (2000) Zonas de produção de moluscos bivalves da Ria de Aveiro. IPIMAR Divulgação nº 12, Lisboa, Portugal
- Sournia A, Chretiennot-Dinet MJ, Ricard M (1991) Marine phytoplankton: how many species in the world?. *Journal of Plankton Research* 13: 1093-1099
- Storer TI, Usinger RL, Stedbins RC, Nybakken JW (1991) *Zoologia geral*, 6th edn. Companhia Editora Nacional, São Paulo, Brasil
- The Open University (1989) *Waves, tides and shallow-water processes*. Pergamon Press, Oxford, England
- Vale P (2004) Biotoxinas marinhas. *Revista Portuguesa de Ciências Veterinárias* 99 (549): 03-18
- Vale P, Cerejo M, Vilarinho MG (2004) Toxin production by *Dinophysis* spp at Ria de Aveiro, Portugal. Article submitted.
- Valiela I (1995) *Marine ecological processes*. Springer-Verlag New York
- Vicente CM (1985) Caracterização hidráulica e aluvionar da Ria de Aveiro. Utilização de modelos hidráulicos no estudo de problemas da Ria. In: *Jornadas da Ria de Aveiro, Vol III – Ordenamento da Ria de Aveiro*. Câmara Municipal de Aveiro, Portugal.

Chapter VI

Conclusions and final considerations

The main goal of this study was to contribute for the optimization of the toxic microalgae monitoring plan currently taking place at Ria de Aveiro, by means of a multidisciplinary study that involved several areas of science such as ecology, toxicology, numerical modelling and oceanography.

After Chapter I, where the frame, aims and structure of this work are described, Chapter II presents the comparison between two techniques of phytoplankton quantification, with the aim of determining the most accurate for phytoplankton abundance estimation in such a way that the best procedure of water sampling in Ria de Aveiro could be established.

In Chapter III a study on the annual cycle of phytoplankton succession is presented as well as on the environmental parameters responsible for the temporal pattern observed both in terms of phytoplankton biomass and community species composition.

Particular emphasis was given to *Dinophysis* cf. *acuminata* and *D. acuta* temporal pattern of distribution, since the syndrome caused by the phycotoxins produced by this genus – DSP – constitutes the most frequent risk for human health in Aveiro region, in what concerns food intoxications by bivalve consumption. Both these species are recurrent every year in the coastal area of Aveiro and for that reason constitute a priority matter in the assessment of harmful algal events in Ria de Aveiro. Chapter IV presents a study on the DSP-toxins and pectenotoxins production by these species in order to provide further data for the full understanding of the toxicity of *Dinophysis* spp..

Concerning the sampling strategy of water and bivalves at Ria de Aveiro, in Chapter V a previously developed lagrangean particle tracking model coupled to a calibrated two-dimensional hydrodynamic model of Ria de Aveiro was applied for the study of the most probable trajectories of microalgae for the interior of the lagoon when transported by the

flood flux allowing, in this way, to evaluate the pre-existent sampling stations and to determine their optimal location.

The site chosen for the collection of samples was considered a success since, beyond its strategic location at the entrance of Ria de Aveiro permitting to obtain a general idea of the community of marine phytoplankton that enters in the lagoon, it also allowed the accomplishment of a high frequency sampling, without interruptions, at slow cost and in reasonable safety circumstances, even when the climate conditions were unfavourable. This high frequency sampling strategy allowed the study of the seasonal phytoplankton succession as well as the study of short-term phytoplankton succession cycles associated with upwelling and upwelling relaxation events.

Several advices can be given for the optimization of the monitoring project for the assessment of marine toxic phytoplankton in Ria de Aveiro, aiming to safeguard public health and to minimize the economic and social negative impacts of bivalve shellfish harvest embargo.

Although the particle tracking model coupled to the hydrodynamic model of Ria de Aveiro has legitimated the location of the water and bivalve sampling stations pre-existent in the lagoon and stipulated by INIAP/IPIMAR, some changes relatively to the initial design are advised: the sampling of bivalve shellfish in Ílhavo channel is considered unnecessary since in all the simulations performed no microalgae transport to that channel was registered. It is believed that it is an unnecessary expense of resources that could be better applied elsewhere. However, it is still advised the sampling in this channel during periods of alert by phycotoxins since, as a branch of Ria de Aveiro, it still receives water of marine source.

The location of the water sampling stations was considered adequate in a general point of view. The Marégrafo and Moacha stations should be maintained without changes while the Mira channel should be sampled with increased periodicity, perhaps bi-monthly, and not only during the occurrence of toxic phytoplankton. Moreover, it should be considered the hypothesis of including another water sampling station at the far end of Espinheiro channel. The Triângulo das Correntes station preservation is a situation of higher controversy since in one hand it is the best spot for collection of bivalve shellfish, particularly blue mussels but, on the other hand and concerning water collection, the

results of phytoplankton quantification obtained from this location tend to be higher than the ones obtained from samples proceeding from Marégrafo, although the similarity of the specific composition of the phytoplankton community between both stations. It is then advised a comparative study between the level of toxicity of bivalve shellfish and the toxic phytoplankton abundance estimated in both sites in order to determine where the best correlation is established. If better correlation is obtained between the toxic microalgae abundance in Marégrafo and the level of contamination of blue mussel, the significance of the water sampling station in Triângulo das Correntes ceases to exist.

The good results obtained with the numerical modelling should not be a reason to exclude further work in this area and consequent improvement of the model. The hydrodynamic model should be upgraded in order to include the vertical pattern of microalgae distribution in such a way that it would be possible to study the influence of such a pattern in the level of toxicity of the bivalves.

In agreement with the results obtained in Chapter II, the Utermöhl technique for estimation of phytoplankton abundance is the most exact and therefore the monitoring of toxic microalgae in Ria de Aveiro should begin to include this technique in the routine work. However, the phytoplankton quantification method currently in use by INIAP/IPMAR (Monitoring technique) should not be relegated, since it continues to be extremely valuable for providing fast results that can accelerate the process of alert by presence of toxic microalgae in the water. In this way, at the sampling station Marégrafo, two water samples should be collected, one to observe by means of the Monitoring technique and other by the Utermöhl technique. The occasional collection of other samples for preservation with other fixatives, like for example Lugol's Solution, should be considered in order to accurately identify certain phytoplankton forms.

The phytoplankton succession cycle observed in the study area follows a pattern typical of temperate zones where oceanographic processes like coastal upwelling are frequent. The seasonal succession of phytoplankton biomass is influenced by the seasonal cycle of surface water temperature (induced by the seasonal cycle of solar irradiance), by the variability of the intensity of upwelling events and by the availability of dissolved nutrients in the surface water layer. As a result of the persistency of the upwelling events it was not observed neither the expected abundance decrease of the phytoplankton in the summer

community, nor the change of the phytoplankton community dominance from diatoms to dinoflagellates during the same period, keeping the succession at its initial stages.

It was found a very significant community of small phytoflagellates, abundant during the entire period of study, and thus very important in terms of primary production. Moreover, many of those organisms are thought to play an important role on the recycling of nutrients through the microbial loop. This task is particularly important because the recycling of nutrients through the microbial loop may be one of the sources of the high concentrations of nitrogen nutrients found in the coastal waters of Aveiro, in parallel with other causes such as: inputs from domestic and industrial sewage effluents; increased deposition of atmospheric nitrogen; and the persistency of upwelling events. All these factors may have a participation in the high concentrations of several forms of nitrogen which can be an indicator of the eutrophication of the coastal waters of Aveiro, situation that should deserve future and careful monitoring.

Proliferations of *Prorocentrum cf. minimum*, a dinoflagellate indicated by several authors as a producer of several types of phycotoxins, were recorded during the entire studied period particularly in spring. At the moment, this species is not included in the set of marine toxic phytoplankton species that are monitored in Ria de Aveiro. It is then advised to include this species in the monitoring program both in terms of phytoplankton quantification and toxin identification and concentration analysis.

During upwelling events, *Pseudo-nitzschia* spp. is the toxic species that can occur in high abundances in the water column. It is a species typical of the second stage of short-term phytoplankton succession cycles associated with upwelling events. Due to the high division rates of this diatom species and other species of diatoms characteristic of upwelled waters, in order to follow the specific pattern of succession associated with upwelling, it is necessary to develop a study where the frequency of the collection of water samples is increased, perhaps from weekly to daily.

Dinophysis cf. acuminata proliferated during spring and beginning of summer while *D. acuta* was most abundant during summer and beginning of autumn. Both occurred during episodes of upwelling relaxation and when nitrogen was in excess.

Once more it was demonstrated the production of DSP toxins and pectenotoxins by *Dinophysis* spp. When *Dinophysis acuta* is the dominant toxic species higher levels of

contamination are found in shellfish, since it is a producer of OA, DTX2 and PTX2. *Dinophysis acuminata* was found to induce contaminations exclusively by OA.

The different levels of toxicity attained by the bivalves during different episodes of toxic microalgae proliferation can be due to different cellular toxin concentration that it was found to increase during the decay of proliferations of *Dinophysis* spp., partially due to lowest rates of cellular division.

Although the calculation of a maximum limit of *Dinophysis* spp. abundance ($700 \text{ cells}\cdot\text{L}^{-1}$) estimated by Utermöhl technique, under which contamination of shellfish does not endanger public health, further work should be made in order to more accurately determine such a limit, perhaps following the same methodology, but appealing to replicates of water and bivalve samples, collected at the same time and location in several sampling stations.

Appendix I

Table 1. Identified species in Ria de Aveiro

BACILLARIOPHYCEAE	<i>Cyclotella</i> (Kützing) de Brébisson
<i>Achnanthes</i> spp.	<i>Cylindrotheca closterium</i> (Ehr.) Reiman & Lewin
<i>Actinoptychus senarius</i> (Ehrenberg) Ehrenberg	<i>Cylindrotheca closterium</i> (Ehr.) Reiman & Lewin (f. peq.)
<i>Actinoptychus splendens</i> (Shadbolt) Ralfs ex Pritchard	<i>Dactyliosolen fragilissimus</i> (Bergon) Hasle
<i>Amphiprora</i> spp.	<i>Detonula pumila</i> (Castracane) Gran
<i>Amphora</i> spp.	<i>Diploneis</i> cf. <i>bombus</i> Ehrenberg
<i>Asterionellopsis glacialis</i> (Castracane) Round	<i>Diploneis</i> sp.
<i>Asterolampra</i> spp.	<i>Ditylum brightwellii</i> (West) Grunow
<i>Asteromphalus flabellatus</i> (Brébisson) Greville	<i>Druridgia compressa</i> (West) Donkin
<i>Asteromphalus sarcophagus</i> Wallick	Epiphyte centric diatoms
<i>Aulacoseira granulata</i> (Ehrenberg) Simons	Epiphyte pennate diatoms
<i>Auliscus</i> spp.	<i>Eucampia zoodiacus</i> Ehrenberg
<i>Auricula</i> spp.	<i>Fragillariopsis</i> Hustedt in Schmidt emend. Hasle
Auricula/amphiprora	<i>Gomphonema acuminatum</i> Ehrenberg
<i>Bacillaria paxillifer</i> (O.F. Müller) Hende	<i>Grammatophora</i> spp.
<i>Bacteriastrum</i> Shadbolt	<i>Guinardia delicatula</i> (Cleve) Hasle
<i>Bellerochea malleus</i> (Brightwell) Van Heurck	<i>Guinardia flaccida</i> (Castracane) Peragallo
<i>Biddulphia alternans</i> (Bailey) Van Heurck	<i>Guinardia</i> spp.
<i>Biddulphia</i> spp.	<i>Guinardia striata</i> (Stolterfoth) Hasle
<i>Campylodiscus</i> spp.	<i>Gyrosigma</i> (Hassal) Cleve
Centric diatoms <10 µm	<i>Haslea wawriake</i> (Hustedt) Simonsen
Centric diatoms >10 µm	<i>Helicotheca tamesis</i> (Shrubsole) Ricard
<i>Cerataulina pelagica</i> (Cleve) Hende	<i>Hemiaulus haukii</i> Grunow in Van Heurck
<i>Cerataulus</i> spp.	<i>Hemiaulus sinensis</i> Greville
<i>Chaetoceros affinis</i> Lauder	<i>Hemiaulus</i> spp.
<i>Chaetoceros danicus</i> Cleve	<i>Lauderia annulata</i> Cleve
<i>Chaetoceros decipiens</i> Cleve	<i>Leptocylindrus danicus</i> Cleve
<i>Chaetoceros densus</i> Cleve	<i>Leptocylindrus mediterraneus</i> (Peragallo) Hasle
<i>Chaetoceros didymus</i> Ehrenberg	<i>Leptocylindrus minimus</i> Gran
<i>Chaetoceros glandazii</i> Mangin	<i>Licmophora</i> sp.
<i>Chaetoceros peruvianus</i> Brightwell	<i>Lithodesmium undulatum</i> Ehrenberg
<i>Chaetoceros pseudocurvisetus</i> Mangin	<i>Melosira</i> cf. <i>artica</i> Dickie
<i>Chaetoceros socialis</i> Lauder	<i>Melosira</i> spp.
<i>Chaetoceros</i> spp.	<i>Meuniera membranacea</i> (Cleve) P. C. Silva
<i>Chaetoceros</i> spp. small forms	<i>Navicula</i> spp.
<i>Cocconeis</i> cf. <i>scutellum</i> Ehrenberg	<i>Nitzschia acicularis</i> (Kützing) Smith
<i>Cocconeis</i> spp.	<i>Nitzschia</i> spp.
<i>Corethron criophilum</i> Castracane	<i>Odontela mobiliensis</i> (Bailey) Grunow
<i>Coscinodiscus</i> affinis <i>centralis/radiatus</i>	<i>Odontela</i> spp.
<i>Coscinodiscus granii</i> Gough	<i>Odontella longicuris</i> (Greville) Hoban
<i>Coscinodiscus perforatos</i> (Ehrenberg)	<i>Paralia sulcata</i> (Ehrenberg) Cleve
<i>Coscinodiscus</i> spp.	Pennate diatoms <10 µm

Pennate diatoms >10 µm	<i>Dinophysis caudata</i> Saville-Kent
<i>Pinnularia</i> sp.	<i>Dinophysis cf. acuminata</i> Claparède & Lachmann
<i>Pleurosigma</i> spp.	<i>Dinophysis fortii</i> Pavillard
<i>Proboscia alata</i> (Brightwell) Sundström	<i>Dinophysis hastata</i> Stein
<i>Proboscia indica</i> (Peragallo) Hernández-Becerril	<i>Dinophysis infundibulus</i> Schiller
<i>Pseudo-nitzschia</i> spp.	<i>Dinophysis</i> morpho. <i>acuta</i>
<i>Rhabdonema adriaticum</i> Kützing	<i>Dinophysis norvegica</i> Claparède & Lachmann
<i>Rhizosolenia</i> affin. <i>styliformis</i> / <i>imbricata</i>	<i>Dinophysis rotundata</i> Claparède & Lachmann
<i>Rhizosolenia setigera</i> Brightwell	<i>Dinophysis</i> spp.
<i>Rhizosolenia</i> spp.	<i>Diploplodinium</i> spp. (<i>Dissodinium</i> spp.)
<i>Skeletonema</i> spp.	Diplopsalis
<i>Stauroneis</i> spp.	<i>Erythrospidinium</i> P.C Silva
<i>Stephanopyxis turris</i> (Arnott in Greville) Raflfs in Pritchard	<i>Gonyaulax birostris</i> Stein
<i>Striatella unipunctata</i> (Lyngbye) Agardh	<i>Gonyaulax cf. digitale</i> (Pouchet) Kofoid
<i>Surirella</i> spp.	<i>Gonyaulax polygramma</i> Stein
<i>Synedra</i> spp.	<i>Gonyaulax spinifera</i> (Claparède & Lachmann) Diesing
<i>Thalassionema fraunfeldii</i> (Grunow) Hallegræf	<i>Gonyaulax</i> spp.
<i>Thalassionema nitzschioides</i> (Grunow) Grunow ex Hustedt	<i>Gonyaulax verior</i> Sournia
<i>Thalassiosira anguste-lineata</i> (Schmidt) Fryxell & Hasle	<i>Gymnodinium catenatum</i> Graham
<i>Thalassiosira rotula</i> Meunier	<i>Gyrodinium cf. spirale</i> (Bergh) Kofoid & Swezy
<i>Thalassiosira</i> spp.	<i>Gyrodinium fusiforme</i> Kofoid & Swezy
<i>Thalassiosira</i> spp. <10	<i>Gyrodinium impudicum</i> Fraga & Bravo
<i>Thalassiosira</i> spp. <5	<i>Gyrodinium lacryma</i> (Meunier) Kofoid & Swezy
<i>Thalassiosira</i> spp. >10 <20	<i>Gyrodinium pingue</i> (Schütt) Kofoid & Swezy
<i>Thalassiosira</i> spp. >20	<i>Gyrodinium</i> spp.
<i>Thalassiosira subtilis</i> (Ostenfeld) Gran	Heterotrophic dinoflagellates
Unidentified diatoms	<i>Katodinium glaucum</i> (Lebour) Loeblich III
DINOPHYCEAE	<i>Mesoporus perforatus</i> (Gran) Lillick
<i>Akashiwo sanguinea</i> (Hirasaka) G. Hansen et Moestrup	<i>Noctiluca scintillans</i> (Macartney) Kofoid & Swezy
<i>Amphidinium cf. globosum</i> Schröder	<i>Oxytoxum</i> sp. I
<i>Amphidinium cf. latum</i> Lebour	<i>Oxytoxum</i> sp. II
<i>Amphidinium cf. sphenoides</i> Wulff	<i>Oxytoxum</i> spp.
<i>Amphidinium</i> sp. I	<i>Peridinium quinquecorne</i> Abé
<i>Amphidinium</i> spp.	<i>Polykrikos</i> spp.
<i>Amphidinium</i> spp. (formas pequenas)	Preperidinium
<i>Amphidoma caudatum</i> Halldal	<i>Prorocentrum cf. minimum</i> (Pavillard) Schiller
<i>Ceratium</i> affin. <i>lineatum/minimum</i>	<i>Prorocentrum compressum</i> (Bailey) Abé
<i>Ceratium cf. kofoidii</i> Jörgensen	<i>Prorocentrum micans</i> Ehrenberg
<i>Ceratium cf. setaceum</i> Jörgensen	<i>Prorocentrum</i> spp.
<i>Ceratium furca</i> (Ehrenberg) Claparède & Lachmann	<i>Protoceratium</i> sp.
<i>Ceratium fusus</i> (Ehrenberg) Dujardin	<i>Proto-peridinium bipes</i> (Paulsen) Balech
<i>Ceratium macroceros</i> (Ehrenberg) Vanhöffen	<i>Proto-peridinium brevipes</i> (Paulsen) Balech
<i>Ceratium massiliense</i> (Gourret) Jörgensen	<i>Proto-peridinium cerasus</i> (Paulsen) Balech
<i>Ceratium pulchellum</i> Schröder	<i>Proto-peridinium cf. conicum</i> (Gran) Balech
<i>Ceratium</i> spp.	<i>Proto-peridinium crassipes</i> (Kofoid) Balech
<i>Ceratium tripos</i> (Müller) Nitzsch	<i>Proto-peridinium curtipes</i>
<i>Cochlodinium</i> spp.	<i>Proto-peridinium depressum</i> (Bailey) Balech
Cysts	<i>Proto-peridinium diabolium</i> (Cleve) Balech
<i>Dinophysis acuta</i> Ehrenberg	<i>Proto-peridinium divergens</i> (Ehrenberg) Balech
<i>Dinophysis acuta</i> morpho. <i>D. dens</i>	<i>Proto-peridinium granni</i> (Ostenfeld) Balech

<i>Protooperidinium leonis</i> (Pavillard) Balech	Unidentified coccolithophorids
<i>Protooperidinium mite</i> (Pavillard) Balech	Unidentified coccolithophorids small
<i>Protooperidinium oblongum</i> (Aurivillius) Parke & Dodge	EUGLENOPHYCEAE
<i>Protooperidinium oceanicum</i> (Vanhöffen) Balech	Euglenophyceae
<i>Protooperidinium ovum</i> (Schiller) Balech	<i>Eutreptiella</i> spp.
<i>Protooperidinium pellucidum</i> (Bergh) Balech	PRASINOPHYCEAE
<i>Protooperidinium</i> sp. A	Prasinophyceae 4 flagella
<i>Protooperidinium</i> spp.	Prasinophyceae 4 flagella small
<i>Protooperidinium steinii</i> (Jørgensen) Balech	CRYSOPHYCEAE
<i>Pyrocystis elegans</i> Pavillard	<i>Dinobryum</i> spp.
<i>Pyrocystis fusiforme</i> Wyville-Thomson ex Murray	<i>Synura</i> spp.
<i>Pyrocystis pseudonocutiluca</i> Thompson ex Murray	DICTYOCHOPHYCEAE
<i>Pyrocystis</i> spp.	<i>Dictyocha crux</i> Ehrenberg
<i>Scrippsiella</i> cf. <i>trochoidea</i> (Stein) Loeblich III	<i>Dictyocha fibula</i> Ehrenberg
Small armoured dinoflagellates	<i>Dictyocha speculum</i> Ehrenberg
<i>Spatolodinium pseudonocutiluca</i> (Pouchet) Cachon & Cachon	<i>Dictyocha</i> spp.
<i>Torodinium robustum</i> Kofoid & Swezy	<i>Octactis octonaria</i> (Ehrenberg) Hovasse
<i>Torodinium</i> spp.	CYANOPHYCEAE
Unidentified dinoflagellate ‘cabaça’	<i>Merismopedia</i> spp.
Unidentified dinoflagellates	CHLOROPHYCEAE
Unidentified unarmoured dinoflagellates	<i>Pediastrum</i> spp.
<i>Warnovia</i> spp.	<i>Scenedesmus</i> spp.
PRYMNESIOPHYCEAE	UNIDENTIFIED
<i>Anoplosolenia brasiliensis</i> (Lohmann) Deflandre	Phytoflagellate
<i>Braarudosphaera bigelowii</i> (Gran & Braarud) Deflandre	Small phytoflagellate
<i>Calcidiscus leptoporus</i> (Murray & Blackman) Loeblich Jr & Tappan	Unidentified Algae (20)
<i>Caliptrosphaera</i> spp.	Unidentified Algae (40)
<i>Cocolithus pelagicus</i> (Wallich) Schiller	PROTOZOA
<i>Coronosphaera</i> spp.	<i>Mesodinium rubrum</i> (Lohmann) Hamburger & Buddenbrock
<i>Emiliana huxleyi</i> (Lohmann) Hay & Mohler	Foraminifers
<i>Gephyrocapsa</i> spp.	Other Zooplâncton
<i>Gephyrocapsa</i> spp. pequena	Radiolaries
<i>Helicosphaera</i> spp.	Tentinnids
<i>Phaeocystis</i> Lagerheim	OTHER CATEGORIES
<i>Rhabdosphaera</i> spp.	Eggs
<i>Scyphosphaera apsteinii</i> Lohmann	Pollen grain
<i>Syracosphaera pulchra</i> Lohmann	Undetermined

Tabela 2. Spring phytoplankton assemblage

Phytoplankton categories	%	cum %	Phytoplankton categories	%	cum %
Small phytoflagellate	29.893	29.893	<i>Protooperidinium steinii</i>	0.055	98.745
<i>Leptocylindrus danicus</i>	26.207	56.100	<i>Skeletonema</i> spp.	0.051	98.795
Small armoured dinoflagellates	9.685	65.786	<i>Gonyaulax</i> spp.	0.051	98.846
<i>Pseudo-nitzschia</i> spp.	9.087	74.873	<i>Ceratium furca</i>	0.051	98.897
<i>Prorocentrum</i> cf. <i>minimum</i>	3.208	78.081	<i>Gyrodinium lacryma</i>	0.051	98.947
<i>Emiliana huxleyi</i>	1.839	79.920	<i>Ceratium</i> cf. <i>kofoidii</i>	0.043	98.990
<i>Scripsiella</i> cf. <i>trochoidea</i>	1.792	81.711	<i>Prorocentrum micans</i>	0.041	99.031
<i>Chaetoceros</i> spp. small forms	1.630	83.341	<i>Proboscia alata</i>	0.040	99.070
<i>Gephyrocapsa</i> spp. small	1.532	84.874	<i>Amphidinium</i> cf. <i>latum</i>	0.039	99.110
<i>Chaetoceros</i> spp.	1.357	86.230	Euglenophyceae	0.038	99.147
<i>Thalassiosira</i> spp. < 5	1.287	87.518	<i>Polykrikos</i> spp.	0.035	99.182
Centric diatoms < 10 µm	1.124	88.641	<i>Leptocylindrus minimus</i>	0.029	99.211
Other Zooplankton	1.110	89.751	<i>Amphidinium</i> sp. I	0.025	99.236
Unidentified unarmoured dinoflagellates	1.076	90.828	<i>Dictyocha speculum</i>	0.025	99.261
Prasinophyceae	0.940	91.768	<i>Thalassiosira</i> spp.	0.024	99.284
Pennate diatoms < 10 µm	0.797	92.564	<i>Protooperidinium bipes</i>	0.024	99.308
Dinoflagelados n. ident.	0.560	93.124	<i>Amphidinium</i> cf. <i>globosum</i>	0.021	99.329
Unidentified dinoflagellates	0.526	93.650	<i>Ceratium</i> cf. <i>setaceum</i>	0.021	99.351
<i>Thalassiosira</i> spp. < 10	0.500	94.150	<i>Prorocentrum</i> spp.	0.020	99.371
Tentinnids	0.431	94.581	<i>Druridgera compressa</i>	0.020	99.392
<i>Ceratium</i> affin. <i>lineatum/minimum</i>	0.346	94.927	<i>Cocconeis</i> cf. <i>scutellum</i>	0.020	99.411
<i>Mesodinium rubrum</i>	0.341	95.267	<i>Erythrospidinium</i> sp	0.019	99.430
<i>Detonula pumila</i>	0.336	95.603	<i>Leptocylindrus mediterraneus</i>	0.019	99.449
Centric diatoms > 10 µm	0.315	95.919	<i>Gyrodinium</i> cf. <i>spirale</i>	0.019	99.468
Pennate diatoms > 10 µm	0.274	96.193	<i>Cocolithus pelagicus</i>	0.019	99.486
<i>Cylindrotheca closterium</i>	0.244	96.436	<i>Amphidinium</i> spp.	0.017	99.503
<i>Guinardia delicatula</i>	0.242	96.678	<i>Cochlodinium</i> spp.	0.017	99.521
<i>Gyrodinium fusiforme</i>	0.207	96.885	<i>Protooperidinium</i> spp.	0.017	99.538
<i>Eutreptiella</i> spp.	0.172	97.056	<i>Stephanopyxis turris</i>	0.017	99.555
<i>Chaetoceros pseudocurvisetus</i>	0.128	97.185	<i>Spatolodinium pseudonoctiluca</i>	0.017	99.572
Diplopsalis	0.115	97.300	<i>Mesoporus perforatus</i>	0.016	99.588
Epiphyte centric diatoms	0.113	97.413	<i>Thalassiosira</i> spp. >20	0.016	99.604
<i>Dinophysis</i> cf. <i>acuminata</i>	0.112	97.525	Heterotrophic dinoflagellates	0.016	99.620
<i>Cerataulina pelagica</i>	0.108	97.633	<i>Syracosphaera pulchra</i>	0.016	99.635
<i>Ceratium fusus</i>	0.100	97.732	<i>Thalassiosira rotula</i>	0.013	99.648
<i>Thalassionema nitzschioides</i>	0.099	97.831	<i>Gyrodinium impudicum</i>	0.013	99.661
<i>Meuniera membranacea</i>	0.098	97.929	<i>Preperidinium</i>	0.012	99.673
<i>Gonyaulax spinifera</i>	0.098	98.027	<i>Protooperidinium depressum</i>	0.012	99.686
<i>Paralia sulcata</i>	0.093	98.120	<i>Protooperidinium diabolium</i>	0.012	99.698
<i>Amphidinium</i> spp. small forms	0.082	98.202	<i>Navicula</i> spp.	0.011	99.709
<i>Chaetoceros socialis</i>	0.080	98.282	<i>Warnovia</i> spp.	0.011	99.721
Phytoflagellate	0.077	98.359	<i>Protooperidinium divergens</i>	0.011	99.732
<i>Katodinium glaucum</i>	0.075	98.434	<i>Licmophora</i> sp.	0.010	99.741
<i>Thalassiosira</i> spp. >10 <20	0.074	98.508	<i>Dactyliosolen fragilissimus</i>	0.010	99.751
<i>Gyrodinium</i> spp.	0.065	98.573	<i>Lauderia annulata</i>	0.010	99.761
<i>Guinardia striata</i>	0.062	98.635	<i>Protooperidinium ovum</i>	0.010	99.771
<i>Asterionellopsis glacialis</i>	0.055	98.690	<i>Haslea wawrikan</i>	0.009	99.780

Phytoplankton categories	%	cum %	Phytoplankton categories	%	cum %
Unidentified diatoms	0.008	99.788	<i>Bellerochea malleus</i>	0.002	99.971
<i>Dinobryum</i> sp.	0.007	99.795	<i>Nitzschia acicularis</i>	0.002	99.972
<i>Oxytoxum</i> spp.	0.007	99.802	<i>Thalassionema fraunfeldii</i>	0.002	99.974
Unidentified coccolithorids	0.007	99.808	Cabaça	0.002	99.975
<i>Dictyocha</i> spp.	0.007	99.815	<i>Diploplodinium</i> spp.	0.002	99.977
<i>Guinardia flaccida</i>	0.007	99.821	<i>Protopteridinium oblongum</i>	0.002	99.979
<i>Thalassiosira anguste-lineata</i>	0.007	99.828	<i>Protopteridinium</i> sp A	0.002	99.980
<i>Gyrodinium pingue</i>	0.007	99.834	<i>Torodinium robustum</i>	0.002	99.982
<i>Helicosphaera</i> spp.	0.006	99.840	<i>Auricula</i> spp.	0.001	99.983
Radiolaries	0.006	99.846	<i>Campylodiscus</i> spp.	0.001	99.984
<i>Diploneis</i> cf. <i>bombus</i>	0.006	99.852	<i>Coscinodiscus</i> spp.	0.001	99.984
<i>Amphidinium</i> cf. <i>sphenoides</i>	0.006	99.857	<i>Melosira</i> spp.	0.001	99.985
<i>Cocconeis</i> spp.	0.005	99.862	<i>Ceratium macroceros</i>	0.001	99.986
<i>Grammatophora</i> spp.	0.005	99.867	<i>Protoceratium</i> sp.	0.001	99.987
<i>Pleurosigma</i> spp.	0.005	99.872	<i>Coronosphaera</i> spp.	0.001	99.988
Foraminifers	0.005	99.877	<i>Actinoptychus senarius</i>	0.001	99.989
<i>Dinophysis acuta</i>	0.005	99.882	<i>Corethron criophilum</i>	0.001	99.989
<i>Dinophysis rotundata</i>	0.005	99.887	<i>Helicotheca tamensis</i>	0.001	99.990
<i>Rhizosolenia</i> spp.	0.004	99.891	<i>Odontela mobiliensis</i>	0.001	99.991
<i>Hemiaulus sinensis</i>	0.004	99.895	<i>Amphidoma caudata</i>	0.001	99.992
<i>Dinophysis norvegica</i>	0.004	99.899	<i>Ceratium macroceros</i>	0.001	99.993
<i>Gonyaulax polygramma</i>	0.004	99.904	<i>Dinophysis infundibulus</i>	0.001	99.993
<i>Amphora</i> spp.	0.003	99.907	<i>Gonyaulax birostis</i>	0.001	99.994
<i>Nitzschia</i> spp.	0.003	99.910	<i>Oxytoxum</i> sp. I	0.001	99.995
<i>Phaeocystis</i> sp.	0.003	99.913	<i>Peridinium quinquecorne</i>	0.001	99.996
<i>Chaetoceros danicus</i>	0.003	99.917	<i>Protopteridinium</i> cf. <i>conicum</i>	0.001	99.997
<i>Gonyaulax</i> cf. <i>digitale</i>	0.003	99.920	<i>Protopteridinium granni</i>	0.001	99.998
<i>Protopteridinium brevipes</i>	0.003	99.923	<i>Protopteridinium oceanicum</i>	0.001	99.998
<i>Pyrocystis fusiforme</i>	0.003	99.926	<i>Calcidiscus leptoporus</i>	0.001	99.999
<i>Acnantes</i> spp.	0.002	99.929	<i>Dictyocha crux</i>	0.001	100.000
<i>Cerataulus</i> spp.	0.002	99.931			
<i>Guinardia</i> spp.	0.002	99.934			
<i>Dinophysis</i> spp.	0.002	99.936			
<i>Pyrocystis</i> spp.	0.002	99.939			
<i>Torodinium</i> spp.	0.002	99.941			
<i>Asteromphalus sarcophagus</i>	0.002	99.944			
<i>Chaetoceros affinis</i>	0.002	99.946			
<i>Prorocentrum compressum</i>	0.002	99.949			
<i>Protopteridinium leonis</i>	0.002	99.951			
<i>Protopteridinium mite</i>	0.002	99.953			
<i>Braarudosphaera bigelowii</i>	0.002	99.956			
<i>Amphiprora</i> spp.	0.002	99.957			
<i>Diploneis</i> sp.	0.002	99.959			
<i>Odontela</i> spp.	0.002	99.961			
<i>Ceratium</i> spp.	0.002	99.962			
<i>Diploplodinium</i> spp. (<i>Dissodinium</i>)	0.002	99.964			
<i>Gephyrocapsa</i> spp.	0.002	99.966			
Prasinophyceae 4 flagella	0.002	99.967			
<i>Rhabdosphaera</i> spp.	0.002	99.969			

Table 3. Summer phytoplankton assemblage

Phytoplankton categories	%	cum %	Phytoplankton categories	%	cum %
<i>Leptocylindrus danicus</i>	14.358	14.358	Phytoflagellate	0.056	98.535
<i>Syracosphaera pulchra</i>	13.118	27.476	<i>Amphidinium</i> spp.	0.055	98.590
<i>Thalassiosira</i> spp. < 10	10.886	38.362	<i>Lauderia annulata</i>	0.047	98.637
<i>Chaetoceros</i> spp. small forms	9.986	48.348	<i>Protoperidinium steinii</i>	0.043	98.680
Small phytoflagellate	9.747	58.095	<i>Chaetoceros affinis</i>	0.042	98.722
<i>Pseudo-nitzschia</i> spp.	7.069	65.164	<i>Detonula pumila</i>	0.041	98.763
Small armoured dinoflagellates	6.934	72.098	<i>Protoperidinium divergens</i>	0.037	98.800
<i>Thalassionema nitzschioides</i>	4.703	76.801	<i>Thalassionema fraunfeldii</i>	0.035	98.836
<i>Scripsiella</i> cf. <i>trochoidea</i>	4.000	80.801	<i>Amphidinium</i> sp. I	0.035	98.871
<i>Emiliana huxleyi</i>	3.708	84.509	<i>Rhabdonema</i> spp.	0.035	98.906
<i>Cylindrotheca closterium</i>	2.858	87.367	<i>Protoperidinium diabolium</i>	0.034	98.940
<i>Gephyrocapsa</i> spp. Small	1.020	88.387	<i>Guinardia</i> spp.	0.034	98.974
Unidentified unarmoured dinoflagellates	0.994	89.381	<i>Navicula</i> spp.	0.034	99.007
Prasinophyceae 4 flagella small	0.882	90.264	<i>Dinophysis</i> cf. <i>acuminata</i>	0.034	99.041
Centric diatoms < 10 µm	0.744	91.008	<i>Ceratium</i> cf. <i>kofoidii</i>	0.032	99.073
Pennate diatoms < 10 µm	0.676	91.684	Cabaça	0.031	99.105
<i>Prorocentrum</i> cf. <i>minimum</i>	0.622	92.306	<i>Thalassiosira</i> spp. >20	0.030	99.135
<i>Ceratium fusus</i>	0.596	92.902	<i>Chaetoceros densus</i>	0.030	99.165
<i>Proboscia alata</i>	0.528	93.430	<i>Thalassiosira</i> spp.	0.028	99.193
Other Zooplankton	0.501	93.931	<i>Coronosphaera</i> spp.	0.026	99.220
Unidentified coccolithorids small	0.400	94.331	<i>Leptocylindrus mediterraneus</i>	0.026	99.246
Unidentified dinoflagellates	0.369	94.700	<i>Thalassiosira</i> spp. >10 <20	0.026	99.272
Centric diatoms >10 µm	0.319	95.019	<i>Meuniera membranacea</i>	0.024	99.297
Prasinophyceae 4 flagella	0.304	95.323	<i>Skeletonema</i> spp.	0.023	99.320
<i>Katodinium glaucum</i>	0.291	95.614	<i>Erythrospidinium</i> sp	0.023	99.342
<i>Chaetoceros</i> spp.	0.251	95.865	Euglenophyceae	0.022	99.364
Pennate diatoms > 10 µm	0.246	96.111	<i>Asteromphalus sarcophagus</i>	0.021	99.385
<i>Amphidinium</i> spp. small forms	0.234	96.346	<i>Gonyaulax spinifera</i>	0.021	99.406
<i>Mesodinium rubrum</i>	0.231	96.576	<i>Chaetoceros didymus</i>	0.020	99.426
<i>Chaetoceros pseudocurvisetus</i>	0.174	96.750	<i>Thalassiosira anguste-lineata</i>	0.020	99.445
Tentinnids	0.157	96.907	<i>Guinardia flaccida</i>	0.018	99.464
Diplopsalis	0.143	97.050	<i>Rhizosolenia</i> spp.	0.018	99.482
<i>Thalassiosira</i> spp. < 5	0.138	97.188	<i>Gyrodinium pingue</i>	0.018	99.499
<i>Prorocentrum micans</i>	0.124	97.312	Heterotrophic dinoflagellates	0.017	99.516
<i>Paralia sulcata</i>	0.120	97.433	<i>Mesoporus perforatus</i>	0.017	99.533
<i>Gyrodinium impudicum</i>	0.118	97.551	<i>Coscinodiscus</i> spp.	0.015	99.549
<i>Cerataulina pelagica</i>	0.109	97.659	Unidentified coccolithophorids	0.015	99.564
<i>Eutreptiella</i> spp.	0.107	97.766	<i>Haslea wawrikan</i>	0.015	99.580
<i>Guinardia striata</i>	0.100	97.866	<i>Dactyliosolen fragilissimus</i>	0.015	99.595
<i>Protoperidinium bipes</i>	0.082	97.947	<i>Protoperidinium</i> spp.	0.014	99.609
<i>Amphidinium</i> cf. <i>latum</i>	0.079	98.026	<i>Phaeocystis</i> sp.	0.014	99.623
<i>Gyrodinium fusiforme</i>	0.077	98.103	Unidentified diatoms	0.014	99.637
<i>Dinophysis acuta</i>	0.074	98.177	<i>Amphidinium</i> cf. <i>globosum</i>	0.014	99.651
<i>Gyrodinium</i> cf. <i>spirale</i>	0.066	98.243	<i>Protoperidinium ovum</i>	0.013	99.664
<i>Guinardia delicatula</i>	0.065	98.307	<i>Prorocentrum</i> spp.	0.012	99.676
<i>Ceratium furca</i>	0.058	98.366	<i>Asterionellopsis glacialis</i>	0.012	99.688
<i>Gyrodinium lacryma</i>	0.057	98.423	<i>Torodinium</i> spp.	0.011	99.699
<i>Gyrodinium</i> spp.	0.056	98.479	<i>Eucampia zodiacus</i>	0.010	99.709

Phytoplankton categories	%	cum %	Phytoplankton categories	%	cum %
<i>Asteromphalus flabellatus</i>	0.010	99.719	Radiolaries	0.002	99.957
<i>Dinophysis acuta</i> morpho <i>D. dens</i>	0.010	99.729	<i>Leptocylindrus minimus</i>	0.002	99.959
<i>Torodinium robustum</i>	0.010	99.739	<i>Ceratium tripos</i>	0.002	99.960
<i>Licmophora</i> sp.	0.009	99.748	<i>Dinophysis norvegica</i>	0.002	99.962
<i>Spatolodinium pseudonocitluca</i>	0.009	99.758	<i>Gonyaulax birostis</i>	0.002	99.963
<i>Chaetoceros decipiens</i>	0.009	99.767	<i>Protopteridinium oceanicum</i>	0.002	99.965
<i>Thalassiosira rotula</i>	0.009	99.775	<i>Protopteridinium pellucidum</i>	0.002	99.967
<i>Amphidinium</i> cf. <i>sphenoides</i>	0.009	99.784	<i>Calcidiscus leptoporus</i>	0.002	99.968
<i>Protopteridinium depressum</i>	0.009	99.793	<i>Amphiprora</i> spp.	0.001	99.970
Prepteridinium	0.008	99.801	<i>Auliscus</i> spp.	0.001	99.971
<i>Dinophysis rotundata</i>	0.008	99.810	<i>Cerataulus</i> spp.	0.001	99.972
<i>Cocconeis</i> cf. <i>scutellum</i>	0.008	99.817	<i>Ceratium</i> spp.	0.001	99.973
<i>Cochlodinium</i> spp.	0.007	99.825	<i>Helicosphaera</i> spp.	0.001	99.974
<i>Hemiaulus sinensis</i>	0.007	99.832	<i>Bellerochea malleus</i>	0.001	99.975
<i>Pyrocystis</i> spp.	0.007	99.838	<i>Chaetoceros danicus</i>	0.001	99.976
<i>Thalassiosira subtilis</i>	0.007	99.845	<i>Lithodesmium undulatum</i>	0.001	99.977
<i>Protopteridinium leonis</i>	0.007	99.852	<i>Melosira</i> cf. <i>artica</i>	0.001	99.978
<i>Ceratium macroceros</i>	0.006	99.858	<i>Nitzschia acicularis</i>	0.001	99.979
<i>Bacteriastrum</i> spp.	0.006	99.869	<i>Ceratium</i> affin. <i>lineatum/minus</i>	0.001	99.981
<i>Protopteridinium mite</i>	0.006	99.875	<i>Protopteridinium oblongum</i>	0.001	99.982
<i>Actinopterychus senarius</i>	0.005	99.880	<i>Protopteridinium</i> sp A	0.001	99.983
<i>Noctiluca scintillans</i>	0.004	99.884	<i>Pyrocystis fusiforme</i>	0.001	99.984
<i>Diploneis</i> cf. <i>bombus</i>	0.004	99.888	<i>Pyrocystis pseudonocitluca</i>	0.001	99.985
<i>Druridgia compressa</i>	0.004	99.892	<i>Chaetoceros socialis</i>	0.001	99.986
<i>Stephanopyxis turris</i>	0.004	99.896	<i>Campylodiscus</i> spp.	0.001	99.986
<i>Pleurosigma</i> spp.	0.003	99.899	<i>Cocconeis</i> spp.	0.001	99.987
<i>Gonyaulax</i> spp.	0.003	99.902	<i>Grammatophora</i> spp.	0.001	99.987
<i>Ceratium</i> cf. <i>setaceum</i>	0.003	99.906	<i>Melosira</i> spp.	0.001	99.988
<i>Peridinium quinquecorne</i>	0.003	99.909	<i>Ceratium massiliense</i>	0.001	99.988
<i>Amphora</i> spp.	0.003	99.912	<i>Polykrikos</i> spp.	0.001	99.989
<i>Dinophysis</i> spp.	0.003	99.914	<i>Protoceratium</i> sp.	0.001	99.990
<i>Odontela mobiliensis</i>	0.003	99.917	<i>Warnovia</i> spp.	0.001	99.990
<i>Rhizosolenia setigera</i>	0.003	99.920	<i>Caliptrosphaera</i> sp	0.001	99.991
<i>Oxytoxum</i> sp. II	0.003	99.923	<i>Synura</i> spp	0.001	99.991
<i>Protopteridinium curtipes</i>	0.003	99.925	<i>Merismopedia</i> sp	0.001	99.992
<i>Hemiaulus</i> spp.	0.002	99.928	<i>Actinopterychus splendens</i>	0.001	99.992
<i>Nitzschia</i> spp.	0.002	99.930	<i>Corethron criophilum</i>	0.001	99.993
<i>Diploplodinium</i> spp. (<i>Dissodinium</i>)	0.002	99.932	<i>Coscinodiscus granii</i>	0.001	99.993
<i>Oxytoxum</i> spp.	0.002	99.934	<i>Coscinodiscus perforatos</i>	0.001	99.994
<i>Dinobryum</i> sp.	0.002	99.936	<i>Ditylum brightwellii</i>	0.001	99.994
<i>Scenedesmus</i> spp.	0.002	99.939	<i>Akashiwo sanguinea</i>	0.001	99.995
<i>Hemiaulus haukii</i>	0.002	99.941	<i>Ceratium massiliense</i>	0.001	99.996
<i>Striatella unipunctata</i>	0.002	99.943	<i>Dinophysis caudata</i>	0.001	99.996
<i>Diploplodinium</i> spp.	0.002	99.945	<i>Dinophysis fortii</i>	0.001	99.997
<i>Prorocentrum compressum</i>	0.002	99.947	<i>Gonyaulax verior</i>	0.001	99.997
<i>Pyrocystis elegans</i>	0.002	99.950	<i>Oxytoxum</i> sp. I	0.001	99.998
<i>Dictyocha speculum</i>	0.002	99.952	<i>Protopteridinium</i> cf. <i>conicum</i>	0.001	99.998
<i>Odontela</i> spp.	0.002	99.954	<i>Protopteridinium granni</i>	0.001	99.999
<i>Pinnularia</i> sp	0.002	99.955	<i>Anoplosolenia brasiliensis</i>	0.001	100

Table 4. Autumn phytoplankton assemblage

Phytoplankton categories	%	cum %	Phytoplankton categories	%	cum %
<i>Syracosphaera pulchra</i>	24.469	24.469	Euglenophyceae	0.074	98.102
Small phytoflagellate	17.830	42.299	<i>Thalassiosira</i> spp. >20	0.072	98.173
<i>Leptocylindrus danicus</i>	12.426	54.725	<i>Meuniera membranacea</i>	0.067	98.240
Small armoured dinoflagellates	8.300	63.026	<i>Cerataulina pelagica</i>	0.064	98.304
<i>Emiliania huxleyi</i>	5.981	69.006	<i>Thalassiosira subtilis</i>	0.064	98.368
<i>Gephyrocapsa</i> spp. Small	4.974	73.981	<i>Prorocentrum micans</i>	0.061	98.429
Prasinophyceae 4 flagella small	2.403	76.384	<i>Guinardia flaccida</i>	0.060	98.490
<i>Pseudo-nitzschia</i> spp.	1.672	78.056	<i>Protoperidinium steinii</i>	0.058	98.548
Diplopsalis	1.515	79.571	Phytoflagellate	0.056	98.604
Centric diatoms < 10 µm	1.481	81.052	<i>Gyrodinium</i> spp.	0.051	98.655
<i>Thalassionema nitzschioides</i>	1.375	82.427	Epiphyte pennate diatoms	0.050	98.706
Epiphyte centric diatoms	1.325	83.752	<i>Asteromphalus sarcophagus</i>	0.047	98.752
<i>Chaetoceros</i> spp. small forms	1.155	84.907	<i>Eucampia zoodiacus</i>	0.046	98.798
Unidentified unarmoured dinoflagellates	1.148	86.055	<i>Protoperidinium diabolium</i>	0.045	98.843
<i>Scripsiella</i> cf <i>trochoidea</i>	1.068	87.122	<i>Detonula pumila</i>	0.040	98.883
Pennate diatoms < 10 µm	0.955	88.077	<i>Prorocentrum compressum</i>	0.037	98.920
<i>Thalassiosira</i> spp. < 5	0.870	88.947	<i>Gyrodinium pingue</i>	0.035	98.955
<i>Guinardia delicatula</i>	0.815	89.762	<i>Erythrospidinium</i> sp	0.032	98.987
Unidentified dinoflagellates	0.747	90.508	<i>Pyrocystis</i> spp.	0.032	99.020
<i>Cylindrotheca closterium</i>	0.728	91.236	<i>Cocconeis</i> cf. <i>scutellum</i>	0.031	99.051
Other Zooplankton	0.705	91.941	<i>Oxytoxum</i> spp.	0.030	99.081
<i>Chaetoceros</i> spp.	0.644	92.585	Unidentified diatoms	0.029	99.110
Cabaça	0.620	93.206	<i>Protoperidinium</i> spp.	0.029	99.139
Pennate diatoms > 10 µm	0.619	93.825	<i>Torodinium</i> spp.	0.029	99.168
Unidentified coccolithorids small	0.475	94.300	<i>Coronosphaera</i> spp.	0.029	99.197
<i>Paralia sulcata</i>	0.448	94.748	<i>Coscinodiscus</i> spp.	0.028	99.225
Centric diatoms > 10 µm	0.343	95.091	<i>Rhabdosphaera</i> spp.	0.028	99.253
<i>Thalassiosira</i> spp. < 10	0.323	95.415	<i>Chaetoceros didymus</i>	0.026	99.279
<i>Katodinium glaucum</i>	0.277	95.692	<i>Leptocylindrus mediterraneus</i>	0.026	99.305
<i>Guinardia striata</i>	0.227	95.919	<i>Gyrodinium lacryma</i>	0.026	99.330
Tentinnids	0.202	96.121	<i>Gyrodinium</i> cf. <i>spirale</i>	0.023	99.354
<i>Chaetoceros decipiens</i>	0.198	96.319	<i>Corethron criophilum</i>	0.022	99.376
<i>Dinophysis acuta</i>	0.170	96.489	<i>Mesoporus perforatus</i>	0.022	99.399
<i>Thalassiosira</i> spp. >10 <20	0.161	96.650	<i>Protoperidinium bipes</i>	0.022	99.421
<i>Mesodinium rubrum</i>	0.145	96.795	<i>Hemiaulus sinensis</i>	0.021	99.442
<i>Prorocentrum</i> cf. <i>minimum</i>	0.133	96.928	<i>Odontela mobiliensis</i>	0.021	99.463
<i>Eutreptiella</i> spp.	0.126	97.054	<i>Chaetoceros danicus</i>	0.020	99.484
<i>Leptocylindrus minimus</i>	0.121	97.175	<i>Lauderia annulata</i>	0.019	99.503
<i>Navicula</i> spp.	0.114	97.289	<i>Rhizosolenia setigera</i>	0.018	99.520
<i>Gyrodinium impudicum</i>	0.104	97.393	<i>Rhabdonema</i> spp.	0.016	99.536
<i>Thalassiosira</i> spp.	0.103	97.496	<i>Cochlodinium</i> spp.	0.016	99.552
<i>Gyrodinium fusiforme</i>	0.098	97.594	<i>Thalassiosira anguste-lineata</i>	0.016	99.567
<i>Chaetoceros pseudocurvisetus</i>	0.097	97.692	<i>Amphidinium</i> cf. <i>sphenoides</i>	0.016	99.583
<i>Haslea wawriake</i>	0.088	97.780	<i>Oxytoxum</i> sp. II	0.016	99.599
<i>Ceratium furca</i>	0.086	97.866	Unidentified coccolithophorids	0.015	99.613
<i>Ceratium fusus</i>	0.082	97.948	<i>Nitzschia</i> spp.	0.013	99.627
<i>Amphidinium</i> sp. I	0.080	98.028	<i>Actinoptychus senarius</i>	0.013	99.640

Phytoplankton categories	%	cum %	Phytoplankton categories	%	cum %
<i>Chaetoceros densus</i>	0.012	99.652	<i>Ceratium macroceros</i>	0.002	99.944
<i>Amphidinium cf. latum</i>	0.012	99.665	<i>Dinophysis</i> spp.	0.002	99.946
<i>Protoperidinium ovum</i>	0.012	99.677	<i>Preperidinium</i>	0.002	99.949
<i>Dactyliosolen fragilissimus</i>	0.011	99.688	<i>Protoceratium</i> sp.	0.002	99.951
<i>Pinnularia</i> sp.	0.010	99.698	<i>Dictyocha</i> spp.	0.002	99.953
<i>Rhizosolenia</i> spp.	0.009	99.707	<i>Chaetoceros affinis</i>	0.002	99.955
<i>Biddulphia alternans</i>	0.009	99.716	<i>Helicotheca tamensis</i>	0.002	99.958
<i>Gymnodinium catenatum</i>	0.009	99.725	<i>Proboscia indica</i>	0.002	99.960
<i>Spatolodinium pseudonoclituca</i>	0.009	99.734	<i>Ceratium macroceros</i>	0.002	99.962
<i>Cocconeis</i> spp.	0.008	99.742	<i>Dinophysis caudata</i>	0.002	99.964
<i>Fragillariopsis</i> spp.	0.008	99.750	<i>Peridinium quinquecorne</i>	0.002	99.966
Heterotrophic dinoflagellates	0.008	99.757	<i>Protoperidinium leonis</i>	0.002	99.969
<i>Proboscia alata</i>	0.008	99.765	<i>Protoperidinium oblongum</i>	0.002	99.971
<i>Dinophysis rotundata</i>	0.008	99.773	<i>Pyrocystis fusiforme</i>	0.002	99.973
<i>Gonyaulax spinifera</i>	0.008	99.781	<i>Dictyocha crux</i>	0.002	99.975
<i>Torodinium robustum</i>	0.008	99.789	<i>Asterolampra</i> sp.	0.001	99.977
<i>Cocolithus pelagicus</i>	0.008	99.797	<i>Diploneis</i> sp.	0.001	99.978
<i>Pleurosigma</i> spp.	0.007	99.803	<i>Gyrosigma</i> spp.	0.001	99.979
<i>Skeletonema</i> spp.	0.007	99.810	<i>Licmophora</i> sp.	0.001	99.980
<i>Polykrikos</i> spp.	0.007	99.817	<i>Surirella</i> spp.	0.001	99.981
<i>Prorocentrum</i> spp.	0.007	99.823	<i>Gonyaulax</i> spp.	0.001	99.982
<i>Amphora</i> spp.	0.006	99.829	<i>Phaeocystis</i> sp.	0.001	99.983
<i>Amphidinium</i> spp.	0.006	99.835	<i>Asteromphalus flabellatus</i>	0.001	99.984
Foraminifers	0.006	99.840	<i>Chaetoceros peruvianus</i>	0.001	99.985
Radiolaries	0.006	99.846	<i>Coscinodiscus granii</i>	0.001	99.987
<i>Diploneis cf. bombus</i>	0.006	99.851	<i>Coscinodiscus perforatos</i>	0.001	99.988
<i>Dinophysis acuta</i> morpho <i>D. dens</i>	0.006	99.857	<i>Odontella longicuris</i>	0.001	99.989
<i>Protoperidinium divergens</i>	0.006	99.863	<i>Ceratium tripos</i>	0.001	99.990
<i>Pyrocystis pseudonoclituca</i>	0.006	99.868	<i>Dinophysis cf. acuminata</i>	0.001	99.991
<i>Cerataulus</i> spp.	0.004	99.873	<i>Dinophysis hastata</i>	0.001	99.992
<i>Melosira</i> spp.	0.004	99.877	<i>Gonyaulax birostis</i>	0.001	99.993
<i>Synedra</i> spp.	0.004	99.882	<i>Protoperidinium cerasus</i>	0.001	99.994
<i>Thalassionema fraunfeldii</i>	0.004	99.886	<i>Protoperidinium crassipes</i>	0.001	99.996
<i>Ceratium cf. kofoidii</i>	0.004	99.890	<i>Protoperidinium depressum</i>	0.001	99.997
<i>Protoperidinium cf. conicum</i>	0.004	99.895	<i>Anoplosolenia brasiliensis</i>	0.001	99.998
<i>Bacteriastrum</i> spp.	0.003	99.898	<i>Scyphosphaera apsteinii</i>	0.001	99.999
<i>Odontella</i> spp.	0.003	99.902	<i>Dictyocha speculum</i>	0.001	100.000
<i>Ceratium</i> spp.	0.003	99.905			
<i>Warnovia</i> spp.	0.003	99.908			
<i>Gephyrocapsa</i> spp.	0.003	99.912			
<i>Helicosphaera</i> spp.	0.003	99.915			
Prasinophyceae 4 flagella	0.003	99.918			
<i>Druridgia compressa</i>	0.003	99.922			
<i>Stephanopyxis turris</i>	0.003	99.925			
<i>Ceratium cf. setaceum</i>	0.003	99.928			
<i>Gonyaulax verior</i>	0.003	99.932			
<i>Noctiluca scintillans</i>	0.003	99.935			
<i>Protoperidinium brevipes</i>	0.003	99.939			
<i>Protoperidinium mite</i>	0.003	99.942			

Table 5. Winter phytoplankton assemblage

Phytoplankton categories	%	cum %	Phytoplankton categories	%	cum %
Small phytoflagellate	34.614	34.614	<i>Guinardia flaccida</i>	0.089	98.645
<i>Chaetoceros</i> spp. small forms	12.427	47.041	<i>Protoperidinium bipes</i>	0.085	98.730
<i>Guinardia delicatula</i>	6.203	53.244	Epiphyte centric diatoms	0.081	98.811
<i>Emiliana huxleyi</i>	4.899	58.143	<i>Cocconeis</i> cf. <i>scutellum</i>	0.081	98.892
<i>Lauderia annulata</i>	4.857	63.000	<i>Gyrodinium</i> spp.	0.060	98.952
<i>Chaetoceros</i> spp.	3.029	66.029	<i>Bacillaria paxillifera</i>	0.060	99.012
<i>Pseudo-nitzschia</i> spp.	2.884	68.913	<i>Corethron criophilum</i>	0.047	99.058
<i>Cylindrotheca closterium</i>	2.543	71.457	<i>Fragillariopsis</i> spp.	0.043	99.101
<i>Thalassiosira</i> spp. >10 <20	2.479	73.936	<i>Chaetoceros danicus</i>	0.043	99.144
<i>Gephyrocapsa</i> spp. Small	2.450	76.386	<i>Thalassiosira rotula</i>	0.038	99.182
Small armoured dinoflagellates	2.237	78.622	<i>Cocolithus pelagicus</i>	0.038	99.220
Centric diatoms < 10 µm	1.917	80.539	<i>Coscinodiscus</i> spp.	0.034	99.254
<i>Chaetoceros socialis</i>	1.551	82.090	Diplopsalis	0.034	99.289
Pennate diatoms > 10 µm	1.397	83.487	<i>Meuniera membranacea</i>	0.034	99.323
Pennate diatoms < 10 µm	1.385	84.872	<i>Pleurosigma</i> spp.	0.030	99.352
<i>Thalassiosira</i> spp. < 10	1.359	86.231	Phytoflagellate	0.030	99.382
Unidentified unarmoured dinoflagellates	1.282	87.513	<i>Pyrocystis fusiforme</i>	0.030	99.412
Other Zooplankton	1.137	88.651	Unidentified diatoms	0.026	99.438
Prasinophyceae 4 flagella small	1.065	89.716	<i>Nitzschia</i> spp.	0.026	99.463
<i>Thalassiosira</i> spp. < 5	0.959	90.674	Foraminifers	0.026	99.489
<i>Paralia sulcata</i>	0.878	91.552	<i>Aulacoseira granulata</i>	0.026	99.514
<i>Mesodinium rubrum</i>	0.626	92.178	<i>Druridgia compressa</i>	0.026	99.540
<i>Scrippsiella</i> cf. <i>trochoidea</i>	0.601	92.779	<i>Hemiaulus sinensis</i>	0.026	99.565
Centric diatoms > 10 µm	0.562	93.341	<i>Calcidiscus leptoporus</i>	0.026	99.591
<i>Navicula</i> spp.	0.494	93.835	<i>Cocconeis</i> spp.	0.021	99.612
<i>Eutreptiella</i> spp.	0.392	94.227	<i>Coscinodiscus granii</i>	0.021	99.634
<i>Cerataulina pelagica</i>	0.375	94.602	<i>Mesoporus perforatus</i>	0.021	99.655
<i>Chaetoceros didymus</i>	0.358	94.960	<i>Licmophora</i> sp.	0.017	99.672
<i>Thalassiosira</i> spp. >20	0.328	95.288	<i>Pediastrum</i> sp.	0.017	99.689
Unidentified coccolithophorids small	0.320	95.608	<i>Diploneis</i> cf. <i>bombus</i>	0.017	99.706
<i>Chaetoceros pseudocurvisetus</i>	0.315	95.923	<i>Thalassiosira anguste-lineata</i>	0.017	99.723
Unidentified dinoflagellates	0.294	96.217	<i>Prorocentrum</i> spp.	0.013	99.736
Euglenophyceae	0.226	96.443	Unidentified coccolithophorids	0.013	99.749
<i>Chaetoceros densus</i>	0.226	96.669	<i>Gyrodinium</i> cf. <i>spirale</i>	0.013	99.761
<i>Chaetoceros affinis</i>	0.209	96.877	<i>Protoperidinium steinii</i>	0.013	99.774
<i>Leptocylindrus danicus</i>	0.204	97.082	<i>Torodinium robustum</i>	0.013	99.787
<i>Prorocentrum</i> cf. <i>minimum</i>	0.170	97.252	<i>Dictyocha speculum</i>	0.013	99.800
<i>Gyrodinium lacryma</i>	0.158	97.410	<i>Amphidinium</i> spp.	0.009	99.808
<i>Actinoptychus senarius</i>	0.149	97.559	<i>Diploplodinium</i> spp. (Dissodinium)	0.009	99.817
<i>Chaetoceros decipiens</i>	0.149	97.708	<i>Protoperidinium</i> spp.	0.009	99.825
<i>Detonula pumila</i>	0.141	97.849	<i>Pyrocystis</i> spp.	0.009	99.834
<i>Gyrodinium fusiforme</i>	0.136	97.985	<i>Dictyocha</i> spp.	0.009	99.842
Tentinnids	0.132	98.117	<i>Leptocylindrus minimus</i>	0.009	99.851
<i>Skeletonema</i> spp.	0.128	98.245	<i>Melosira</i> cf. <i>artica</i>	0.009	99.859
<i>Guinardia striata</i>	0.107	98.351	<i>Odontela mobiliensis</i>	0.009	99.868
<i>Rhabdonema</i> spp.	0.102	98.454	Cabaça	0.009	99.876
Radiolaries	0.102	98.556	<i>Biddulphia</i> spp.	0.004	99.889

Phytoplankton categories	%	cum %
<i>Campylodiscus</i> spp.	0.004	99.893
<i>Cyclotella</i> spp.	0.004	99.898
<i>Diploneis</i> sp.	0.004	99.902
<i>Pinnularia</i> sp	0.004	99.906
<i>Stauroneis</i> spp.	0.004	99.911
Heterotrophic dinoflagellates	0.004	99.915
<i>Erythrospidinium</i> sp	0.004	99.919
<i>Oxytoxum</i> spp.	0.004	99.923
<i>Polykrikos</i> spp.	0.004	99.928
<i>Warnovia</i> spp.	0.004	99.932
<i>Coronosphaera</i> spp.	0.004	99.936
<i>Helicosphaera</i> spp.	0.004	99.940
<i>Asteromphalus flabellatus</i>	0.004	99.945
<i>Asteromphalus sarcophagus</i>	0.004	99.949
<i>Bellerochea malleus</i>	0.004	99.953
<i>Gomphonema acuminatum</i>	0.004	99.957
<i>Haslea wawrikan</i>	0.004	99.962
<i>Amphidinium</i> sp. I	0.004	99.966
<i>Ceratium furca</i>	0.004	99.970
<i>Gonyaulax spinifera</i>	0.004	99.974
<i>Oxytoxum</i> sp. II	0.004	99.979
<i>Peridinium quinquecorne</i>	0.004	99.983
<i>Prorocentrum micans</i>	0.004	99.987
<i>Pyrocystis elegans</i>	0.004	99.991
<i>Scyphosphaera apsteinii</i>	0.004	99.996
<i>Dictyocha crux</i>	0.004	100.000
